THE UNIVERSITY OF
SYDNEY

The role of ARNT in liver and myeloid cell function

Christopher Scott

This thesis was submitted as part of the requirement for a Doctor of Philosophy in the Faculty of Medicine, Westmead Clinical School at The University of Sydney, Australia.

Diabetes and Transcription Factors Group

Department of Immunology and Inflammation

Garvan Institute of Medical Research

Supervisor: A/Prof. Jenny E. Gunton

Co-supervisor: Prof. Jacob George

Declaration

The studies presented in this thesis are the results of original work carried out whilst the author was enrolled in the degree of Doctor of Philosophy in the Faculty of Medicine, University of Sydney. Any contribution made to the research by others, whom I have worked with at USYD or elsewhere is explicitly acknowledged in the thesis.

These studies were conducted at the Garvan institute of Medical Research, Darlinghurst Sydney. Ethical approval for all animal studies was granted by the Garvan Animal Ethics Comittee. Ethical approval for the collection of human monocytes was granted by the Sydney Health District Human Research Ethics Committee.

The work presented in this thesis has not been submitted for a degree of diploma at any other university.

Signed .....

Christopher Scott

Acknowledgements

I would first and foremost like to thank my supervisor Dr Jenny Gunton, I could not have hoped for better supervisor. I honestly don't think I would have undertaken a PhD if I had not found such a great and knowledgable mentor. She had faith in me and gave me the opportunity to complete my PhD whilst concurrently studying medicine, while the vast majority of people thought I had gone insane! Her patience, support and guidance have been absolutely remarkable. I would also like to thank my co-supervisor Dr Jacob George for his invaluable guidance and expertise.

I would like to acknowledge the contributions of our collaborators Sue McLennon, Steven Twigg and James Bonner for advice and assistance with the wound healing studies. I would particularly like to thank James Bonner, for technical assistance with the wound healing histology. In addition I would like to thank Philip Boughton for technical assistance with the wound tensile strength testing and Andrew Clouston for the NASH scoring of HFD mouse livers. I also want to thank the Biological Testing Facility for looking after our mouse lines.

At the Garvan a special thanks to Bec, for teaching me so much and being a good mate. To Stacey for teaching me how to perform skin transplants. To all our lab members past and present for their help and friendship; Tash, Kim, Kuan, Sue Mei, Sue Lynn, Ken, Matt, and Christian. To the Immunology department at the Garvan which has been such a great place to work, in particular to previous members Jess Stolp, Hynn Lee and Kendle Maslowski for all their technical advice. I would also generally like to thank everyone, staff and students, at the Garvan with whom I sought advice over the course of this work.

And of course I could not have done this without my family and close friends. I thank you for believing in me as well as providing me with ongoing support and encouragement.

Abbreviations

Acetyl CoA	Acetyl coenzyme A
ADP	Adenosine diphosphate
AhR	Aryl hydrocarbon receptor
ARNT	Aryl hydrocarbon receptor nuclear translocator
ATP	Adenosine triphosphate
AUC	Area under the curve
BCS	Bovine calf serum
bHLH-PAS	Basic helix-loop-helix Per-ARNT-single minded
BMI	Body mass index
CHREBP	Carbohydrate-responsive element-binding protein
CPT-1	Carnitine palmitoyltransferase 1
DFO	Deferoxamine
DMEM	Dulbecco's modified eagle medium
DNL	De novo lipogenesis
ECM	Extracellular matrix
FACS	Fluorescent automated cell sorting
$FADH_2$	Flavin adenine dinucleotide
FBP	Fructose-1,6-bisphophate
FC	Floxed control
F16BPase	Fructose-1,6-Bisphosphatase
F6P	Fructose 6-phosphate
FIH	Factor inhibiting HIF
GK	Glucokinase
GAP	Glyceraldehyde 3-phosphate
G6P	Glucose-6-phosphate
G6Pase	Glucose-6-phosphotase
Glut	Glucose transporter
GTP	Guanosine triphosphate
GTT	Glucose tolerance test
HbA1c	Glycated haemoglobin
HDL	High-density lipoprotein
HFD	High fat diet

HGP	Hepatic glucose production
Hif-1α	Hypoxia inducible factor-1α
Hif-2α	Hypoxia inducible factor-2α
Hk	Hexokinase
HMG-CoA	3-hydroxy-3-methylglutaryl-coenzyme A
HSC	Hepatic stellate cell
Ir	Insulin receptor
Irs-1	Insulin receptor substrate-1
Irs-2	Insulin receptor substrate-2
ITT	Insulin tolerance test
KC	Kupffer cell
LDL	Low-density lipoprotein
MCP-1	Monocyte chemoattractant protein-1
MetS	Metabolic syndrome
NAD	Nicotinamide adenine dinucleotide
NADP	Nicotinamide adenine dinucleotide phosphate
NALFD	Non-alcoholic fatty liver disease
NASH	Non-alcoholic steatohepatitis
NEFA	Non-esterified fatty acid
FAS	Fatty acid synthase
FA	Fatty acid
PBS	Phosphate buffered solution
PEPCK	Phosphoenolpyruvate carboxykinase
PCT	Pyruvate challenge test
ROS	Reactive oxygen species
RPMI	Park Memorial Institute-1640 medium
R5P	Ribose 5-phosphate
SC	Subcutaneous
SCD-1	Stearoyl-CoA desaturase-1
Srebp-1c	Sterol regulatory element binding protein 1C
T1D	Type 1 diabetes
T2D	Type 2 diabetes
TCA	Tricarboxylic acid
TG	Triglyceride

TGF-β	Transforming growth factor beta-1
TNF-α	Tumour necrosis factor alpha
VEGF	Vascular endothelial growth factor
Vhl	von Hippel-Lindau
VLDL	Very-low-density lipoprotein
WAT	White adipose tissue

Abstract

Aryl hydrocarbon receptor nuclear translocator (ARNT) is a transcription factor which acts as a general partner for members of the bHLH/PAS family of transcription factors. Previous research has found that ARNT mRNA was decreased in the islets and in the livers of type 2 diabetes (T2D) patients. This hinted at a potentially global downregulation of this factor in the setting of T2D. To investigate the effect of long term loss of ARNT in hepatocyte and myeloid cells, 2 lines of mice with ARNT deletion in these cell types. In common with T2D, mice lacking hepatocyte ARNT had impaired glucose tolerance, increased gluconeogenesis, decreased ATP and increased post-prandial serm triglycerides. However, in contrast to T2D hepatic ARNT deletion actually resulted in decreased liver steatosis. Importantly, these changes became non-significant after high fat diet (HFD), although we did not find a significant reduction in total ARNT protein fed HFD.

Deletion of ARNT in myeloid cells led to decreased cytokine expression, decreased phagocytosis, decreased bactericidal activity, impaired response to infection, and impaired wound healing. Again, the phenotype of impaired wound healing between knockout and control animals equilibrated in a diabetic milieu. It was then found the full effects of the the iron chelator Desferasirox (DFO) on improving diabetic wound healing require myeloid cell ARNT. In addition mice lacking ARNT in myeloid cells displayed impaired glucose tolerance on HFD and paradoxically increased liver inflammation. In human monocytes it was found that ARNT mRNA correlated negatively with key serum cytokine levels including IL-6, IL-8, MCP-1 and TNF-α, although there was no significant difference in monocyte ARNT mRNA in T2D patients compared to controls. This data demonstrates that ARNT has important roles in hepatocyte and myeloid cell function and suggests that modulation of this transcription factor could be used in future therapy for diabetes and disorders of immune function.

Publications and presentations arising from this thesis

Ning Ding, Ruth T. Yu, Nanthakumar Subramaniam, Mathias Leblanc, Caroline Wilson, Renuka Rao, Mingxiao He, Sally Coulter, Christopher Scott, Mara Sherman, Sue L. Lau, Annette R. Atkins, Grant D. Barish, Jenny E. Gunton, Christopher Liddle, Michael Downes, Ronald M. Evans. *A Master Cistromic Circuit Governing Hepatic Fibrogenesis*. **Cell**. 2013, Accepted (in Press).

Girgis, CM., Cheng, K., Scott, CH., Gunton, JE., *Breathing badly: Novel links between HIFs, type 2 diabetes, and metabolic syndrome (review)*, **Trends in Endocrinology and Metabolism**, 2012, 23: 372-380.

Cheng, K., Ho, K., Stokes, R., Scott, C., Lau, SM., Hawthorne, WJ., O'Connell, PJ., Loudovaris, T., Kay,TW., Kulkarni, RN., Okada, T., Wang, XL., Yim, SH., Shah, Y., Grey, ST., Biankin, AV., Kench, JG., Laybutt, DR., Gonzalez, FJ., Kahn, CR, Gunton, JE., *Hypoxia-inducible factor-1α regulates β-cell function in mouse and human islets,* **Journal of Clinical Investigation**, 2010, 120(6): 2171-2183.

Papers in draft

Christopher Scott, James Bonner, Philip Boughton, Rebecca Stokes, Stacey Walters, Kendle Masolowski , Frederic Sierro , Stephen Twigg , Sue McLennon & Jenny E Gunton. *Loss of ARNT in myeloid cells results in Immune suppression and delayed wound healing.*

Christopher Scott, Jason Ngai, Natasha Deters, Jiang Changtao, Kim Cheng, Rebecca A. Stokes, Matthew Adams, Kenneth W. K. Ho, Jacob George, Frank J. Gonzalez, Jenny E. Gunton. *Hepatic Aryl hydrocarbon Receptor Nuclear Translocator Regulates Metabolism in Mice but is not required for DFS action.*

Christopher Scott, Jacob George, Frank J. Gonzalez, Jenny E. Gunton. *Hepatic specific deletion of Aryl hydrocarbon Receptor Nuclear Translocator Results in Decreased Fibrosis in the Thioacetamide Model of Liver Fibrosis.*

Poster presentations:

C. Scott, S. Walters, J. E. Gunton. *Loss of ARNT in macrophages and neutrophils delays skin transplant rejection and impairs wound healing*. St Vincents and Mater Health Sydney Research Symposium, Sydney (2008).

C. Scott, A. Clouston, J. George, J. E. Gunton. *ARNT in macrophages plays a role in whole body glucose metabolism*. Australian Diabetes Society Meeting, Adelaide (2009).

Christopher Scott , Kim Cheng , Matthew Adams, Rebecca Stokes, Kenneth Kheong Ho, Jacob George, Frank J. Gonzalez, Jenny E. Gunton. *Hepatocyte Aryl hydrocarbon Receptor Nuclear Translocator (Arnt) Regulates Metabolism in Mice and Arnt Is Decreased by High-Fat Diet*. Australian Diabetes Society Meeting, Perth (2011).

Contents

List of figures

List of Tables

Chapter 1. Introduction

1.1 The liver

The liver is the largest solid organ in the body and occupies the right upper quadrant of the abdomen. This organ is uniquely placed between blood returning from the digestive tract and the systemic circulation such that it is the first port of call for nutrient enriched blood after a meal (1). The liver has been labeled the most important metabolic organ in the body (2) and it functions to process dietary amino acids, carbohydrates, lipids, vitamins and micronutrients. The liver is also responsible for secretion of bile for fat absorption, the removal of microbes and toxins from the blood returning from the digestive tract, synthesis of a range of plasma proteins, and detoxification of endogenous wastes and pollutant xenobiotics.

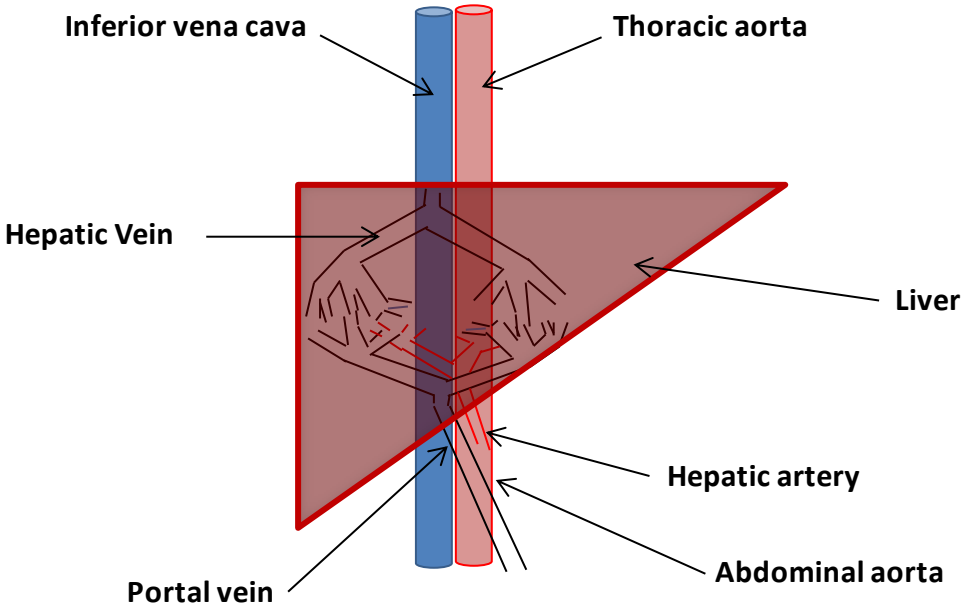

Figure 1.1 Blood supply to the liver.
Blood from the hepatic artery and nutrient rich portal vein enters the liver and mixing in the sinusoids before draining via the hepatic vein to the inferior vena cava.

These crucial functions of the liver are performed by a limited number of cell types. Within the liver cells are bathed in a mixture of arterial 30-40% and portal vein 60-70% blood (1) (Figure 1.1). Blood from the branches of the hepatic artery and portal vein flows from the periphery of the lobule into large expanded capillary spaces called sinusoids which run between rows of hepatocytes. As shown (Figure 1.2), the richly perfused hepatocytes line the outside of the sinusoids and make up 80% of the cell volume of the liver and it is these cells that perform the metabolic and detoxification processes (1). To allow the hepatocytes direct access to larger blood components endothelial cells lining the

sinusoids have a discontinuous fenestrated anatomy with no basement membrane. Hepatocytes also extend microvillus into the space of Disse, which lies between the endothelial cells and hepatocytes, to increase the surface area in contact with blood components. Between rows of hepatocytes are bile canaliculi where bile is secreted to aid in digestion along with conjugated non-aqueous waste products for elimination in the faeces. The remaining 20% of the liver mass is comprised of endothelial cells, hepatic stellate cells, Kupffer cells and lymphocytes (3). The Kupffer cells are the macrophage cell of the liver and line the sinusoids, engulfing and destroying old red blood cells and microbes (1). Hepatic stellate cells are found in the space of Disse. Given the important functions of the liver it is clear that dysfunction of this organ will have far reaching implications.

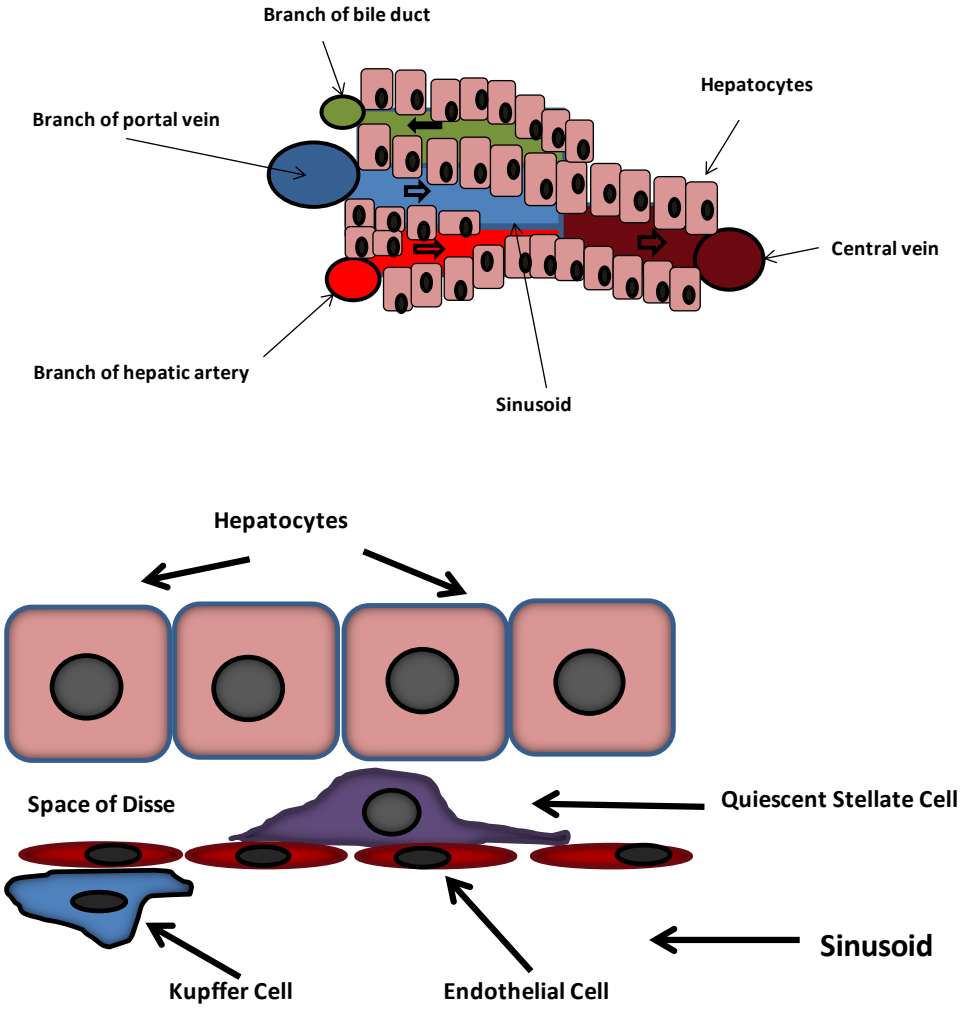

Figure 1.2 Microstructure of liver sinusoids and cell types.
A stylised cross section of a liver sinusoid is shown in the upper panel. Blood flows from portal vein and hepatic artery branches and flows between rows of hepatocytes. Blood drains from sinusoids into branches of the central vein. Bile is synthesized by hepatocytes and secreted into bile duct branches. The lower panel shows the major cell types and their relations within the liver sinusoids.

1.2 Normal liver metabolism

The liver is involved in key functions in metabolism, including maintenance of blood glucose levels through glucose uptake and storage, glycogen breakdown, and gluconeogenesis, and lipid homeostasis (1, 2). As such a discussion of normal liver function is warranted.

1.2.1 Liver glucose metabolism

In order to achieve its function as a glucose 'buffer' the liver expresses a specific glucose transporter (GLUT-2) (4). This transporter protein primarily occurs in the liver and pancreatic β cells and has a high capacity with low affinity. Essentially this transporter allows linear uptake of glucose in proportion to extracellular glucose concentration. In comparison, the GLUT-1 isoform is required to ensure basal uptake of glucose into cells to maintain respiration and is expressed only at low levels in the normal liver (4). Glycolysis is a universal cellular pathway whereby glucose is converted into 2 pyruvate, 2 ATP and 2 NADH molecules in the cell cytosol (Figure 1.3). Pyruvate can then be converted to Acetly-CoA and enter the tricarboxylic acid cycle (TCA), the products of which are used in oxidative phosphorylation to produce even greater amounts of ATP. Glycolysis consists of ten enzymatic reactions. The first step of the glycolytic pathway is the phosphorylation of glucose to glucose-6-phosphate (G6P) by hexokinase (HK) using ATP (Figure 1.3). Importantly to whole body metabolism the liver predominantly expresses an isoform of HK called glucokinase (GK). Interestingly again this isoform is also expressed in pancreatic β-cells. GK has different kinetics to the HK expressed in the majority of tissues (4). GK has a low binding affinity for glucose at low concentrations and increasing activity with increasing glucose concentration. This ensures that the liver does not compete with the other tissues when glucose levels are low but acts to efficiently take up extra glucose in times of glucose excess. GK is also not inhibited by physiological concentrations of G6P allowing the liver to take up extra glucose for storage as triglyceride (TG) or glycogen (4). In this way the liver has the ability to act as a "glucose buffer" for the plasma glucose concentration. In the liver the process of glucose uptake is thus regulated by circulating glucose. G6P is a key intermediate in the liver which can be used for synthesis of glycogen, new glucose, ribose-5-phosphate (R5P) and NADPH and acetyl-CoA (Figure 1.4).

The next two reactions catalysed by phosphoglucose isomerise (PGI) and then phosphofructokinase (PFK) converts G6P to fructose-6-phosphate (F6P) and then phosphorylates F6P in an irreversible

action to produce fructose-1, 6-bisphophate (FBP). PFK plays a key role in glycolysis as it is one of the rate determining reactions. The following reactions ultimately result in the formation of two pyruvate molecules ATP and NADH as mentioned previously.

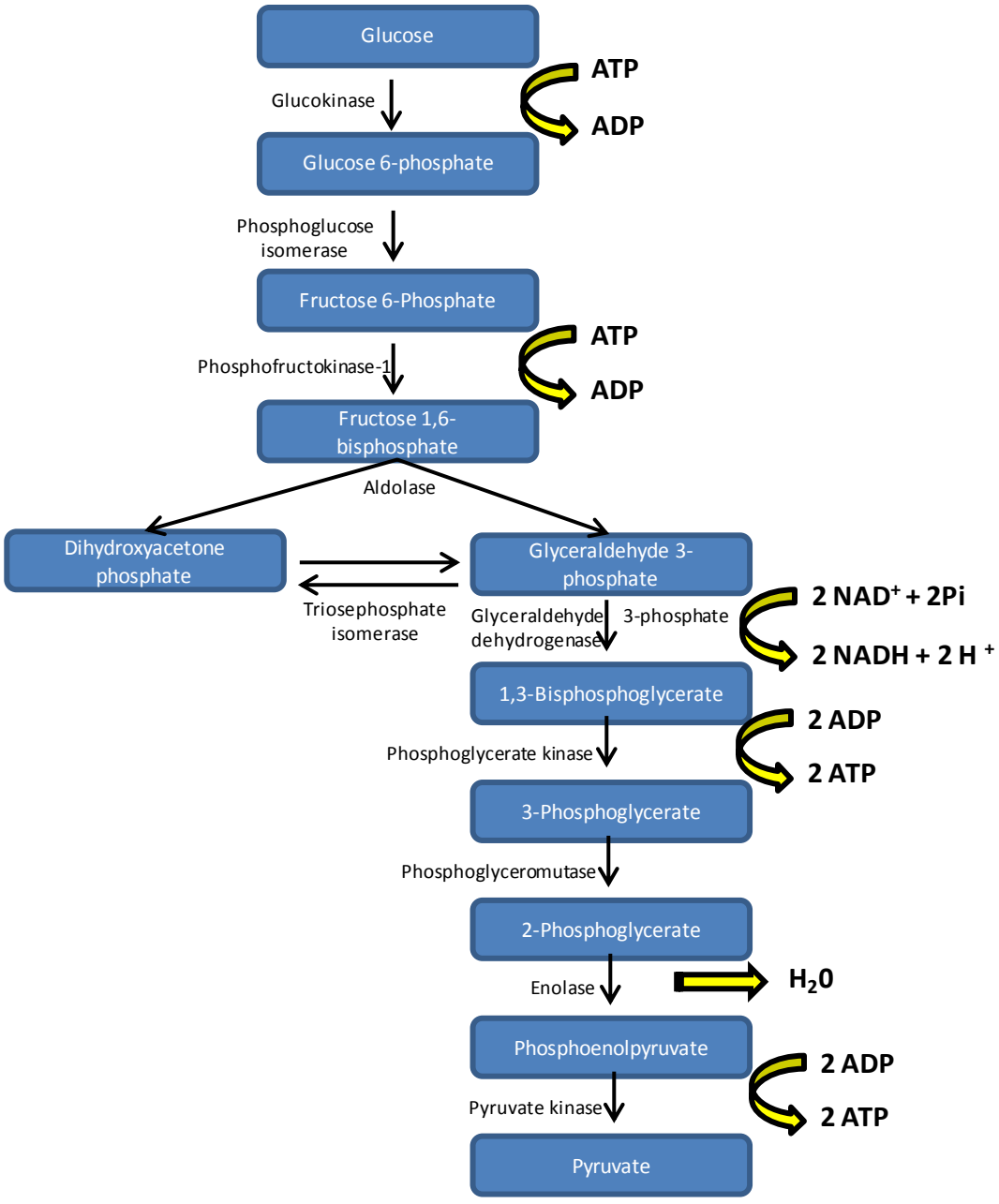

Figure 1.3 The glycolytic pathway.
The liver glycolytic pathway is shown with intermediates in blue boxes. The enzymes catalysing each step are also shown.

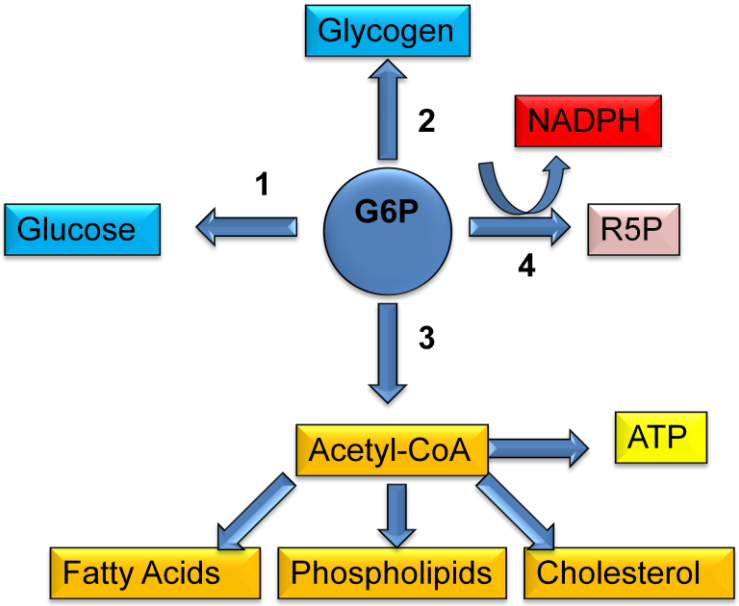

Figure 1.4 Alternate fates of G6P.
G6P can be converted to glucose (1) or to glycogen for storage (2). Acetyl coenzyme A (acetyl-CoA) derived from its degradation can be used for oxidative phosphorylation in the mitochondria. Acetyl-CoA also be used for lipid synthesis (3). Finally G6P can be diverted to the pentose phosphate pathway for NADPH and Ribulose-5-phosphate (R5P) for nucleotide synthesis (4).

1.2.1.1 Pentose phosphate pathway.

Many reactions, notably the reductive synthesis of fatty acids and cholesterol, require NADPH in addition to ATP. The two key products of the pentose phosphate pathway are Ribulose-5-phosphate (R5P) and NADPH. R5P is used in nucleotide biosynthesis. Excess R5P is converted into glycolytic intermediates fructose-6-phosphate (F6P) and glyceraldehyde-3-phosphate (GAP). Around 30% of glucose taken up by liver cells is shunted into the pentose phosphate pathway reflecting the high rates of synthesis of fatty acids and cholesterol (4). Entry of G6P into the pentose phosphate pathway is regulated positively by increasing NADP+ concentration which acts on glucose-6-phosphate dehydrogenase.

1.2.1.2 Anaerobic glycolysis

In situations where oxygen levels may be depleted and it is necessary for the glycolytic pathway to keep functioning to provide the cell with ATP, anaerobic glycolysis can occur. In this case, pyruvate is not shuttled off but instead recycled and converted to lactate and nicotinamide adenine dinucleotide (NAD^+) through the actions of lactate dehydrogenase (LDH) (4). The liver is able to take up lactate from the circulation and convert it back into glucose by the process of gluconeogenesis (see below).

1.2.1.3 Tricarboxylic acid (TCA) cycle

The molecules of pyruvate produced by glycolysis can also be converted to acetyl-CoA via the sequential actions of the pyruvate dehydrogenase enzyme. Acetyl-CoA can be used to generate energy by oxidative phosphorylation in the mitochondria or be converted into fatty acids. In order to generate energy acetyl-CoA must cycle through the TCA cycle producing 3 NADH, one FAD and one GTP molecule which can then donate their electrons to the oxidative phosphorylation chain in the mitochondria producing large amounts of ATP (12 per acetyl-CoA, or 38 per glucose) (Figure 1.5).

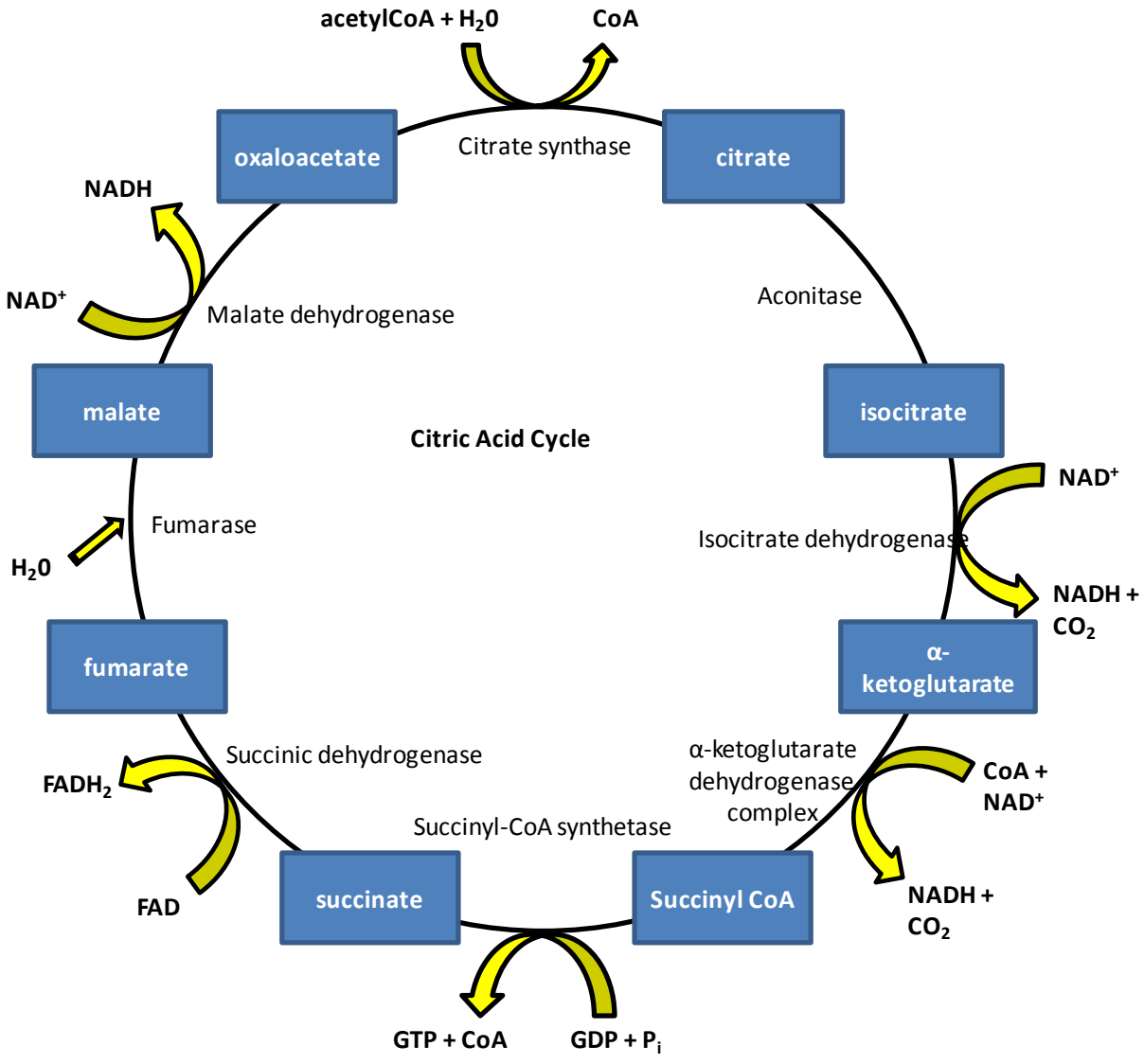

Figure 1.5 The Tricarboxylic Acid Cycle.
Intermediate molecules are shown in blue boxes. Enzymes catalyzing each step and key substrates and products are also shown.

1.2.1.4 **Gluconeogenesis**

When serum glucose is low, the liver responds by glycogenolysis (breakdown of glycogen) and gluconeogenesis (glucose synthesis) to provide glucose to the rest of the body (4-6). Gluconeogenesis provides a substantial fraction of the glucose produced in fasting humans, even within hours of feeding. The liver and to a lesser extent the kidney have the highest capacity for gluconeogenesis (4). Gluconeogensis enables these tissues to convert organic compounds such as glycolysis products (lactate and pyruvate), citric acid cycle intermediates and the carbon skeletons of many amino acids to derive glucose which is then released into the circulation. Thus the liver has an important role in maintaining blood glucose levels through glycogen breakdown and gluconeogenesis. Essentially the reactions in gluconeogenesis are the reverse for those of glycolysis except for the addition of four enzymes: pyruvate carboxylase, phosphoenolpyruvate carboxykinase (PEPCK), fructose 1,6-bisphosphatase (F16BP) and glucose-6-phosphatase to catalyse the non-reversible steps (Figure 1.6).

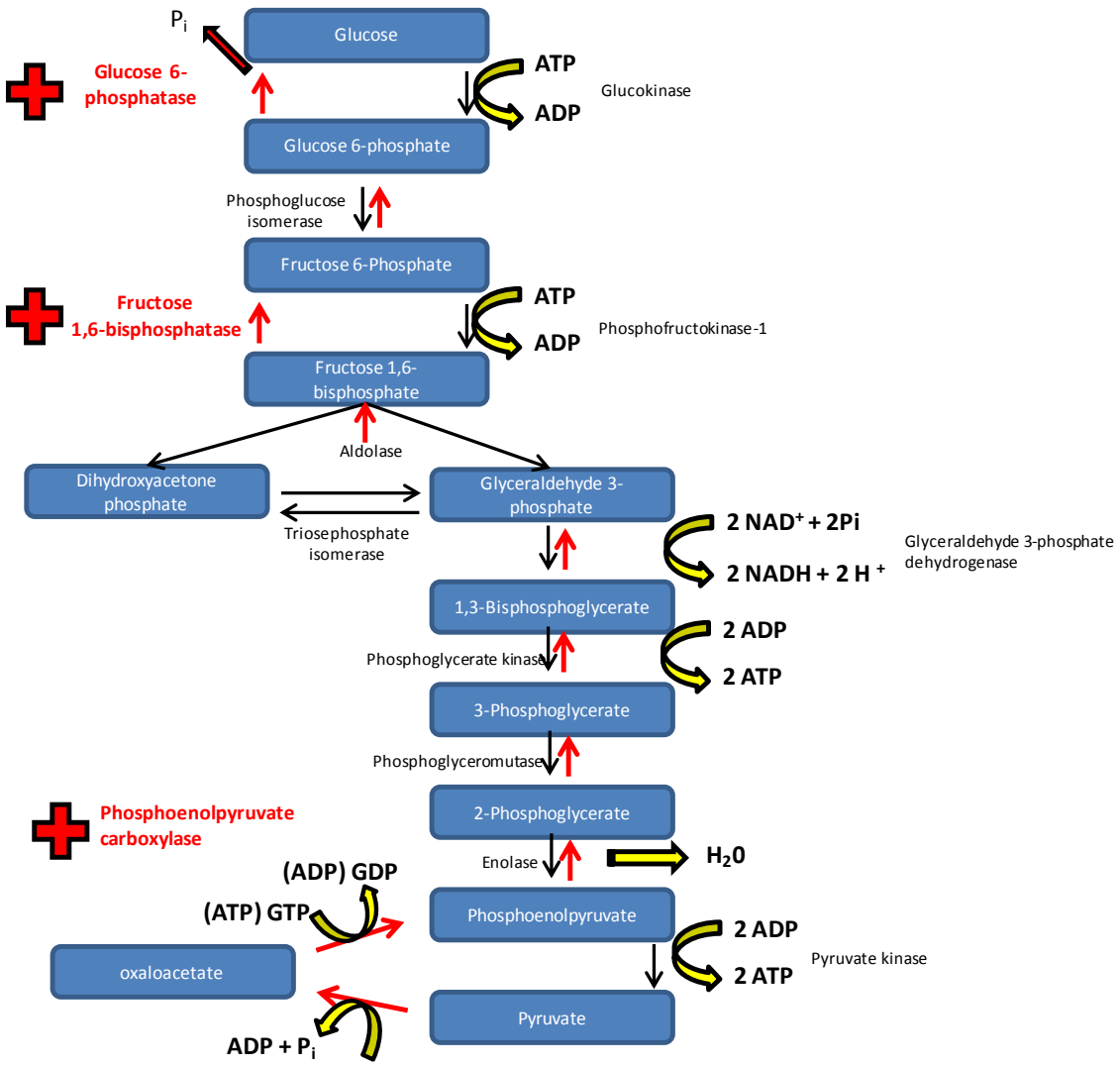

Figure 1.6 Gluconeogenesis.
This diagram shows gluconeogenesis (red arrows) and glycolysis (black arrows). Irreversible steps requiring the addition of purely gluconeogenic enzymes are highlighted in red text.

1.2.2 Liver fat metabolism.

Triglycerides (TG) constitute 90% of the dietary lipid and are the major medium for energy storage in humans (4). After eating, dietary TG are delivered to the liver and other tissues from the intestine in the form of chylomicrons (via the lymphatic and portal systems) (1, 4). Chylomicrons are large lipoprotein particles that transport dietary lipids from the intestines to other locations in the body like adipose tissue. Additionally the secretion of insulin that occurs after eating stimulates hepatic TG synthesis from available free fatty acids (FFA) and glycerol (7). FFA can either be from plasma non-esterified fatty acid (NEFA) or from de novo lipogenesis in the liver (DNL). The NEFA pool is derived from FFA released from adipocytes which are transported in the blood bound to albumin. Excessive TG is stored as lipid droplets within the liver and it is the expansion of these hepatocyte lipid stores that is a hallmark of non-alcoholic fatty liver disease (NAFLD)(8). Endogenous TG from the liver is

secreted into the blood in the form of very low density lipoprotein (VLDL). These VLDL particles can then be absorbed by adipose tissue as TGs or metabolised and used as an energy source in tissues throughout the body (1, 4).

The metabolic process of DNL in the liver appears to be tightly regulated, and in the state of energy excess surplus glucose is used as a FA substrate (8). Citrate formed from the TCA cycle is shuttled into the cytosol via the tricarboxylate transport system where FA synthesis takes place. Citrate is converted to acetyl-CoA by ATP citrate lysate. Acetyl-CoA is then converted to malonyl-CoA by Acetyl-CoA carboxylase 1 (ACC1) and it is this molecule that is used by fatty acid synthase (FAS) to add 2 additional carbon groups to the fatty acid with each additional cycle of FAS (Figure 1.7)(4).

In comparison the hepatic uptake of FA from the NEFA pool is not regulated and as a result serum FFA influx into the liver is directly related to serum FFA concentration (8). TG are synthesised from fatty acyl-CoA esters using glycerol-3-phosphate or dihydroxyacetone phosphate from glycolysis of glucose as the backbone. This TG synthesis can occur in the mitochondria and the endoplasmic reticulum in the case of glycerol-3-phosphate or in the endoplasmic reticulum and peroxisomes in the case of dihydroxyacetone phosphate (4).

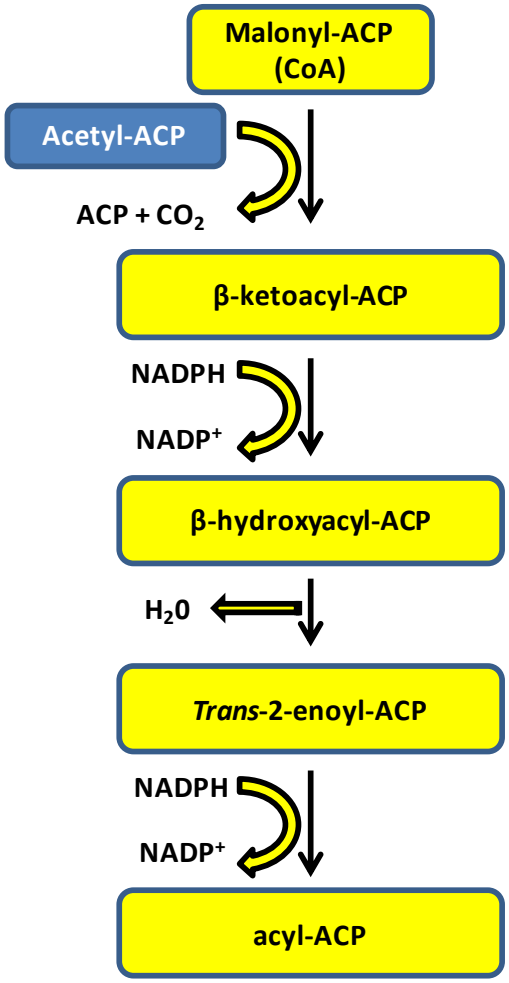

Figure 1.7 Fatty acid synthesis.
The synthesis of fatty acids involves a number of reactions catalysed by the multi-enzyme Fatty Acid Synthase complex. These reactions result in the addition of 2 carbon atoms per cycle and consume 2 x NADPH. Initially Malonyl-CoA serves as the backbone for FA synthesis. Acyl Carrier Protein = ACP.

Two key transcriptional regulators of lipid metabolism are sterol regulatory element-binding protein (SREBP1-c) and carbohydrate response element-binding protein (ChREBP)(9). Insulin regulates SREBP1-c activation through the downstream effectors of phosphoinositide 3-kinase (PI3K), atypical protein kinase C (aPKC) and protein kinase B (PKB/Akt) (10). It has been postulated that lipid synthesis in the liver is primarily controlled by the activation of aPKC. However, the mechanisms involved in selective insulin resistance to insulin effects upon gluconeogenesis on a background of increased DNL are still lacking a satisfactory explanation. Mice lacking aPKC have both reduced expression of SREBP1-c and decreased TAG content (10). SREBP1-c transcriptionally activates most genes involved in DNL including ACC, FAS SCD-1 and long-chain elongase (ELOVL6) and it also activates ACC-2 to produce more malonyl-CoA at the mitochondrial membrane (11). An increase in malonyl-CoA inhibits CPT-1 mediated transport of fatty acyl-CoA in to the mitochondria and therefore decreases oxidation of FA (4). SREBP1-c is also regulated by liver X-activated receptors

(LXRs). Insulin signalling results in LXR activation and transcriptional activation of SREBP-1c. LXRs also directly regulate the expression of lipogenesis genes FAS, SCD1 and ACC (9). LXRs play a key role in the sensing of intracellular sterol levels and regulate the expression of genes that control absorption, storage and transport of cholesterol (12).

Excess carbohydrate is mainly converted to TG in the liver both through the effects of insulin and hyperglycaemia itself (9, 13). High glucose levels can directly stimulate lipogenesis by activating carbohydrate response element binding protein (ChREBP) (13). Importantly ChREBP induces expression of liver-type pyruvate kinase (L-PK) which catalyses the production of increased pyruvate and hence citrate generation and lipognesis (14). ChREBP also induces genes involved in NADPH production (glucose-6-phosphate dehydrogenase, transketolase, malic enzyme etc.) and gluconeogenesis (G6Pase) (14). ChREBP also increases transcription of genes directly involved in lipogenesis including ACC and FAS (14). ChREBP inactivation is thought to be regulated by glucagon, epinephrine and direct AMP effects. Increased glucagon and epinephrine occurring in the fasting state increase cAMP and activate cAMP activated protein kinase (PKA) (15). PKA then phosphorylates ChREBP and inactivates it. Increased AMP accumulation in states of low glucose inhibits ChREBP through activation of AMP-activated protein kinase (AMPK) and phosphorylation of ChREBP (15). Glucose activates ChREBP through the hexose monophosphate shunt (HMP) via activation of protein phosphatase 2A delta (PP2Adelta) and subsequent dephosphorylation of ChREBP(15). It appears that ChREBP can respond to glucose in another way as mutants lacking the PKA phosphorylation sites are still responsive to glucose. In addition the levels of ChREBP RNA are regulated and increased in fed states. LXR also regulated transcription of ChREBP (15).

1.2.2.1 **FA and TG oxidation.**

Oxidation of FA occurs in the mitochondria, peroxisomes and microsomes (4). The majority of fatty acid oxidation occurs in the mitochondria. The peroxisomes and microsomes oxidise and shorten long chain and very long chain fatty acids and then the process is completed in the mitochondria (16).

Peroxisomal β oxidation shortens fatty acids > 22 carbon atoms in length. These very long chain fatty acids (VLCFAs) simply diffuse into peroxisomes and are activated by a long chain acyl-CoA synthetase (16). It is noteworthy that peroxisomal oxidation results in the production of H_2O_2 which then needs to be converted back to H_20 and O_2 by catalyse. Peroxisomal oxidation also yields 2 fewer ATP per

cycle compared to mitochondrial beta oxidation (4, 16). Peroxisomal oxidation proceeds until FA acyl-CoA are 8 carbon atoms in length, and then these shortened FA acyl-CoA molecules are converted to their carnitine esters by carnitine acyltransferases. These carnitine esters can then diffuse out of the peroxisome and be transported into the mitochondria and undergo complete oxidation (4).

The rate-limiting step of mitochondrial fatty acid oxidation is entry of FA into the mitochondria (4). To gain entry into the mitochondria FA must first be converted to fatty acyl-CoA by the actions of fatty acyl-CoA synthase in the cytosol then transported into the mitochondria by carnitine acyltransferase I (CPT-1). This process involves the transfer of the acyl group to carnitine, transport of this carnitine ester into the mitochondria and transfer of the acyl group back to CoA in the mitochondrial pool (4). The Degradation of fatty acyl-CoA oxidation in the mitochondria occurs in four reactions (Figure 1.8).

The first step catalysed by acyl-CoA dehydrogenase and results in the formation of 1 $FADH_2$ then results in the immediate formation of 2 ATP through the electron transport chain in the mitochondria. Like the formation of fatty acids the four step reaction ultimately results in the formation of 1 FADH + 1 NADH + 1 Acetyl-CoA and 1 fatty acyl-CoA which is 2 carbon atoms shorter in length (Figure 1.8). Acetyl-CoA can then be oxidised via the TCA cycle and generates further ATP. Importantly, in the liver mitochondria a significant fraction of acetyl-CoA is converted to acetoacetate or D-β-hydroxybutyrate (ketone bodies). These molecules can be used as an alternate energy source in peripheral tissues particularly the heart and skeletal muscle (4). During this process 3-hydroxy-3-methyl-glutaryl-CoA (HMG-CoA) is formed by HMG-CoA synthase, and this product is also a precursor to cholesterol biosynthesis.

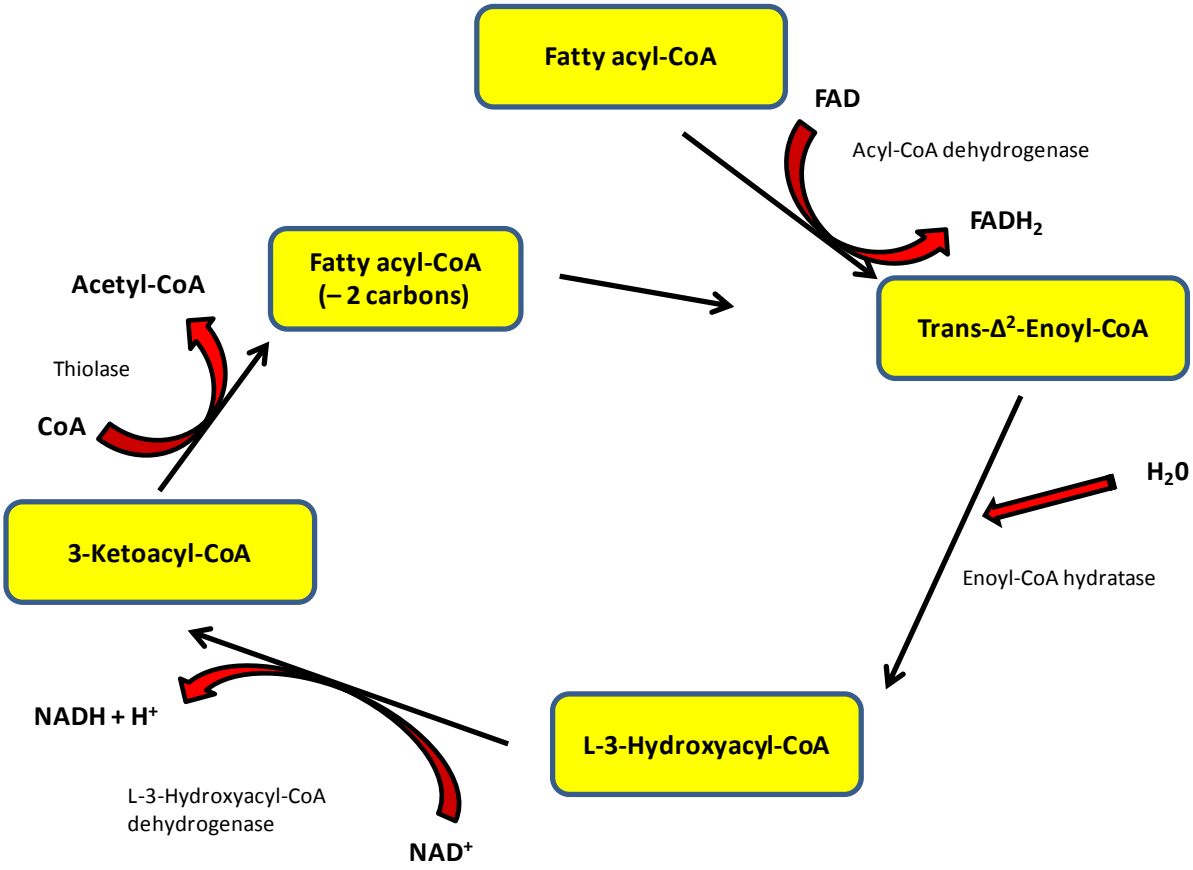

Figure 1.8 Fatty Acid oxidation.
This diagram shows the cycle and products of the oxidation of 2 carbons from a fatty acyl CoA. Intermediate molecules are shown in yellow boxes. Enzymes required to catalyse each reaction are also shown.

1.2.2.2 Cholesterol biosynthesis.

Cholesterol is a vital constituent of all cell membranes and is also used in the production of steroids and bile acids (1, 4). Cholesterol also plays a role in the pathogenesis of atherosclerosis leading to cardiovascular disease and stroke (17). In healthy organisms there is a fine balance between biosynthesis, utilisation and transport such that the harmful effects of cholesterol are kept to a minimum. Dietary cholesterol is transported to cells from the intestines by way of chylomicrons and cholesterol biosynthesis can also occur within cells. Within the body cholesterol circulates between the liver and peripheral tissues via LDL (from liver to periphery) and HDL (from periphery to liver) (4). Excess cholesterol can be disposed of as bile acids. Accumulation of cholesterol in arteries leads to atherogenesis and is promoted by increased LDL levels (17). Conversely elevated HDL has been linked with protection from cardiovascular disease.

It has been shown that cholesterol is synthesised from molecules of acetate (4). To be used in cholesterol synthesis acetate must first be converted to isoprene units. Once condensed to form a linear molecule the carbons cyclise to form the four-ring structure of cholesterol. Acetyl-CoA is converted to isoprene units by a series of steps that begin with formation of HMG-CoA. HMG-CoA synthesis requires thiolase and HMG-CoA synthase. Isoforms of these two enzymes are located in the mitochondrion and are also responsible for the formation of HMG-CoA for ketone synthesis. The cytosolic isozymes of these two enzymes are responsible for the formation of HMG-CoA that is used in cholesterol synthesis. A number of reactions are required to convert HMG-CoA molecules into cyclic cholesterol molecules (4). Cholesterol synthesised in the liver can be used by hepatocytes in cell membrane formation, hormone synthesis, bile production or exported to the rest of the body (4). If cholesterol is to be exported it is esterified by acyl-CoA: cholesterol acyltransferase (ACAT) to form esters. These hydrophobic compounds are transported throughout the body in lipoprotein packages as a component of VLDL. These particles mature into LDL as triglycerides and apolipoproteins are removed. LDL particles are taken up in cells by receptor mediated endocytosis via LDL receptors. Once inside the cell cholesterol esters are hydrolysed into cholesterol which can be incorporated into cell membranes or re-esterified by ACAT and stored as cholesterol ester droplets (4).

Cholesterol levels are regulated by controlling HMG-CoA reductase activity, LDL receptor synthesis and the rate of esterification of cholesterol by ACAT (4). HMG-CoA reductase is the rate-limiting enzyme in cholesterol biosynthesis and is subject to rapid regulation by phosphorylation by an AMP-dependent kinase in response to decreased cellular ATP. Phosphorylated HMG-CoA is less active than the non phosphorylated form (4). Expression of HMG-CoA reductase is also regulated at the mRNA level and degradation can also be inhibited. SREBP-2 is a transcription factor thought to be key regulator of cholesterol biosynthesis in the liver (18). SREBP-2 responsive genes include HMG-CoA synthase, HMG-CoA reductase, farnesyl diphosphate synthase and squalene synthase. SREBP-2 is regulated through cholesterol sensing by the SREB processing protein SREBP cleavage activating protein (SCAP) (18). When cholesterol levels are low SCAP delivers SREBP-2 from the ER to the golgi where it is activated through proteolytic cleavage.

Removal of LDL from the circulation is controlled by the expression of LDL receptors. The expression of these receptors is thus another mechanism for reducing circulating cholesterol levels. High intracellular concentrations of cholesterol suppresses the expression of the LDL protein (4).

1.3 Non-alcoholic fatty liver disease (NAFLD) and non-alcoholic steatohepatitis (NASH).

Non-alcoholic fatty liver disease is the accumulation of macroscopically visible lipid in hepatocytes in the absence of excess alcohol consumption (<20g of ethanol/day) (19) . Histologically NALFD has been defined by the accumulation of fat in more than 5% of hepatocytes (9). It is often a patchy process with some areas having the majority of cells affected and relative sparing in others. The spectrum of NAFLD includes a range of pathological features from mild steatosis to non-alcoholic steatohepatitis (NASH) and cirrhosis with increasing levels of liver dysfunction (Figure 1.9) (20).

The diagnosis of NASH and grading of NAFLD and NASH varies between pathologists and numerous criteria have been proposed. Matteoni et al (table 1.1) proposed a staging system linking histological features to progression to cirrhosis and liver related death (21). In this system staging included a score of (1) fatty liver alone; (2) fat accumulation and lobular inflammation; (3) fat accumulation and ballooning degeneration; and (4) fat accumulation, ballooning degeneration, and either Mallory hyaline or fibrosis.

It is noteworthy that more recently a NAFLD activity score was proposed by Kleiner et al (2005) based on the histological features identified by multiple pathologists which were independently associated with the diagnosis of active NASH. The scoring system in this study suggested a staging system where the score is defined as the cumulative scores for steatosis (0-3), lobular inflammation (0-3), and ballooning (0-2) (22). Fibrosis activity (Table 1.1) was included as a separate score as the diagnosis of active NASH does not correlate well with fibrosis progression (23).

Table 1.1 Criteria for histological grades.

	1	2	3	4
NAFLD grade	fatty liver alone >5%	fat accumulation and lobular inflammation	fat accumulation and ballooning degeneration	Fat accumulation, ballooning degeneration, and either Mallory hyaline or fibrosis.
Fibrosis grade	Perisinusoidal or periportal = 1 Mild, zone 3, perisinusoidal=1A Moderate, zone 3, perisinusoidal=1B Portal/periportal =1C	Perisinusoidal and portal/periportal	Bridging fibrosis	Cirrhosis

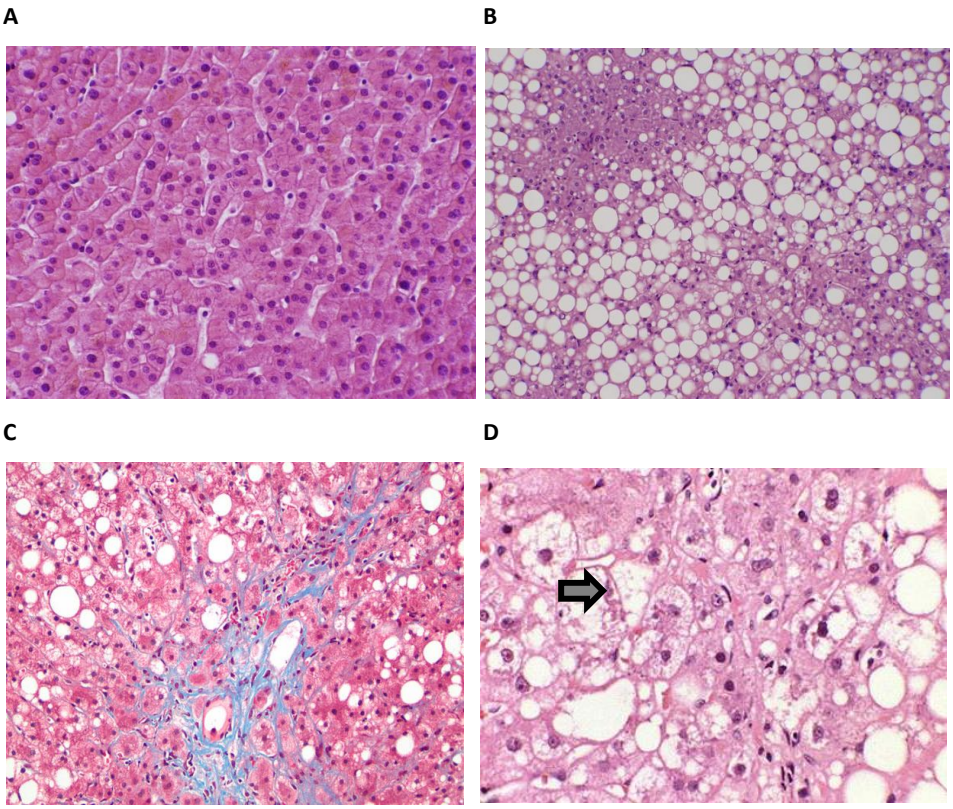

Figure 1.9 Histological staging of NALFD.
(A) Normal liver. (B) Liver with steatosis. (C) Masson trichrome stain of NASH with fibrosis in grey (from http://emedicine.medscape.com/article/2038493-overview). (D) Mallory body within ballooning hepatocyte - grey arrow (from http://www.medscape.com).

Available evidence suggests that NAFLD is the cause of around 80% of elevated liver enzyme levels in America (24). Conversely, it has also been estimated that 79% of those with NAFLD do not have

raised serum alanine transferase levels (25). Using magnetic resonance spectroscopy (MRS) it was found that NAFLD was present in up to 34% of the general population in the USA (25). NAFLD/NASH are also noted to have a high prevalence in South America, much of the Asia Pacific region (including Australia), the Middle East and Europe (26).

Most NAFLD patients have increased liver fat content alone but some (10%-30%) go on to develop NASH (26, 27). NASH involves hepatocyte steatosis with addition of signs of inflammation characterised by lobular inflammation, hepatocyte ballooning (Figure 1.9) and fibrosis (21). NASH can in turn lead to increasing liver fibrosis and cirrhosis, liver failure and hepatic carcinoma (HCC) (28, 29). Rates of cirrhosis development have been estimated to be between 5 – 20% over 10 years of follow up (26). Cirrhosis carries with it the risk of complications including ascites, renal failure, variceal bleeding, hepatic encephalopathy and HCC (30). In one study of 420 NAFLD patients the rate of liver-related mortality at 7 years was 1.7% and accounted for 13% of all deaths compared to <1% in the general population (30). Current treatment of end-stage liver disease requires liver transplant. It is predicted that NAFLD will soon become the leading cause of chronic liver disease and reason for liver transplants (8). Important risk factors for NAFLD are obesity, diabetes and the metabolic syndrome (MetS) (27). As might be expected as alcohol consumption can also lead to steatosis, cross-sectional studies also support a role for heavier alcohol consumption (>60g/day) and increased steatosis and injury in obese individuals (31). As the prevalence of these metabolic risk factors are increasing the prevalence of liver chronic disease related to NASH/fibrosis can be expected to rise with it. It is clear that genetics also play a role as evidenced by the different prevalence of NAFLD in different ethnic groups of similar socioeconomic status. The frequency of NAFLD was found to be 45% in Hispanics, 33% in Whites and 24% in Blacks. Correspondingly there was increased insulin resistance and obesity in Hispanics but there was no association of the lower rates of steatosis in blacks with these factors, suggesting a strong independent genetic component. The rates of NAFLD were also found to be higher in males 42% than females 24% (25). Important risk factors for progression of NASH fibrosis include obesity, type 2 diabetes (T2D) and initial fibrosis severity (26).

1.3.2 **Obesity**

Obesity is defined by the World Health Organisation as excess weight for a given height (32). Functionally this is calculated as body mass index (BMI). Obesity as defined as BMI ≥over 30 (WHO) and has become a global epidemic as a result of sedentary lifestyles and the availability of processed high calorie foods and soft drinks in industrialised countries. Currently, around 35% of American adults are overweight (BMI 25-29.9) and 30% are obese (32). In 2005 in Australia 36% of the

population were overweight and 18% obese and this percentage is constantly increasing (33). Further, it is estimated that the cost of obesity and its associated illnesses in Australia in 2005 was 21billion. This high cost to society is primarily due to the association of obesity with metabolic derangements and the resultant pathologies. One such association is that of obesity and the development of insulin resistance**.** In fact the vast majority of obese individuals are insulin resistant (34) and insulin resistance is a key component of NAFLD, Metabolic syndrome (MetS) and T2D (35).

There is a clear association of obesity and NALFD with a prevalence of 3-24 % of non-obese patients compared with 76% in obese patients and 90% in morbidly obese (BMI=35+ (26, 36, 37). Obesity is also a risk factor for NASH, particularly central obesity (26). Obesity clearly contributes to NAFLD and NASH through oversupply of lipids but also contributes to disease through its role in inflammation as discussed later. Importantly visceral fat in particular has been found to correlate with the extent of hepatic inflammation and fibrosis, potentially through increased IL-6 levels (38).

1.3.3 **The metabolic syndrome**

In recent years there has been a dramatic increase the prevalence of the controversial MetS, which parallels the increase in obesity (35). MetS is a clustering of features intrinsically linked to obesity and insulin resistance. Table 1.2 shows the definitions of the metabolic syndrome WHO, American Diabetes Association, The National Cholesterol Education Program's Adult Treatment Panel III guidelines (NCEP:ATPIII) and International diabetes federation (IDF). NAFLD has been named the liver component of the metabolic syndrome (MetS). It was found that over 90% of NALFD patients have at least one feature of the metabolic syndrome (27) and 1/3 have the complete syndrome (by the National Cholesterol Education Program's Adult Treatment Panel III guidelines) (39). Interestingly, the combination of the full gamut of MetS and NAFLD confers an increased likelihood of development of NASH at an odds ratio of 3.2, and liver fibrosis at 3.5 (27). Definitions of the metabolic syndrome vary between organisations, however they have been sought as it was recognised early on that that patients with features such as obesity, central obesity, high serum triglycerides, low HDL (good cholesterol), high blood pressure and high blood glucose had an increased risk of cardiovascular events and T2D (1). In fact is has been estimated that such patients have approximately twice the risk of cardiovascular events and five times the risk of development of T2D. Using this definition the prevalence of MetS has been estimated to be 22%, increasing to 45% of those over the age of 50 (27, 35). The prevalence of NAFLD in the US is remarkably similar at 22% (26) and again increases with age (40).

1.3.4 **Diabetes mellitus**

Approximately 75% of T2D patients have NAFLD (26). And the presence of diabetes has been identified as a risk factor for NASH with a 2.6 fold increase in hyperglycaemic patients (41). It is also clear that alterations in liver function play a role in the pathogenesis of T2D (1). A key feature of T2D is hyperglycaemia and this is generally caused by a combination of peripheral resistance to insulin action and inadequate insulin secretion by β-cells (42). However B-cell dysfunction can lead to T2D in the absence of peripheral resistance but B-cell dysfunction or a failure of β-cell compensation must occur to get T2D from peripheral insulin resistance (42). The incidence of T2D has increased rapidly in parallel with increasing levels of obesity and the MetS. In 2007-8 721, 000 people were reported as having type 2 diabetes in Australia (43). The complications of this disease are severe and include damage to kidneys, eyes, and blood vessels. It also contributed to 14, 3000 deaths in Australia in 2009 as either a direct cause or associated cause (43). Cardiovascular events such as heart attacks,and cerebrovascular incidents are the most common cause of death in long standing diabetic patients. These events result from the increased rates of atherosclerosis in these patients, estimated to be 3- 7.5 times greater incidence than the general population (42).

Table 1.2. Diagnostic criteria for the metabolic syndrome.

WHO	**NCEP:ATPIII**	**IDF**
T2D, Insulin resistance, or impaired glucose tolerance (IGT) and 2 of;	Three or more of;	3 or more of;
Waist-to-hip ratio >0.90 in men or >0.80 in women	WC> 40 inches for men, >35 for women.	Waist circumference >102 cm (40.2 in) in men and >88 cm (35.6 in) in women
Serum triglycerides ≥150 mg/dl or HDL cholesterol <35 mg/dl in men and <39 mg/dl in women	Triglycerides ≥ 150 mg/dl	Serum triglycerides ≥150 mg/dl
Blood pressure ≥140/90 mmHg	HDL-C:<40mg/dl for men, <50mg/dl for women	Blood pressure ≥130/85 mmHg
Urinary albumin excretion rate >20 mg/min or albumin-to-creatine ratio≥30 mg/g.	BP ≥ 130/85 mm Hg	HDL cholesterol <40 mg/dl in men and <50 mg/dl in women
	Fasting plasma glucose ≥ 110mg/dl	Serum glucose ≥110 mg/dl (≥100 mg/dl may be applicable)

1.4 Pathogenesis of NAFLD

The exact pathogenic mechanisms of NAFLD and NASH remain elusive. The available studies suggest that environmental factors such as diet, exercise and/or toxins play a role (9, 44, 45). In particular fructose consumption has been found to be a risk factor for NAFLD (46). As mentioned a genetic component is suggested by studies indicating the prevalence of NAFLD varies in different ethnic groups and that disease progression varies between individuals with similar risk factors (18, 25, 26). On a more basic level, in order to get deposition of triglyceride (TG) in the liver there needs to be an imbalance in fat deposition and metabolism, especially of free fatty acids (FFA).

1.4.1 Insulin resistance in NAFLD

Insulin resistance is an almost universal finding in NAFLD and NASH. Importantly, it has been shown that the elevated insulin levels in states of hepatic steatosis fail to suppress adipose fatty acid flux to the liver (7, 47). As expected liver insulin resistance as occurs in NAFLD and T2D results in uninhibited hepatic glucose production (48). Unexpectedly this failure of insulin to suppress hepatic glucose production occurs on a background of increased hepatic lipogenesis and steatosis (49). The mechanism(s) for this disconnect are unclear. In the setting of complete insulin resistance in hepatocytes, that is in mice with liver specific knockout of the insulin receptor (LIRKO), there was increased inappropriate gluconeogenesis and decreased lipogenesis, suggesting either that insulin resistance seen in metabolic disease must occur downstream of the insulin receptor or that complete insulin-resistance results in other compensatory changes (48). The idea that a disconnection of insulin effects could exist was confirmed in studies of patients with mutations disrupting either insulin receptor or AKT2 function (50). Disruption of insulin receptor function exhibited low serum TG and low liver fat content whereas those with AKT2 had elevated liver fat, and hypertriglyceridemia (50). Studies using short hairpin RNAs (shRNAs) directed against IRS-1 and IRS-2 in the liver suggested that IRS-1 and IRS-2 may play complementary roles in liver metabolism. Results suggested that IRS-1 mediated insulin suppression of hepatic glucose production, while IRS-2 was involved in suppression of lipogenesis (51). However, it has also been reported that in ob/ob mice there was a reduction in IRS-2 mRNA alongside increased SREBP-1c mRNA (52). It has been proposed that the 'SREPB1-c' mediated arm of the insulin signalling pathway remains insulin sensitive while the PI3k/Akt arm mediating the gluconeogenic effects becomes resistant to insulin mediated suppression.

The mechanisms of fat accumulation in the liver are thus two-fold. There is both increased delivery of FA to the liver via insulin resistant adipocytes and increased lipogenesis within the liver itself (47).

The contributions of liver fat from these 2 sources were quantified by Donnelly et al (2005). It was found that the plasma NEFA pool accounted for 60% of liver TG suggesting that peripheral insulin resistance and increased FA flux to the liver plays a major role (7). Importantly the uptake of fatty acids into the liver is not regulated and as a result plasma FA levels have a direct impact upon liver steatosis. In addition de novo lipogenesis (DNL) in the liver is also dysregulated in hyperinsulinaemic subjects with NAFLD. In hyperinsulinaemic NAFLD patients DNL accounted for 26% of liver TG (7). Measurement of VLDL-TG is reported to parallel DNL. In healthy human subjects DNL has been reported to contribute as little as 5% (VLDL-TG) in the fasted state and is elevated to 23% (VLDL-TG) after feeding (53). In NAFLD patients this DNL was elevated at fasting and did not undergo further elevation in the fed state (53). Interestingly the export of fatty acids in the form of VLDL is also altered in NAFLD patients. It has been found that apoprotein B-100 which is required for VLDL synthesis is decreased in patients with NAFLD compared to healthy controls and may also contribute to steatosis in these patients (54). It is worth noting that there is a compensatory increase in B-oxidation of fatty acids in both animal (55, 56) and patients with NASH (57-59). Clearly this upregulation is unable to reduce hepatic steatosis sufficiently and may actually contribute to the damage caused by fatty acid accumulation in the liver (60). Hepatic triglyceride content is also an indicator for whole body insulin action. A recent study suggests that hepatic triglyceride content is in fact a better predictor for insulin action in liver, skeletal muscle and adipose tissue insulin action than visceral fat (61).

1.4.2 **Animal studies.**

In line with the mechanisms of fat accumulation in the liver it is clear from the literature that diets rich in fat or sugar can lead to fatty liver and obesity in humans and animal models (9, 62-64). Interestingly it is also reported that there may be increased delivery of LPS from the gut to the liver in obesity, which could contribute to progression to NASH (see below) and increased steatosis through inflammation leading to insulin resistance (65-67). The Ob/Ob and Db/Db mouse models contain a spontaneous mutation in the leptin gene and receptor respectively rendering these mice hyperphagic, inactive, obese and diabetic. These mice exhibit marked hepatic steatosis showing that increased dietary intake is sufficient to induce steatosis. However, these mice do not progress to NASH unless a secondary insult is provided (see below for a discussion of NASH) (68).

There have been a number of knockout mice generated which give more clues to the potential aetiology of NAFLD. The importance of SREBP-1c and ChREBP has been confirmed in this manner. As

might be expected deletion of these key transcription factors resulted in a reduction in lipogenic genes (14, 69). Ob/Ob mice have a mutation in the the leptin gene rendering them leptin deficient, these mice exhibit hyperphagia, obese and diabetic (70, 71). It has been found that Ob/Ob mice x SREBP1 -/- mice had decreased hepatic steatosis (69). To add to the involvement of SREBP-1c hepatic specific over expression also produces steatosis, however again steatohepatitis was not evident although ALT levels were raised (72). SREBP1-c and SREBP-2 expression are also induced by HFD feeding of C57BL/6 mice (73).

In addition there are examples of mice with defects in fatty acid oxidation which develop steatosis. The peroxisome-proliferator-activated receptor (PPAR) family includes PPAR-α, PPAR-δ and PPAR-γ, the PPARs have different tissue distributions with distinct and overlapping functions (74, 75). In general this family is involved in regulation of genes involved in fatty acid metabolism (76). PPAR-α is most highly expressed in tissues such as the liver, heart, and brown fat. PPAR-αis activated by ligands including fatty acids and fenofibrate (74). PPAR-α activation results in upregulation of genes involved in fatty acid transport and genes involved in β-oxidation in mitochondria and peroxisomes (77). PPAR-α in particular has been shown to play a crucial role in liver lipid metabolism (78, 79). The PPAR-α knockout mouse line does not accumulate fat under normal fed conditions but fail to up-regulate fatty acid oxidation when delivery to the liver increases during fasting and develop severe steatosis, without additional signs of NASH (78). Another example is the mitochondrial trifunctional protein (MTP) heterozygote mouse. MTP is reported to regulate β-oxidation in the mitochondria. Heterozygote mice exhibit hepatic steatosis, raised ALT and lower antioxidant levels consistent with oxidative stress, in the absence of NASH (80).

1.5 NASH Pathogenesis

As suggested by the above models, many factors are known to induce NAFLD, but less is known about the factors leading to progression to NASH. The two-hit hypothesis has been proposed to describe the mechanism of progression from simple NAFLD to NASH (81, 82). In this model it is believed that FA deposition in the liver is a "first hit" which sensitises hepatocytes to future insults. It is thought that NASH develops as a result of the liver's inability to deal with cumulative secondary insults, particularly oxidative stress (68). For example Ob/Ob mice can progress to NASH if the mice are injected with a small amount of lipopolysaccharide (LPS), or administered ethanol at concentrations leading to no negative effects in control animals (83, 84). A study by Yamaguchi et al 2007 would suggest TG synthesis itself may actually be protective. In this study inhibition of TG synthesis by diacylglycerol acyltransferase 2 (DGAT2) antisense oligonucleotide led to reduced hepatic steatosis in a model of diet induced obesity (85). However, DGAT2 antisense oligonucleotide treatment combined with the MCD diet resulted in increased cytochrome P450 2E1 (CYP2E1, discussed below), markers of oxidant stress, inflammation and fibrosis (86).

A potential mechanism for the potential elimination of excess fat in NAFLD is to increase mitochondrial oxidation of FA's in the mitochondria. Increased fatty oxidation has in fact been demonstrated in ob/ob mice and in patients with NASH (55, 56, 87). Increased hepatic FA could clearly lead to increase FA oxidation on its own, however upregulation of the key β-oxidation gene CPT-1 has also been found in animal models of diabetes (55, 88). Interestingly PPAR-α has also been found to be up-regulated in a number of animal models of diabetes, its targets being genes involved in both mitochondrial and peroxisomal fatty acid oxidation (including CPT-1) (78, 89). As expected from increased PPAR-α expression there is a proliferation of peroxisomes in patients with fatty liver (90). Uncoupling protein-2 (UCP-2) as the name suggests uncouples the respiratory chain from the membrane potential leading to increased catabolism at the expense of ROS production and is also a target of PPAR-α (91, 92). Accompanying the increased production of ROS it has been found that patients with steatosis have increased expression of endotoxin receptors in Kupffer cells (83). This increased expression leads to increased sensitivity of Kupffer cells to activation with TNF-α and ROS release (60, 93). Importantly products of lipid peroxidation due to ROS and ROS themselves impair mitochondrial function (60). Added to this TNF-α which is increased in obese patients also increases mitochondrial permeability and ROS generation (60). This increased oxidation coupled with increased ROS and damaged mitochondria are believed to lead to a vicious cycle where increasingly damaged mitochondria are less able to quench ROS produced by both increased FA delivery and a damaged respiratory chain.

Oxidative stress has been implicated in the progression of a number of liver diseases (94). In concordance with the idea that increased ROS plays a role in NASH, markers of oxidative stress have been demonstrated in the MCD model of NASH including decreased glutathione (GSH) and S-adenosylmethionine (95). Oxidant stress has also been indicated in humans by mitochondrial DNA depletion and structural alterations in patients with steatohepatitis (57, 60, 96). As mentioned it is believed that fatty acid oxidation in the mitochondrion itself is a major source of reactive oxygen species (ROS) in NAFLD. It is also thought that the oversupply of FA overwhelms the B-oxidation capacity of the mitochondria and oxidation takes place through peroxisomes and in the endoplasmic reticulum (97). Although oxidation of FA in the mitochondria produces some ROS and superoxide anions the majority are safely dissipated in healthy mitochondria. On the other hand oxidation of FA in extra-mitochondrial sites generate ROS without the capacity to deal with these reactive products hence the oxidative stress of the hepatocyte increases (97). When the antioxidant capacity of the cell is overwhelmed cellular macromolecules are damaged including DNA and membranes leading to the release of proinflammatory cytokines (18). This proapoptotic state and further loss of mitochondrial function exposes the cell to further oxidative stress. Concordantly mice on the methionine/choline-deficient model (MCD) and ob/ob mice show increased ROS production and mitochondrial damage (98).

Evidence suggests that impaired β-oxidation and increased ROS an important mechanism of MCD induced liver inflammation and fibrosis (99). It is also evident in MCD, NASH patients and alcoholic steatohepatitis patients there is an upregulation of the cytochrome P450 2E1 (CYP2E1) enzyme which again would tend to increase ROS production (100). CYP2E1 is a member of the cytochrome P450 family of proteins which function in metabolism of xenobiotics and endogenous substrates (101). It is responsible for the metabolism of substances such as alcohol, paracetamol, fatty acids and steroids. Expression of CYP2E1 is induced by both alcohol and high fat diet feeding (102, 103). It has been proposed that increased CYP2E1 activity leads to increased production of ROS as a by product, which further adds to oxidative stress in NAFLD and NASH (101). The activity of the nuclear factor kappa B (NFκB) family of transcription factors has been linked to liver inflammation and insulin resistance in models of obesity (104, 105). NFκB members regulate a wide variety of genes from those involved in cell growth and development to inflammation and the immune response (106, 107). Inactive complexes of NFkB and IκB reside in the cytoplasm, activation in the majority of cases involves phosphorylation of IκB by an IκB kinase (IKK) and subsequent degradation which releases NFkB complexes and allows transcriptional activity. IKK may be activated by a range of stimuli

including cytokines, free fatty acids and high concentrations of glucose (108). NFkB activity appears to be upregulated in models of NASH and obesity where in this context it appears to mediate liver inflammation and insulin resistance (104, 105, 109). In addition CYP2E1 is also known be up-regulated by NFkB activation (110, 111). It has been shown that ROS mediated lipid peroxidation leads to the generation of longer acting and more inflammatory reactive aldehydes such as malondialdehyde (MDA) and 4-Hydroxynonenal (4-HNE). HNE is known to act as a chemoattractant for neutrophils (112). Increased ROS generation in the liver then leads to increased expression of transforming growth factor B (TGF-β), TNF-α and IL-8 which further attract inflammatory cells which contribute to liver inflammation (60). Fas ligand is also upregulated on ROS damaged hepatocytes which would lead to increased apoptosis or necrosis of these cells in NASH (60).

TNF-α is believed to play a central role in the pathogenesis of NASH and there have been studies which indicate TNF polymorphisms which lead to increased TNF production may lead to increased NASH progression (113). Indeed NAFLD and NASH are associated with increased levels of TNF-α as is obesity, the mechanisms of which are discussed later (113, 114). In addition it has been found that serum levels of TNF-α, IL-6 were increased in NASH patients compared to those with simple steatosis (115). Increased TNF-α can arise from a number of sources, including fat ladened adipocytes, fat ladened hepatocytes and Kupffer cells (114, 116). This increased TNF-α leads to increased hepatocyte damage and apoptosis and hence perpetuates the inflammation associated with the pathology of NASH.

1.6 Liver fibrosis

Liver fibrosis from NASH is increasingly becoming a cause for liver transplant. Liver fibrosis is the result of chronic damage to the liver with concurrent deposition of extracellular matrix (ECM) proteins and occurs in most types of chronic liver disease (2). Histological progression of fibrosis in NASH has been found to be between 32 and 37 %, however regression appears to also be possible and occurs in 18-29% (26). Obesity, diabetes and established fibrosis are associated with progression (26). Increasing NASH activity also predisposes to fibrosis development. The central pathogenic process is progressive fibrosis with distortion of the normal liver architecture (2). In healthy liver collagens I and III are concentrated in portal tracts and around central veins and occasionally in the Space of Disse. The collagen supporting hepatocytes in the space of Disse is composed of type IV collagen. With fibrosis progression collagen I and III are progressively deposited within the liver parenchyma disrupting blood flow and hepatocyte function (117). It has been estimated that over 10 years 5-20% of NASH patients may progress to cirrhosis (26). Cirrhosis itself is defined by bridging fibrous septae linking portal tracts and portal tracts with hepatic veins. Parenchymal nodules which contain proliferating hepatocytes encircled in fibroblasts are also a feature (2). Finally, disruption of the architecture of the whole liver occurs. In particular secretion of proteins such as albumin, clotting factors and lipoproteins are greatly impaired. The complications of liver cirrhosis include ascites, renal failure, hepatic encephalopathy and variceal bleeding (117).

The major source of collagen in liver fibrosis, in both animal and human liver fibrosis, has been found to be hepatic stellate cells (HSCs) (2). HSCs are found in the Space of Disse and serve as a major store of vitamin A. HSC undergo rapid activation in response to profibrogenic cytokines released from hepatocytes and Kupffer cells (KC), the most potent being TGF-β. Platelet derived growth factor mainly derived from KCs also plays an important role as do ROS (118). Upon activation these cells change from a lipocyte phenotype to a transitional myofibroblast phenotype, with increased capacity for ECM production (119). Activated HSCs also secrete inflammatory cytokines such as TGF-β, MCP-1, IL-10, RANTES, IL-8, TNF-α and cause recruitment and activation of lymphocytes (118). It is predominately the cytokines secreted by activated KCs, the macrophage of the liver, and other inflammatory cells that activated these cells (117).

KCs as mentioned are the macrophage of the liver and represent 80-90% of all tissue macrophages in the body (120). KC are responsible for the elimination of bacteria, old red blood cells and foreign antigens (121). Like other macrophages KCs sense danger signals from cells and microbes and respond by activation. KC secrete cytokines, ROS, nitric oxide (NO) and recruit immune cells such as

natural killer (NK) T cells, NK cells and macrophages (122). As such KC may escalate the inflammatory response in NAFLD and increased CD68 positive KC correlate with histological severity of human NAFLD (123). Further the pattern of KC distribution is altered in NASH from diffuse to perivenular aggregates (124). To add to the importance of KC in liver injury 'selective' deletion of large cells by gadolinium chloride attenuates liver injury from thioacetamide, CCl4 and alcohol. Clondrate elimination of macrophages also reduces steatohepatitis from alcohol and MCD deficiency diet (122). However, there were also alterations in cytokines which could interfere with regeneration (125, 126). Correspondingly, a paper by Duffield et al (2005) demonstrated the importance of KC in the processes of both inflammation and resolution of fibrosis (127). In this paper a model was developed which allowed for selective deletion of macrophages via way of expression of diphtheria toxin receptor in CD11b cells. Diphtheria toxin was then added at different phases of liver fibrosis either during progression of fibrosis (during CCl4 treatment) or in the recovery phase (after cessation of CCL4 treatment). Deletion of macrophage cells during the progression phase resulted in decreased fibrosis and fewer activated HSCs. Macrophage deletion in the recovery phase of fibrosis on the other hand lead to persistence of fibrosis and with a failure with 50% more collagen III in the livers of mice with macrophage depletion 7 days after the recovery phase. Importantly it was found that macrophages in liver injury were associated with high levels of TGF-β in response to injury (127, 128).

A key molecule in the process of fibrosis is transforming growth factor β (TGF-β) (129). In the liver TGF-β can arise from injured hepatocytes, Kupffer cells or HSCs (118). TGF-β is a pleotrophic molecule mediating anti-inflammatory and immunomodulatory roles. Homozygous KO mice die due to leukocyte infiltration and inflammation of multiple organs (130). Studies using overexpression of TGF-β or inhibition of TGF-β have demonstrated that in the context of liver injury TGF-β is profibrotic (131, 132). Importantly TGF-β released form hepatocytes and macrophages activates HSCs (117). TGF-β mediates its effects through increasing the expression of connective tissue growth factor (CTGF) and increasing the expression of metalloproteinase inhibitors (TIMPs) and downregulating the ECM degradative enzymes matrix metalloprotinases (MMPs) (133-135). CTGF has been found to play a key role in mediating the effects of TGF-β on fibrosis (136). Further the level of CTGF can induce TGF-β in a feed forward loop. siRNA mediated disruption of CTGF resulted in significantly reduced HSC activation and liver fibrosis. An important finding has been that liver fibrosis is potentially reversible, however the treatment for patients with advanced cirrhosis currently require transplant.

1.7 Diabetes and liver disease

A key feature linking NAFLD, NASH, MetS, obesity and T2D is insulin resistance (35, 42, 137, 138). Importantly insulin resistance in the liver and periphery is known to play a role in NALFD and NASH and has been found to contribute to the severity of NAFLD. Normally glucose homeostasis is tightly regulated, both by controlling glucose production in the liver and glucose uptake and use in the tissues (42). The hormone insulin is crucial in regulation of these processes. Insulin is generated in the β cells of the pancreas. Upon stimulation with elevated blood glucose levels after a meal the β-cells release insulin. Intestinal hormones, certain amino acids, and the autonomic nervous system can also stimulate insulin release, however elevated blood glucose is the most important stimulus (1, 42).

Insulin acts to control serum levels of glucose, and regulates lipids and amino acids. Insulin receptors are present on all cell types, and are expressed at high levels in important tissues for metabolism including the liver, adipocytes and skeletal muscle (139). Insulin is an anabolic hormone, acting to increase uptake and storage of these building blocks in times where they are in excess in the serum, while decreasing their synthesis (see Figure 1.10). The principal effect of insulin is to increase glucose uptake and storage. Glucose is stored as glycogen in striated muscle and liver and triglycerides in adipocytes. Insulin also controls lipid metabolism acting to increase storage and inhibit release of fatty acids by adipose tissue. Insulin also promotes uptake of amino acids and their incorporation into protein (42).

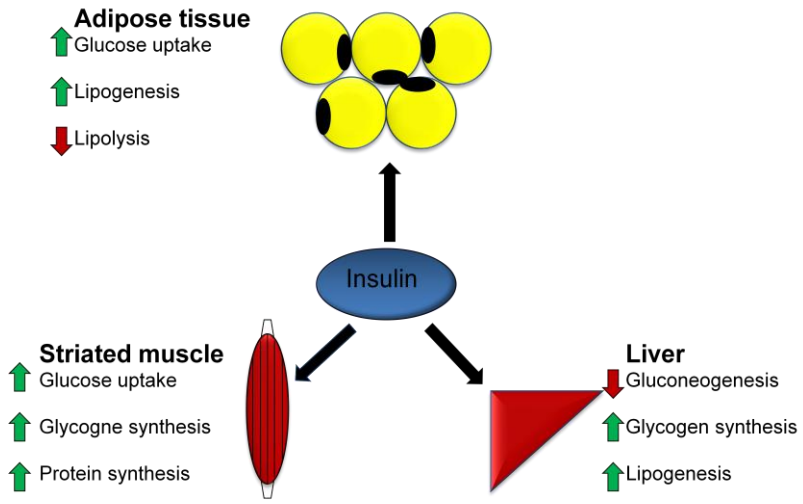

Figure 1.10 Insulin Action on Tissues.
General insulin action on adipose tissue, muscle and the liver are shown.

Insulin resistance is defined as resistance to the effects of insulin on glucose homeostasis (42). That is, resistance to the effect of insulin on metabolism or storage of glucose. Insulin resistance is often detected years before the development of T2D, is a key component of the metabolic syndrome and is a good predictor for the future development of T2D (35, 140). This insulin resistance combined with β-cell dysfunction leads to elevated blood glucose levels through a decrease in insulin mediated glucose uptake in tissues such as muscle and adipose and a failure to suppress gluconeogenesis in the liver (141). Interestingly an index incorporating insulin resistance and insulin secretion was found to be the best predictor for future T2D (140). Insulin resistance results in detectable alterations in the insulin signalling pathway within target tissues including; decreased insulin receptor protein, decreased tyrosine phosphorylation (activation) of the insulin receptor and decreased levels of activated downstream signalling intermediates (42, 142, 143). Insulin signalling and changes in insulin resistance are shown in Figure 1.11 and Figure 1.12.

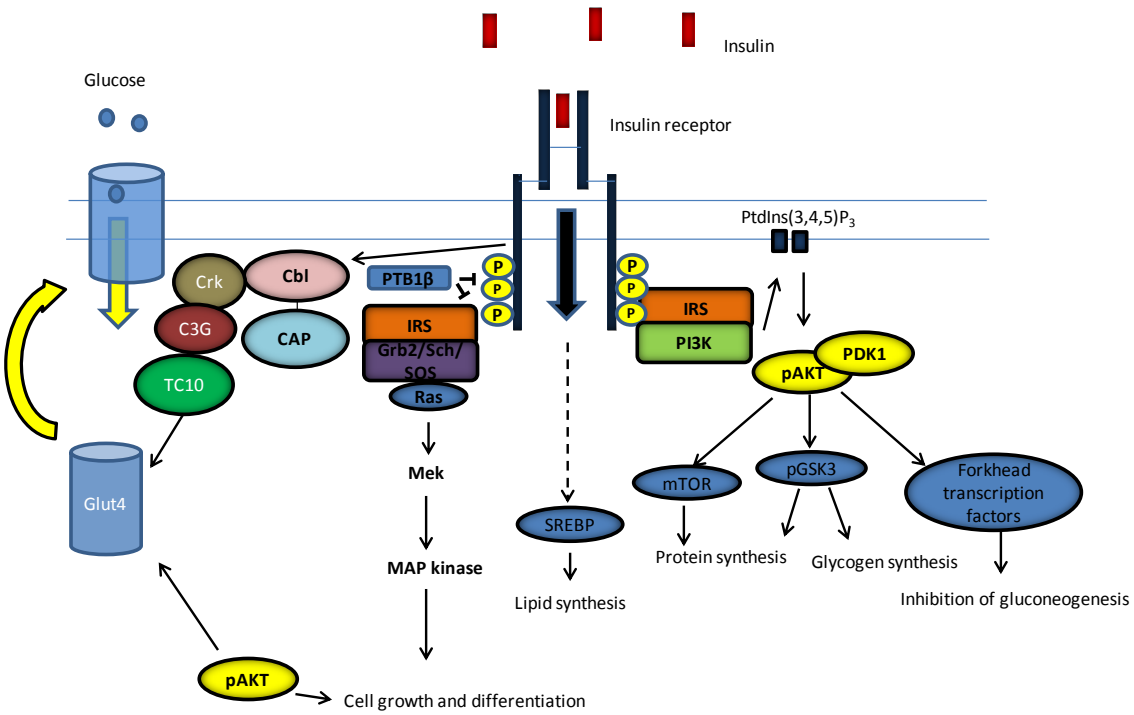

Figure 1.11 Insulin signalling.
The insulin receptor is a tyrosine kinase that undergoes autophosphorylation upon insulin binding. The receptor in turn catalyses the phosphorylation of the IRS proteins, Cbl and Shc. These activated proteins then interact with binding partners resulting in signaling pathway activation and alterations in cellular functions Casistas B-Lineage lymphoma protein (Cbl), Insulin receptor substrate (IRS), Son of Sevenless (SOS), Growth factor receptor bound protein 2 (Grb2), Protein tyrosine phostphatase 1 β (PTP1β), CRK SH3-binding GNRP (C3G), Glucose transporter type 4 (Glut4), Sterol Regulatory Element-Binding protein (SREBP), Phosphatidylinositol 3-kinase (PI3K), Phosphatidylinositol -3,4,5-phosphate (PtdIns(3,4,5)P_3), phosphoinositide-dependent protein kinase-1 (PDK1), glycogen synthase kinase 3 (GSK3), mammalian target of rapamycin (mTOR).

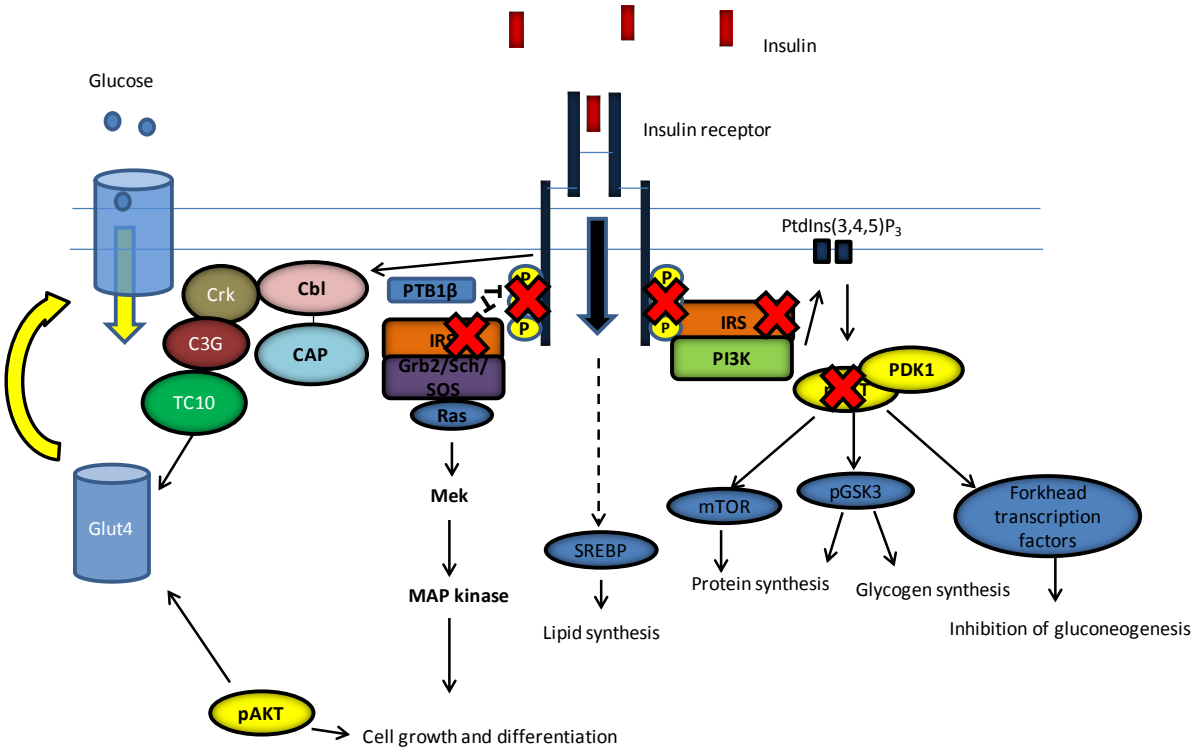

Figure 1.12 Alterations to signalling in insulin resistance.
Activation of PKCε (not shown) by increased lipid leads to impairment of IR activation and inhibitory IRS-1 serine phosphorylation. PKC ζ can also bind to and sequester AKT2. Activation of inflammatory pathways result in serine phosphorylation of IRS proteins and insulin resistance as discussed in section 1.9.2. Casistas B-Lineage lymphoma protein (Cbl), Insulin receptor substrate (IRS), Son of Sevenless (SOS), Growth factor receptor bound protein 2 (Grb2), Protein tyrosine phostphatase 1 β (PTP1β), CRK SH3-binding GNRP (C3G), Glucose transporter type 4 (Glut4), Sterol Regulatory Element-Binding protein (SREBP), Phosphatidylinositol 3-kinase (PI3K), Phosphatidylinositol -3,4,5-phosphate (PtdIns(3,4,5)P_3), phosphoinositide-dependent protein kinase-1 (PDK1), glycogen synthase kinase 3 (GSK3), mammalian target of rapamycin (mTOR).

In metabolically healthy individuals an increase in insulin resistance in the tissues is countered by an increase in insulin release in the pancreas and an increase in β-cell function and / or β-cell mass (144). In individuals where the β-cells are unable to compensate for increasing insulin resistance T2D develops. Interestingly this event is accompanied by β-cell apoptosis in animal models and reduced β-cell mass has been demonstrated in both animal models of diabetes and in humans with diabetes (145, 146) .

Importantly liver metabolic dysfunction is known to occur in T2D. Increased fat accumulation in the form of NAFLD and liver fibrosis from NASH are known to have increased prevalence in diabetic individuals as mentioned previously (147, 148). In a recent mechanistic study it was found that HFD feeding of mice alone was sufficient to increase hepatic lipid and induce hepatic macrophage infiltration, two features of NASH (149). However, induction of diabetes via streptozotocin increased fibrosis and was required to increase collagen in the perisinusoid space. Intriguingly

concurrent treatment with insulin reduced fibrosis, this indicated that β-cell failure and progression to overt diabetes could lead to NASH progression.

Apart from being affected by diabetes a dysfunctional liver actively contributes to the diabetic phenotype through its action on blood glucose and serum lipid. Indeed diabetes is known to be associated with both inappropriate hepatic glucose production (HGP) when glucose is normal or even raised, and impaired insulin-mediated suppression of HGP (49, 150, 151). The increased HGP observed in diabetic patients occurs at lower insulin levels (150pmol/L) suggesting that increased HGP is more important in raising bgls in fasting conditions (152). Hence inappropriate HGP in turn can result in elevated fasting glucose, another key feature of T2D. Moreover, HGP is higher in diabetic patients even after controlling for higher circulating levels of the HGP-inducing hormone glucagon, which is also present in diabetic patients (153, 154). Hepatic glucose production can come from gluconeogenesis or glycogenolysis, both of which are increased in severely diabetic patients (154). Although gluconeogenesis may be increased only in response to increased glucagon as after clamping studies with equivalent insulin, elevated blood glucose and glucagon only glycogenolysis was still raised. Importantly this increase in glycogenolysis occurred in mildly diabetic and severely diabetic patients (154). In addition hepatic glucose uptake is decreased in diabetic patients and may contribute to elevated blood glucose in this manner (152). Importantly decreased hepatic uptake was observed at higher insulin concentrations of 300p/mol/L (155). Further evidence suggested that decreased uptake in the liver accounts for 1/3 of the decrease in glucose disappearance in people with T2D. It has been found that the activity of the uptake rate limiting enzyme GK activity is decreased in the liver of T2D patients which may account for decreased uptake (156).

Dyslipidemia is a recognized feature of the metabolic syndrome and T2D where it is characterized by increased serum triglycerides (TG) and low high density lipid cholesterol, often with pronounced post-prandial hypertriglyceridemia (48, 157, 158) thereby contributing to the increased risk of cardiovascular complications in people with diabetes or the metabolic syndrome. Overproduction of VLDL TG is a key feature in insulin resistant and diabetic patients and is driven by increased FA flux from insulin resistant adipocytes, increased VLDL uptake, increased chylomicron remnants and increased de novo lipogenesis (157, 159). It has been shown that increased FA levels lead to increased VLDL secretion (160). However, insulin resistance in the liver is also associated with failure of insulin to stimulate ApoB degradation and this is accompanied by increased VLDL synthesis in humans and in animal models of insulin resistance (161-165). Thereby the insulin resistant liver

actively increases VLDL TG levels in the serum of diabetic patients. The systemic effects of a insulin resistant liver is shown in Figure 1.13.

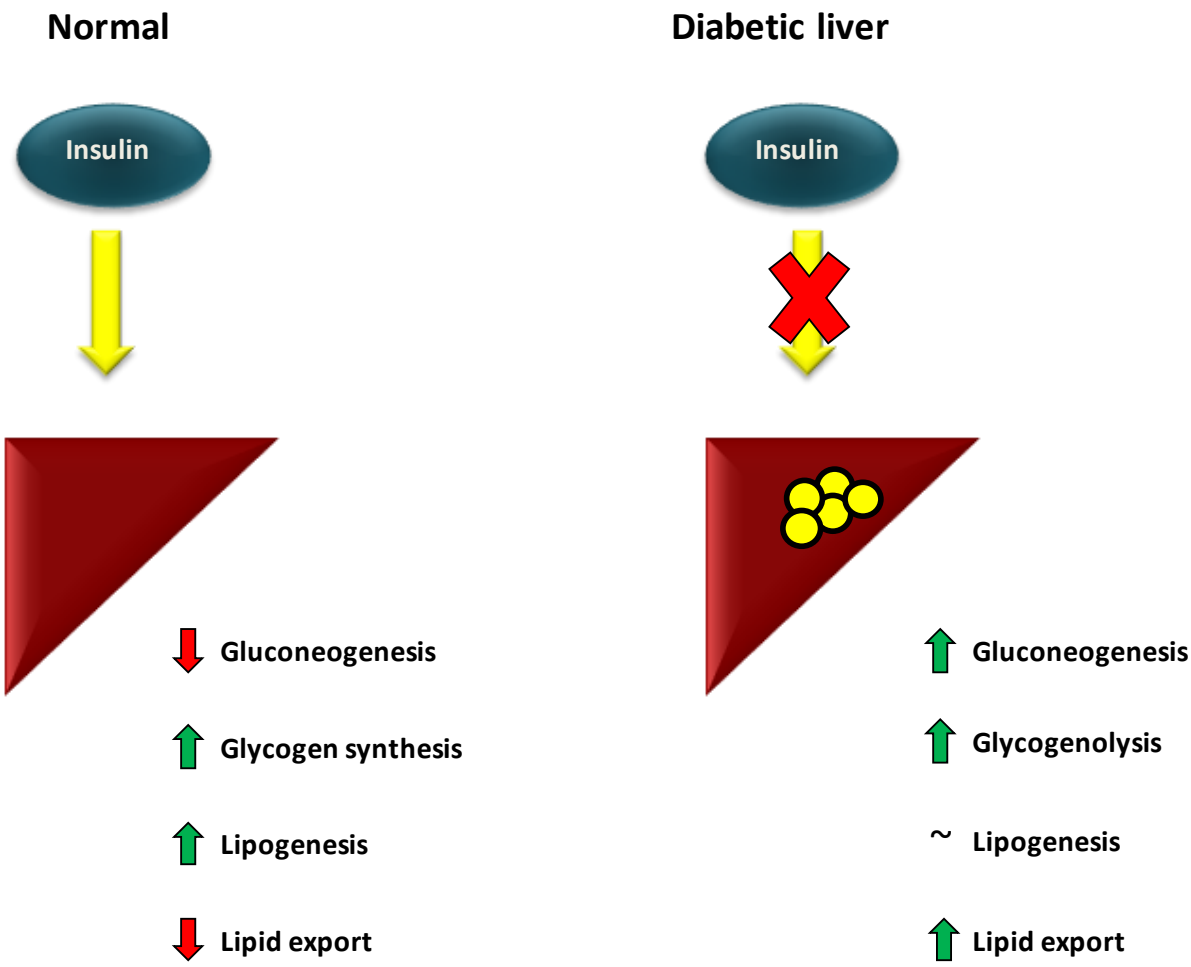

Figure 1.13 The outcome of hepatic insulin resistance.
The insulin resistant liver continues gluconeogenesis and glycogenolysis at lower insulin levels resulting in increasing fasting blood glucose. Lipogenesis is increased basally and fails to decrease VLDL export in response to insulin.

1.8 Obesity, inflammation and insulin resistance

One culprit identified as mediating insulin resistance is obesity. Although not all obese individuals develop metabolic derangements the majority are insulin resistant (34). In particular visceral obesity has been strongly linked with insulin resistance (138). The effect of obesity on insulin resistance is at least partially mediated through an increase in free fatty acids (FFA) (61, 166). Population studies have clearly demonstrated an inverse correlation between fasting plasma FFAs and insulin sensitivity. Correspondingly, acute infusions of FA have been shown to induce insulin resistance (61, 166). The role of inflammation in obesity has emerged as an important factor in mediating disease in the last decade (167). Obesity and the MetS have been associated with chronic low grade inflammation as measured by altered cytokine production, increased acute phase proteins and activation of inflammatory pathways (168). The pro-inflammatory cytokine TNF-α is also known to mediate insulin resistance in a number of rodent models (169, 170). It has been documented that individuals with the metabolic syndrome have increased levels of TNF-α mRNA in white adipose tissue (WAT) and increased serum levels of TNF-α (171, 172). In addition it has been found that the expression of many other cytokines including IL-6, IL-1β and IL-8 are elevated in models of obesity or hyperglycaemia (167). The production of the adipocyte derived anti-inflammatory molecule adiponectin is also decreased (173). As discussed, in NAFLD and NASH TNF-α and inflammation in the liver play an important role in mediating disease. Correspondingly it was found that serum levels of TNF-α, IL-6 were increased in NASH patients compared to those with simple steatosis (115). It is now recognised that visceral adipose tissue is an active endocrine organ regulating both metabolism and inflammation (174). Interestingly, it has been documented that there are increased numbers of macrophages in obese WAT (175). Further studies have suggested that macrophage infiltration may be a key component of the inflammatory phenotype of the adipose tissue (176). Intriguingly it has also been recognised by transcriptional profiling that macrophages and adipocytes are in fact closely related, and there has even been evidence to suggest transdifferentiation of adipocytes into macrophages (177, 178).

1.8.1 The innate immune system in obesity induced inflammation

It is thought that dysregulation of the macrophages of the innate immune system which populate metabolic organs play a key role in the chronic low grade inflammation which link diet-induced obesity to insulin resistance (179, 180). Macrophages are the sentinels of the immune system and assume different morphological forms and functions in response to environmental signals relating to microbes and tissue damage (181). In this manner the macrophage senses the environment and

orchestrates a response to eliminate infectious agents and/or repair damage. Supporting the importance of macrophages in metabolism a number of myeloid and macrophage specific knockout mice which alter macrophage function have been found to have altered insulin resistance and changes in glucose metabolism (182-186). The idea of two activation states of macrophages has been a useful concept and defines macrophages into two polarised populations characterised by different markers and functions (187). Although, in reality macrophages display a range of gene expression patterns along the continuum. The classical inflammatory macrophage activation state termed M1 is stimulated by exposure of macrophages to TH1 cytokines like IFNγ and bacterial products. M1 activated macrophages secrete high levels of cytokines TNF-α, IL-6 and IL-12 and also have increased bactericidal activity with upregulation of inducible nitric oxide synthase (iNOS) to catabolise production of NO. The alternative activation state M2 is stimulated by TH-2 cytokines like IL-4 and 13. M2 activated macrophages have anti-parasitic functions with decreased TNF-α, IL-6 and IL-12 in relation to M1 macrophages and are also thought to function in tissue repair while being thought of as anti-inflammatory (188).

Adipose tissue of lean mice is populated by macrophages with alternative activation markers such as arginase 1 (Arg1) and CD301 (189). It has been shown that macrophages isolated from animals with diet-induced obesity have increased inflammatory properties such as elevated IL-6 and iNOS (189, 190). Further work suggests that macrophages infiltrating adipose tissue during weight gain predominantly express a classically activated phenotype (191, 192). Correspondingly, genetic deletion of TNF-α or iNOS reduced insulin resistance in obese mice (193, 194). It has also been shown that it is the macrophage and pre-adipocyte fraction of adipose tissue which is responsible for the majority of cytokine expression (176). Furthermore, in this fraction it is the macrophages which seem to be responsible for the majority of cytokine production. Correspondingly obesity induced macrophage recruitment is associated with elevated MCP-1 expression in adipocytes of db/db mice (195). Correspondingly transgenic upregulation of MCP-1 expression in adipocytes resulted in increased macrophage recruitment and insulin resistance, while acute expression of a dominant negative mutant had the opposite effect (195, 196). An opposing study however showed that mice lacking MCP-1 had similar levels of macrophage recruitment to adipose tissue in response to HFD, and that these mice had mildly impaired glucose tolerance and increased serum insulin compared to controls (197). This suggested that MCP-1 may have other effects apart from macrophage recruitment and that compensation can occur. Another molecule which may be involved is osteopontin (OPN). OPN was increased in serum of HFD mice and displayed elevated macrophage

expression (198). Mice lacking OPN had improved metabolic parameters with no change in weight gain and a concurrent reduction in macrophage recruitment to adipose tissue.

There is also evidence of tissue inflammation in islets of T2D patient with corresponding increases in cytokines and chemokines (199-201). In fact immune cell islet infiltration has been found in animal models and human patients with T2D, indicating the possibility that tissue inflammation may directly impact T2D through impairment of islet function (201). In line with this data there is an increased number of islet associated macrophages after 8 weeks of HFD, and this corresponds to a decrease in B-cell function. B-cells express high levels of IL-1β receptor and express this cytokine along with resident macrophages (202). IL-1β is known to be induced by high glucose and along with upregulation of Fas contributes to impairment of glucose stimulated insulin secretion (199, 203). FFAs have recently been shown to increase IL-1β expression, including oleate, palmitate and stearate (202). Interestingly expression of IL-1 receptor antagonist (IL-1Ra) is induced by IL-1β and is a mechanism by which the body attempts to dampen down excessive IL-1β signalling. Correspondingly increased IL-1Ra is elevated in prediabetes and obesity with a sharp increase before the onset of T2D (204). It is possible that islet inflammation is exacerbated by infiltrating inflammatory macrophages and leads to impairment of islet function.

Research in the past decade has led to some insight as to how classical activation of macrophages may be favoured in obesity. Cells of the innate immune system express receptors for common microbial ligands which allow them to quickly detect and respond to various infectious agents. TLR4 is a toll-like receptor which responds to lipopolysaccharide (LPS) which is a cell wall component in gram negative bacteria (205). The receptor also responds to a number of other ligands including fungal mannans, parasitic phospholipids, viral envelope proteins and host heat shock proteins. Ligation of this receptor leads to inflammatory signalling via induction of nuclear factor kappa-light-chain-enhancer of activated B cells (NFkB) to trigger release of M1 macrophage cytokines such as IL-6, TNF-α and IL-12, and iNOS (206). Importantly it has been shown that TLR4 responds to saturated fatty acids in a dose dependant manner (207). These include palmitic, myristic and stearic fatty acids and free fatty acids are known to be increased in obesity (208, 209). Indeed mice lacking TLR4 have blunted inflammatory responses to FFA and were protected from FFA infusion induced insulin resistance, although the insulin sensitising phenotype did not occur in male mice suggesting gender effects. Male mice did however have less inflammatory cytokine expression in adipose and liver (207).

Importantly while an obesogenic diet rich in saturated fats is thought to lead to inflammation through classical macrophage activation, alternatively activated macrophages are favoured in adipose tissue of lean mice and by diets containing monounsaturated fatty acids like oleic acid (189, 210). Studies have shown PPAR activation is required to maintain alternative activation. PPAR-δ activation by oleic acid alongside IL-4 stimulation has also been shown synergise to drive alternative activation of macrophages (210). It was also shown that in mice lacking PPAR-γ in myeloid cells there were decreased numbers of alternatively activated macrophages and had impaired glucose tolerance, increased insulin resistance and diet induced obesity on HFD (186). Mice lacking PPAR-δ in haematological cells lead to increased diet induced obesity and insulin resistance. It was further shown that the alternative activation of KCs in the liver was affected (210). While mice lacking PPAR-δ in myeloid cells were again predisposed to increased insulin resistance and reduced numbers of alternative activation of adipose macrophages (211). Interestingly macrophages also accumulate in adipose tissue in response to weight loss (212). In this case macrophages did not promote inflammation but lipolysis and did not express mRNA for alternative activation, suggesting another phenotype of macrophages in this situation. In conjunction with stimulation of TLR4 leading to increased inflammation and potentially decreased PPAR activation leading to decreased alternative activation, cellular stress in response to nutrient overload can also mediate insulin resistance and inflammation in metabolic parenchymal and immune cells.

1.8.2 **Common intracellular pathways of insulin resistance and inflammation.**

A major metabolic consequence of the chronic inflammation that occurs with obesity appears to be insulin resistance (137, 167). This insulin resistance in obese patients can be triggered by increased cytokine production from stressed cells and activated immune cells as discussed (108). In NAFLD and NASH inflammatory cytokines such as TNF-α can arise from fat-ladened adipocytes, hepatocytes and the liver Kupffer cells (60, 114, 116). It is not entirely clear how intracellular stress is detected however it seems the endoplasmic reticulum plays a role through the Unfolded Protein Response (UPR). Stress in the form of unfolded protein, hypoxia, infections, toxins, nutrient overload or energy deprivation can trigger the response (108). The UPR leads to upregulation of chaperone proteins and proteins involved in protein degradation. The UPR response also leads to inflammatory signals and can activate apoptosis if ER homeostasis is not restored (213). This sustained UPR activation can in turn lead to activation of JUN N-terminal Kinase (JNK) via inositol-requiring kinase 1 (IRE1) (214). Inflammatory pathways triggered by cytokines and intracellular stress, kinases like (JNK) and $I_K\beta$

kinaseβ(I_{Kk}β) are activated leading expression of inflammatory genes and in the case of JNK to direct serine phosphorylation and inhibition of IRS proteins (214-216). More specifically hepatocyte JNK can be activated by proinflammatory cytokines, free fatty acids, ROS and pathogens (108). Not surprisingly JNK1 deficient mice are protected from insulin resistance induced by diet and genetic models (217). Correspondingly JNK-1 deficient mice also have decreased expression of TNF-α and IL-6 in high fat diet induced obesity (217). Likewise hepatic specific activation of IkkB increased inflammation and insulin resistance in this tissue and to a lesser degree systemically, while hepatic deletion produced the opposing result in the liver (104, 105). Reactive oxygen species (ROS) are also generated in conditions of ER stress and as discussed are important in mediating cellular damage (218). It is known that high sustained levels of glucose and nutrients themselves can engage the UPR and NF-kB pathways and initiate inflammation (219). Saturated fatty acids have also been shown to initiate the UPR in a number of tissues including liver and macrophages (108). As might be predicted from their role activating inflammatory cellular pathways Ικκβ and JNK1 may be required for classical macrophage activation in obesity (105). Mice deficient in Ικκβ in myeloid cells including macrophages and neutrophils had lower levels of tissue inflammation after HFD and decreased insulin resistance (105). Mice lacking JNK in haemopoetic cells led to decreased hepatic and adipose tissue inflammation and increased insulin sensitivity after HFD (220). Interestingly lack of JNK in non-haemopoetic cells protected mice from obesity. NAFLD and especially NASH are characterised by insulin resistance and inflammation leading to disruption of normal liver functioning, and these pathways clearly play a role. The mechanisms of inflammatory induced insulin resistance are shown in Figure 1.14.

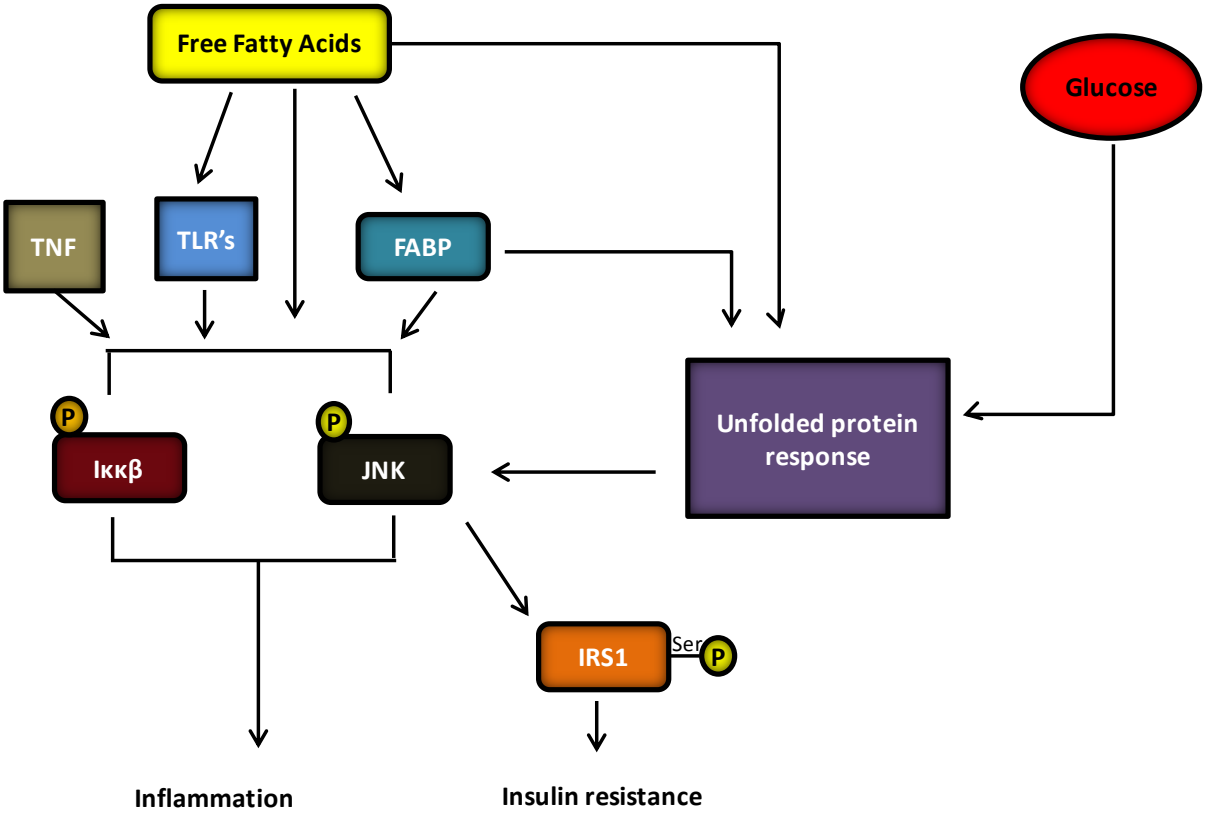

Figure 1.14 Metabolism and inflammation.
Impairment of insulin signaling can be induced by cytokines like tumor necrosis factor (TNF). TLR4 and 2 can be activated by fatty acids. Fatty acid binding proteins (FABP) have also been found to activate inflammatory response in the presence of saturated fatty acids. Excess free fatty acids and glucose themselves can activate the unfolded protein response in the endoplasmic reticulum. All these activation signals lead to activation of Ikkβ or JNK which activate inflammatory pathways and alter the metabolic response through serine phosphorylation of IRS1.

1.9 ARNT and its partners in metabolic liver disease and diabetes

bHLH-PAS (Basic helix-loop helix / PER/ARNT/single minded (SIM)) homology domain) proteins are transcription factors which regulate cellular programs relating to development and physiological responses (221). These functions include cellular responses to hypoxia, circadian rhythm and the dioxin response pathway (222). ARNT and some other family members are ubiquitous, and their activity is signal regulated, and they recognise sequences that diverge from the prototypical E-box (CANNTG) (223). These proteins combine a specific partner for an environmental signal with a generic partner to mediate different responses. This family is characterized by a DNA binding region adjacent to a helix-loop-helix dimerisation region both of which are required to form a function transcription factor (223). The PAS domain consists of two repeated amino acid sequences of around 130 amino acids termed PAS A and PAS B, which has been conserved throughout evolution (221). When the PAS domain is activated by its environmental ligand the protein conformation is altered allowing it to dimerise with a second bHLH/PAS partner and mediate transcription of its target genes. The PAS domain also functions to define which bHLH/PAS partners may be selected with PAS A being essential for interaction with other bHLH/PAS proteins and PAS B interacting with other classes of proteins including HSP90, p23, Ara9 and small molecules (222, 224).

ARNT acts as a general partner for members of the bHLH/PAS family of transcription factors. It heterodimerises with other bHLH/PAS family members including Hypoxia-Inducible Factor-1-α (HIF-1α), Hypoxia-Inducible Factor-2-α (HIF-2α) and Aryl hydrocarbon Receptor (AhR) to form active transcription complexes which regulate genes involved in hypoxic-responses, cell survival, proliferation, glycolysis, angiogenesis and response to xenobiotics (225-228). In its inactive state AhR is found in the cytoplasm associated with two molecules of heat shock protein 90 (Hsp90), p23 and hepatitis B virus associated protein (XAP2/AIP/Ara9) (221). Following ligand binding the complex translocates to the nucleus where Hsp90 is exchanged for ARNT and the complex drives transcription of target genes. The endogenous ligand for AhR remains highly contentious; bile acids and cAMP are reported to be potential candidates, while a recent paper points to other ligands in breakdown products from cruciferous vegetables (229-231). Each of these putative ligands has obvious relevance to the liver. HIF-1α and HIF-2α are regulated by cellular oxygen content, under normal conditions (20%) oxygen the majority of these proteins are rapidly degraded by the ubiquitin-proteosome pathway (232). This degradation is mediated by an oxygen dependent degradation domain (ODD), which is distal to the PAS domains. In the absence of other signals proline residues in the ODD are

hydroxylated by prolyl-hydroxylases (PHD1 -3) in the presence of oxygen and iron (233, 234). These hydroxyl motifs act as docking sites for the von Hippel-Lindau tumour suppressor protein (Vhl). Vhl then forms a complex with elongins B and C, Cullin 2 and RBX1 to form a E3 ubiquitin ligase which targets HIFs for degradation (235). Importantly HIF proteins are also hydroxylated at asparagine residues by factor inhibiting HIF (FIH) to prevent interactions with co-activators (236). Although HIF levels are decreased in normoxia these factors are expressed basally under normoxia in brain, kidney, liver and heart tissue (237). Interestingly elevation in response to hypoxia shows a different time course in different tissues. It is now known HIF-1α is also stabilized by inflammation, TGF, PDGF, EGF, IGF-1 and IL-1β (221, 238-240). It has also been shown that maximal HIF-1α expression is dependent on functional NFKB in fibroblasts and macrophages. Further that NFKB signaling controls HIF-1α mRNA expression under both hypoxic and basal conditions (241). Within the liver cells are exposed to a range of oxygen concentrations from 60mmHg in periportal blood to 30-35mmHg in the perivenous areas (242). Correspondingly, expression of enzymes involved in glucose metabolism differ according to location in the liver with periportal hepatocytes specialising in oxidative metabolism, synthesis of bile and glucose metabolism while perivenous cells take up more glucose, synthesize glutamine and metabolise xenobiotics (242).

The first studies showing that ARNT and its partners did in fact play a role in liver function came with the characterisation of the AhR knockout mouse. Among many phenotypes this animal displayed transient hepatic steatosis, increased hepatocyte apoptosis and fibrosis driven by increased TGF-β expression (243-245). Another study suggested that signalling through AhR may actually sensitise hepatocytes to Fas induced apoptosis (246). Interestingly it was further found that the phenotype of liver fibrosis was reversed if AhR -/- mice were fed a diet deficient in vitamin A, suggesting retinoid excess contributes to fibrosis in these mice (247). It was suggested this activation may be due to excess retinoid accumulation in AhR -/- mice which activated tissue transglutaminase type II in HSCs which in turn activated latent TGF-β. Subsequent studies investigating AhR in liver metabolism showed that AhR activation also led to hepatic steatosis (248, 249). It was found that AhR activation led to increased expression of fatty acid translocase (CD36) and this potentially led to preferential accumulation of serum TG in the liver. Interestingly whole body knockout animals also have improved insulin sensitivity, glucose tolerance and decreased gluconeogenic and lipid oxidation gene expression in the liver (250).

In 2005 and 2010 Gunton et al identified that ARNT and HIF-1α were reduced in the islets of patients with T2D (225, 251). It was further found that β-cell ARNT or HIF-1α deletion in mice resulted in

impaired glucose tolerance due to decreased β-cell function, the latter being exacerbated by HFD (225, 251). These experiments hinted at the possibility both factors could play wider roles in tissue dysfunction in metabolic disease. During the course of this thesis it was determined that ARNT mRNA is also reduced in the livers of T2D patients (252). This study found that short term hepatic ablation of ARNT using injection of Adenoviral-Cre led to decreased hepatic steatosis. In addition deletion of ARNT was accompanied by an increase in HGP and impaired glucose tolerance (252). These studies went on to demonstrate that ARNT mRNA and protein were reduced in the livers of mice treated with streptozotocin, a model of type 1 diabetes, showing liver ARNT was actively down-regulated in a type 1 diabetic milieu.

A number of studies have linked the apneic- episodes of obstructive sleep apnoea with elevation of liver enzymes and NASH (253, 254). This suggested that increased HIF expression may play a role in these conditions. One animal model of increased HIF expression is the Vhl +/- mouse line. Livers of Vhl +/- mice developed steatosis and blood filled cavities and increased areas of increased vascularisation (255). Recently it was shown that acute increases in the level of liver HIF-1α and HIF-2α induced by complete Adenoviral-Cre mediated deletion of Vhl led to fatty liver together with decreased serum glucose and ketone levels, which if left untreated resulted in death (256). This phenotype was accompanied by suppressed mitochondrial respiration and could be rescued by simultaneous ARNT inactivation (256). Further studies using a combination of Vhl deletion and inactive HIF-1α or HIF-2α mutants showed that steatosis and impaired fatty acid β- oxidation was dependent on functional HIF-2α (257). It was then shown using a model of acute hepatocyte specific double deletion of Vhl and HIF-1α or HIF-2α under control of the Cre-ER system, that elevated HIF-2α resulted in increased liver inflammation and fibrotic mRNA expression (258). Interestingly HIF-1α has been found to be elevated in a mouse model of alcohol induced steatosis (259). HIF-1α deletion in hepatocytes protected mice from liver steatosis and hepatomegaly following alcohol feeding, and from elevated ALT levels following subsequent LPS challenge. The steatotic effects after alcohol feeding and LPS challenge were subsequently found to be regulated by hepatocyte MCP-1 (259). HIF1-α is also known to regulate the expression of fibrosis inducing factors TGF-β and CTGF, and is itself stabilised by TGF-β. In addition hypoxia was found to activate HSCs (260-262). In contrast to the harmful effects of elevated HIFs suggested by these studies HIF-1α accumulation in fatty liver was shown to be protective in a model of ischaemia reperfusion injury and also to be required for gluconeogenesis in regenerating liver (263, 264). Hepatic HIF-1α deletion was further shown to impair glucose tolerance in animals given a high fat/sucrose diet (265).

As outlined in Section 1.8.1 previous studies have demonstrated an important role for myeloid cells in regulating metabolism (182-186). The first evidence that HIF-1α in myeloid cells was impotant for innate immune function was demonstrated by Cramer et al in 2003 then others where it was shown that myeloid cell specific knockout of HIF-1α impaired acute response in terms of motility, cytokine production, bacterial killing, survival, and phagocytosis (238, 266-268). Another link between HIF-1α and inflammation is that NF-κB expression has also been found to be crucial for maximal HIF-1α mRNA expression, while HIF-1α may also increase levels of NF-κB (241). An important potential role for myeloid cell ARNT in liver pathology has been shown by work where ARNT deletion in Kupffer cells prevented the upregulation of PDGF-β, VEGF, angiopoetin-1 and MCP-1 (269). In addition it is known that adipose tissue becomes hypoxic in obesity and that macrophages accumulate (270-273). A number of studies have used the AP2 promoter to investigate the effect of adipose HIF-1α. These studies have shown that increased adipose HIF-1α expression seems to drive adipose tissue inflammation and impaired glucose tolerance (274-277). Importantly the AP2 promoter used in these experiments is also expressed in macrophages, thus perturbation of HIF-1α signaling in macrophages may have contributed to these findings (278, 279).

1.10 Wound healing

1.10.1 Normal wound healing

The ability of an organism to repair tissue damage is essential to survival. In mammals the majority of tissues are not able to repair damage in a way that completely replicates the original tissue (280, 281). In most cases tissue is repaired through healing where the original structure of the tissue is restored with some loss of function by way of scarring. Wound healing in mammals occurs via progression through three overlapping phases (1) inflammation, (2) new tissue formation and (3) remodelling. The inflammatory phase occurs immediately after tissue injury and haemostasis is generally initially achieved by the formation of a platelet clot which is overlain with a fibrin matrix. This clot re-establishes haemostasis, serves as a matrix for cell migration, limits microbial entry into the tissue and holds tissue in place so healing can proceed (281, 282). Platelets play a key role in clot formation but also in initiation of the healing response via release of mediators such as platelet derived growth factor (PDGF), Epidermal growth factor (EGF) and transforming growth factor beta 1 (TGFβ1) which serve as chemoattractants and or stimulate epidermal and fibroblast proliferation and migration (283-286). Recent research suggests that another important molecule in initiation of wound healing is Hsp90α (287). This work by Cheng et al (2011) indicates that Hsp90α is released early in wound healing in response to tissue damage and stimulates migration firstly of keratinocytes then fibroblasts and endothelial cells. Hsp90α is regulated by HIF-1α which is expressed throughout wound healing and is known to also regulate genes involved in angiogenesis (288, 289). Correspondingly application of a fragment of Hsp90α greatly accelerated wound healing (287).

Within hours neutrophils appear at the edge of the wound, attracted to damaged tissue in response to activation of complement, degranulation of platelets, and bacteria (290). Neutrophils act to clear infection or foreign tissue and then apoptose and are phagcytosed by infiltrating macrophages (291). They also deposit basement membrane components as they migrate through the wound (292). Monocytes infiltrate the wound and become activated macrophages which dominate the wound by 72hours. Macrophages release more growth factors such as PDGF and VEGF which lead to granulation tissue formation (281). Macrophages also release other proinflammatory cytokines such as TNF-α, and other molecules like IL-1, TGFβ, and Insulin like growth factor I (IGF-I) which increase growth factor expression and further stimulate re-epithelialisation (293, 294).

The second stage of repair fibroblasts, epithelial and endothelial cells migrate and proliferate to fill the wound (292). Hsp90α, growth factors and cytokines such as TGF-β,EGF, PDGF, FGF, IL-1, Il-6

released from platelets, immune cells (particularly macrophages) and activated endothelium stimulate proliferation and migration of cells (294, 295). Epithelialisation of wounds begins within hours and by 3-7 days spurs of epithelial cells from the wound edges have fused in the midline beneath the scab to reform a thin epithelial layer. Epithelial cells migrate through the wound in such a manner that they dissect the wound between viable and eschar tissue (281). Subsequently epithelial cells proliferate to thicken the epidermal layer and reconstitute the original architecture. It has been shown that hepatocyte growth factor (HGF) signalling in keratinocytes in particular is a requirement for normal re-epithelialisation (296). HGF binds to and activates the MET receptor and mice with keratinocyte MET deletion had strongly delayed re-epithelialisation. It was further found that the keratinocytes which eventually reformed the epithelial layer contained functional MET and thus escaped MET deletion, suggesting an absolute requirement for MET signalling. FGF and EGF growth factors also positively regulate epithelialisation (294). Beneath the regenerating epithelium the granulation tissue which began to invade the wound around day 3 fills the incisional space by day 5 (292). This granulation tissue is composed of fibrous connective tissue with inter-dispersed fibroblasts, macrophages and new blood vessels. By day 5 collagen fibrils begin to branch the wound. Macrophages along with other cell types are thought to supply a continuing source of growth factors such as PDGF, TGFβ1 and VEGF which support fibroblast and blood vessel proliferation (281, 284, 297).

Fibroblasts are responsible for the synthesis, deposition, and remodelling of the extracellular matrix (292). Fibroblasts gradually replace the provisional matrix of fibrin, fibronectin and hyaluronic acid with collagen. Once sufficient collagen deposition has been achieved cells within the granulation tissue undergo apoptosis. During the second week of healing fibroblasts differentiate into myofibroblasts, and it is these cells which are key to contraction and compaction of the wound (295). Contraction appears to require TGFβ1 and β2 and again PDGF, and progresses when cross linkage between collagen filaments is present (298-300). For contraction to proceed there must be low turnover of collagen and this is achieved through the action of matrix metalloproteinases (MMPs). MMPs are secreted by a number of cell types including macrophages, epidermal cells, endothelial cells and fibroblasts and are expressed throughout wound healing (281, 292, 301). Tissue inhibitors of matrix metalloproteinases (TIMPs) are able to regulate the activity of MMPs and are also expressed throughout wound healing. Elevated MMP expression is associated with chronic wounds and an increased MMP9/TIMP-1 ratio correlates negatively with healing (302, 303). Importantly though, effective wound healing requires controlled degradation of ECM in order for cell migration, epithelialisation, angiogenesis and remodelling to proceed (304-307). Correspondingly the use of

non-specific MMP inhibitors has been shown to reduce keratinocyte migration and myofibroblast function in rat wounds, or delay epithelialisation in human skin, resulting in delayed healing (308-310). Wounds have around 20% of their final strength at three weeks and remodelling continues in the following months to achieve a maximal tensile strength of 60% of the original tissue (311, 312). Over this period the ECM is remodelled from mainly collagen type III to one composed of predominantly collagen type I (313).

1.10.2 The innate immune system in wound healing

Neutrophils and then macrophages migrate into the wound in response to injury and are thought to play a key role in wound healing in aseptic conditions (292). Only when infection has been eliminated and repair is completed will these cells disappear from the wound site. The primary function of neutrophils in particular is thought to be the elimination of invading microbes (291). Neutrophils achieve this role via phagocytosis of infectious agents although in the process often release free radicals which lead to death of host cells. Importantly, elimination of neutrophils in sterile conditions did not impair healing and in fact increased healing speed (314, 315).

Macrophages which arrive in the wound shortly after neutrophils operate to remove cell debris, fibrin matrix and spent neutrophils (316). Defective macrophage phagocytosis has been postulated to play a role in impaired persistence of inflammatory neutrophils in diabetic wounds, and macrophages are known to propagate inflammation in the sodium lauryl sulphate skin inflammation model (317, 318). As mentioned macrophages also produce a number of cytokines and growth factors which are thought to play an important role in regulation of fibroblasts and angiogenesis (281). Elimination of macrophages was shown in early experiments to delay removal of damaged cells, fibrin and tissue debris (316). However the importance of macrophages in repair in sterile conditions with a concurrent lack of neutrophils has recently come into question. PU.1-null mice, which lack both neutrophils and macrophages, show slightly increased rates of re-epithelialisation and heal without fibrosis (319). These mice did have delayed clearance of cell debris but in the absence of neutrophils this did not delay healing. Wound healing in mouse embryos is also known to occur without a functional immune system and again without scarring (320). Importantly these studies were performed in sterile conditions and in neonatal antibiotic treated mice in the case of the PU.1-null animals.

The importance of macrophages in normal adult wound healing were recently confirmed using Diphtheria toxin (DT) mediated elimination of macrophages, although this would also be expected to

impair neutrophil clearance in the early phase . LysM-DT mediated macrophage deletion throughout wound healing resulted in increased neutrophils, delayed healing, disturbed angiogenesis and increased MIP-2, MCP-1 and IL1β expression (321). Blood monocyte accumulation was not assessed specifically in this study. Cd11b –DT mediated macrophage deletion led to delayed re-epithelialisation, reduced collagen deposition, impaired angiogenesis, increased TNFalpha and reduced TGFβ1 in wounds (322). Of note monocyte and neutrophil accumulation in wounds still occurred. A third study looked at the effect of macrophage deletion in early, mid or late wound healing (323). Monocytes were depleted 24 hours after macrophages in this model. It was found that elimination of macrophages in the early inflammatory phase (Day -1 to 5) led to reduced vascularisation of granulation tissue, delayed epithelialisation, reduced wound contraction but reduced scar formation. Deletion of macrophages in mid wound healing resulted in reduced granulation tissue maturation with concurrent haemorrhage, fibrin and serum exudates from newly formed blood vessels into the wound. Subsequently, increased endothelial apoptosis was demonstrated. A significant reduction in VEGF and TGFβ was also evident. Wound contraction was also ablated and epithelial wound edges became atrophic. Importantly in instances where epithelialisation was complete no increase in neutrophils was observed, but increased haemorrhage was still present. Deletion of macrophages late in wound healing (day 9-14) did not appear to inhibit wound maturation, although tensile strength was not assessed.

The results of these studies suggest firstly that neutrophils are not required for wound healing in aseptic conditions. Secondly, macrophages are required in a host with normal immune function in early and mid wound healing for wound healing to progress at a normal speed in terms of epithelialisation, granulation tissue angiogenesis and wound contraction. And that these functions can deteriorate in mid wounding in some cases in the absence of increased neutrophils. This data also suggests the increased wound healing speed facilitated by macrophages comes at a cost of increased scarring. These studies are consistent with the fibrotic role of liver macrophages in the carbon tetrachloride model of liver fibrosis, although a role for liver macrophages in matrix degradation after fibrosis was also demonstrated and not thoroughly assessed in these wound healing studies (127).

1.10.3 **Impaired wound healing and innate immune dysfunction in diabetes.**

An increasingly common cause for impaired wound healing is diabetes, this impaired healing can progress to a chronic wound (282, 324). In fact it was found that HbA1c was the best predictor of wound healing speed in a panel of patient characteristics (325). Due to impairments in wound healing chronic wounds in the form of ulcers can occur in up to 15% of diabetic patients (326). An unhealed wound is then a portal to infectious agents which can lead to sepsis and subsequent amputation. Importantly ulceration preceeds approximately 84% of lower leg amputations in diabetic patients (327). The global factors leading to this delay in wound healing include repeated trauma to the wound due to loss of sensation and ischemia (282, 324). In addition multiple impairments occur in models of diabetic wound healing throughout all phases of healing and include defective cell function, decreased angiogenesis, impaired epithelialisation, impaired keratinocyte proliferation and migration, decreased collagen content and impaired cytokine and growth factor production (317, 328, 329).

In terms of impaired cellular components, impaired macrophage function has been demonstrated in terms of phagocytic clearance of necrotic tissue (317). Studies have demonstrated impaired chemotaxis, phagocytosis and killing of bacteria in diabetic polymorphonuclear cells and monocytes/macrophages compared to normal controls (330-332). Accumulation of macrophages has been reported in chronic diabetic ulcers and in wounds of Ob/Ob mice (333-335). In a primate model of diabetes macrophages were initially decreased but both neutrophils and macrophage numbers failed to decrease by week 4 (336). In the chronic diabetic wound the idea of excessive inflammation appears to be supported by increased numbers of inflammatory cells with an absence of cellular growth and migration over the wound (335, 337). Impaired innate immune system function in diabetic patients may also impact wound healing through increased infection, an important source of morbidity in diabetic patients (338). An important factor in infection is the decreased immune function in diabetic patients (331). Correspondingly bacterial infection has been shown to correlate negatively with diabetic ulcer healing, and persistent infection would also prolong the inflammatory phase (339). In addition fibroblasts at the diabetic wound site have impaired proliferation and differentiation (340, 341), while chronic wound keratinocytes at the callus exhibit impaired migration, hyperproliferation and reduced differentiation (342-344). Endothelial progenitor cell (EPC) function is also compromised in diabetic patients and contributes to impaired angiogenesis in diabetic wounds (345-347). Importantly stromal cell-derived factor-1α has been shown to mediate EPC recruitment from bone marrow progenitors to wounds, and decreased levels are found in

diabetic patients (347). Also mobilisation of EPCs from bone marrow is impaired due to decreased hypoxia response and decreased VEGFA release from ischaemic wound fibroblasts, macrophages and epithelial cells (327, 348, 349). Mobilisation of bone marrow EPCs via hyperoxia and subsequent homing to wounds by application of SPF-1α was correspondingly shown to improve wound healing in diabetic mice (347). VEGF is a potent stimulator of all steps in angiogenesis including; degeneration of extracellular matrix of old vessels, migration and proliferation of capillary endothelial cells (350).

A number of key growth factors are decreased in chronic wounds of diabetic patients including IGF-1, TGFβ1 and PDGF (351-353). Decreased levels of these growth factors have also been found in acute wounds of diabetic wounds of mice and application of these agents to diabetic animal models accelerates healing (354, 355). IGF-1 is involved in epithelialisation, keratinocyte and fibroblast proliferation and endothelial cell chemotaxis (281). However the role of transforming growth factor beta 1 (TGF-β1) which has important functions throughout wound healing including chemotactic, growth factor stimulating, angiogenesis and ECM deposition is more complex (285). As evidenced in a model of constitutive expression of TGF-β1 in keratinocytes, in which a delay in wound healing was found concurrently with increased inflammation (356). A putative negative regulator of TGF-β1, TGF-β3, has also been found to be increased in diabetic foot ulcers (352). Platelet derived growth factor (PDGF) is another growth factor which is expressed throughout wound healing and serves multiple functions including; chemotactic, growth factor secretion and production of ECM components (284). Keratinocyte growth factor (KGF) involved in epithelialisation. Nerve growth factor (NGF) in involved in keratinocyte and endothelial proliferation, neutrophil survival and monocyte differentiation (324). Both KGF and NGF, are reduced in diabetic human wounds and animal wound models (357-360). While growth factors have been found to be decreased, a prolonged expression of inflammatory cytokines TNF-α, IL-1β and chemokines MCP-1 and MIP-1α has been reported in ob/ob diabetic mice (335). However, leptin receptor deficiency also impairs immune function and no increase in TNF-α in streptozotocin treated acute mouse wounds were found (361, 362). In fact a decrease in IL-6 at later time points of healing was reported. In diabetic rabbits IL-6 and IL-8 were found to be increased in skin basally compared to control animals. However expression of these cytokines and their receptors failed to increase after wounding as is the case in non-diabetic control animals (363). As mentioned, patients with diabetes also display impaired angiogenesis with insufficient activation of angiogenesis. This may be attributable in part to reduced proangiogenic factors TGF-β1, VEGF and bFGF in diabetic models. Correspondingly treatment of mice with VEGF or bFGF accelerated wound healing while increasing angiogenesis in diabetic animals (364, 365).

Generation of reactive oxygen species (ROS) is important for elimination of invading organisms from the wound (366). However, recent studies suggest elevated ROS impair proper angiogenesis (367). In normally healing wounds ROS peaks in the early inflammatory phase then declines. Impaired wound healing is associated with persistence of elevated ROS within the wound (366), this is likely attributed in part to the increased inflammation observed in chronic diabetic wounds. However, ROS generation is required for optimal wound healing as mice lacking the ability to produce superoxide also display impaired wound healing (368). Nonetheless, decreased levels of the key cellular antioxidant glutathione are found in wounds of mice with diabetes and in human diabetic ulcers, and topical glutathione application accelerated wound healing in diabetic mice (369).

There have been a number of ECM alterations documented in diabetic patients and diabetic wounds which contribute to impaired wound healing. For example the collagen content of normal skin and wounds of diabetic animals has been found to be reduced (370, 371). These lower levels have been associated with decreased synthesis by fibroblasts (324, 372-374). Added to this ECM components become glycated in the presence of high glucose and that this glycation disrupts assembly and fibroblast attachment (375, 376). A number of studies have also shown increased levels of MMPs in chronic diabetic wounds including MMP-2, MMP-8 and MMP-9 with a corresponding decrease in TIMP expression, this environment favours ECM breakdown and would disrupt ECM deposition as well as decrease the availability of growth factors (301-303, 324). Elevated inflammatory cytokines such as TNF-αa in chronic wounds could decrease the amount of TIMP synthesised by fibroblasts and could thus contribute to the imbalance, while reduced TGF-β1 which enhances TIMP production and is decreased in diabetic wounds may also play a role (335, 377-379).

In the past decade evidence has accumulated for the importance of HIF-1α in wound healing. It has been shown that HIF-1α activity is reduced at high glucose concentrations in human fibroblasts and diabetic animals (380-383). HIF-1α expression was also found to be decreased in human diabetic ulcers and with increasing age in db/db mice (383, 384). Artificially elevating the level of HIF-1α through desferoxamine (DFO), $CoCl_2$ or constitutively active HIF-1α producing constructs lead to improved wound healing in models of diabetes (381, 382). Interestingly IGF-1 was also found to regulate HIF-1α expression in db/db mice, and treatment with recombinant IGF-1 resulted in increased HIF-1α and improved wound healing (240). HIF-1α mediates its effects on wound healing in part by increasing expression of VEGF in response to hypoxia in fibroblasts (380). Importantly DFO treatment of mouse wounds led to increased angiogenesis and granulation tissue. In addition high

glucose has been found to induce a defect in HIF-1α transactivation and reduce binding to the coactivator protein p300. This was mediated through covalent modification by methylglycoxal at high glucose concentrations (380). In support of a role for HIF-1α in endothelial cell mediated angiogenesis it has also been reported that deficiency of either HIF-1α or its partner ARNT in endothelial cells delayed wound healing, reduced vascularisation and reduced EPC mobilisation to wounds (385). HIF-1α is also known to regulate the release of Hsp90α by human dermal fibroblasts in response to ischaemia (386). In line with decreased HIF-1α in diabetic wounds treatment of mice with the F -5 peptide fragment of Hsp90alpha was shown to greatly increase wound healing speed in diabetic animals, although not to normal healing speeds (287). The importance of HIF-1α in innate immune function was shown by Cramer et al (238) who found decreased immune function in mice with myeloid cell deletion of this gene. Subsequently it was found that HIF-1α was important in regulating apoptosis, phagocytosis and bacterial killing which has similarities with the diabetic innate immune phenotype (238, 266, 267). It is clear that increasing the levels of HIF-1α and its products have been shown to improve wound healing speeds, and importantly the agents used to increase HIF-1α have not been specific. The levels of HIF-1α may be decreased in other cell types, including myeloid cells, in the diabetic environment and further contribute to impaired wound healing.

1.11 Conclusions

The results of numerous studies support a role for ARNT and its partners in the function of the liver. These processes include lipid accumulation, glucose homeostasis, inflammation and fibrosis. However many of the models employed to investigate the role of the HIF's use acute adenoviral mediated deletion of Vhl which results in non-physiological elevation in the levels of the HIFs. In addition HIF in this situation would still be modified, having been hydroxylated on proline and asparagines residues which is known to affect function (236). The result of long-term reduction in liver ARNT remains unknown.

It is also clear that ARNT in myeloid cells is likely to play a role in innate immune function. And that innate immune function can impact upon whole body metabolism and contribute to the diabetic phenotype. In addition it is clear that innate immune function is involved in adult wound healing in aseptic conditions, and that reduced HIF-1α plays a role in normal healing which is compromised in diabetes and with increasing age.

1.12 Hypothesis and aims

At the beginning of this thesis it was known that ARNT was reduced in the islets of patients with Type 2 Diabetes and was essential for normal islet function. It was hypothesised that ARNT may be regulated during the course of metabolic disease and also contribute to tissue dysfunction. More specifically

1) ARNT may be reduced in the liver of patients with metabolic disease and this long-term decrease in ARNT could contribute to or reduce the development of Non-alcoholic fatty liver disease, Non-alcoholic steatohepatitis and liver fibrosis.

2) Liver ARNT may also contribute to metabolic dysfunction of the liver and the diabetic phenotype.

It was also known that loss of HIF-1α in cells of the innate immune system impaired immune function in animal models but the role of its partner ARNT was not known.

3) ARNT may play a role in innate immune function.

4) ARNT may play a role in innate immune function in diabetes and also contribute to the diabetic phenotype.

1.12.1 **Aims**

To create the hepatocyte-specific *ARNT*-knockout (LARNT) mouse line by using the Cre-LoxP system with Cre expression under control of the albumin promoter and

1) To characterise LARNT mice on chow diet in terms of markers of Non-alcoholic fatty liver disease, Non-alcoholic steatohepatitis and whole body metabolism of glucose and lipids.

2) To characterise LARNT mice in the High Fat Diet model of Type 2 Diabetes including; assessment markers of Non-alcoholic fatty liver disease, Non-alcoholic steatohepatitis and whole body metabolism of glucose and lipids.

3) To characterise LARNT mice in the thioacetamide model of liver fibrosis in terms of collagen production and histology.

To create the myeloid-specific *ARNT*-knockout (LAR) mouse using the Cre-LoxP system with Cre expression under control of the LysM promoter and

1) Characterise LAR mouse immune function and wound healing in terms of; Gene expression, phagocytosis, bacterial killing, in vivo models of immune function and wound healing.

2) To characterise metabolism of LAR mice on chow and in the high fat model of Type 2 Diabetes including; Assessment of markers of Non-alcoholic fatty liver disease, Non-alcoholic steatohepatitis and whole body metabolism.

Chapter 2. Materials and methods

2.1 Buffers and solutions

Chemicals and other reagents were purchased from Sigma-Aldrich (Australia) unless otherwise specified.

Acid ethanol

1 % 1 M HCl

Made up with 70 % ethanol

Bovine calf serum (BCS)

Bovine calf serum (Hyclone, USA) was heat inactivated for 30 minutes at 56 °C before use.

Cell lysis buffer

10 mM	Tris-HCl
1 %	Triton X-100
0.5 %	NP-40
150 mM	Sodium chloride
10 mM	Sodium phosphate
100 mM	Sodium fluoride
1 mM	EDTA
1 mM	EGTA
10 mM	Sodium orthovanadate
10 mM	Sodium orthophosphate

One tablet per 50 ml of Complete protease inhibitor cocktail tablets (Roche, Germany) was added and pH 7.4.

DNA isolation buffer

670 mM	Tris pH 8.8
166 mM	Ammonium sulphate
65 mM	Magnesium chloride
10 %	β-mercaptoethanol
5 %	Triton X-100

Kreb's buffer

115 mM	Sodium chloride
4.7 mM	Potassium chloride
1 mM	Magnesium sulphate
1.2 mM	Potassium sulphate
25 mM	Sodium bicarbonate
1 mM	Sodium pyruvate
10 mM	Hepes
pH 7.4	

Phosphate buffered solution (PBS)

3.6 %	Disodium hydrogen orthophosphate
0.2 %	Potassium chloride
0.24 %	Potassium dihydrogen orthophosphate
8 %	Sodium chloride

Red Blood Cell Lysis Buffer (RBC lysis buffer)

8.29g	NH_4Cl
1g	$KHCo_2$
200µl	EDTA

Made up to 1L in distilled water

RIPA cell lysis buffer

0.5 %	Sodium deoxycholate
10 mM	Hepes
1 %	NP-40
0.1 %	SDS
pH 7.4	

RPMI media

10%	BCS
2 mM	L-glutamine

Made in Roswell Park Memorial Institute-1640 medium (RPMI-1640, Invitrogen, USA).

Minimal essential media (MEM)

10%	BCS
2 mM	L-glutamine
25 mM	Hepes

Made from MEM powder from

High glucose minimal essential media (MEM)

10%	BCS
2 mM	L-glutamine
25 mM	Hepes
+ 19mM	Glucose

Made from MEM powder from

DMEM media low glucose

10%	BCS
2 mM	L-glutamine
5mM	Glucose

Added to 0mmol/L Dulbecco's Modified Eagle Medium (DMEM, Invitrogen, USA).

DMEM media high glucose

10%	BCS

2 mM	L-glutamine
25mM	Glucose

Added to 0mM glucose Dulbecco's Modified Eagle Medium (DMEM, Invitrogen, USA).

Sirius Red Stain

0.1%	Direct Red 80
0.1%	Fast Green FCF

Made up in 1.3 % Saturated picric acid solution.

Perl's stain

Solution A

20%	Aqueous Hydrochloric Acid
20ml	Hydrochloric acid, 1M
80ml	Distilled water

Solution B

10%	Aqueous Solution of Potassium Ferrocyanide
10g	Potassium ferrocyanide, Trihydrate
100ml	Distilled water

Milligan's Trichrome stain solutions

Solution A

2.25g	Potassium dichromate
2.25ml	Hydrochloric acid
25ml	Ethanol, 95%
75ml	Distilled water

Solution B

0.1g	Acid fuchsin
100ml	Distilled water

Solution C

1g	Phosphomolybdic acid

100ml	Distilled water

Solution D

2g	Orange G
1g	Phosphomolybdic acid
100ml	Distilled water

Solution E

1ml	Acetic acid, glacial
100ml	Distilled water

Solution F

0.1g	Fast green FCF
0.2ml	Acetic acid, glacial
100ml	Distilled water

Todd Hewitt broth (THB) media

Todd Hewitt broth (Sigma, Australia) was made up as per manufacturer's instruction. THB agar was made with the addition of 15g of Agar per Litre. Solutions were sterilised by autoclaving before use.

Reducing sample buffer

75%	distilled water
2%	SDS
0.0625 mol/L	Tris-HCl pH 6.8
25%	glycerol
0.5%	bromophenol blue
0.5 ml	2MeOH

Streptozotocin buffer (Strep Buffer).

0.1M Citric Acid	(A)
0.1M Sodium Citrate	(B)

28mls (A) added to 25.5mls (B) made up to pH 4.21 in distilled water.

Transfer buffer

20%	methanol
0.1 mol/L	Tris
80 mmol/L	Glycine
1mmol/L	$NaPO_4$

Western SDS running buffer

3g	Tris
14.4g	Glycine
1g	SDS

Made up in 1000mL deionised water

2.2 Cell culture

2.2.1 Cell lines

HuH7 and RAW cell lines were maintained in a tissue culture incubator with 5% CO_2 at 37 °C. Cells were passaged as needed at 70-80% confluence by washing with PBS then incubation with 0.05% trypsin-EDTA (Invitrogen, USA) for 5 minutes at 37 °C. Trypsin was neutralised by the addition 2 x the volume of complete media and cells were divided into new flasks. HuH7 cells were maintained in MEM media. For experiments using high glucose cells were maintained in MEM with high glucose. RAW cells were maintained in DMEM with high or low glucose.

2.2.2 Bacteria

Group A streptococcus (GAS) were a gift from St Vincent's Hospital Pathology. Cells were grown in THB in stationary cultures overnight at 37°C. Cultures were grown to logarithmic phase OD 600 = 0.6 for the GAS infection study. Isolated bacteria were grown on THB agar plates overnight at 37°C.

2.3 Animals

All animals received humane care according to the criteria outlined in the "Australian code of practice for the care and use of animals for scientific purposes" prepared by the National Health and Medical Research Council (2004).

2.3.1 **Mouse lines**

The LAR and LARNT lines are tissue specific Aryl-hydrocarbon Receptor Nuclear Translocator (ARNT) knockout mice generated on a C57Bl/6 background using the Cre-lox system. Cre-lox recombination involves the targeted splicing of a specific DNA sequence using a site specific Cre recombinase in order to create a tissue-specific knockout. Exon 6, encoding the conserved basic-helix-loop-helix domain of the protein ARNT was flanked by *lox-p* sites (flox) and introduced into the *ARNT* gene by standard gene disruption techniques using embryonic stem cells to produce homozygous ARNT *flox/flox* mice (387).

2.3.1.1 **LARNT mice**

To create the hepatocyte specific ARNT knockout mice (LARNT) floxed ARNT mice were interbred with mice expressing *Cre*-recombinase under control of the albumin promoter (Alb-*Cre*) (a kind gift from David James, obtained from Jackson laboratories, Boston). Alb -Cre is expressed in hepatocytes. Mice were generated to be homozygous for floxed *ARNT* and either heterozygous or wild type for Alb-*Cre.* Alb-*Cre* positive ARNT *flox/flox* mice are hepatocyte ARNT knockout animals (LARNT), and Alb-Cre negative ARNT flox/flox mice are floxed controls (FC). Only one copy of *Cre* is required to produce the hepatocyte-specific phenotype, thus the phenotype is inherited in an autosomal dominant manner. Mice were C57Bl/6 for more than 12 generations to ensure genetic homogeneity. *Arnt* mRNA expression in FC compared to LARNT mice is shown in Figure 3.1b. An example of ARNT protein expression in FC compared to LARNT animals is shown in Figure 2.1**.**

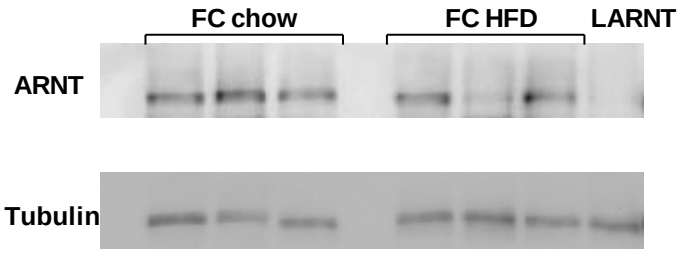

Figure 2.1 ARNT protein expression by western blot in LARNT animals.
An example of ARNT protein expression in a LARNT mouse is shown. In this western blot ARNT protein was assessed in female FC chow fed (FC chow) and HFD fed animals (FC HFD). Protein from a LARNT animal was run as a control (LARNT). Alpha Tubulin (Tubilin) was used as a loading control.

2.3.1.2 LAR mice

To create the myeloid specific ARNT knockout mice (LAR) floxed ARNT mice were interbred with mice expressing *Cre*-recombinase under control of the lysosome M (LysM) promoter (LysM-*Cre*), which is expressed in myeloid cells (388). As above, mice were generated to be homozygous for floxed *ARNT* and either heterozygous or wild type for LysM-*Cre.* LysM-*Cre* positive ARNT *flox/flox* mice are myeloid cell ARNT knockout animals (LAR), while LysM-Cre negative ARNT flox/flox mice are floxed controls (FC). As above, mice were C57Bl/6 for more than 12 generations to ensure genetic homogeneity.

2.3.2 Housing

Animals were housed in the Biological Testing Facility at the Garvan Institute of Medical Research, which employs a 12 hr on-off light cycle (0700-1900 on, 1900-0700 off). Mice were housed in standard filtered boxes, sterilised bedding was used.

2.3.3 Feeding

2.3.3.1 Chow

LAR and LARNT mice were provided with standard chow food containing 59.9 %, 26.7 % and 13.4 % calories from carbohydrate, protein and fat respectively (Agrifood technology, Australia) unless otherwise stated and water *ad libitum.*

2.3.3.2 **Hugo's high fat diet**

The Hugo's High Fat Diet (HFD) was prepared according to Rodent Diet D12451 from Research Diets Incorporated. The ingredients are as follows:

261 g	Casein
230 g	Sucrose
193 g	Starch
51 g	Bulking mineral mix
14.8 g	Trace minerals
57 g	Bran
3.4 g	Methionine
23 g	Gelatine
4.6 g	Choline bitartrate
29.6 g	AIN Vitamin Mix 76A (ICN Biomedicals, Australia)
68 g	Safflower oil
500 g	Melted Allowrie lard

Dry ingredients were mixed thoroughly before addition of oil and lard.

Water was provided *ad libitum*.

2.3.4 **Genotyping**

Genotyping for *Cre* and *Arnt* were performed by PCR and separation on 1.5 % agarose gels using genomic DNA from tail tips. Tips were digested overnight in 200 µl DNA isolation buffer with 0.5 µl proteinase K (Roche, Germany) at 65 °C. PCR was performed using standard protocols with 5 µl of GoTaq Master Mix Taq polymerase (Promega, USA), 1 µl of DNA solution, 2 µl of *Cre* or *Arnt* primers, and 2 µl of *Irs-2* primers (control). *Irs-2* primers were included in every *Cre* genotyping reaction as a positive control which confirmed successful DNA amplification for *Cre* negative samples. For primers and PCR program is shown below. Example PCR gels, performed by Kuan Cha, are shown in Figure 2.2.

Cre and ARNT genotyping

Primers:

Arnt forward: TTCTTTTGGGTGGATGATTTTT

Arnt reverse: GAGGGAGGGGAAAAGAAAGG

Cre forward: AGGTGTAGAGAAGGCACTTAGC

Cre reverse: CTAATCGCCATCTTCCAGCAGG

Irs-2 forward: GTAGTTCAGGTCGCCTCTGC

Irs-2 reverse: TTGGGACCACCACTCCTAAG

PCR program:

Initial melt step 5 minutes at 95 °C

35 cycles

- Denature 45 seconds at 95 °C
- Anneal 45 seconds at 60 °C
- Extend 45 seconds at 72 °C

Final extension 6 minutes at 72 °C

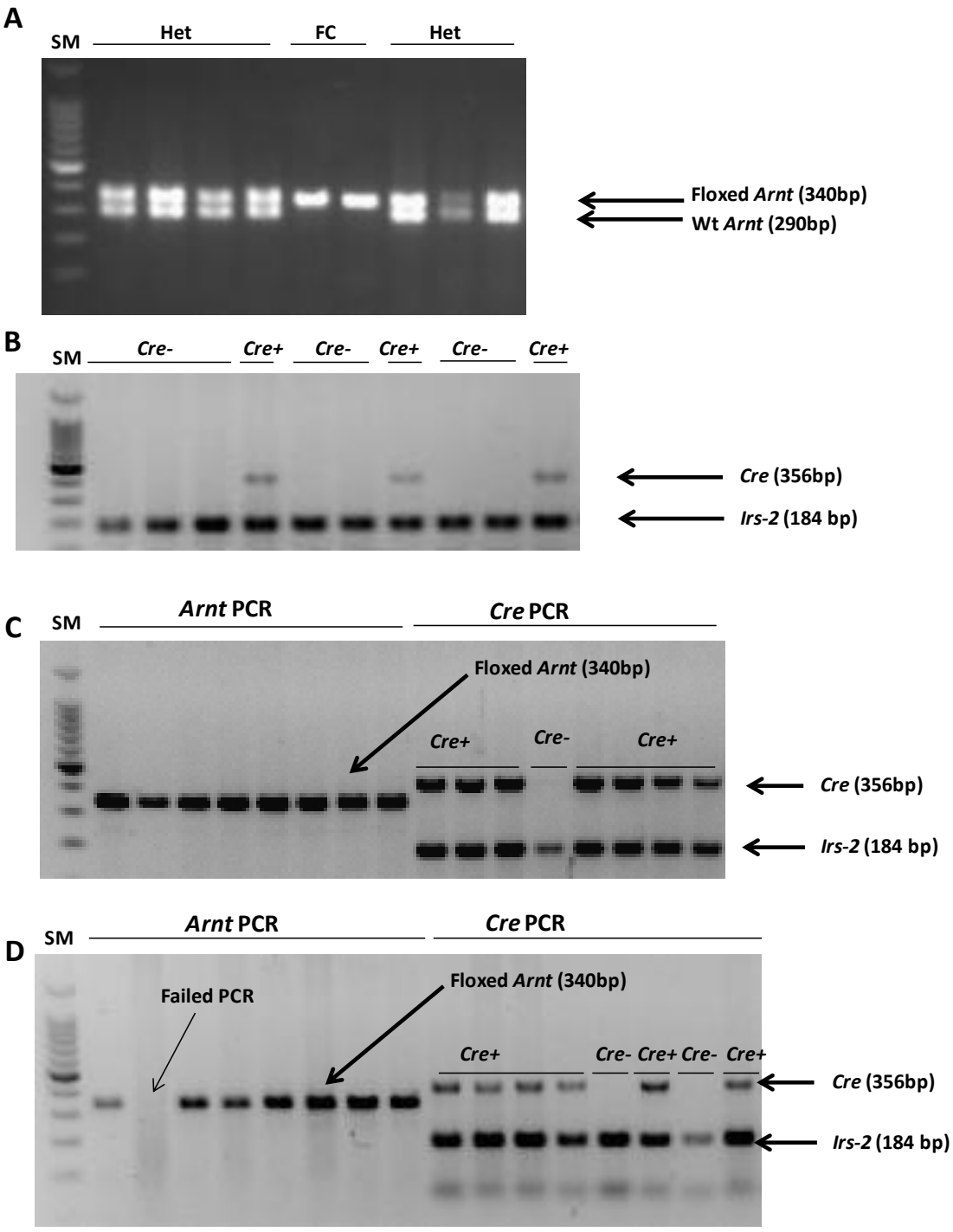

Figure 2.2 Example PCR gels

(A) An example gel from the *Arnt* pcr. PCR of animals containing a floxed *Arnt* allele results in a product of 340 bp. PCR of animals containing the wild-type allele (Wt) produced a product of 290bp. **(B)** An example gel from the *Cre* PCR. The *Irs-2* PCR was used as a control of PCR quality and produced a product of 184bp. Animals were either positive (*Cre+*, product at 356bp) or negative for *Cre* (*Cre-*). **(C)** Example gel from LARNT line genotyping with *Arnt* and *Cre* PCR. All animals contain 2 alleles of floxed ARNT and are either positive or negative for *Cre*. **(D)** Example gel from LAR line genotyping with *Arnt* and *Cre* PCR. All animals contain 2 alleles of floxed ARNT and are either positive or negative for *Cre*. In lane 2 of the ARNT PCR the PCR has failed and no product is present. Standard DNA marker (SM), Floxed control (FC), Heterozygote *Arnt* (Floxed *Arnt*/ Wt *Arnt* = Het).

2.4 *In vivo* experiments

2.4.1 Metabolic tests

2.4.1.1 Glucose tolerance tests

LARNT mice were fasted overnight for 16 hours. LAR mice were fasted for 6 hours. Glucose was administered at a dose of 2 g/kg by intraperitoneal injection in the form of a 20 % dextrose solution. Tails were nicked with a scalpel blade and blood glucose was measured via the Accucheck Advantage II glucometer (Roche, Australia) prior to, and at 15, 30, 60, 90 and 120 minutes after the dextrose injection

2.4.1.2 Insulin tolerance tests

LARNT mice were fasted overnight for 16 hours. LARNT HFD fed mice and all LAR mice were fasted for 6 hours. Chow fed female mice were injected with 0.25 units of insulin per kilogram. Male and all HFD mice were injected with 0.5 units per kg of Insulin (diluted in 1x PBS with 1% bovine serum albumin) delivered by intraperitoneal injection. Tails were nicked with a scalpel blade and blood glucose was measured via glucometer prior to, and at 10, 20, 30, 45 and 60 minutes after the insulin injection.

2.4.1.3 Pyruvate tolerance tests

Mice were fasted overnight for 16 hours. Pyruvate was administered at a dose of 2 g/kg by intraperitoneal injection in the form of a 20 % pyruvate in PBS solution. Tails were nicked with a scalpel blade and blood glucose was measured via the Accucheck Advantage II glucometer (Roche, Australia) prior to, and at 15, 30, 45, 60 and 90 minutes after the dextrose injection

2.4.2 Tissue collection

2,2,2-tribromoethanol or ketamine+xylzaine was administered by intraperitoneal injection to achieve deep anaesthesia. Tissues were divided for formalin fixation (10% Neutral Buffered Formalin, Australia Biostain PTY LTD), snap-freezing in liquid nitrogen or in OCT (Tissue-Tek, Thuringowa, Australia) for frozen sections.

2.4.2.1 Plasma

After deep anesthesia with 2, 2, 2-tribromoethanol or ketamine+xylzaine 500µl of blood was collected by cardiac puncture and placed in an eppendorf containing 40 µl of 0.5M EDTA. After centrifugation, the supernatants were stored at -80°C.

2.4.2.2 Liver and fat

After metabolic studies LARNT mice were sacrificed after an overnight fast and LAR animals were sacrificed after 6 hours of fasting, unless otherwise specified. Mice were sacrificed at least 1 week after the last test. Liver, epigonadal and subcutaneous fat were collected and weighted before processing samples as described above

2.4.2.3 Skin

Skin samples were obtained from animals with free access to food before sacrifice. Skin samples were divided as described above. For measuring tensile strength mice were de-gloved and skin stored flat at -80°C.

2.4.3 HFD studies

HFD studies were commenced on mice of age 10-12 weeks. Mice were initially weighed and had a baseline glucose tolerance test before commencing on HFD. Mice were weighed weekly and received subsequent metabolic tests before sacrifice and tissue collection as illustrated below (Figure 2.3).

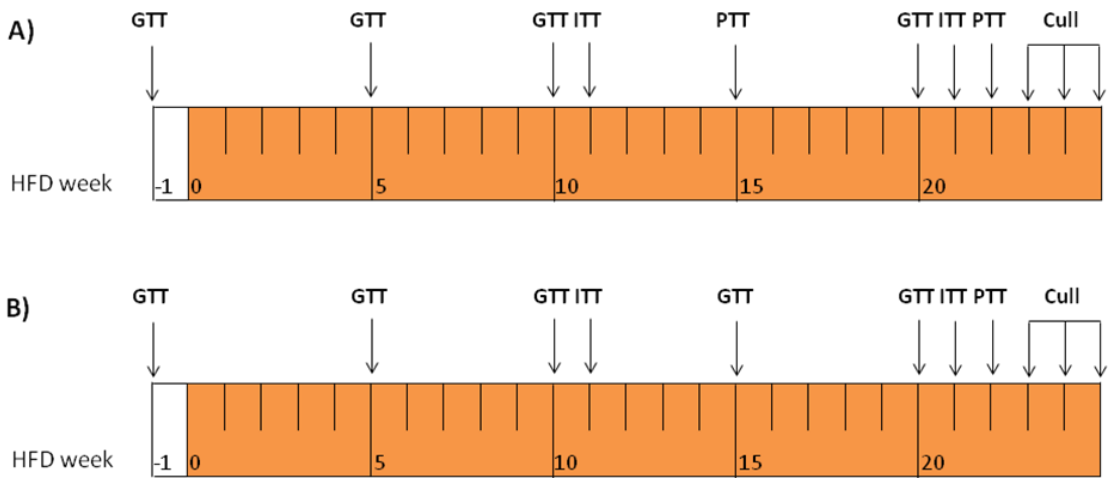

Figure 2.3 HFD timeline.
LARNT mice (A) and LAR mice (B).

2.4.4 Re-feeding studies

For re-feeding studies mice receiving chow diet or HFD (for two weeks) were fasted overnight. Mice were then re-fed with chow or HFD. Six hours later mice were sacrificed and serum and liver collected as described.

2.4.5 Thioacetamide (TAA)-induced liver fibrosis model

LARNT mice at 10 weeks of age were injected twice weekly with 0.15 and 0.056mg/g body weight for 15 weeks. At the end of the study mice were fasted for 6 hours before sacrifice and tissue collection as described.

2.4.6 Skin transplant study

Mice were anaesthetised with inhaled isoflurane and shaved. Skin grafts were taken from Balb/c mice (H-2d) and transplanted onto LysM-ARNT (KO) or floxed-controls (FC) (C57Bl/6, H-2b). Grafts were sex-matched but full-MHC-mismatched. The reciprocal transplant was also performed. Transplant performance was scored blinded to mouse genotype until complete rejection.

2.4.7 GAS study

Mice were anaesthetised with isoflurane, shaved and residual hair was removed with Nair (Church & Dwight, Australia). GAS bacteria were grown to OD 600= 0.6 ($5x10^7$ CFU) as described. The following day mice were weighed and injected subcutaneously on their flank with 50µl of bacteria plus 50µl of sterile THB. Mice were weighed and wounds measured daily. On day 4 (96 hours) final measurements were taken and mice were culled. Whole blood, spleen and wounded skin were taken for bacterial counts. Spleen and skin were homogenized in cold PBS to a concentration of 100mg/ml. Blood was also homogenized and kept on ice. 30ul of homogenates were plated onto THB in serial dilutions and colony forming units calculated.

2.4.8 Skin irritation study

Mice were anaesthetised with isoflurane, shaved and residual hair was removed with Nair. They were left to recover for 3 days. Then 5% sodium dodecyl sulphate (SDS) was then painted onto skin twice daily for 5 days. Mice were then sacrificed and skin was fixed in formalin for histology. Skin was scored blinded to genotype.

2.4.9 Wound healing studies

Mice were anaesthetised with isoflurane, shaved and residual hair was removed with Nair. They were left to recover for 3 days. Mice were again anaesthetised with isolfurane and skin was swabbed with ethanol. Two 0.5cmx0.5cm squares of epidermis and dermis were removed from behind the shoulder blade of each mouse. Mice wounds were then bandaged and assessed every second day by tracing wound margins. Day 0 is taken as the day following wounding as wounds stretched to varying degrees after wounding. Bandaids were removed on day 6. Wounds were collected at day 4 for RNA and histology.

2.4.9.1 Wound healing with diabetes

Mice were rendered diabetic by streptozotocin (STZ) injection 180mg/kg delivered in strep buffer. Mice were considered diabetic if mice had random blood glucose levels of > 15mmol/L on two consecutive days. Wound healing experiments were then conducted as above.

2.4.9.2 Wound healing with DFO and diabetes

Mice were rendered diabetic by Alloxan injection 100mg/kg delivered dissolved in sterile water. Mice were considered diabetic if mice had random blood glucose levels of > 15mmol/L on two consecutive days. Wound healing experiments were then conducted as above with the addition of 20µl of 0.0125µM deferoxamine (DFO) wounds starting at Day 0, then every second day when wounds were assessed.

2.4.9.3 Tensile strength

Non diabetic mice were culled and de-gloved when all wounds had completely healed (day 18 of wounding). Skin was stored in foil at -80 until tensile strength testing. Skin was cut into approximately 1cm x 1cm squares and paddle pops glued to each end to attach at the site of clamping (Figure 2.4). Tensile strength was determined at room temperature. Tissue ends with paddle pops were clamped with an Elf 3400 Tensinometer (BOSE EnduraTec, Minnetonka, MN, USA). Exact cross sectional area was obtained using calipers and Young's Modulus was calculated (Tensile Strength).

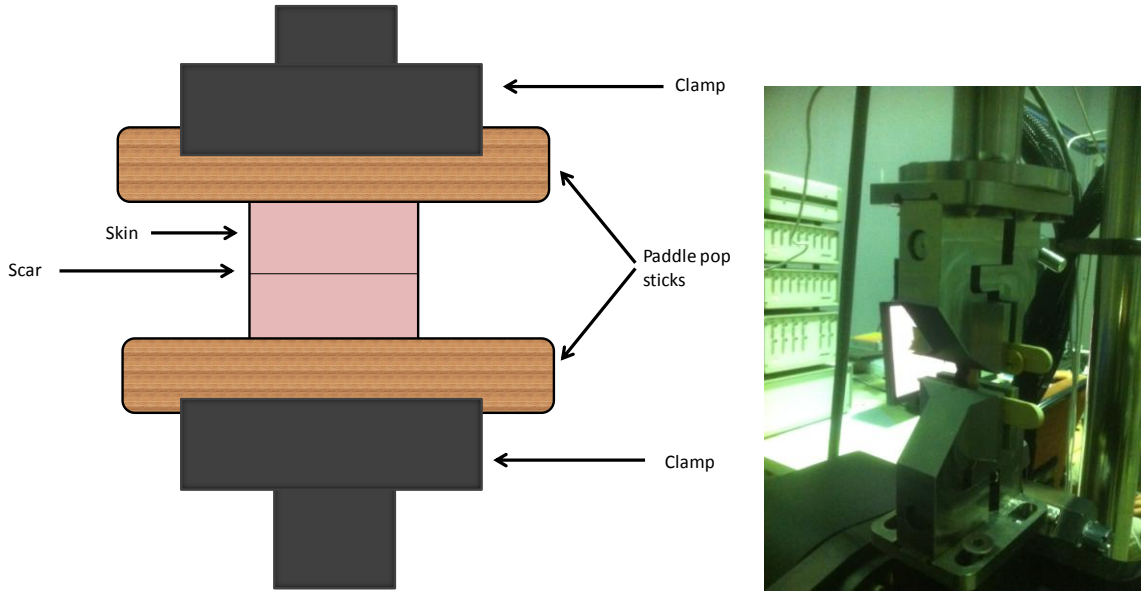

Figure 2.4 Tensile strength testing.
Left shows a schematic of clamp set up in relation to scar tissue. On the right is a picture of the Elf 3400 Tensinometer with skin clamped..

2.5 Primary cell studies

2.5.1 Thioglycollate elicited macrophages

Macrophages were isolated by injection of 2ml of 3% thioglycollate media 4 days before harvest. At day 4 mice were culled by cervical dislocation and 10ml ice-cold PBS was injected and incubated for 1min with agitation. Lavage fluid was removed and cells were resuspended in RPMI media and plated. Non-adherent cells were removed by washing with room temperature PBS and the remaining cells were used in experiments. 100ng/ml of lipopolysaccharide was used to stimulate primary macrophages for 16 hours. Cells were harvested in RLT buffer for mRNA quantification.

2.5.2 Primary hepatocytes

Mice were anaesthetised and the portal vein cannulated. Saline was passed through the liver and the inferior vena cava and abdominal aorta were cut. The cannulated liver was then flushed with Krebs + 0.5mM EGTA. Liver was then pulsed with serum free MEM with 5mmol/L $CaCl_2$ containing Collagenase D at 0.05g/100ml. Liver was removed and diced before passing through a 100micron sieve. Cells were washed in normal media and plated at 1x 10^6 cells per 25cm^2 tissue culture flask.

Isolated hepatocytes were cultured overnight in 25cm^2 flasks in complete MEM medium. The following day cells were washed twice with PBS, and incubated in Krebs buffer plus 0.25 % fatty acid free BSA (Sigma-Aldrich, USA) containing 6mM glucose, 0.125 mM palmitate and 0.25 µCi/ml of [1-^{14}C]-palmitic acid (GE Healthcare, USA) for 24 hours at 37 °C with 5 % CO_2. Filter paper soaked in 5 % KOH was suspended over the cells and the flasks sealed shut. The reaction was stopped by the addition of 500 µl of 40 % perchloric acid. Radioactivity was counted in 4 ml Microscint-20 (Perkin Elmer, USA) using the LS 6500 Scintillation Counter (Beckman Coulter, USA). Results were corrected for total protein using the assay described in 1.9.1

2.5.3 Phagocytosis assay.

Blood was collected via tail bleed into heparin-containing eppendorf tubes. 50ul of blood was placed into v-well plate and incubated with 0.5x10^6 Staphylococcus Aureus bioparticles labelled with BIODIPY FL (Invitrogen, Australia) for 30 minutes. Cells were fixed in 2-4% formaldehyde and red blood cells lysed in RBC lysis buffer. Fixed cells were resuspended in FACS buffer and bacterial uptake assessed by flow cytometry (FACS Calibur, Becton Dickson, Australia). Granulocyte and

monocyte populations were determined by Forward Scatter (FSC) and Side Scatter (SSC) characteristics. Blood granulocytes, which include neutrophils, are characterised by high SSC. Blood monocytes are characterised by lower SSC and higher FSC (Figure 2.5)

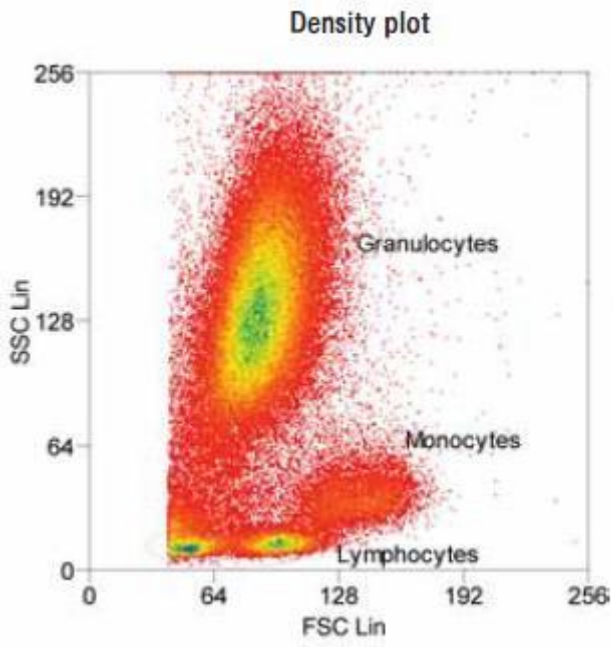

Figure 2.5 (SSC) and FSC characteristics of granulocytes and monocytes.
FSC and SSC characteristics of granulocyte and monocyte populations.
(from http://www.assay-protocol.com/index.php?page=flowcytometry-diagrams).

2.6 Histology

Five µm thick sections were cut from paraffin-embedded, formalin fixed tissues. Sections were incubated at 70 °C for 10 minutes prior to de-waxing with xylene and standard progressive ethanol rehydration. After staining sections were dehydrated and coverslips mounted using GVA Mount non-aqueous mounting solution (Zymed, USA).

2.6.1 Haematoxylin and Eosin staining

After de-waxing sections were

1) Incubated in Haematoxylin (Haematoxylin Instant from Thermo Fisher Scientific) for 1 minute.
2) Rinsed with distilled water.
3) Incubated in 1% Acid alcohol for 10seconds (1M HCL- 4mL and 400mL 70% Ethanol).
4) Rinsed with water from the hot water tap and letting it run from cold to hot (1min).
5) Incubated with 70% ethanol for 1min.
6) Incubated with 95% ethanol for 1min.
7) Incubated with Eosin – 2 quick dips (Eosin Y solution with Phloxine, 1L from Sigma-Aldrich).
8) Incubated with 95% ethanol for 30 seconds.
9) Incubated with 95% ethanol for 1min.
10) Incubated with 100% ethanol for 2min.
11) Incubated with 100% ethanol for 2min.
12) Allowed to dry in oven (1-2min).
13) Coverslipped.

2.6.2 Sirius red

Hydrated sections were stained for collagen in sirius red staining solution for 45 minutes (See Section 1.2).

2.6.3 Pearls stain

Sections were stained for iron using standard Perl's staining solutions described in section 1.2. Solutions A and B were mixed and hydrated slides were incubated in stationary solution for 20min. Sections were counterstained in Nuclear Fast Red solution (Vector Lab Inc, USA).

2.6.4 F4/80 staining

Staining was performed using the DakoCytomation EnVision+ Dual Link System-HRP (DAB+) Kit (Dako, USA) as per manufacturer's instructions. After antigen retrieval Rat F480 monoclonal antibody (Abcam, USA) was diluted 1:100 in Antibody Diluent (Dako, USA). After staining, slides were counterstained using a standard haematoxylin and ethanol dehydration protocol.

2.6.5 Trichrome

Standard Milligan's Trichrome staining was performed using solutions A-F listed in section 1.2.

2.7 mRNA expression

2.7.1 RNA Isolation

Tissues were homogenised using an electric homogeniser (Silent Crusher M, Heidolph, Germany) in RLT buffer (Buffer RLT Lysis Buffer, Qiagen USA), RNA was extracted and purified from stored tissues using a biopolymer shredding spin column (QIAshredder #79654, Qiagen USA) and the RNeasy Mini Kit (#74104, Qiagen) according to the manufacturer's instructions. RNA from cells was obtained by lysing cells in RLT buffer and proceeding immediately to RNA extraction with the RNeasy kit. RNA was quantitated using a nanodrop ND-1000 (Thermo Fisher Scientific, Scoresby, Victoria) RNA was stored at -80°C in sterile RNAse free water.

2.7.2 CDNA synthesis

Complementary DNA was synthesised from 0.5-1 µg of RNA using random hexamer primers and the Superscript III RT kit (Invitrogen, USE) according to the manufacturer's instructions.

2.7.3 Real time PCR

Real time PCR was performed using Sybr Green PCR Master Mix (Applied Biosystems, UK) as per Cheng et al (251) with an ABI 7900HT thermal cycler (Applied Biosystems, UK). A full list of primers can be found in Table 2.1. Primers were designed using Primer 3. After design the primer sequences were blasted using Blastn against genomic mouse and transcript sequences to ensure specificity. After running the RTPCR the reaction product was run on an agarose gel to ensure a single product of the expected size. All results from RTPCR were normalised to the house-keeping gene, TATA box

binding protein (TBP) which did not differ between experimental groups. Fold change of mRNA expression was calculated using the $2^{\Delta\Delta CT}$ method.

2.8 Western immuno-blotting

2.8.1 Protein preparation

Cells were washed with PBS then lysed in cell lysis buffer. Tissue was homogenised in cell lysis buffer. Protein was measured using the *DC* Protein Assay Kit (Bradford, USA) according to manufacturer's instructions.

2.8.2 Western blotting

25µg of sonicated protein was run on an 8% sodium dodecyl sulphate-polyacrylamide (SDS-PAGE) gel in Western SDS running buffer using a Biorad Protein 3 apparatus. Protein was transferred onto a polyvinylidene difluoride (PVDF) membrane using a semi-dry method. Membranes were blocked with 5% skim milk-PBST at RT for 1 hour. Membranes were then incubated on a shaker overnight at 4°C in a solution containing 5% skim milk- PBST plus primary antibody. A 1/500 dilution of ARNT (BD Bioscience Pharmingen, Australia) and a 1/1000 dilution of Alpha Tubulin (Abcam, San Francisco, CA) primary antibody was used. Membranes were washed for 3 x 5min in PBST at room temperature (RT) before incubation with secondary antibodies. Membranes were then incubated with anti-mouse secondary antibodies linked to Horse Radish Peroxidase at a dilution of 1/1000 for 1 hour at RT (HRP, Immunopure Rat IgG thermoscientific). Membranes were again washed for 3 x 5min in PBST before incubation with Western Blot Luminol Reagent (Santa Cruz Biotechnology, Santa Cruz, California, USA) to visualize the protein bands via chemiluminescence on a ChemiDoc XRS (Biorad, Berkeley, California, USA). Alpha Tubulin was used as a loading control and signal intensity were quantitated by densitometry using ImageJ to calculate ARNT protein level relative to Alpha Tubulin level.

2.9 Assays

2.9.1 ATP

Intracellular ATP content was measured using the ATP Bioluminescence Assay Kit CLS II (Roche, Australia. Assay was performed according to manufacturer's instructions and measurement of ATP

was performed using the TopCount NXT (Packard, USA). Results were corrected for total protein as described in 2.5.3.

2.9.2 Triglyceride assay

Liver was homogenized (30-40mg per mouse) and used to determine total liver TG content which was expressed as µg/mg of liver. Serum and liver TG content was assayed using the Roche TG kit (GPO-PAP, Mannheim, Germany). Absorbance was quantitated on SpectraMax™ Plus 384 (Molecular Devices, USA).

2.9.3 Collagen assay quantification

Collagen was quantified by staining liver sections with sirius red solution without Fast green (FCF). The percentage of red staining section (collagen) was calculated using ImageJ software.

2.9.4 Insulin assay

Serum insulin was measured by ELISA (Crystal Chem, USA) as per manufacturer's instructions and absorbance quantified on SpectraMax™ Plus 384.

2.9.5 Alanine transaminase (ALT) and Aspartate aminotransferase (AST) assay.

Plasma ALT and AST levels were assayed by St Vincents Hospital Pathology.

2.10 Statistical analysis

For all figures, error bars indicate ± SEM. For Students t-test, unpaired 2-tailed tests with unequal variance were used, calculated by Excel. For repeated measures ANOVA, results were calculated using PRISM 5. Pearson's correlations were calculated and p-value from 2-tailed analysis also calculated with PRISM 5. For non-parametric data, tests were performed using SPSS (v14). A p-value of < 0.05 was considered significant.

Table 2.1 RTPCR primer list

mRNA	Fwd primer	Reverse Primer
Human ARNT	aacctcacttcgtggtggtc	caatgttgtgtcgggagatg
Human TBP	gttgagttgcagggtgtgg	ctcaaaccaacttgtcaacagc
Mouse Ahr	agcagctgtgtcagatggtg	ctgagcagtcccctgtaagc
Mouse Akt2	cctgaggcttttctcaaacg	cctcagtctcagcctcatcc
Mouse AldoB	agcacctctggctcaacaat	gcttgatggcctctctgaac
Mouse Arnt	tctccctcccagatgatgac	caatgttgtgtcgggagatg
Mouse Cd36	tgctggagctgttattggtc	caacagacagtcaaggct
Mouse Collagen alpha 1	taggccattgtgtatgcagc	acatgttcagctttgtggacc
Mouse Cpt-1	cttccatgactcggctcttc	agcttgaacctctgctctgc
Mouse Chrebp	gcatcctcatccgaccttta	gatgcttgtggaagtgctga
Mouse CXCL1	tggctgggattcacctcgaa	tatgacttcggtttgggtgcag
Mouse Elastin	atcctcttgctcaacctcct	gcccctggataatagactcc
Mouse Fas	gaggacactcaagtggctga	gtgaggttgctgtcgtctgt
Mouse F16bp	gaccctgccatcaatgagta	gttggcggggtataaaaaga
Mouse F480	ctttggctatgggcttccagtc	gcaaggaggacagagtttatcgtg
Mouse G6pase	tcggagactggttcaacctc	acaggtgacagggaactgct
Mouse Gk	gagatggatgtggtggcaat	accagctccacattctgcat
Mouse Glut-1	acctatggccaaggacacac	ctggtctcaggcaaggaaag
Mouse Glut-2	catgctgagctctgctgaag	acagtccaacggatccactc
Mouse Hif1a	tcaagtcagcaacgtggaag	tatcgaggctgtgtcgactg
Mouse Hif2a	ctccaggagctcaaaaggtg	agtgaagctggcaggtcaag
Mouse Hmgr	caaagtttgccctcagttca	gtgccaactccaatcacaag

Mouse Hmgs	gccgtgaactgggtcgaa	gcatatatagcaatgtctcctgcaa
Mouse Il-6	ccagagatacaaagaaatgatgg	actccagaagaccagaggaaat
Mouse Ir	taccgcattgagctgcaggc	aagacaaagatgaggggtcc
Mouse Irs-1	tcccaaacagaaggaggatg	cattccgaggagagcttttg
Mouse Irs-2	gtagttcaggtcgcctctgc	ttgggaccaccactcctaag
Mouse Mcp-1	ggtccctgtcatgcttctgg	cctgctgctggtgatcctct
Mouse Mmp9	gaaggcaaaccctgtgtgtt	agagtactgcttgcccagga
Mouse Pepck	ctaacttggccatgatgaacc	cttcactgaggtgccaggag
Mouse Pfk	atggcaaagctatcggtgtc	acacagtcccatttggcttc
Mouse Pgc1α	gtcaacagcaaaagccacaa	tctggggtcagaggaagaga
Mouse Pgm	cgaacttcaccttgctctcc	tcaggccattgaggaaaatc
Mouse Ppara	tggcgtacgacaagtgtgat	gtttgcaaagcctgggatag
Mouse Pparg	gaataccaaagtgcgatcaaagta	ccaaacctgatggcattgtgagac
Mouse Scd-1	cctgcggatcttccttatca	gtcggcgtgtgtttctgag
Mouse Sma	gagaagcccagccagtcg	ctcttgctctgggcttca
Mouse Srebp1-c	gagccatggattgcacattt	ctcaggagagttggcacctg
Mouse Tbp	atgatgactgcagcaaatcg	tatcactcctgccacaccag
Mouse Timp-1	aggtggtctcgttgatttct	gtaaggcctgtagctgtgcc
Mouse Tgfβ1	tgagtggctgtcttttgacg	ggttcatgtcatggatggtg
Mouse Tnfα	ccagaccctcactagatca	cacttggtggtttgctacgac

Chapter 3. The role of ARNT in liver metabolism and fibrosis

3.1 Introduction

In healthy individuals, the liver prevents hypoglycemia HGP from glycogenolysis and gluconeogenesis. The liver also plays a key role in regulating serum lipids (157). T2D is associated with inappropriate HGP in the setting of normal or raised glucose, and impaired insulin mediated suppression of HGP (49, 150). Dysregulation of HGP results in elevated fasting glucose levels, a key feature of T2D. HGP is higher in diabetic patients even after controlling for higher circulating glucagon (153). T2D is associated with dyslipidaemia, characterized by increased serum TG, often with pronounced postprandial hypertriglyceridaemia (48, 157, 158). Dyslipidaemia contributes to the increased risk of cardiovascular complications in people with diabetes or the metabolic syndrome. Studies in animal models show that liver dysfunction can be sufficient to lead to T2D and components of the metabolic syndrome (150, 389, 390). The elucidation of the mechanisms leading to alterations of glucose and lipid metabolism in the liver is thus of importance to understanding the pathogenesis of T2D and the metabolic syndrome. It was previously reported that there is decreased expression of *ARNT* in isolated pancreatic islets of patients with T2D (391). While these studies were underway it was reported that ARNT was also reduced in the liver of T2D patients, and that short-term adenovirus-induced hepatic ARNT deletion caused increased HGP and impaired glucose tolerance (252).

The development of NASH and cirrhosis is a liver complication with increased prevalence in obesity and diabetes. Obesity and diabetes related liver failure due to progression of NAFLD to NASH and cirrhosis is predicted to become the major cause for liver transplantation (8). Interestingly acute increases in the level of liver ARNT partners HIF-1α and HIF-2α, via adenoviral-Cre mediated deletion of von Hippel-Lindau (Vhl) in the liver, leads to fatty liver with decreasing serum glucose levels (256). Also AhR activation and deletion both lead to hepatic steatosis (244, 248, 249). Of particular relevance, increased liver *Hif2α* has been linked to increased hepatic inflammation and AhR deletion been shown to increase liver fibrosis (243, 258).

To create mice with hepatocyte deletion of ARNT the Cre-LoxP system was used with Cre expression under control of the hepatocyte specific albumin promoter. This results in Cre expression in the majority of hepatocytes with reported deletion efficiency in whole liver of 80% by southern blot in whole liver (392). This promoter has a liver specific expression pattern with no recombination observed in pancreas, brain, liver, heart, spleen or kidney tissue.

It is clear from previous studies that liver ARNT and its partners are involved in liver metabolism, NASH and fibrosis. Given the fact that ARNT is reduced in people with type 2 diabetes the potential role of this gene in these processes was investigated.

3.1.1 Aims and strategies

To investigate the effects of long-term ARNT deletion in the liver, liver-specific ARNT-knockout (LARNT) mice were studied in three models:

1) Mice were studied on standard chow diet.

2) Mice were studied on high fat diet to determine the effect of reduced liver ARNT in a model of high fat diet-induced diabetes.

3) In order to study the potential contribution of liver ARNT to liver fibrosis mice were studied in the thioacetamide model of liver fibrosis model.

3.2 LARNT mice on chow fat diet

LARNT mice on chow diet were of equivalent weight to their FC littermates at all time points assessed. Mice weight at 10 weeks of age is shown (Figure 3.1A). 20 week old LARNT mice had a reduction of whole liver ARNT mRNA to 20.4±1.4% of FC (Figure 3.1B). LARNT mice also had significantly reduced liver ATP to 38.9 % of FC levels (P=0.0182) (Figure 3.1C).

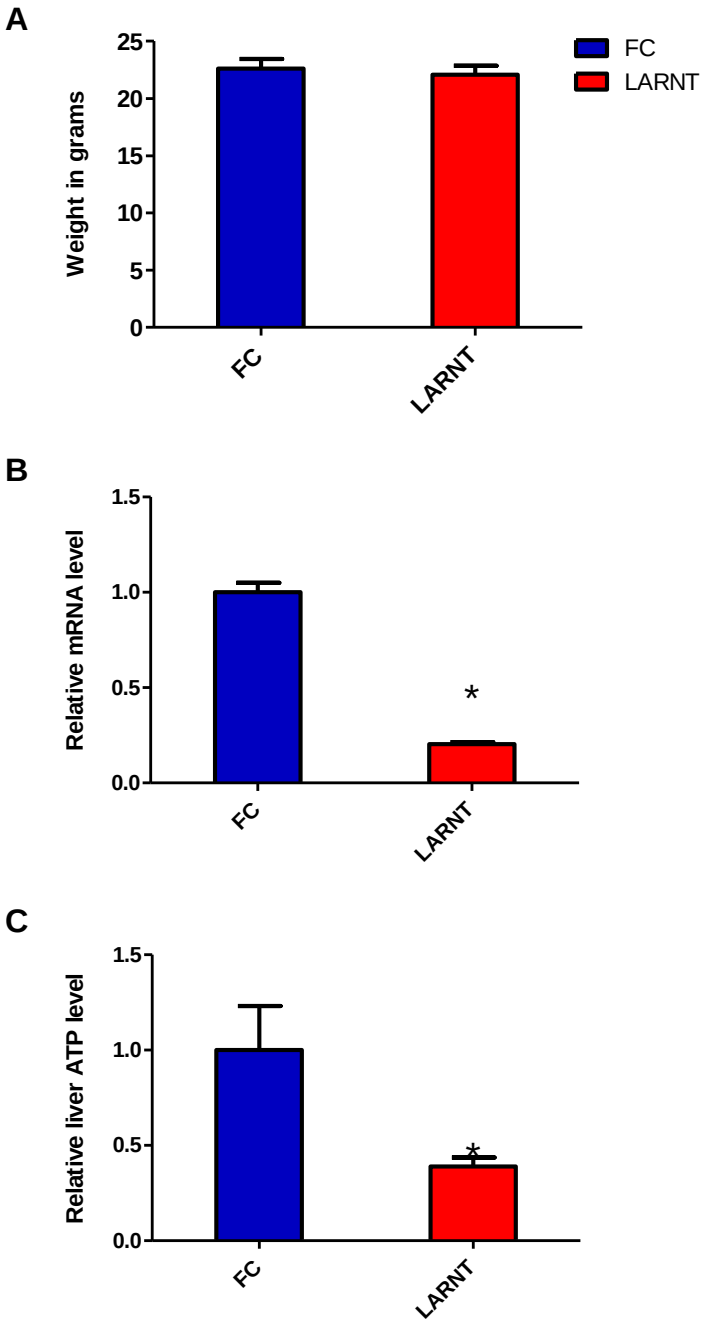

Figure 3.1 Chow fed LARNT and FC weight, knockdown and ATP.
Chow fed female mice data. (A)Weights FC (shown in blue bars) compared to LARNT (shown in red) (n=8/group). (B) Relative *Arnt* mRNA level in whole liver in FC compared to LARNT mice (n=5-6/group). (C) relative liver ATP in FC compared to LARNT mice (n=8-10/group). $p<0.05$=* by students ttest. SEM shown

There were no obvious changes in liver histology in LARNT mice at 20 weeks of age compared to FC using H&E and Sirius Red staining (Figure 3.2).

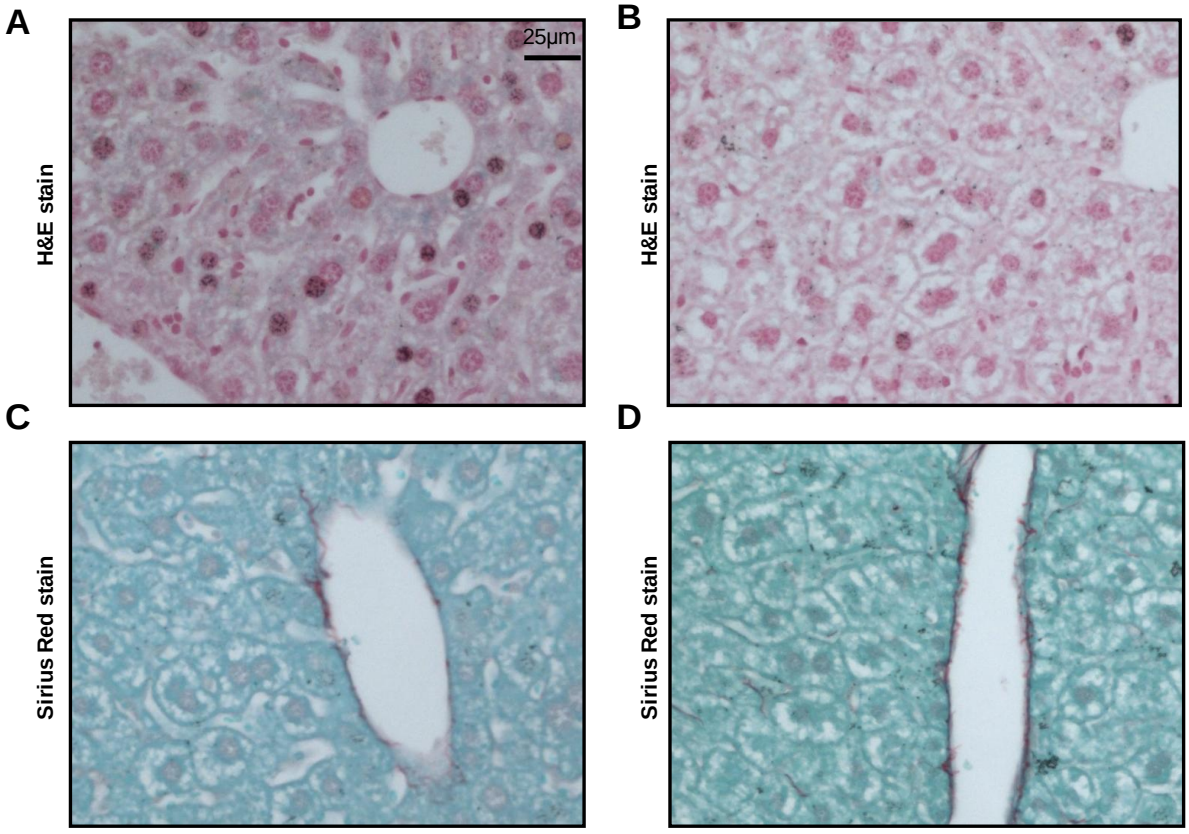

Figure 3.2 Histology of LARNT and FC chow fed liver.
Haematoxylin and Eosin staining of liver sections from 20 week old FC (A) and LARNT (B) mice. Sirius Red staining from FC (C) and LARNT (D) mice. Representative results are shown (n=5-7/group).

3.2.2 Metabolism

Fasting glucose levels were normal in floxed controls, and 42% higher in LARNT mice ($p<0.001$,Figure 3.3A). LARNT mice had mildly but significantly worse glucose tolerance than floxed-controls, shown in Figure 3.3B. Area under the curve of glucose tolerance was increased by 19% ($p=0.026$), Figure 3.3C.

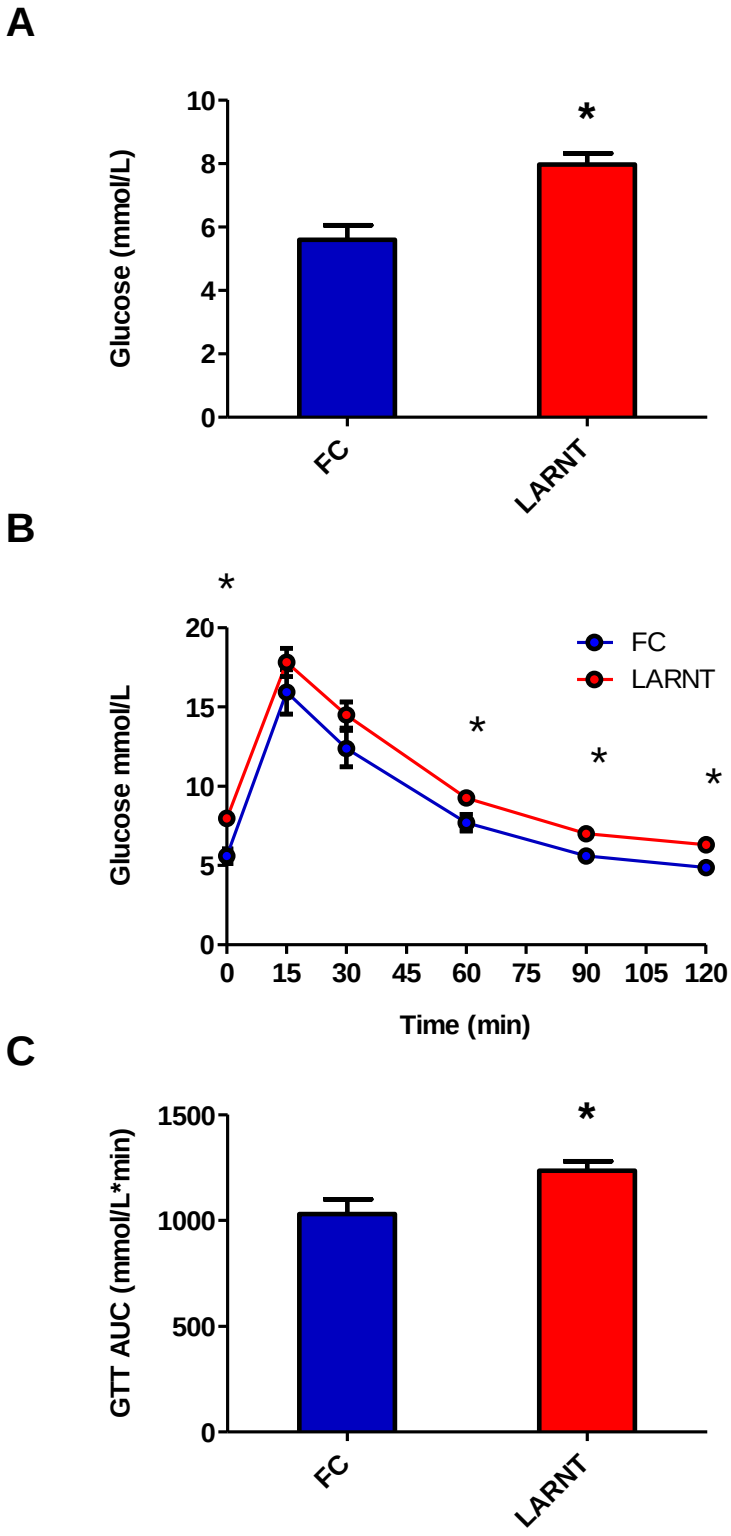

Figure 3.3 Glucose metabolism in chow fed LARNT mice.
(A) Average fasting blood glucose levels in floxed control mice (FC) in blue and LARNT mice in (red). (B) Glucose tolerance test FC (blue) and LARNT (red circles). (C) Area under the curve of glucose tolerance test. FC (blue) and LARNT mice (red bar). $p<0.05$=*by students ttest. SEM shown (n=8-13/group)

Fasting serum insulin did not differ (Figure 3.4A). To assess whole-body insulin sensitivity, ITTs were performed. Results are presented as percentage fall from baseline because LARNT mice had higher fasting glucose. LARNT and control mice had similar whole-body insulin sensitivity (Figure 3.4B).

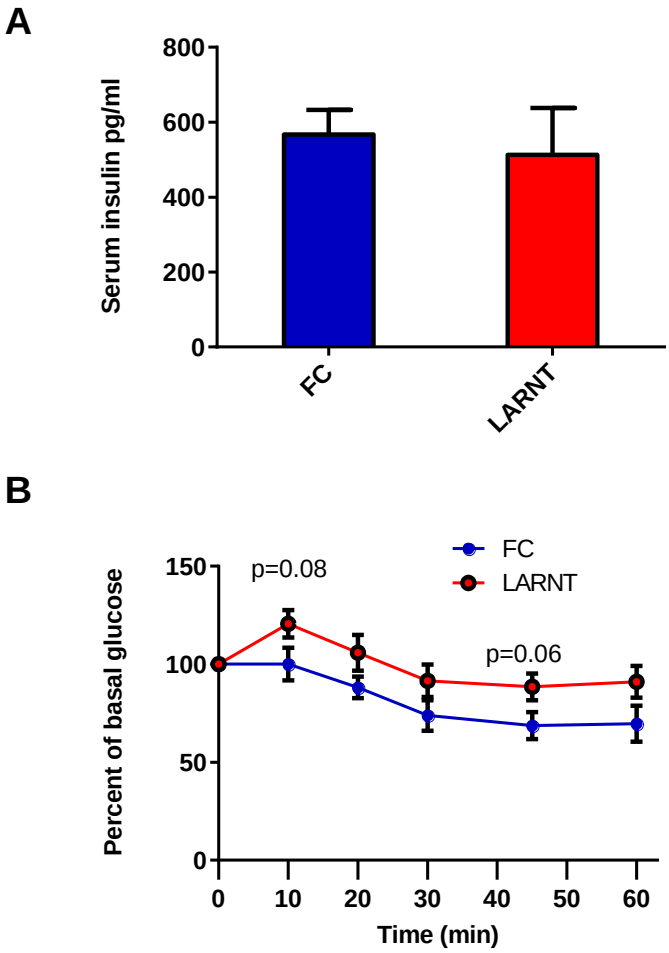

Figure 3.4 Serum insulin and insulin resistance in chow fed LARNT and FC mice.
(A) Average fasting serum insulin levels. (B) Insulin tolerance test (ITT) of female FC (blue circles) and LARNT mice (red circles). Levels are expressed as a percentage of blood glucose level at 0 min. $p<0.05$=*by students ttest. SEM shown (n=5-6/group)

To examine the effect of hepatic ARNT deletion on HGP, pyruvate challenge tests were performed. After overnight fasting, fasting glucose levels were higher, and glucose levels were significantly greater after pyruvate loading in LARNT mice (Figure 3.5A, $p=0.005$ by ANOVA for repeated measures). Because the fasting glucose was greater, the results are also presented as the AUC of the *increase* from baseline fasting glucose. This was 22% higher in LARNT mice following pyruvate challenge (Figure 3.5B, $p=0.021$).

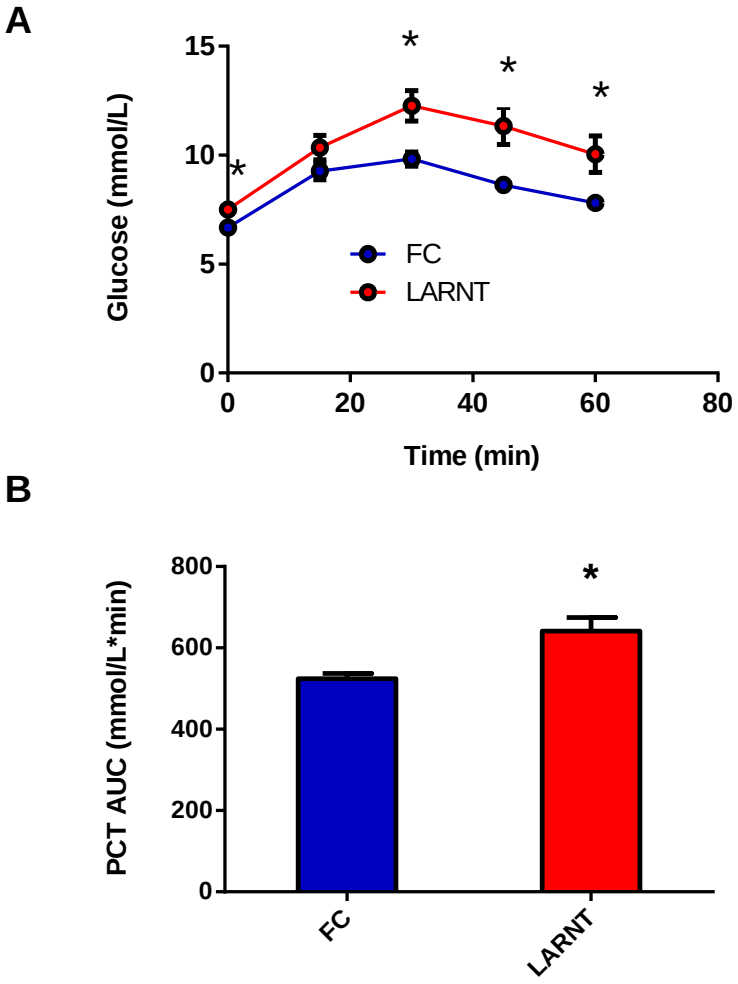

Figure 3.5 Hepatic glucose production (HGP) in chow fed LARNT and FC mice.
(A) Pyruvate challenge tests (PCT) in FC and LARNT KO female mice. FC mice are shown in blue circles LARNT mice are shown in red circles. (B) Area under the curve (AUC) of PCT on female mice. FC mice AUC shown by the blue column and LARNT mice in red. $p<0.05$=*by students ttest. SEM shown (n=14-19/group).

3.2.3 Lipid handling

Liver triglyceride content was equivalent in fed but was 26% lower in LARNT mice after 16 hour fasts (Figure 3.6A). Fasting reduced liver triglyceride content in FC and LARNT mice by 40% and 66% respectively (Figure 3.6A). To investigate the cause of reduced triglyceride content we assessed rates of lipid oxidation in LARNT hepatocytes. Figure 3.6B shows that lipid oxidation was reduced in isolated LARNT hepatocytes so this did not account for the reduced hepatic triglyceride content in LARNT mice. ATP concentrations were correspondingly reduced in LARNT livers to 38.9 % of FC levels ($p=0.0182$, Figure 3.1C).

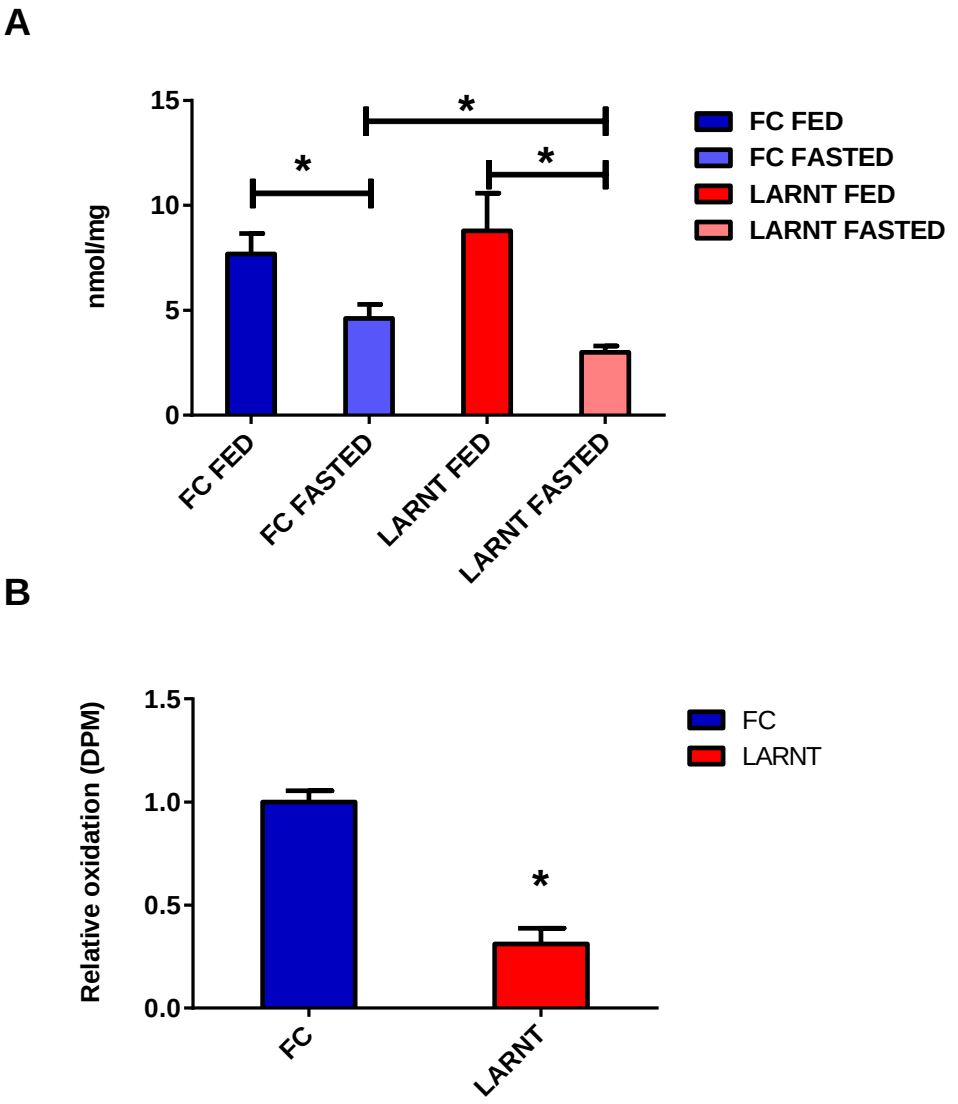

Figure 3.6 Liver lipid, hepatocyte palmitate oxidation and liver ATP.
(A) Liver triglyceride levels in FC and LARNT female mice. Liver TG is shown in fed and fasted states (darker and lighter bars respectively. FC blue and LARNT red (n=5-6/group). (B) Lipid oxidation in isolated hepatocytes from male FC (blue bars) or LARNT animals (red bars), (n=9-11/group). $p<0.05$=*by students ttest. SEM shown.

Serum triglyceride levels were then assessed. They were not different in mice after fasting (Figure 3.7A). However, serum triglycerides were significantly higher 6 hours after feeding ($p=0.0187$, Figure 3.7B).

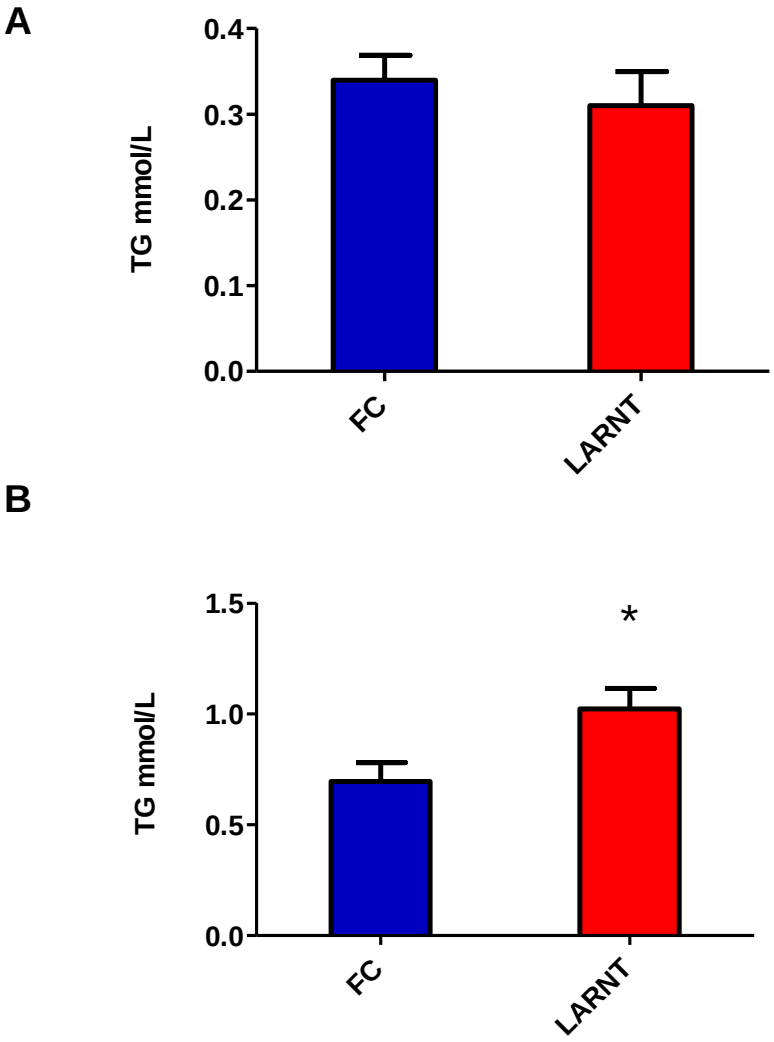

Figure 3.7 Serum triglycerides in LARNT and FC chow fed mice.
(A) Serum TG's in male FC and LARNT animals after a 16hr fast (n=5-6/group). (B) Serum TG in FC 6 hours after feeding with HFD (n=8-10/group). $p<0.05$=*by students ttest. SEM shown.

3.2.4 **Gene expression**

In the liver of LARNT mice, expression of glucose transporters 1 (Glut1) and 2 (Glut2) were decreased, expression of the transcription factor Carbohydrate responsive element binding protein (Chrebp) was increased and there was no significant change in Glucokinase (Gk) (Figure 3.8A). There was a trend to increase in phosphoenolpyruvate carboxykinase (*Pepck)* expression, and there was increased Glucose 6-phosphatase *(G6Pase)* (Figure 3.8B). There were also significant decreases in mRNA for Insulin receptor (*IR*) and Insulin receptor substrate 2 (*Irs2*), with a trend to decreased Insulin receptor substrate 1 (*Irs1*) and *Akt2* which may explain the trend to impaired ITT in LARNT mice (Figure 3.8B). In line with increased *Chrebp* expression LARNT mice had significantly increased levels of lipogenic genes Stearoyl Co-A-desaturase 1 (*Scd-1*), Fatty-acid synthase (*Fas*) and HMGCoA-synthase (*Hmgs*) (Figure 3.8C). No changes were present in HMGCoA-reductase (*Hmgr*) (Figure 3.8C). No changes were present in other lipogenic genes including peroxisome proliferator-activated receptor alpha (*Ppar-α)* and gamma (*Ppar-γ)* (Figure 3.8D). There were no significant changes in the glycolytic genes phosphofructokinase (*Pfk*), Aldolase B (*Aldob*) or *Phosphoglucomutase* (*Pgm*) (data not shown).

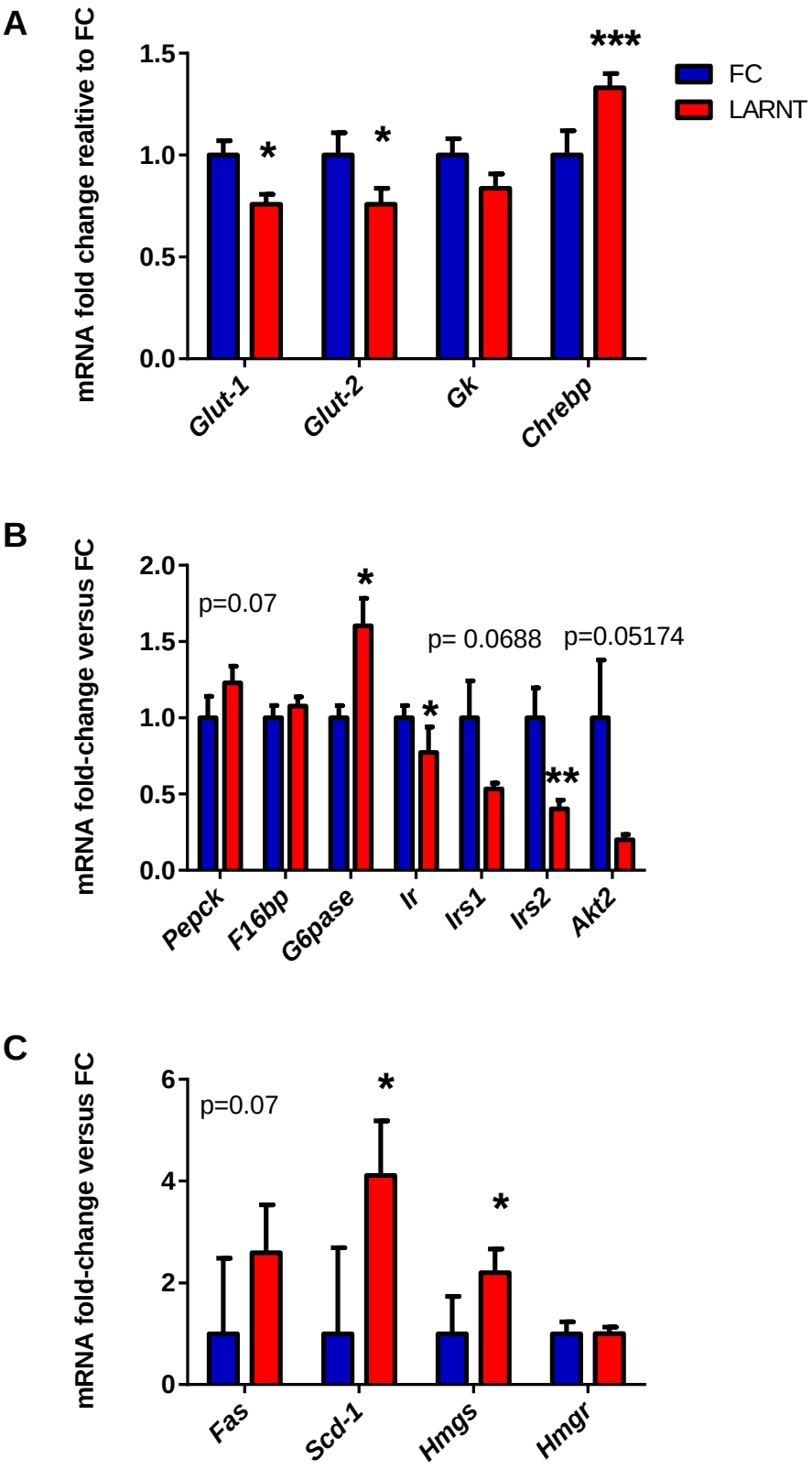
A
mRNA fold change realtive to FC
1.5
1.0
0.5
0.0
*
*
***
FC
LARNT
Glut-1
Glut-2
Gk
Chrebp
B
mRNA fold-change versus FC
2.0
1.5
1.0
0.5
0.0
p=0.07
*
p= 0.0688
p=0.05174
*
**
Pepck
F16bp
G6pase
Ir
Irs1
Irs2
Akt2
C
mRNA fold-change versus FC
6
4
2
0
p=0.07
*
*
Fas
Scd-1
Hmgs
Hmgr

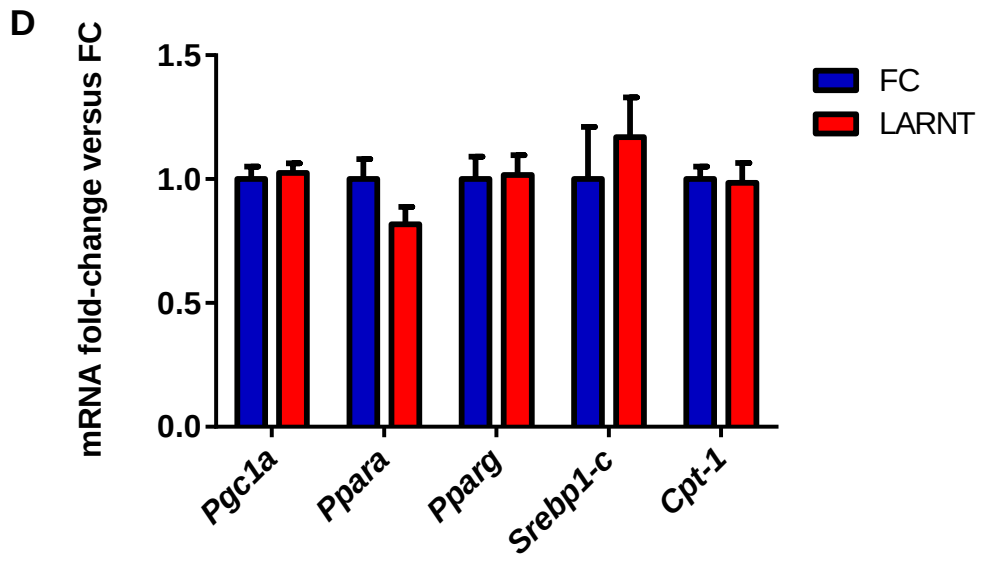

Figure 3.8 mRNA expression changes in female 20 week old FC and LARNT mice.
(A) Relative mRNA levels of glucose transporter 1 (*Glut-1*), Glucose transporter-2 (*Glut-2*), Glucokinase (*Gk*) and Carbohydrate response element-binding protein (*Chrebp*), (D) Relative mRNA levels for Phosphoenolpyruvate carboxylase 1 (*Pepck*), Fructose-1-6-bisphosphatase (*F16bp*), Glucose-6-phosphatase (*G6pase*), Insulin receptor (*Ir*), Insulin receptor substrate 1 (*Irs1*), Insulin receptor substrate 2 (*Irs2*) and *Akt2*,. (E) Relative mRNA levels of Fatty acid synthase (*Fas*), Stearoyl-CoA-desaturase (*Scd-1*), HMG-CoA-Synthase (*Hmgs*) and HMG-CoA-Reductase (*Hmgr*). (F) Relative mRNA levels of Peroxisome Proliferator-Activated Receptor-Gamma, Coactivator-1 Alpha (*Pgc1a*), Peroxisome Proliferator-Activated Receptor-Alpha (*Ppara*), Peroxisome Proliferator-Activated Receptor-Gamma (*Pparg*), Sterol regulatory element-binding protein (*Srebp1-c*) and Carnitine Palmitoyltransferase 1 (*Cpt-1*). (n=5-6/group).*p<0.05. **p<0.01, *** p<0.001 by students ttest. SEM is shown.

3.3 LARNT mice on a high fat diet

3.3.1 Metabolism on HFD

Both FC and LARNT female mice gained approximately 12g after 12 weeks of high fat diet and body weights were not significantly different (Figure 3.9A) At 20 weeks the average weight of LARNT mice was lower than FC this change was not significant (Figure 3.9B).

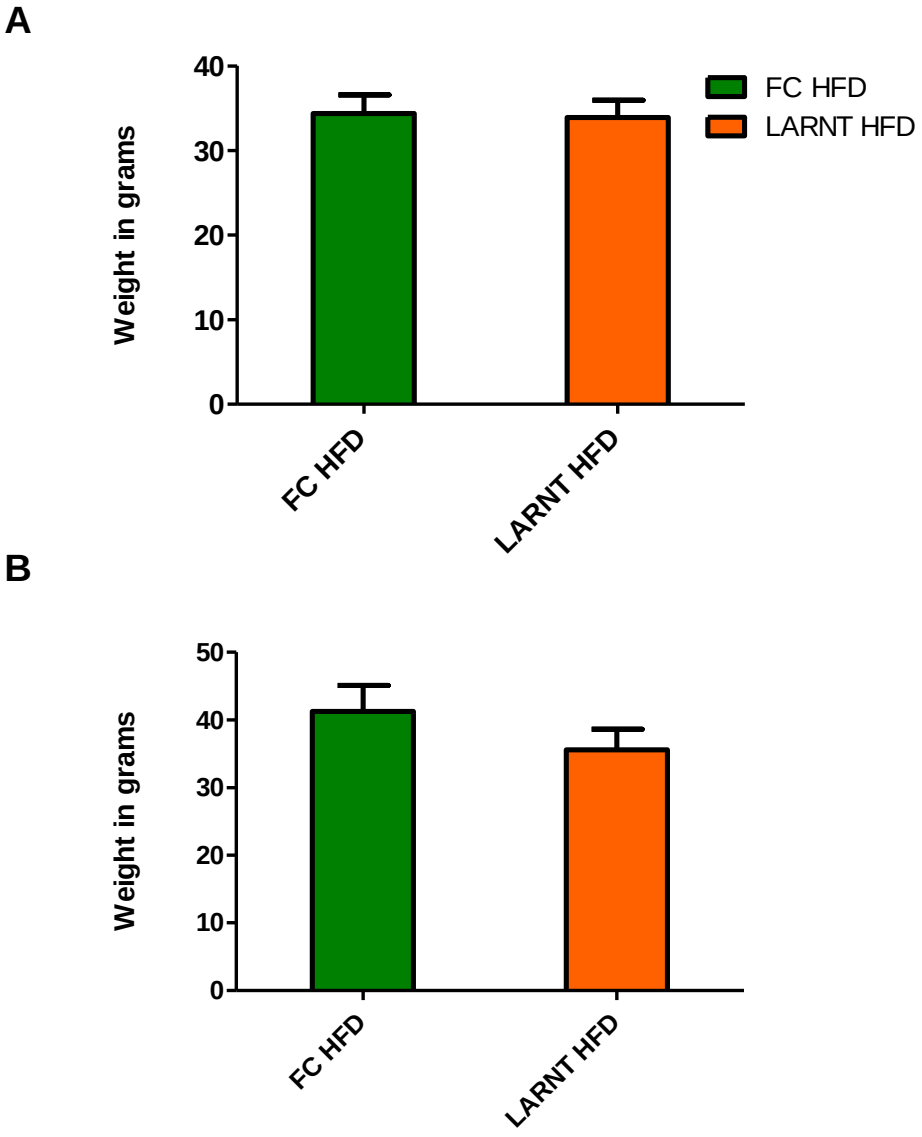

Figure 3.9 Weight of female FC and LARNT mice on HFD.
LARNT compared to FC mice on HFD. Standard error bars are shown. * p <0.05. Weight was not significantly different between FC and LARNT mice fed HFD at 12 weeks (A) or 20 weeks (B). (n=8-10/group), p<0.05=*by students ttest. SEM shown.

Histology was variable but overall there appeared to be no consistent significant patterns of fatty liver or of fibrosis (Figure 3.10).

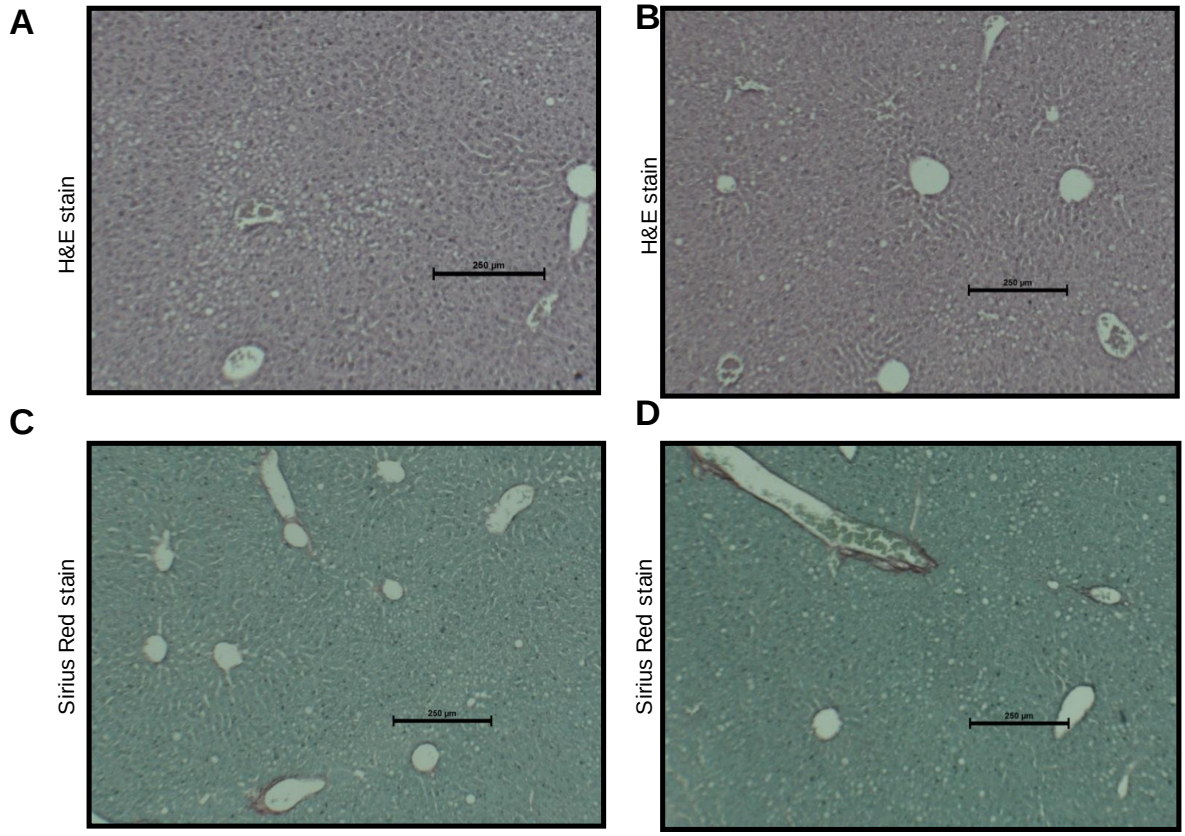

Figure 3.10 Histology of HFD fed FC and LARNT mice.
Representative Haematoxylin and Eosin staining of liver sections from female FC (A) and LARNT (B) mice after 20 weeks of HFD. Sirius Red staining from HFD treated FC (C) and LARNT (D) mice. (pictures taken at 4X magnification). 250µM scale bar is shown.

Surprisingly, there was no longer a significant difference in glucose tolerance although glucose tolerance deteriorated as expected for both groups at 10 weeks of HFD (Figure 3.11A). Insulin tolerance tests were identical at 11 weeks of HFD (Figure 3.11B). A small, late difference persisted in response to pyruvate challenge at 15 weeks of HFD but the AUC was no longer significantly different (Figure 3.12A and B).

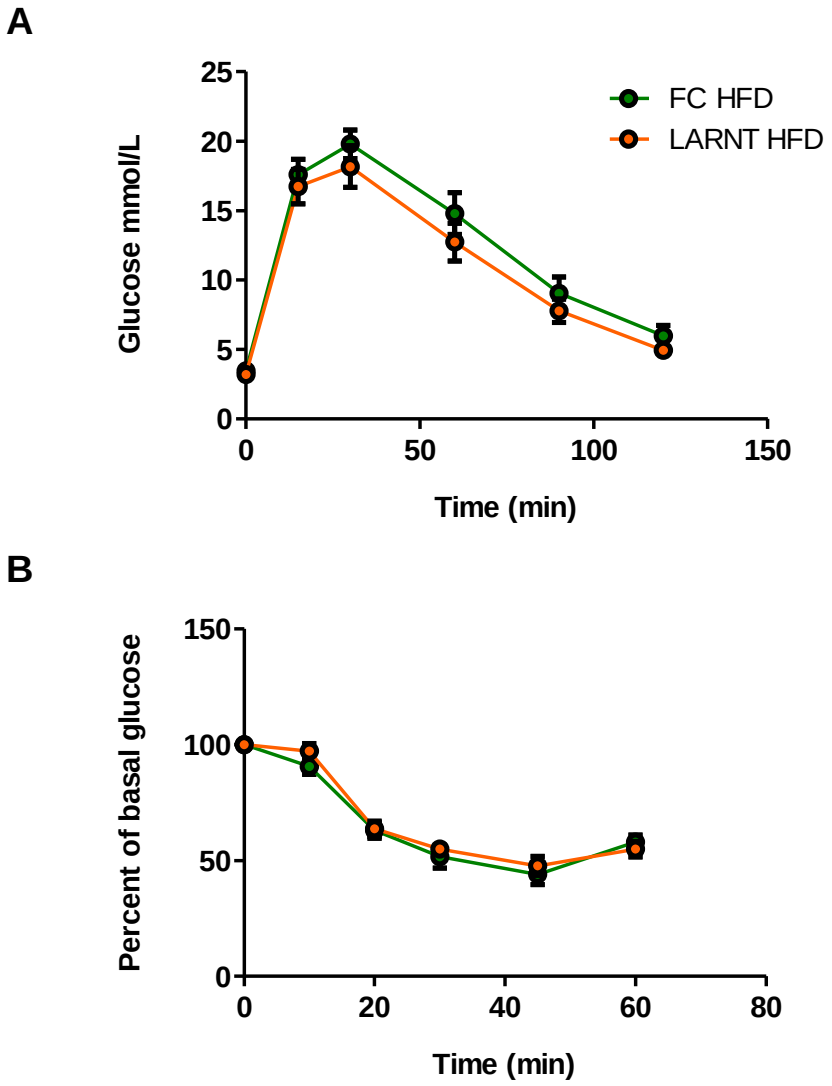

Figure 3.11 Glucose and insulin tolerance in HFD fed mice.
Glucose tolerance tests after HFD (A). Insulin tolerance test (ITT) of FC and LARNT mice (B) expressed as a percentage of baseline blood glucose. (n=8-10/group), $p<0.05$=*by students ttest. SEM shown.

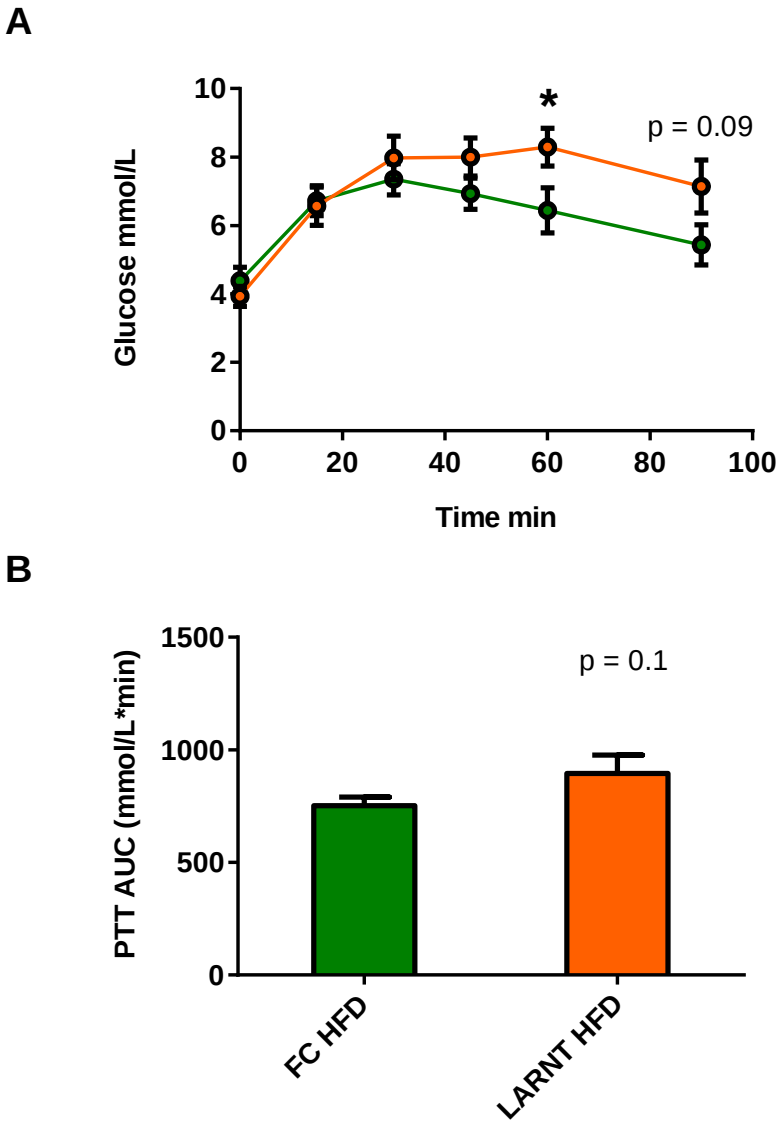

Figure 3.12 Hepatic glucose production in HFD fed FC and LARNT mice.
Pyruvate challenge tests (PTT) in FC and LARNT KO female mice (A). Area under the curve (AUC) of PTT (B). (n=8-10/group), p<0.05=*by students ttest. SEM shown.

3.3.2 **Lipid handling**

HFD fed LARNT mice had a trend to reduced hepatic TG content after overnight fasting (p= 0.09, Figure 3.13A). ATP was no longer significantly different in LARNT compared to FC mice on HFD (p=0.119, Figure 3.13B).

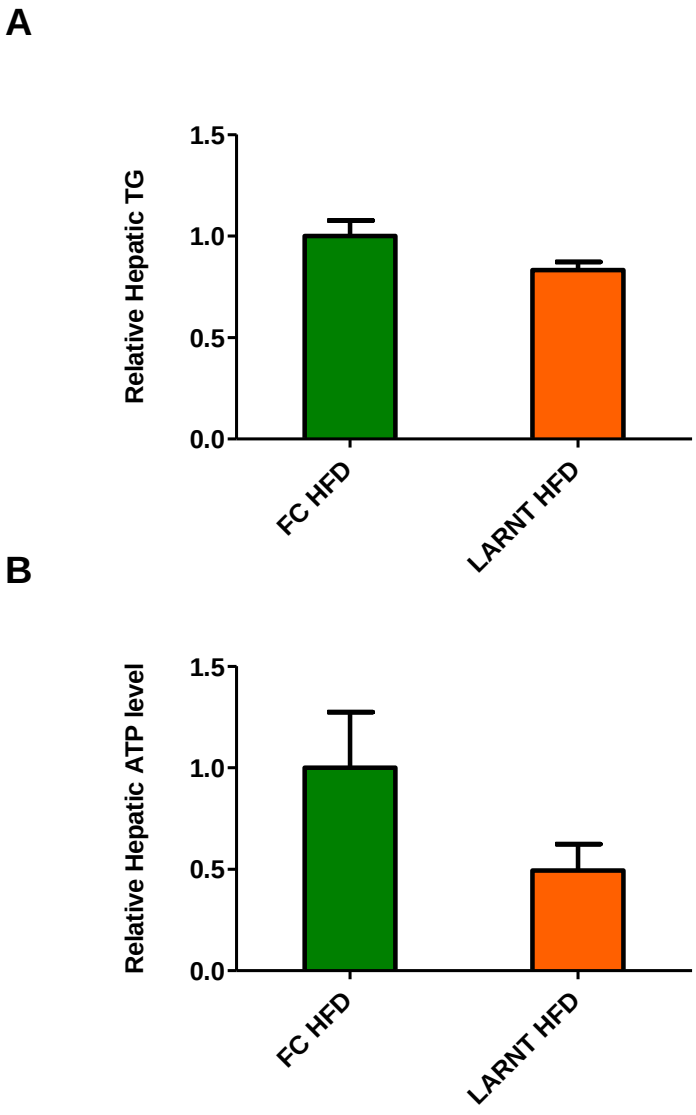

Figure 3.13 HFD hepatic triglyceride and ATP levels.
Standard error bars are shown *p<0.05. (A) Triglyceride levels in whole liver in fasted HFD animals (P=0.09). (B) Hepatic ATP content in HFD mice (P=0.119). (n=5-6/group), p<0.05=*by students ttest. SEM shown.

Serum TGs were equivalent in HFD LARNT and FC animals after fasting or re-feeding (Figure 3.14A and B).

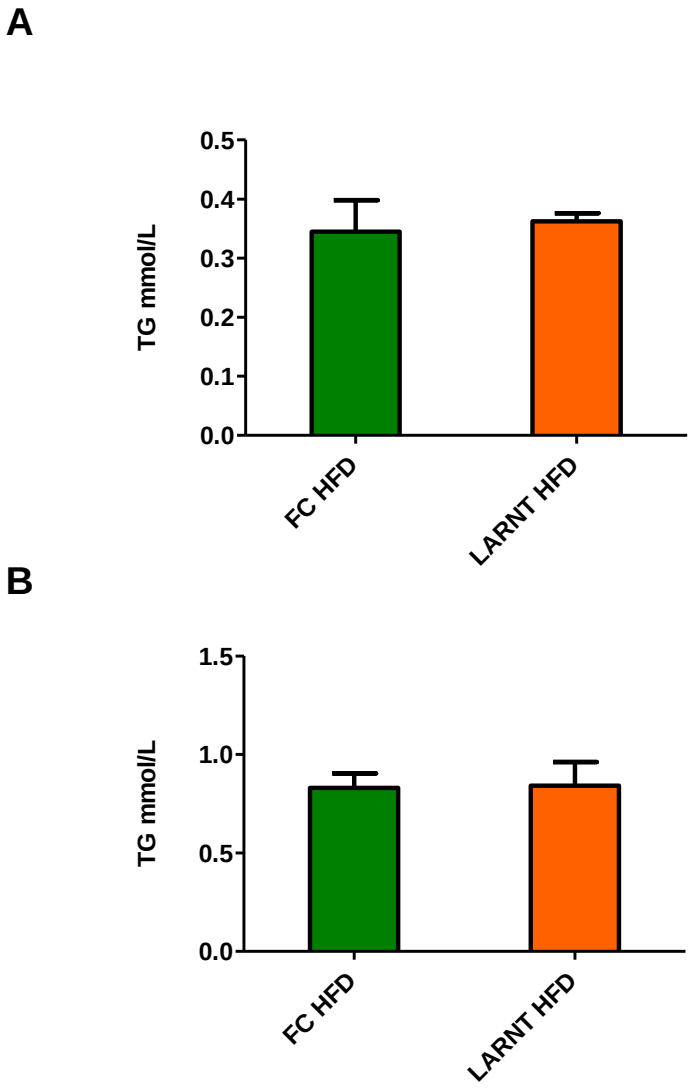

Figure 3.14 Serum triglyceride levels in HFD FC and LARNT mice.
Serum triglyceride levels in fasted HFD fed mice (A). Re-fed serum triglycerides in HFD fed mice (B). (n=5-6/group), p<0.05=*by students ttest. SEM shown.

3.3.3 Gene Expression

With the previous report that hepatic *ARNT* is decreased in people with T2D (252), we hypothesized that the loss of phenotype with HFD might be due to HFD decreasing hepatic ARNT in controls. This was confirmed. HFD treatment reduced the level of *Arnt* to 71% of chow fed levels (p=0.0007) (Figure 3.15A). Protein levels were examined by Western immunoblotting (Figure 3.15B) and surprisingly, although highly variable, we found that ARNT protein was, if anything, increased. This was not significant (p=0.223, Figure 3.15C, Western performed by Dr Natasha Langley). Figure 3.16 shows that the mRNA for ARNT binding partner *Hif2a* was increased by 23% (p=0.0002) and *Chrebp* by 28%

(p=0.019). There was a trend to increased *Hif1a* but this did not reach significance (p=0.1, Figure 3.16).

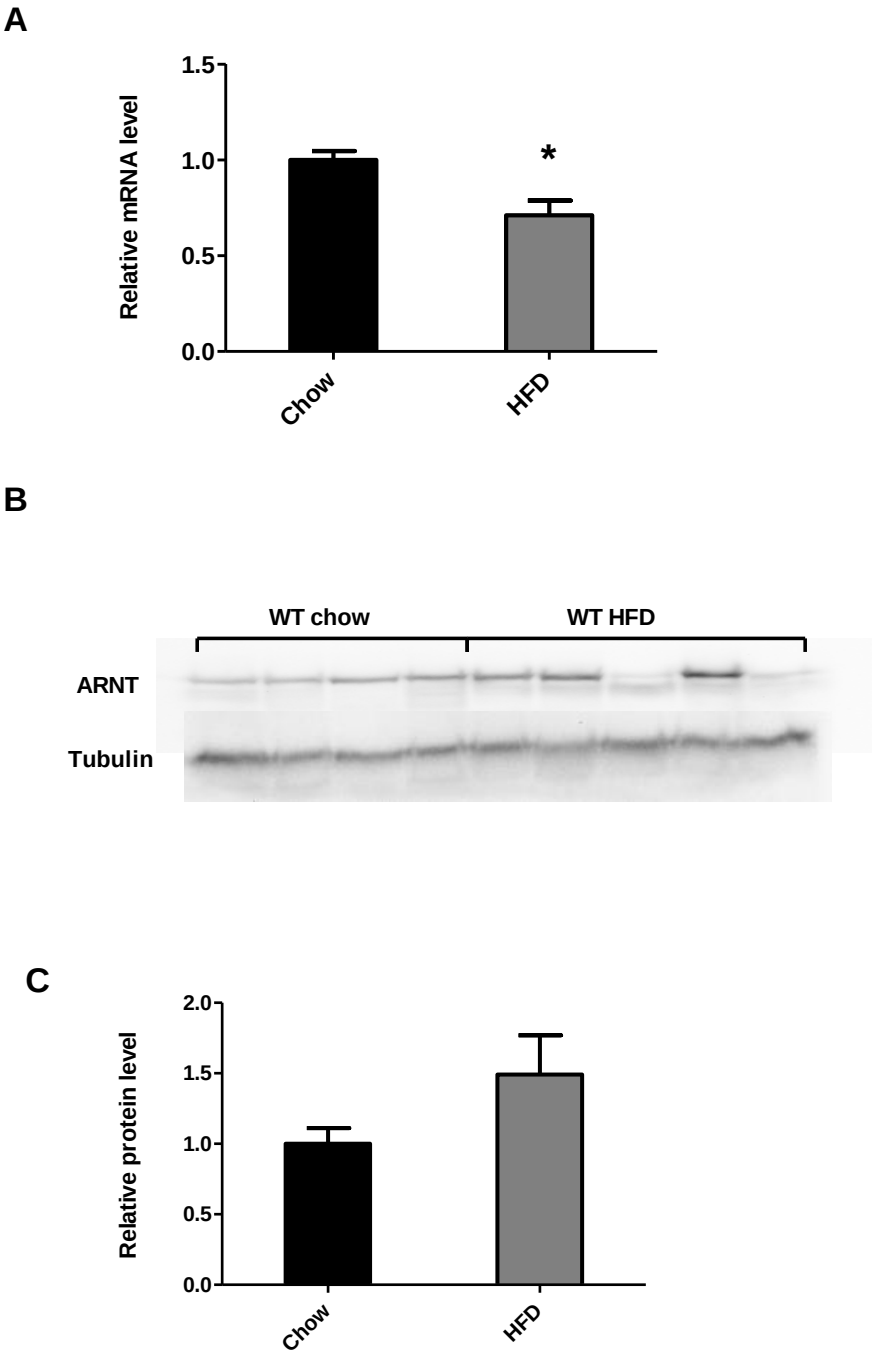

Figure 3.15 ARNT expression in FC on chow and HFD.
Changes in ARNT expression after HFD. Standard error bars are shown *p<0.05 (A) ARNT mRNA in FC animals fed chow (black) or HFD (grey). (B) Representative western blot for ARNT in WT chow fed compared to HFD fed animals. Alpha Tubulin shown as loading control. (C) Densitometry of ARNT western blot. ARNT levels were normalised to tubulin expression. Relative levels shown. (n=5-6/group), p<0.05=*by students ttest. SEM shown.

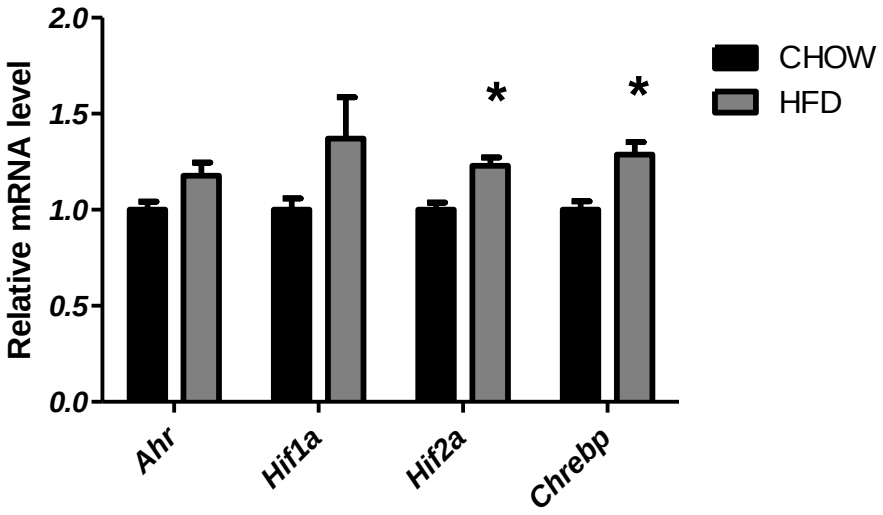

Figure 3.16 mRNA changes in FC on HFD.
Changes in gene expression after HFD. Standard error bars are shown *p<0.05. Relative level of *Ahr*, *Hif1a* and *Hif2a* and *Chrebp* mRNAs in FC animals fed chow or HFD. (n=5-6/group), p<0.05=*by students ttest. SEM shown.

Some significant alterations in gene expression remained between LARNT and FC mice receiving HFD. High fat fed LARNT mice had reduced *Chrebp* mRNA (p=0.00332) (Figure 3.17A), increased expression of *Glut1* (p=0.01) and a trend to increased *Glut2* (p=0.063). There was also increased *Pepck* (P=0.00493) (Figure 3.17A), however *G6pase* was no longer significantly different. *Fas* and *Srebp1c* mRNAs were increased in LARNT HFD fed mice (p=0.000143 and p=0.0000046), but *Scd1* was not (Figure 3.17B). *Cpt-1* was significantly increased while *Hmgs* was reduced (p=0.035 and p=0.02). There was no difference in and *Hmgr* expression.

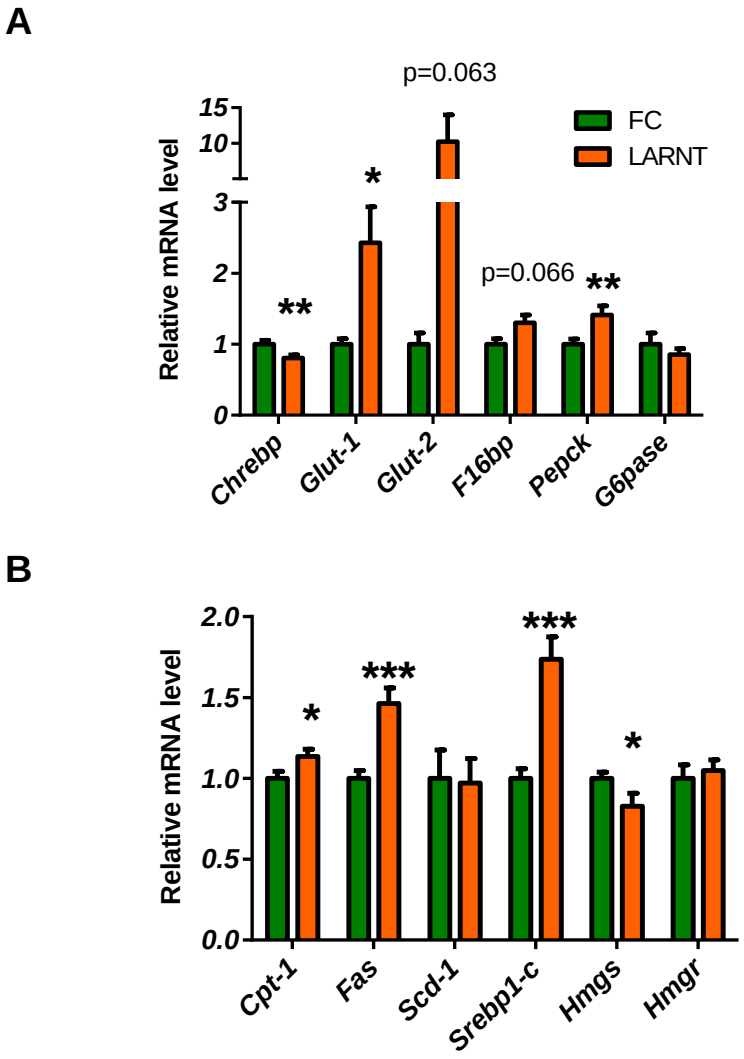

Figure 3.17 mRNA expression in FC and LARNT mice at 20 weeks HFD.
Changes in gene expression after HFD. Standard error bars are shown. (A) Relative mRNA levels of *Chrebp*, *Glut-1*, *Glut-2*, *F16bp*, *Pepck* and *G6pase*. (B) Relative mRNA levels of *Cpt-1*, Fas, *Scd-1*, *Hmgs* and *Hmgr*. *p<0.05. **p<0.01, *** p<0.001 by students ttest, (n=6/group), SEM shown.

3.4 Thioacetamide-induced liver fibrosis

To investigate the potential role of ARNT in liver fibrosis we studied LARNT and FC mice on the thioacetamide (TAA) model of liver fibrosis. After 13 weeks of TAA treatment there was no obvious difference in the extent of fibrosis via histology (Figure 3.18). To confirm observations collagen content was assessed by quantitating histological collagen staining with ImageJ. There was a significant reduction in collagen content in LARNT mice compared to FC (Figure 3.19, p =0.019).

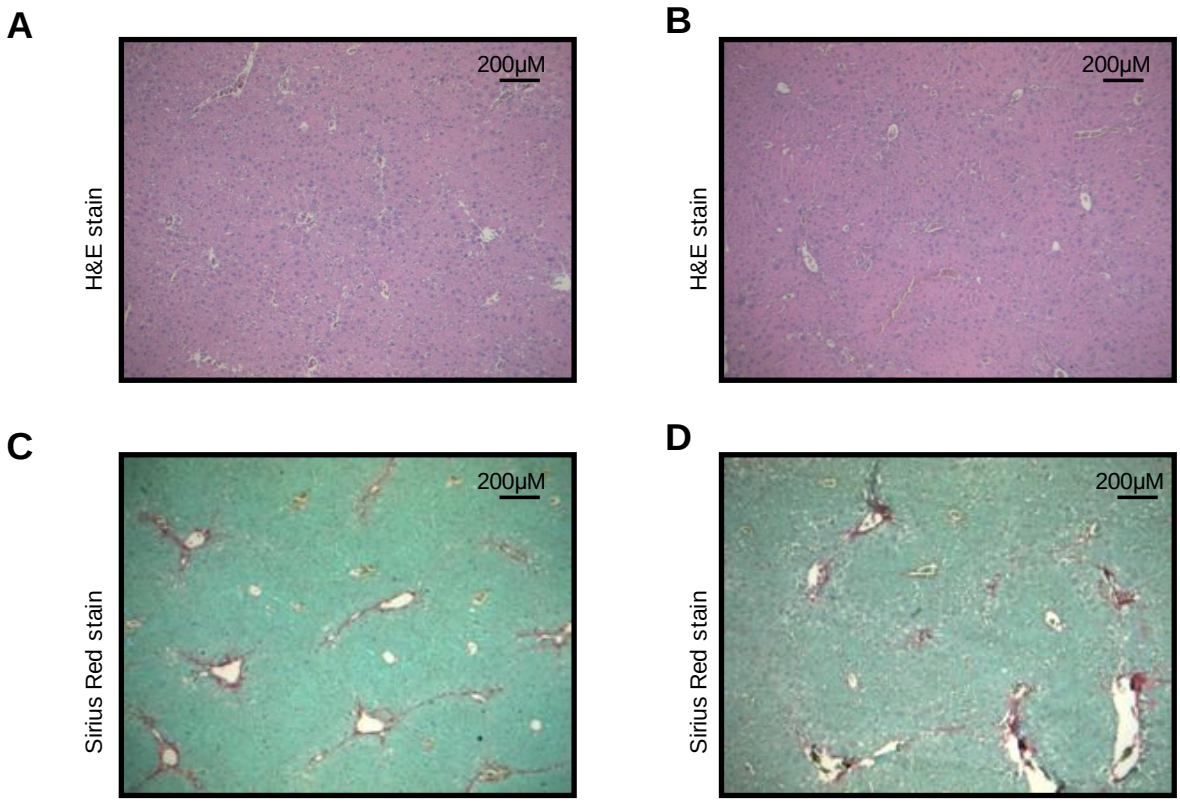

Figure 3.18 Histology from TAA treated FC and LARNT mice.
Representative Haematoxylin and Eosin staining of liver sections from male FC (A) and LARNT (B) mice after 13 weeks of TAA injection. Sirius Red staining from TAA treated FC (C) and LARNT (D) mice. (Pictures taken at 4X magnification). (n=6-7/group).

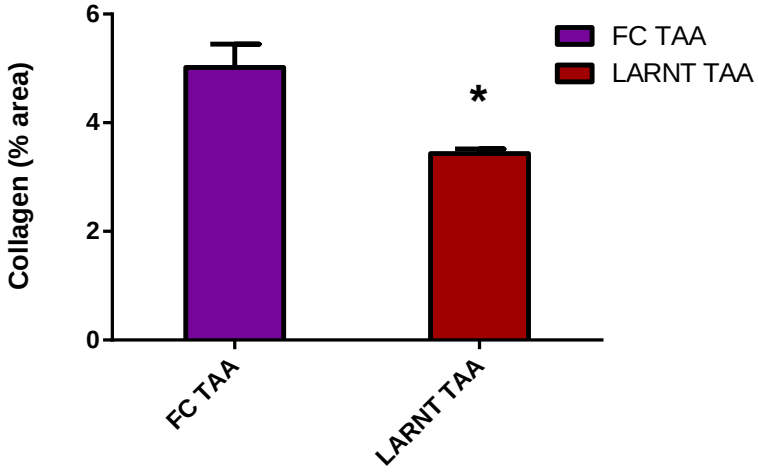

Figure 3.19 Average collagen content in TAA treated mice.
Percentage of histological area covered by collagen in FC (purple column) and LARNT (red column) livers after TAA treatment, (n=5-7/group), p<0.05=*by students ttest. +/- SEM is shown.

3.5 Discussion

Hepatocyte ARNT deletion resulted in impaired glucose tolerance, increased glucose production after pyruvate challenge and increased postprandial serum triglycerides. These changes are similar to changes seen in people with T2D and metabolic syndrome. Assessment of liver ATP and triglyceride content showed that both were significantly reduced in LARNT mice in fasted animals, however these alterations became non-significant with HFD feeding. HFD caused a reduction in liver *Arnt* mRNA in control animals, but surprisingly no apparent reduction in total ARNT protein.

People with T2D have increased HGP (6). PEPCK is a critical enzyme in gluconeogenesis (393, 394) and is increased in the setting of T2D (395). G6Pase catalyses the final step in gluconeogenesis and is increased in diabetic animals (394, 396). We have found increased expression in *G6pase* and a trend to increased *Pepck* in chow fed LARNT mice.

It has recently been demonstrated that by magnetic resonance spectroscopy that both ATP and flux through ATP (fATP) are reduced in the livers of T2D patients compared to age matched controls (397, 398). Further liver ATP correlated with hepatic insulin sensitivity even after controlling for hepatocyte lipid content (398). We found that hepatic ARNT deletion in LARNT animals resulted in basally decreased liver ATP and this reduction in ATP occurred alongside increased HGP.

In contrast to the results of acute ARNT ablation using adenoviral Cre-recombinase (252) in this study we found no change in fasting insulin level. In common with short-term deletion, long-term loss of ARNT also led to alterations in gluconeogenic and lipogenic mRNAs in the liver, and increased HGP. Mice lacking ARNT in the long-term also had mildly worsened glucose tolerance. Short term ARNT deletion also led to reduced hepatic triglyceride after fasting. Interestingly a decrease in ARNT protein after streptozotocin induced diabetes was also reported (252). We report here a reduced level of *Arnt* mRNA after HFD, which is also found in the liver of type 2 diabetic patients, although we did not find a reduction in total ARNT protein (252). It is also known that the activity of *Hif1α* is reduced in the setting of diabetes (380, 383). These studies are supportive of a role for perturbations in the regulation or function of ARNT and its partners in the diabetic milieu. We hypothesise that the decrease in *Arnt* mRNA may be mediated by ChREBP in response to increased glucose, as is the case in pancreatic β-cells (399), and we found increased *Chrebp* expression in FC mice after HFD. Quantification of the relative proportions of nuclear versus cytoplasmic ARNT protein would give a

more accurate indication of the amount of active transcription by ARNT and its partners and would be interesting in future studies.

Perturbations resulting in increased *Hif1α* and *Hif2α* have been found to result in hepatic steatosis, reduced serum glucose levels, reduced HGP and reduced lipid oxidation, which, if left un-countered results in death (256, 258). In particular increased liver *Hif2α* has been linked to hepatic steatosis and inflammation (257, 258). The present data complements these studies finding the reverse phenotype in respect to serum glucose levels after fasting, HGP and reduced liver TG content after fasting in the setting of reduced ARNT. It is also noteworthy that there was increased *Hif2α* and a trend to increased *Hif1α* mRNA in HFD fed FC mice, although protein levels or activity were not assessed. HIF-1α has also been found to be elevated in a mouse model of alcohol induced steatosis (259). HIF-1α deletion in hepatocytes protected mice from liver steatosis and hepatomegaly following alcohol feeding, and from elevated ALT levels following subsequent LPS challenge in this study. The steatotic effects after alcohol feeding and LPS challenge were subsequently found to be regulated by hepatocyte MCP-1 (259). However, in a recent study the opposite effect was found in terms of steatosis (400).

The alterations in lipid handling following ARNT deletion are noteworthy in that despite hepatic insulin resistance, these mice showed reduced hepatic lipid content on fasting compared to controls. Lipogenic gene expression was increased in these animals and lipid oxidation was reduced in culture, suggesting that liver triglyceride content should have been elevated. The mechanism for this effect is unclear, but may relate to alterations in lipid import into the liver. With feeding, serum triglyceride increased in ARNT knockout mice, suggesting that increased fatty acid synthesis and reduced lipid oxidation may also result in increased hepatic triglyceride export. Again, the lipid handling differences were abrogated on high fat feeding.

Although increased *Fas* and *Srebp1-c* expression remained in LARNT mice on HFD again this did not result in increased triglyceride levels in the livers of these mice. Interestingly HFD mice had increased *Cpt-1* expression which may indicate an increased lipid oxidation in the liver of LARNT mice on HFD resulting in decreased export and a possible explanation for the equivalent serum TG levels.

It was also found that long term ARNT deletion decreased collagen content in TAA treated mice, although it did not change the extent of fibrosis as scored by the criteria outlined by Kleiner et al

(2005). This is in line with the reported increased inflammation and fibrogenic gene expression in mice over expressing *Hif2a* in the liver (258). Importantly this indicates that hepatocyte ARNT and its partners are not an absolute requirement for fibrosis initiation but instead influence the extent of collagen deposition.

These results demonstrate that ARNT is an upstream regulator of hepatic glucose and lipid homeostasis. The increased HGP reduced hepatic ATP and increased fasting serum triglyceride in ARNT deleted mice are also found in the diabetic liver. These findings combined with that of reduced mRNA in HFD fed mouse liver suggested that this pathway is perturbed in the setting of diabetes, although surprisingly we did not find a corresponding reduction in total ARNT protein. The mechanisms of this disconnect are unclear; however modulation of the activity of ARNT and its partners may hold future promise in the management of diabetes.

Chapter 4. The role of myeloid cell ARNT in metabolism and NASH

4.1 Introduction

In the past decade evidence has accumulated for the role of chronic low grade inflammation in the development of insulin resistance and T2D (167, 179). Obesity and the metabolic syndrome are associated with chronic low grade inflammation as measured by elevated cytokine production, increased acute phase proteins and activation of inflammatory pathways (168, 401). It is thought that this inflammation is mediated in large part by inflammatory activation of macrophages populating metabolic tissues. In line with this, obesity is known to be associated with inflammatory macrophage infiltration of adipose tissue with osteopontin and MCP-1 playing a role (175, 195, 198). Furthermore, a reduction of adipose infiltration by macrophages by Resolvin D1 treatment is associated with improvement of metabolic parameters (402). Further supporting the importance of macrophages in metabolism a number of myeloid and macrophage specific knockout mice which alter macrophage function have been found to have altered insulin resistance and changes in glucose metabolism (182-186).

NASH is the most common chronic liver disease in developed countries, and is associated with insulin resistance, obesity and type 2 diabetes (147, 403). Liver macrophages have also been shown to play a key role in the development of non-alcoholic steatohepatitis (NASH) and fibrosis, both in the inflammatory and resolution phase (122-124, 127). Of particular relevance, Adenoviral-Cre mediated deletion of von Hippel-Lindau (Vhl) leading to increased liver *Hif2α,* a partner of ARNT, has been linked to increased hepatic inflammation (258). AhR deletion, another ARNT binding partner, has also been shown to increase liver fibrosis (243, 258).

The importance of HIF-1α in myeloid cell immune function was shown by Cramer et al (2003) who found decreased immune function in mice with myeloid cell deletion of this gene. Subsequently it was found that HIF-1α is important in regulating apoptosis, chemotaxis, phagocytosis and bacterial killing in myeloid cells (238, 266). To date the potential role of myeloid cell ARNT in glucose homeostasis and non-alcoholic steatohepatitis has not been investigated. The results presented in this chapter show that deletion of ARNT in myeloid cells results in impairment of GTT and increased NASH on HFD.

4.1.1 Aims and strategies

To investigate the effects of long-term ARNT deletion in innate immune cells on metabolism, myeloid cell-specific ARNT-knockout mice were studied on chow and high fat diet:

1) Metabolism was assessed on chow diet.

2) Mice were studied on high fat diet to determine what effect myeloid cell ARNT deletion had on whole body metabolism, weight gain and markers of Non-alcoholic steatohepatitis.

4.2 LAR mice metabolism on chow and HFD

Myeloid cell-specific ARNT-knockout (LAR) and FC female and male mice had equivalent weight on chow diet (Figure 4.1A and B). Glucose tolerance was also equivalent on chow diet, however male mice had a slight trend towards impaired glucose tolerance (p=0.1 by repeated measures ANOVA, Figure 4.2B).

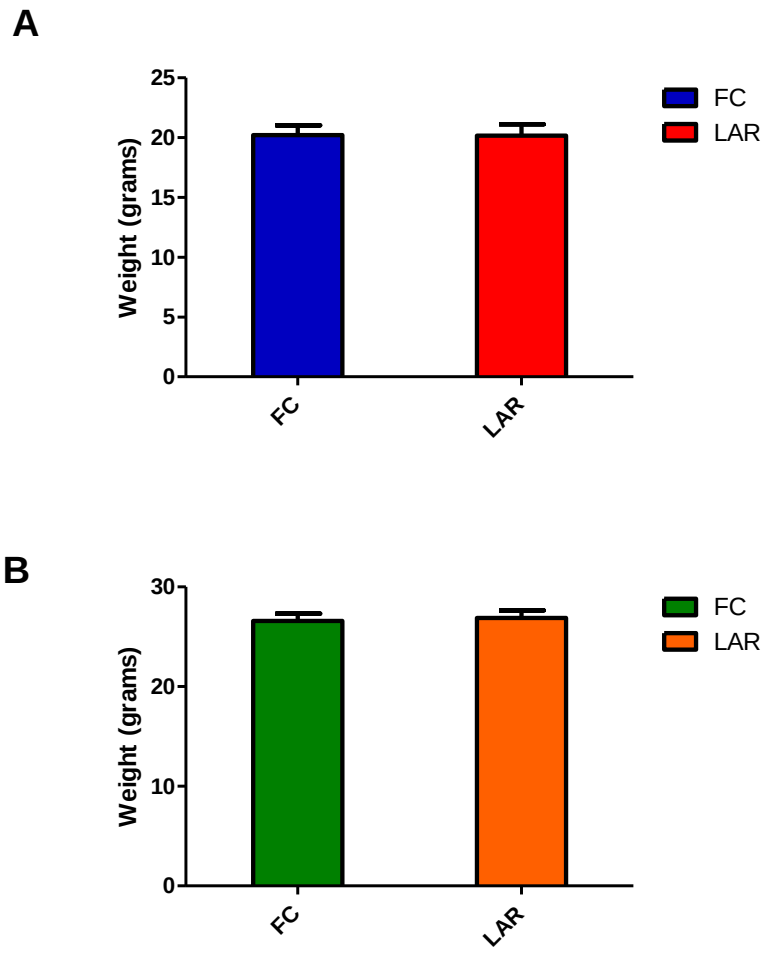

Figure 4.1 LAR weight on chow diet.
FC female mice shown in blue, LAR female mice in red, FC male mice in green and male LAR mice in orange. (A) Female FC and LAR weight on chow diet, (n=13-14/group). (B) Male FC and LAR mice on chow diet, (n=12-14/group). p<0.05=*by students ttest. +/- SEM is shown.

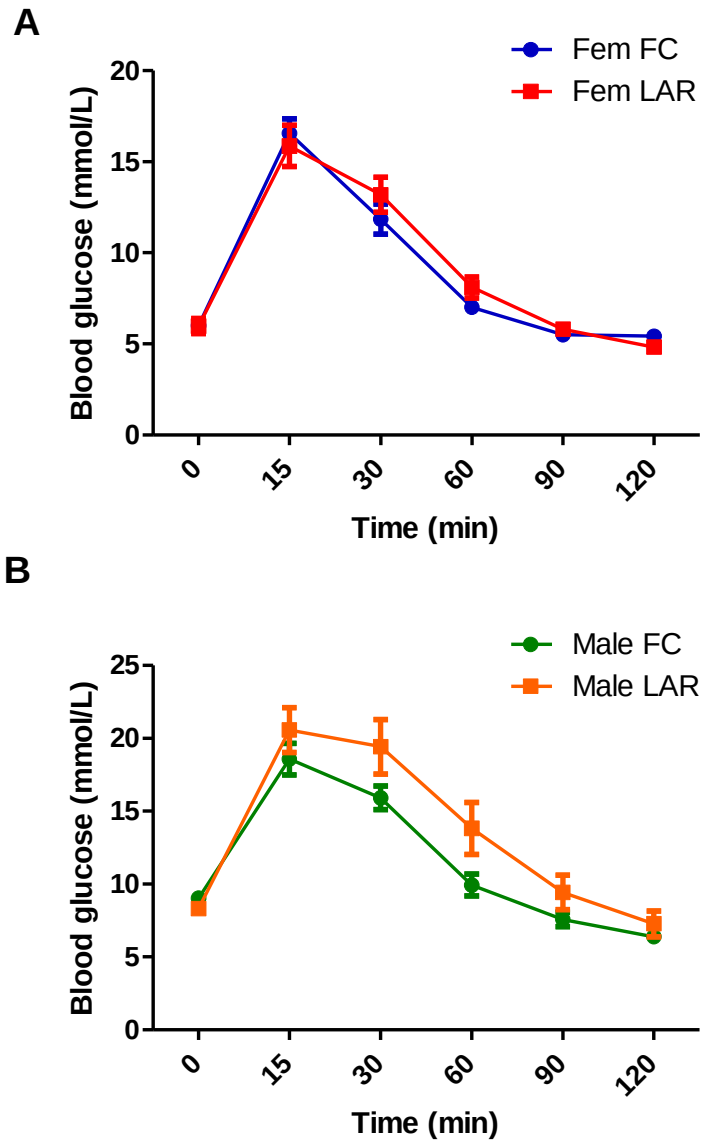

Figure 4.2 Glucose tolerance in chow fed mice.
FC female mice shown in blue, LAR female mice in red, FC male mice in green and male LAR mice in orange. (A) GTT of female FC and LAR mice on chow diet, (n=13-14/group). (B) Male LAR mice had a trend to impaired GTT compared to FC, (n=14-16/group). $p<0.05$= # by repeated measures ANOVA. +/- SEM is shown.

At 5 and 10 weeks of HFD both female LAR ($p = 0.04$, $p = 0.0036$ by repeated measures ANOVA, Figure 4.3A and C) and male LAR mice ($p = 0.01$ and $p = 0.02$ by repeated measures ANOVA Figure 4.3B and D) had impaired glucose tolerance compared matched FC. A subsequent ITT showed no significant difference by repeated measures ANOVA but a small significant increase in blood glucose level in female LAR mice at 20 and 45 minutes (Figure 4.3E, $p=0.05$ and 0.03 respectively by students ttest). Surprisingly male LAR mice had significantly decreased blood glucose level compared to FC mice at 60 minutes by students ttest (Figure 4.3F, $p=0.03$). This suggests no major decrease in peripheral insulin sensitivity to account for impaired glucose tolerance in LAR mice.

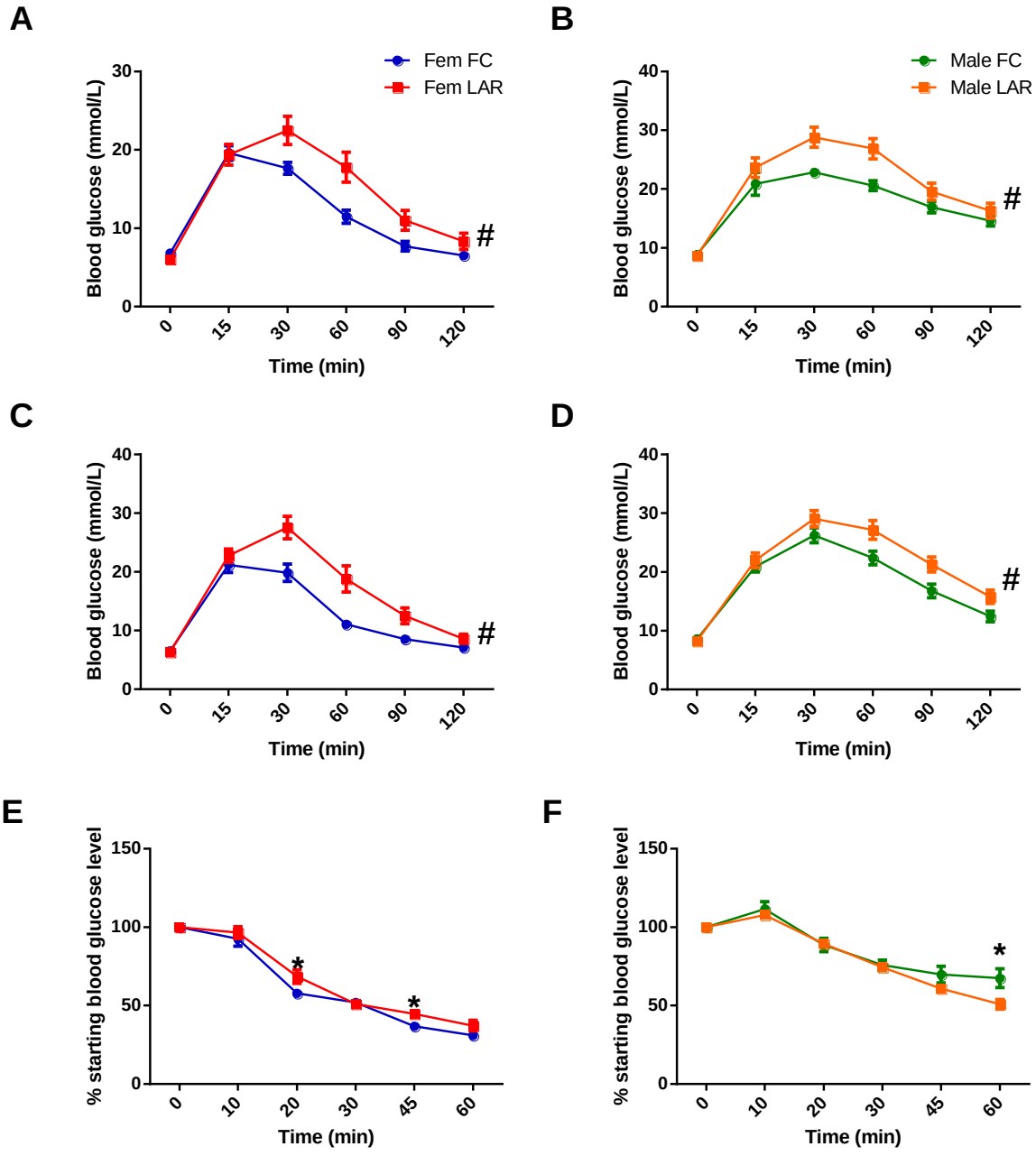

Figure 4.3 Metabolism in mice after 5 and 10 weeks of HFD.
FC female mice shown in blue, LAR female mice in red, FC male mice in green and male LAR mice in orange. (A) Glucose tolerance after 5 weeks of HFD in female mice, (n=13-14/group). (B) Glucose tolerance after 5 weeks of HFD in male mice, (n=14-16/group). (C) Glucose tolerance after 10 weeks of HFD in female mice, (n=13-14/group). (D) Glucose tolerance after 10 weeks of HFD in male mice, (n=14-16/group). (E) Insulin tolerance after 11 weeks of HFD in female mice, (n=8-9/group). (F) Insulin tolerance after 11 weeks of HFD in male mice, (n=10-13/group). Average +/- SEM is shown. * $p<0.05$ by students t-test. # $p< 0.05$ by repeated measures ANOVA.

At 15 and 20 weeks of HFD female glucose tolerance remained impaired compared to FC animals (p=0.01 for both by repeated measures ANOVA, Figure 4.4A and C). At 15 weeks of HFD male LAR mice had equivalent GTT to FC animals (Figure 4.4B). At 20 weeks fasting blood glucose levels were significantly decreased in LAR males (students ttest, p=0.045) and there was a trend to decreased glucose levels throughout the glucose tolerance test (Figure 4.4D, p=0.0637 by repeated measures ANOVA). It is noteworthy that the average blood glucose levels in both LAR and FC male and female mice were significantly decreased compared to GTT results at 15 weeks.

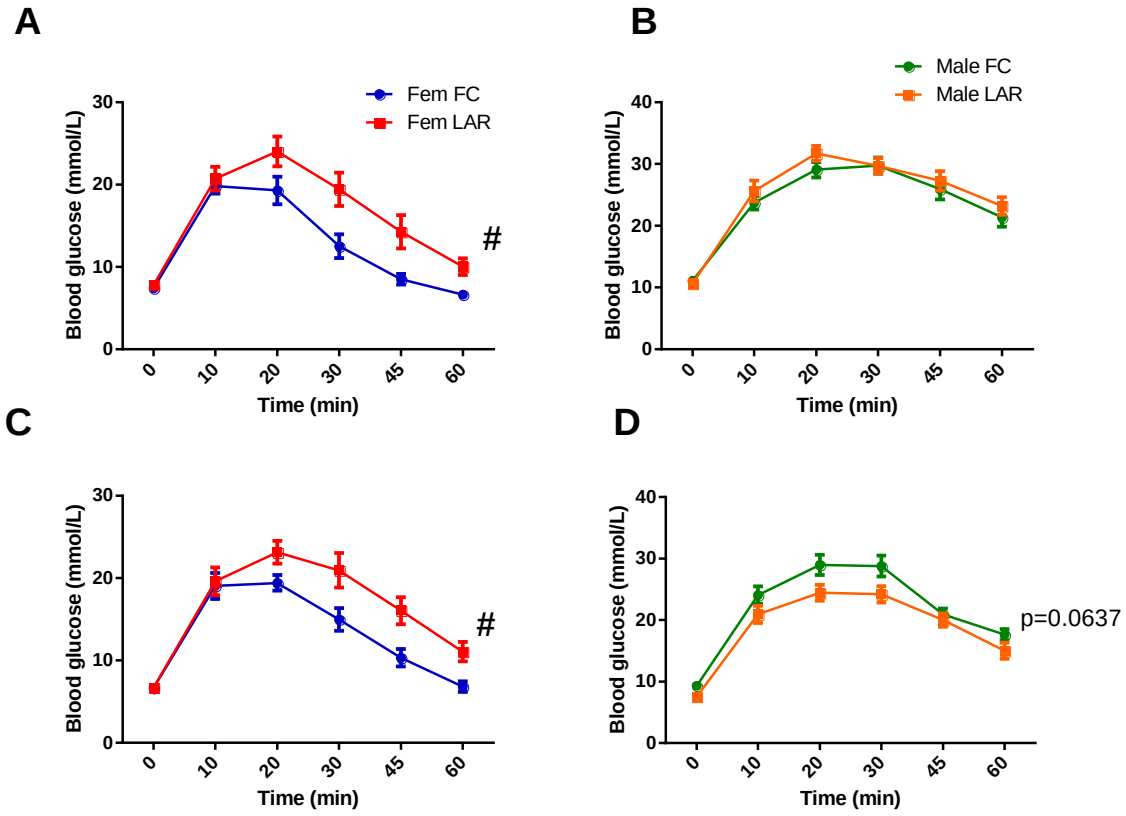

Figure 4.4 Glucose tolerance tests after 15 and 20 weeks of HFD.
FC female mice shown in blue, LAR female mice in red, FC male mice in green and male LAR mice in orange. (A) Glucose tolerance after 15 weeks of HFD in female mice, (n=13-14/group). (B) Glucose tolerance after 15 weeks HFD in male mice, (n=11-13/group). (C) Glucose tolerance after 20 weeks in female mice, (n=13-14/group). (D) Glucose tolerance after 20 weeks in male mice, (n=12-14/group). Average +/- SEM is shown. # $p<0.05$ by repeated measures ANOVA.

At 20 weeks of high fat diet there was no significant difference in PTT results of female LAR and FC mice (Figure 4.5A). There was a trend to decreased blood glucose level in male LAR mice after pyruvate challenge (p=0.09 by repeated measures ANOVA, Figure 4.5B). And blood glucose was again decreased in male LAR mice after fasting (Time 0, p=0.02 by students ttest). There was no overall difference in ITT results by repeated measures ANOVA for LAR mice compared to FC in either sex. However, female LAR mice still showed a small increase in blood glucose at 45 minutes (p=0.05 by students ttest) and male LAR mice a small trend to a decrease in blood glucose compared to FC mice at 60 minutes (p=0.065 by students ttest, Figure 4.5C and D).

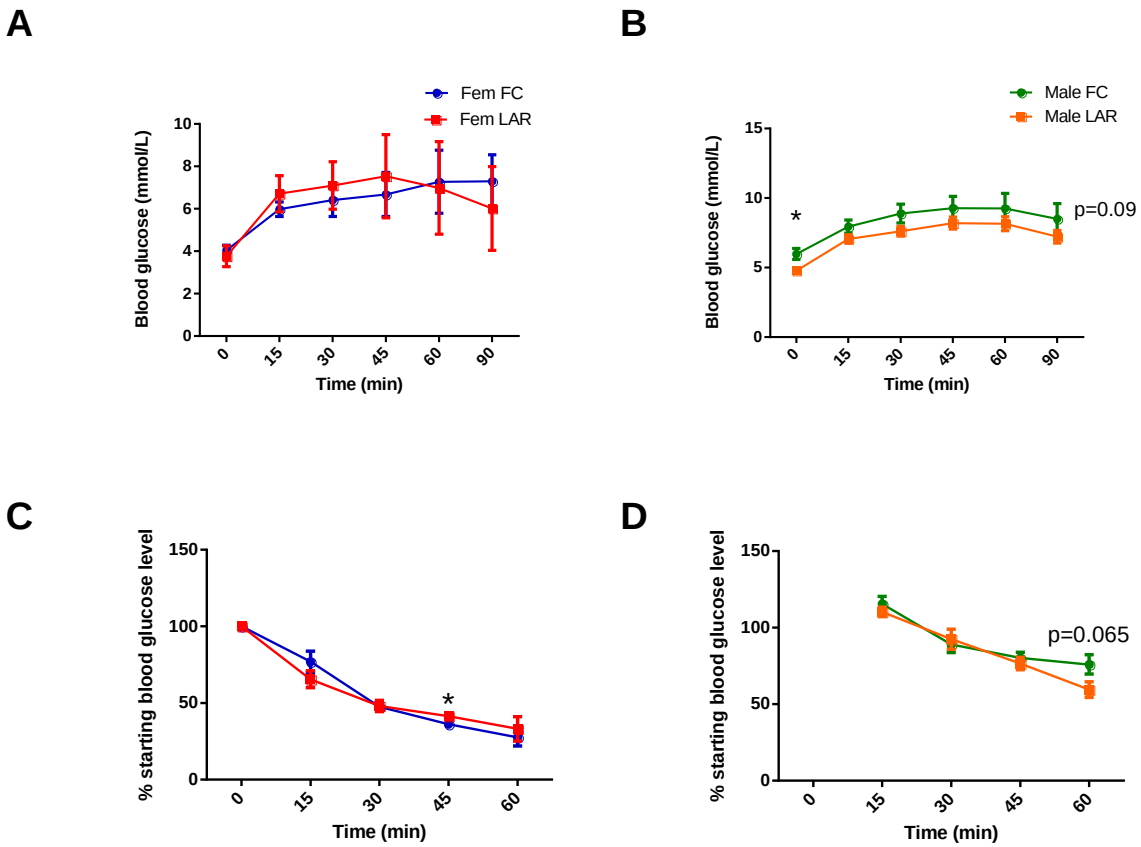

Figure 4.5 Pyruvate challenge and insulin tolerance tests at 20 weeks.
FC female mice shown in blue, LAR female mice in red, FC male mice in green and male LAR mice in orange. (A) Pyruvate challenge results in female mice after 20 weeks of HFD, (n=6-7/group). (B) Pyruvate challenge results in male mice after 20 weeks of HFD, (n=8-13/group). (C) Insulin tolerance for female mice after 20weeks HFD, (n=6-7/group). (D) Insulin tolerance test for male mice after 20 weeks, (n=7-10/group). Average +/- SEM is shown. * p<0.05 by students t-test. # p< 0.05 by repeated measures ANOVA.

4.3 Weight gain in LAR mice on HFD

Male LAR mice had equivalent weight gain throughout the study (Figure 4.6A). Female mice had increased weight or a trend to increased weight at weeks 8-14 (P= 0.05, 0.07, 0.04 and 0.06 by students t-test, Figure 4.6A). When expressed as weight gain female LAR mice gained weight more rapidly than their FC counterparts (p=0.04, by repeated measures ANOVA, Figure 4.6B), although total weight gain at completion of the study was not significantly different (p=0.19 at 20 week time point, by students t-test).

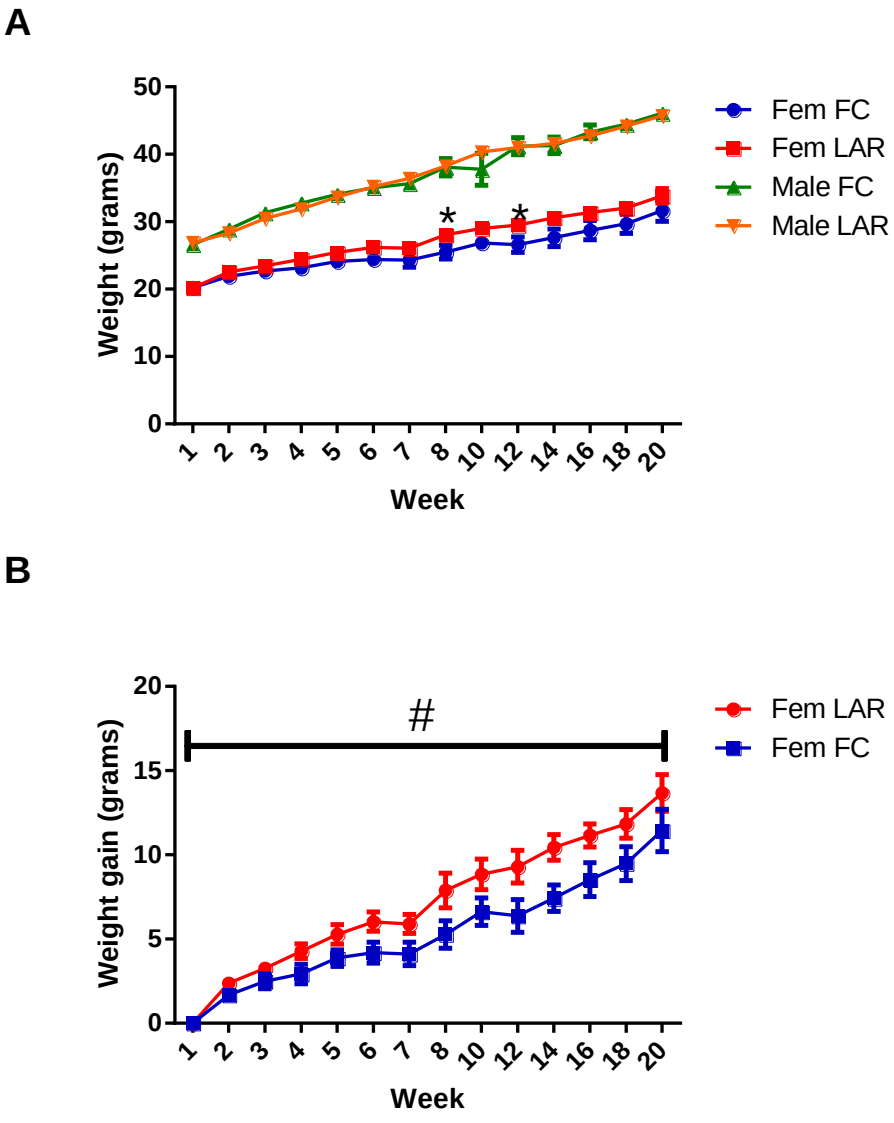

Figure 4.6 LAR weight gain on HFD.
FC female mice shown in blue, LAR female mice in red, FC male mice in green and male LAR mice in orange. (A) Weight in LAR and FC male (n=14-16/group) and female mice (n=13-14/group) during the HFD study. (B) Weight gain in female mice during the HFD study, (n=13-14/group). Average +/- SEM is shown. * p<0.05 by students t-test. # p< 0.05 by repeated measures ANOVA.

4.3.2 **Tissue weights after HFD.**

Female LAR mice had equivalent tissue weight compared to FC after 20 weeks of HFD (Figure 4.7A). Although male LAR mouse body weight did not differ from FC weight throughout the experiment they had a significant increase in subcutaneous fat (p=0.04, by students ttest, Figure 4.7B). There was also a trend to reduced liver weight in male LAR mice after HFD (p=0.092, by students ttest).

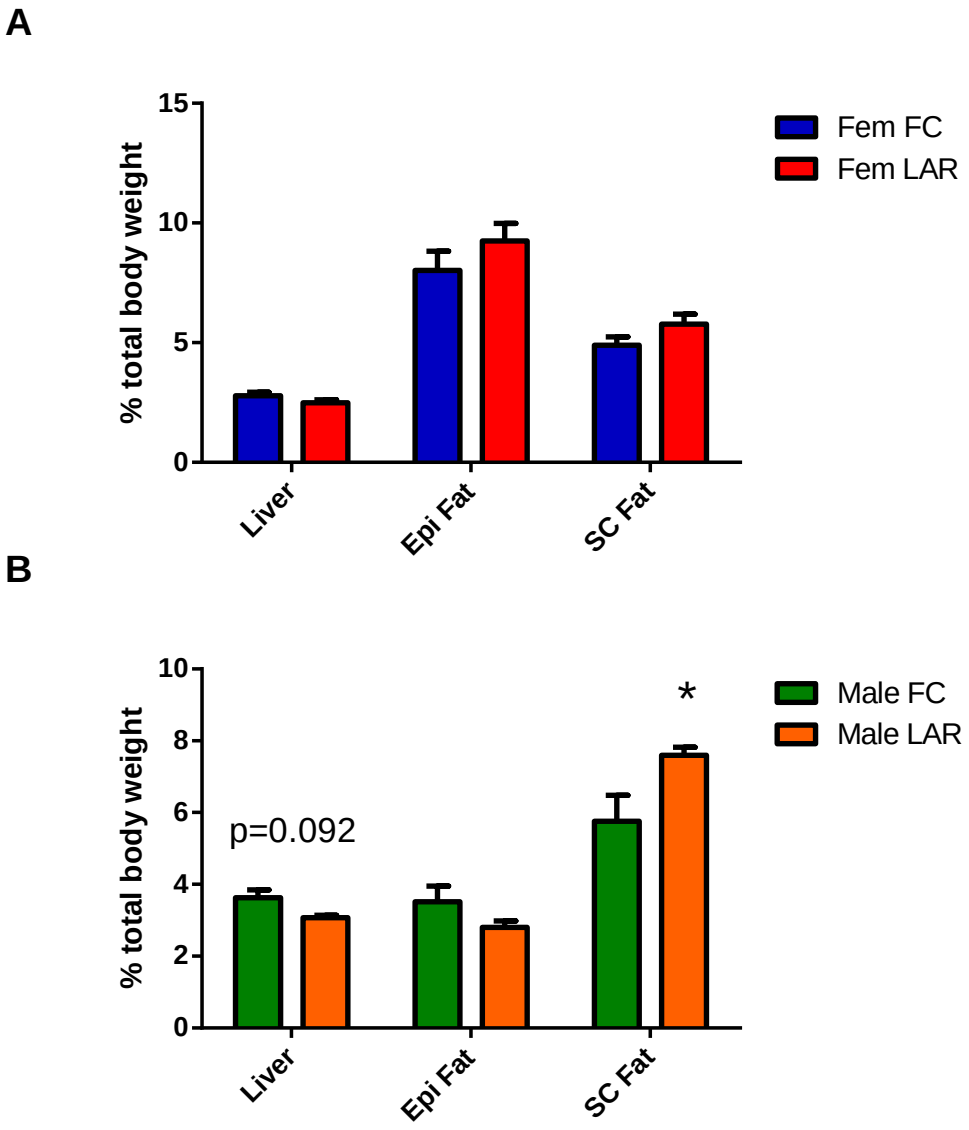

Figure 4.7 Tissue weights after HFD.
FC female mice shown in blue, LAR female mice in red, FC male mice in green and male LAR mice in orange. (A) Female tissue weights after 20 weeks HFD, (n=12/group). (B) Male tissue weights after 20 weeks of HFD, (n=13-15/group). Epigonadal fat pad (Epi), subcutaneous fat pad (SC). Average +/- SEM is shown. * p<0.05 by students t-test.

4.3.3 **Fat cell size quantification of male LAR mice.**

Although the average epigonadal fat pad weight was equivalent in LAR male mice after 20 weeks of HFD there was a trend for increased fat cell size (p=0.075 by students ttest, Figure 4.8A and B, Figure 4.9). As expected there was a significant increase in subcutaneous fat cell size after 20 weeks of HFD in male LAR mice compared to FC (p=0.04 by students ttest, Figure 4.8C and D, Figure 4.9).

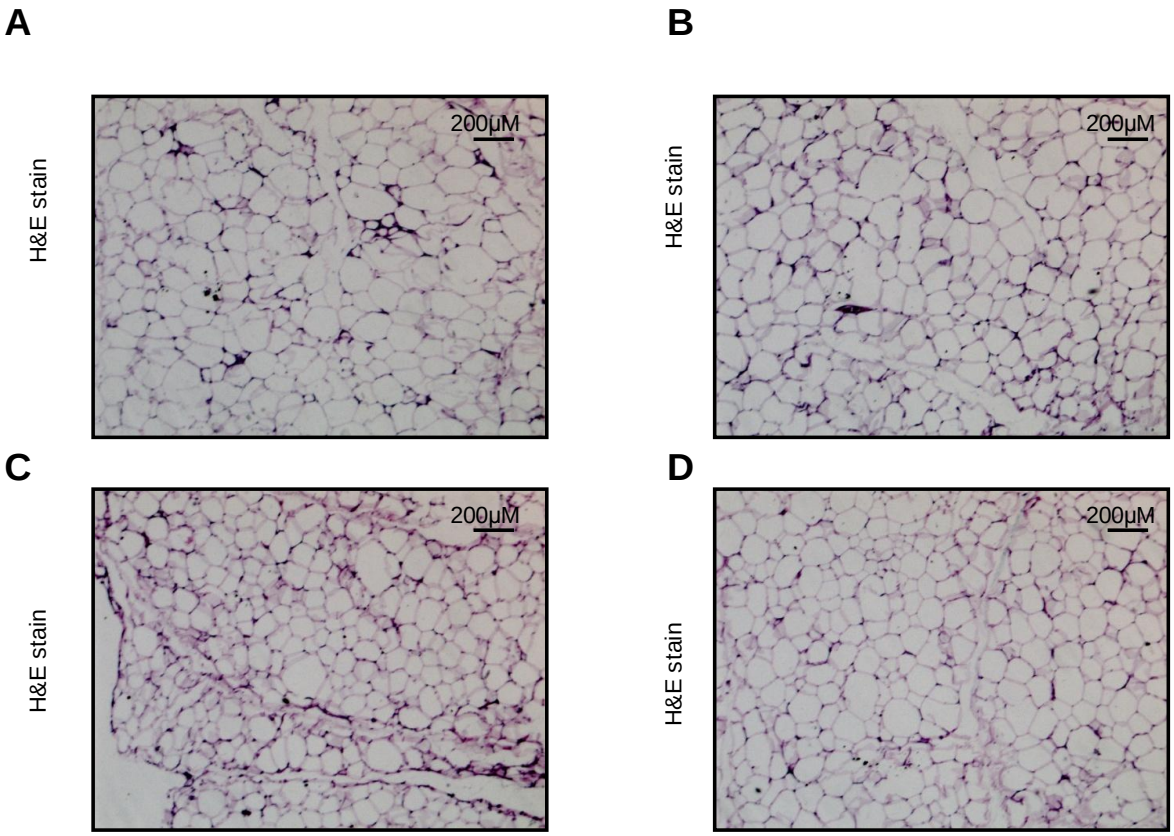

Figure 4.8 Epigonadal and SC fat after 20 weeks HFD.
Representative pictures taken at 4X magnification scale bars shown. FC and LAR male epigonadal fat H&E (A and B). FC and LAR male subcutaneous fat H&E (C and D).

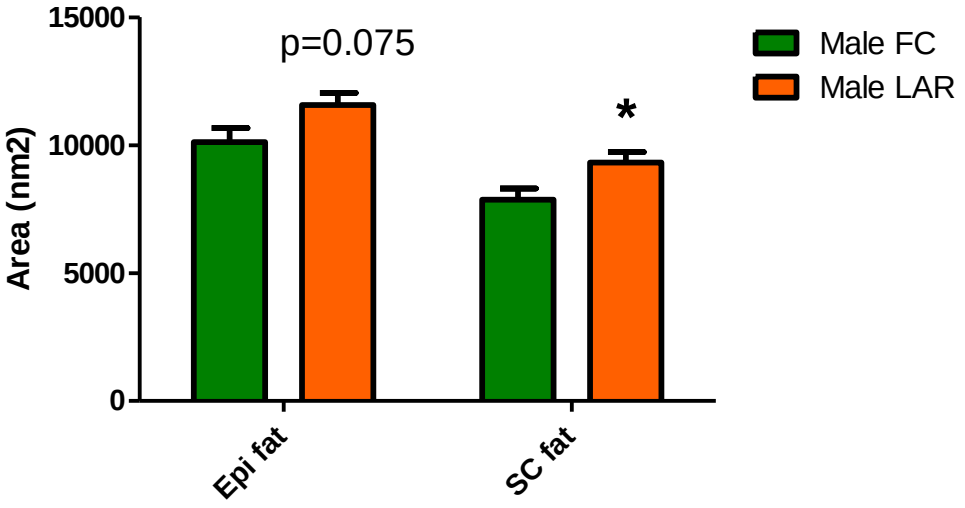

Figure 4.9 Quantification of fat histology.
FC mice shown in green and LAR mice in orange. Average size of fat cells is shown. Epigonadal fat pad (Epi), subcutaneous fat pad (SC). Average +/- SEM is shown. * $p<0.05$ by students t-test, (n=5-7/group).

4.4 NASH and fibrosis in LAR mice

In order to assess the potential contribution of myeloid cell ARNT to development of NASH we next assessed liver histology. Histology of mice which had revieved HFD for 20 weeks was assessed by a blinded and independent pathologist, Andrew Clouston, for the inflammatory changes of NASH and fibrosis using the scoring system outlined by Kleiner et al 2005 (22). Representative histology results for male FC and LAR mice are shown in Figure 4.10. As a percentage female LAR mice had increased prevalence of fatty liver diagnosis compared to FC, and one female LAR mouse had NASH Table 4.1). More male mice had NASH than female mice with 9 of 14 male LAR mice qualifying as having NASH, and only 3 of 10 FC mice (Results summarised inTable 4.1). Male LAR mice had a small but significant increase in inflammation score (LAR average = 0.9285, FC = 0.3, p =0.041293 by students ttest). NASH Activity Score (NAS) was also significantly elevated in LAR male mice compared to FC (Average LAR NAS= 4.5, average FC NAS = 2.25, p=0.033727 by students ttest)

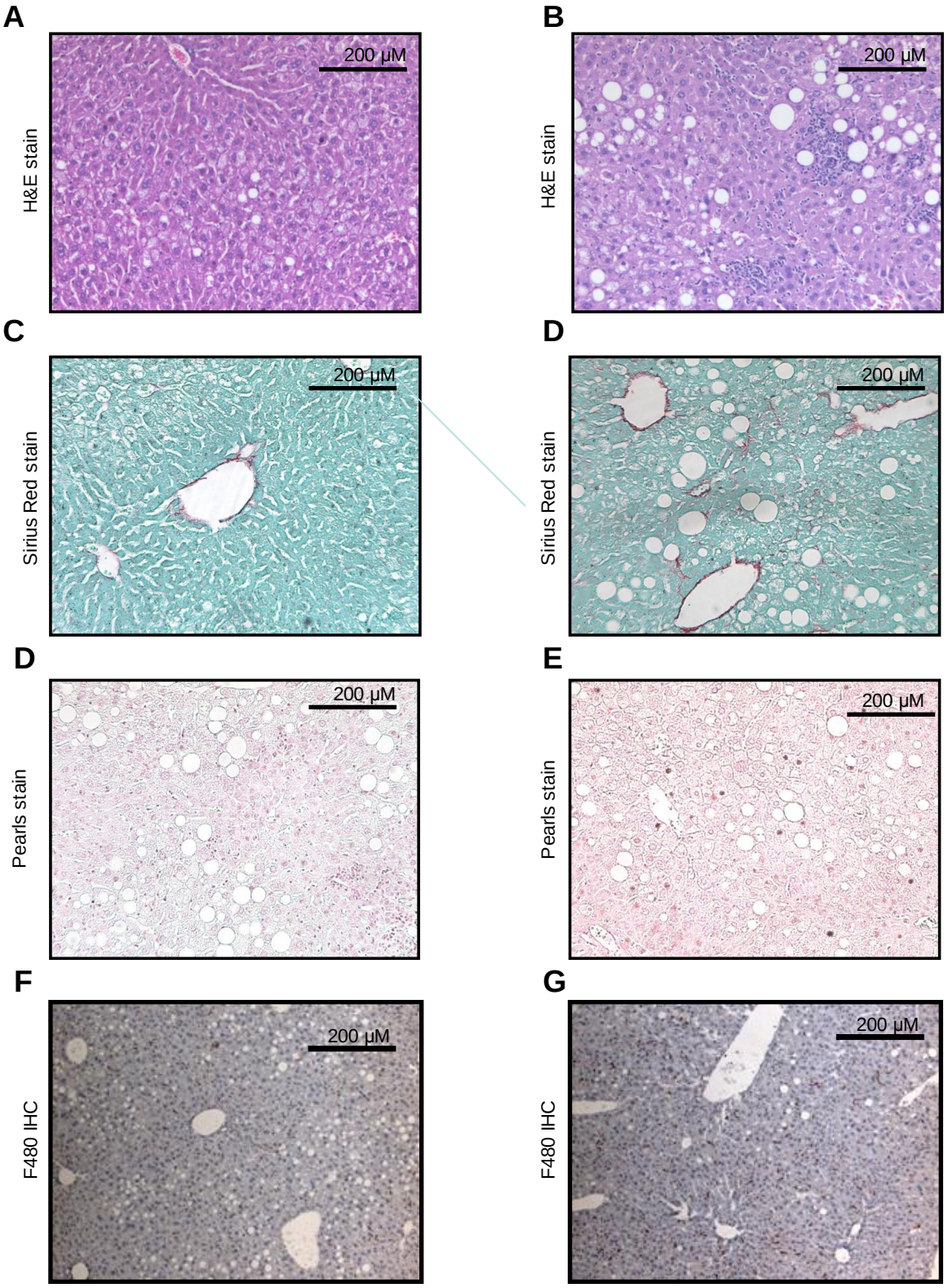

Figure 4.10 Liver histology in LAR mice.

Representative Haematoxylin and Eosin staining of liver sections from FC HFD (A) and LAR HFD (B) mice. Sirius Red staining from FC HFD (C) and LAR HFD (D) mice. Pearls stain liver from FC HFD (D) and LAR HFD (E). F480 staining of FC (F) and LAR HFD (G) fed mice. F480 positive cells are brown.

Table 4.1 Summary of histological NASH scoring for male LAR mice after HFD. Average +/- SEM is shown. Results of students t-test comparing FC and LAR scoring for each gender is shown. Females (n=10/group), males (n=10-14/group).

Gender and Genotype	Steatosis grade	Hepatocye Ballooning	Lobular Inflammation	NAS	Fibrosis (METAVIR)	Diagnosis NAFLD	Diagnosis NASH
Male FC	2.2±0.25	0.7±0.21	0.3±0.15	2.5±0.48	0.2±0.13	70%	30%
Male LAR	2.42±0.14	0.92±0.22	0.66±0.25	4.5±0.78	0.29±0.13	35.7%	64.3%
ttest	0.09	0.13	0.03	0.03	0.21		
Fem FC	0.3±0.15	0	0	-	0	30%	0%
Fem LAR	0.9±0.28	0.1±0.1	0.2±0.2	-	0.1±0.1	50%	10%
ttest	0.08	0.34	0.34	-	0.34		

On quantification there was a trend to increased TG content in livers of LAR HFD fed male mice (p=0.1 by student ttest), and there was no significant change in collagen content compared to FC using Image J to quantitative collagen content (Figure 4.11A and B)

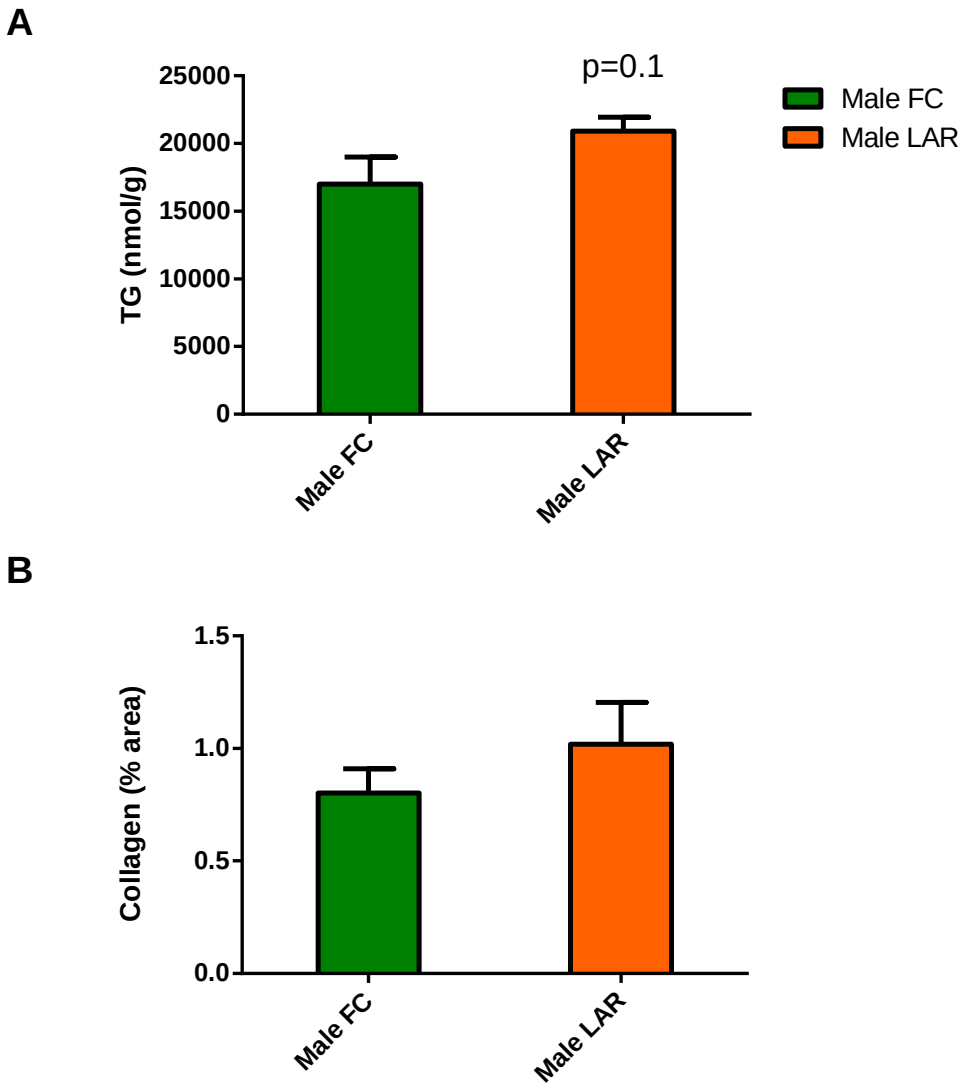

Figure 4.11 Liver TG and collagen content.
FC shown in green and LAR in orange. (A) TG content of FC and LAR HFD liver, (n=5-7/group). (B) Collagen % surface area of FC and LAR liver, (n=5-9/group). Average +/- SEM is shown. * p<0.05 by students t-test.

The increased macrophage infiltration hinted at by F480 staining (Figure 4.10 F and G) was confirmed by assessing liver mRNA expression of *F4/80*, which was significantly increased in LAR HFD mice (p=2.59E-7 by students ttest, Figure 4.12A).

Due to the increased inflammatory changes observed by histology in male LAR mice, the expression of cytokine mRNA was examined (Figure 4.12B). Expression of *Mcp-1*, *Tnf-α* and *Tgf-β1* were significantly increased (p=6E-5, 6.7E-8 and 0.002 respectively by students ttest). There was no change in *Il-6* mRNA expression.

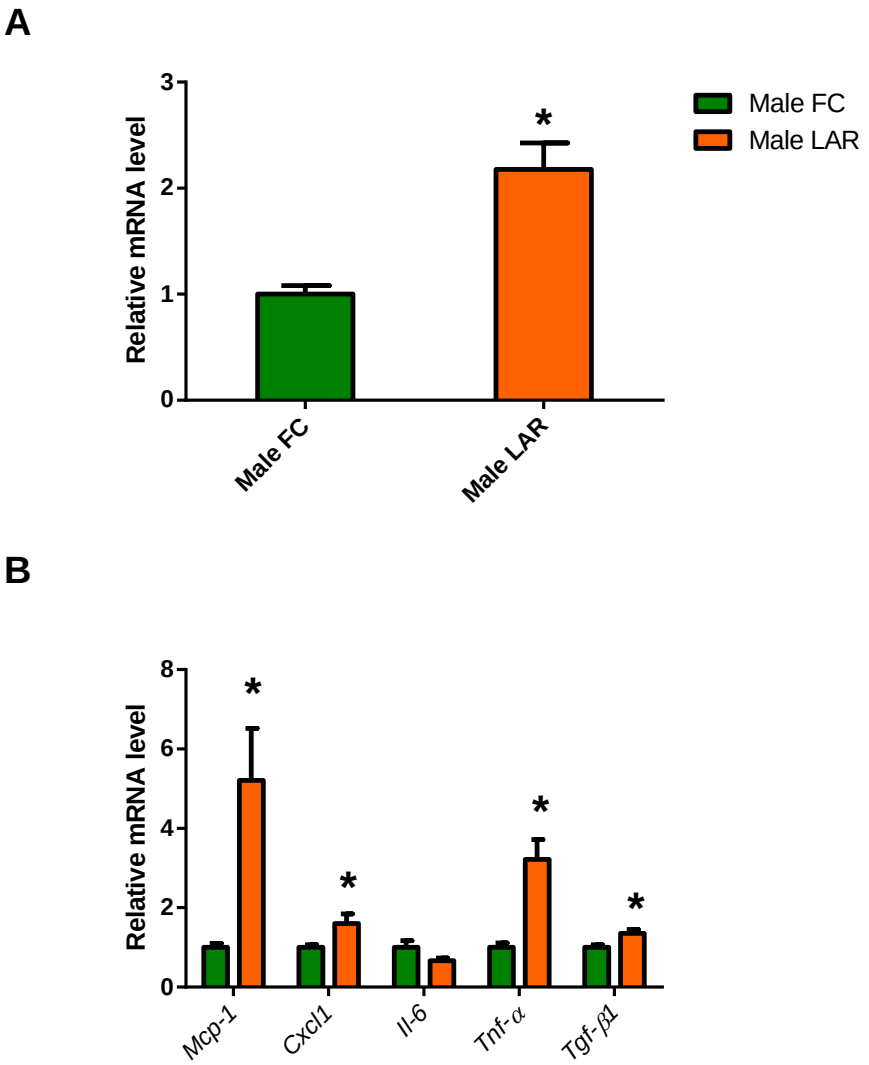

Figure 4.12 F4/80 and cytokine mRNA expression in liver.
FC liver expression show in green and LAR liver expression in orange. (A) Expression of mRNA for macrophage marker *F480* in liver. (B) Expression levels of *Mcp-1*, *Il-6*, *Tgf-β1* and *Tnf-α*. Average +/- SEM is shown. * p<0.05 by students t-test, (n=5-6/group).

Although NASH was evident histologically there was no significant difference in serum levels of alanine transaminase (ALT) or aspartate transaminase (AST) (Figure 4.13A and B).

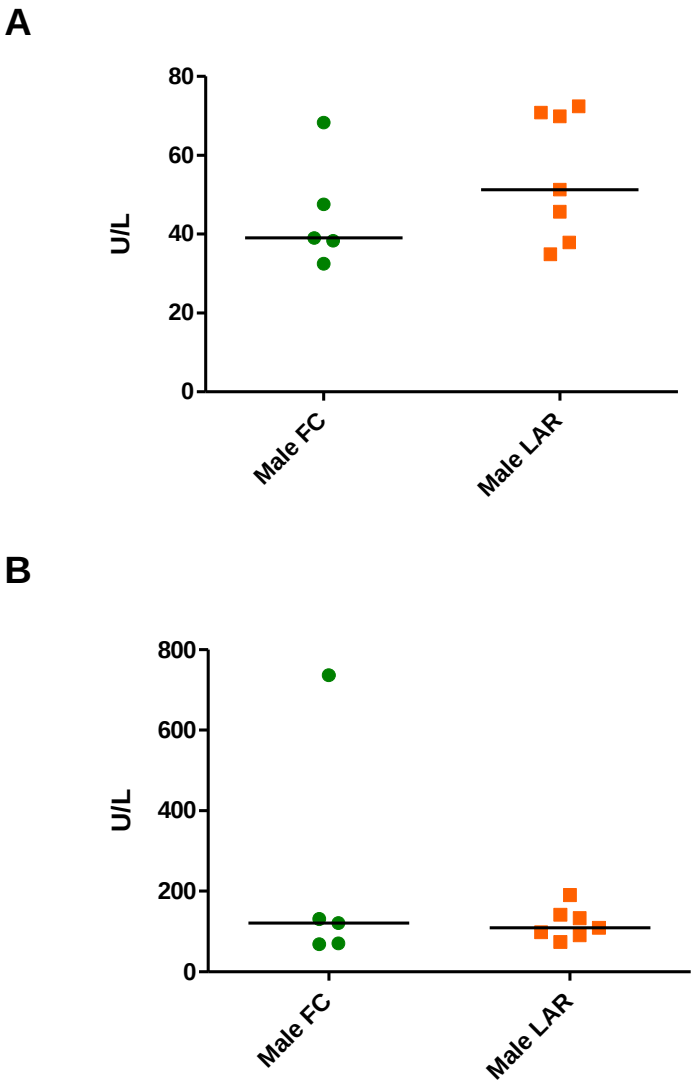

Figure 4.13 Liver function tests.
FC results shown in green and LAR in orange. Median is shown. (A) Serum ALT levels. (B) Serum AST levels. Average +/- SEM is shown. * $p<0.05$ by students t-test, (n=5-7/group).

4.5 Discussion

Mice lacking myeloid cell ARNT had impaired glucose tolerance after 5 - 10 weeks of HFD. Female LAR mice had impaired GTTs throughout the study with a small increase in insulin resistance as assessed by ITT at 11 and 20 weeks. Female LAR mice gained weight on HFD more rapidly than their FC counterparts, whereas male LAR mice showed equivalent weight gain to FC animals. After 20 weeks HFD female LAR mice had a higher prevalence of histologically defined fatty liver, while male LAR mice had increased NASH with increased liver macrophage infiltration and inflammatory cytokine expression.

The results of this chapter add to the growing list of myeloid cell perturbations which result in altered metabolic function. The cause of this impairment of glucose tolerance is unclear. In female LAR mice the impaired glucose tolerance may in part be explained by the small but significant increase in insulin resistance as assessed by ITT. In male mice the mechanism requires further investigation, with a lack of peripheral insulin resistance being demonstrated. However ITT's were not performed at time points earlier than 11 weeks and at 15 weeks of HFD glucose tolerance was equivalent in FC and LAR male mice. Increased cytokine production and in particular IL-1β are known to impair B-cell function (199, 404). It has also been shown that IL-1β blockade is effective in increasing B-cell function in human trials (405). It is known that macrophages associate with islets during HFD (406). It may be that increased macrophage cytokine expression led to impairment of β-cell function and insulin secretion during the first 10 weeks of high fat diet, but β-cell function of LAR mice on HFD remains to be determined.

It is noteworthy that male FC and LAR blood glucose levels were both decreased after glucose challenge at 20weeks compared to 15weeks of HFD, although blood glucose levels in LAR mice decreased further. This corresponded to increased prevalence of NASH in male mice compared to females and a further increase in LAR males compared to FC. This increased NASH was also accompanied by decreased fasting glucose levels in male LAR mice and a trend to reduced gluconeogenesis as assessed by PTT, which suggested impaired HGP in LAR male mice. This also corresponded to a trend to reduced liver weight in LAR mice compared to FC, in the face of a trend to increased TG content. Importantly mRNA for *Tnf-α* was found to be increased in LAR animals and increased TNF-α is associated with disease progression in humans (113). TNF-α is believed to play a

central role in the pathogenesis of NASH through increasing hepatocyte damage and apoptosis (114). The non-significant elevation in collagen content of LAR HFD livers may also hint at a role for macrophage ARNT in liver fibrosis. Assessment of liver collagen of these mice using the TAA model of liver fibrosis would be useful to answer this, unfortunately this study could not be undertaken due to time constraints. The finding of increased cytokine expression and inflammation in the liver after HFD is unexpected when taken together with work showing decreased immune function in acute models in myeloid Hif-1α (238, 266, 267) and ARNT knockout animals (presented in the following chapter). Nonetheless this is congruent with the clinical picture of T2D, where patients have increased markers of chronic inflammation alongside defective immune function with an increased risk of infection and sepsis (167, 179, 331).

These results suggest myeloid cell ARNT may be therapeutic target to reduce liver inflammation in diabetes and other causes of liver cirrhosis. Although supraphysiological elevations of ARNT and hence the ARNT/Hif-2α pair should be avoided because of the recent finding that increased in liver Hif-2α also drives inflammation (258). It is noteworthy that the known human polymorphism (Arg554Lys) of the transactivation domain of AhR has recently been shown to reduce both AhR and ARNT expression in white blood cells (407). The correlation of this polymorphism to prevalence and outcome of liver disease and particularly NASH patients give some information about the contribution of ARNT to human liver disease.

The results in this chapter show that myeloid cell ARNT regulates whole body metabolism and development of NASH. The mechanism of the impaired glucose tolerance requires further investigation, but may be explained in part in female mice by impairment in insulin sensitivity. It is apparent that loss of myeloid cell ARNT drives increased cytokine transcription and inflammation in the liver and exacerbates HFD induced liver damage. Myeloid cell ARNT may be a therapeutic target to reduce blood glucose levels and liver injury in obese and diabetic patients.

Chapter 5. The role of myeloid cell ARNT in immune function and wound healing.

5.1 Introduction

The innate immune system functions as the first line of defence against infection. Mononuclear phagocytes and neutrophils are the key effector cells and function in elimination of pathogens, modulation of the adaptive immune system and tissue repair. An increasingly common cause of immune dysfunction is diabetes mellitus. Diabetes increases the risk of infection, ulcer formation and delayed wound healing (324, 331, 408). Monocyte and neutrophil dysfunction are involved in these processes (317, 331, 333, 409, 410). Studies demonstrate impaired chemotaxis, phagocytosis and killing of bacteria in diabetic polymorphonuclear cells and monocytes/macrophages compared to normal controls. Wound healing in diabetes is delayed compared to controls and is characterised by alterations in number and function of myeloid cells, with available evidence pointing to a persistence of dysfunctional macrophages (317, 333, 335, 409, 410).

ARNT is a transcription factor of the bHLH-PAS family (basic helix-loop-helix Per/ARNT/Sim). In immune cells ARNT binds with its partners Aryl hydrocarbon Receptor (AhR) and Hypoxia Inducible Factor 1 Alpha (HIF-1α) to mediate responses to environmental toxins, immune function (AhR) and the hypoxic response (HIF-1α)(221). The importance of HIF-1α in innate immune function was shown by Cramer *et al* (238) who found decreased immune function in mice with myeloid cell deletion of this gene. Subsequently it was found that HIF-1α was important in regulating apoptosis, phagocytosis and bacterial killing (238, 266, 267).

HIF-1α activity is reduced at high glucose concentrations in human fibroblasts and diabetic animals (380-382), and is decreased in human diabetic ulcers and with increasing age in db/db mice (383, 384). Correspondingly, artificially elevating the level of HIF-1α through desferoxamine (DFO), $CoCl_2$ or constitutively active HIF-1α producing constructs lead to improved wound healing in models of diabetes (381, 382). We previously reported that ARNT is decreased in islets and in the liver of T2D patients and reduction of ARNT in both these tissues results in impairment of function (225, 252). Intriguingly high glucose has been found to reduce ARNT expression in islets via ChREBP activation, demonstrating another direct link between glucose and the functioning of ARNT and its partner HIF-1α (399). From this accumulating evidence it is possible that diabetes also causes alterations in the ARNT expression in multiple tissues and cell types and this further contributes to the diabetic phenotype.

To create myeloid cell ARNT deletion we used the Cre-LoxP system with Cre expression under control of the Lysozyme M promoter (388). Lysozyme M is an antimicrobial protein expressed in

granulocytes, macrophages and their precursers (411). Although recent studies have demonstrated that LysM expression is not completely restricted to myeloid cells, with LysM expression evident in alveolar type II cells of the lung and in myocardial cells which form the intraventricular septum, this is an accepted system which has been used in multiple studies to investigate the function of myeloid cells (411-413). LysM Cre mice were initially described as having high deletion efficiency in macrophages and neutrophils (75-95% and 79-99% respectively), with 16% deletion in CD11c-positive DC and minimal deletion in T and B cell lymphocytes (388). Subsequent studies have shown reduced effectiveness with a variable percentage of Enhanced green fluorescent protein (EGFP) expression reported in peritoneal macrophages isolated from LysM-EGFP mice (around 60%) and blood monocytes isolated from LysM-Cre × Rosa26-stop flox EGFP mice (55-75%) in previous studies, with a higher deletion efficiency (93%) in neutrophils (414, 415).

As the required partner, ARNT integrates signals from HIF1α, HIF2α and AhR. To date the role of macrophage and neutrophil ARNT in immune function and wound healing has not been examined. Here we present evidence that myeloid cell ARNT plays a key role in immune function and wound healing. The results suggest reduced macrophage ARNT/ HIF-1α transcription may be a component of impaired wound healing in diabetes and represent a therapeutic target to improve immune function and wound healing in diabetic patients.

5.1.1 Aims and strategies

To investigate the effects of long-term ARNT deletion in myeloid cells including; response to infection, inflammation and wound healing. Myeloid cell-specific ARNT-knockout mice were studied on chow diet:

1) To investigate the effect of myeloid cell ARNT deletion on immune function.

2) To investigate the role of myeloid cell ARNT in models of infection and inflammation.

3) To investigate the role of myeloid cell ARNT on wound healing with or without diabetes.

5.2 The role of ARNT in myeloid cell function.

The average number of thioglycollate elicited macrophages isolated from myeloid cell-specific ARNT-knockout (LAR) mice was similar to that in controls suggesting grossly similar migration (FC average $14.7x10^6$ and LAR average $14.3x\ 10^6$, p>0.9, by students ttest). Macrophage *Arnt* mRNA was reduced to 50% of control levels in thioglycollate elicited LAR macrophages after 24 hours of LPS treatment (Figure 5.1A). This relatively modest deletion efficiency is consistent with previous studies (414, 415). After 24 hours of LPS stimulation, LAR macrophages had significantly reduced *Cxcl1* (p=0.0002), *Mcp-1* (p = 2.78E-07), *Tgf-β1* (p = 1.62E-05) and *Il-6* (p = 0.002) expression by students ttest. There was no change in *Tnf-α* (p = 0.2) (Figure 5.1A).

Blood monocyte and granulocyte phagocytosis was next assessed in whole blood. LAR animals showed reduced bacterial uptake compared to FC animals in blood granulocytes 80% (p<0.001 by students ttest) and a trend to reduced monocyte uptake (76% of FC, p=0.08 by students ttest, Figure 5.1B). Although LAR granulocytes phagcytosed fewer bacterial particles than FC, there were approximately 10 times the number of surviving Group A streptococcal (GAS) intracellular bacteria isolated from whole blood lymphocytes (p=0.01 by students ttest). This suggests both impaired phagocytosis and severely impaired bactericidal activity (Figure 5.1C).

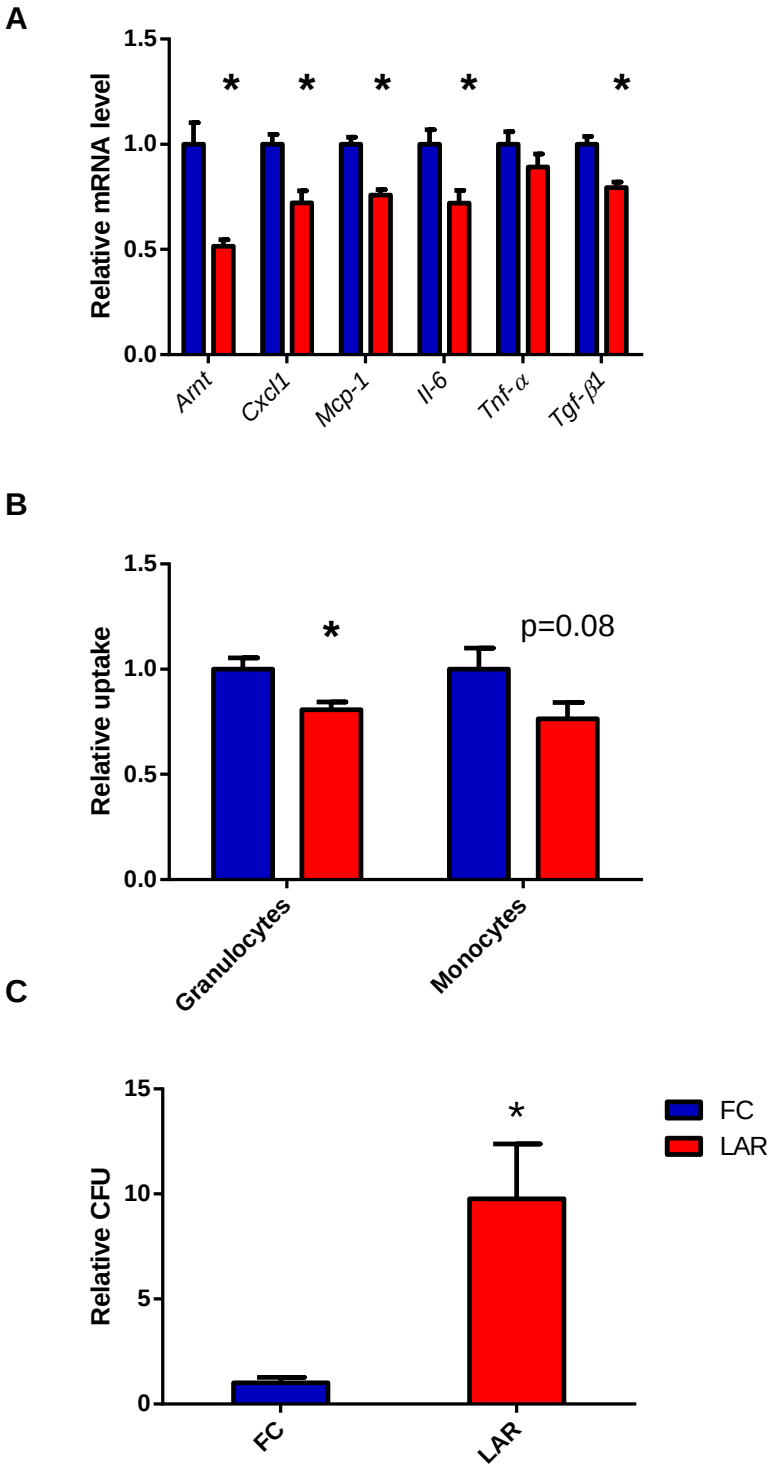

Figure 5.1 Myeloid cell function in LAR mice.

FC male mice shown in blue, LAR male mice in red. (A) Thioglycollate elicited macrophage mRNA expression after 24 hours incubation with 100ng/ml LPS, (n=5/group). (B) Phagocytosis of labelled bacteria in whole blood, (n=10-11/group). (C) Intracellular GAS bacteria isolated after incubation with whole blood. Results shown is the average of a total of 15 replicates per group performed with whole blood from 3xFC and 3xLAR male mice over two experiments. *=<0.05. Average -/+ SEM is shown. Colony-forming unit (CFU).

5.3 The role of myeloid cell ARNT in models of inflammation and immune function.

We next assessed the *in vivo* function of LAR myeloid cells. Cutaneous inflammatory response was reduced in LAR animals following SDS treatment. As expected, skin in FC animals was irritated after SDS treatment, showing erythema and keratosis, and these gross findings were markedly reduced in LAR animals (Figure 5.2A). Inflammatory response in FC animals was marked by vasodilation, epidermal hyper-proliferation and oedema (Figure 5.2B). Inflammatory response was scored by two independent observers blinded to genotype using a semi-quantitative scale of inflammation which included signs of infiltrate, edema and epidermal proliferation. Sections were scored from 0-4 with 0 being no skin inflammation and 4 being maximal inflammation observed. Results are shown graphically (Figure 5.2C).

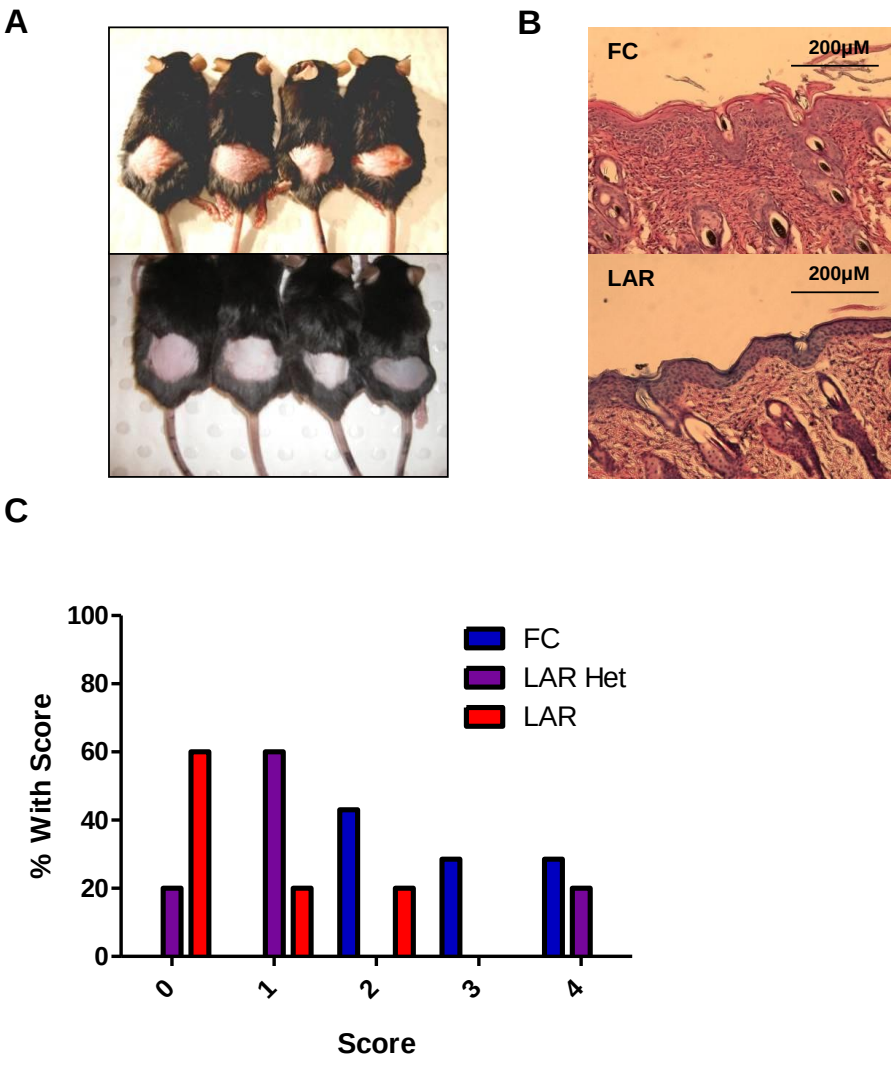

Figure 5.2 The SDS skin irritation model.
(A) Photograph of male FC mice treated with SDS (upper panel) and male LAR mice treated with SDS (lower panel). (B) H&E of male FC and LAR skin after SDS study. (C) Histology after SDS was scored for signs of inflammation by two observes blinded to genotypy. Results in male mice expressed as the average % of mice with inflammation score FC (blue) LAR het (purple) and LAR (red). (n=5-6/group).

The response of LAR mice to infection was then assessed by a model of GAS subcutaneous infection. LAR had significantly accelerated wound formation and size and increased bacteraemia following subcutaneous Group A streptococcal (GAS) injection (Figure 5.3). There was no significant difference in weight loss between groups by repeated measures ANOVA, although LAR mice had a trend towards less weight loss at day 1 ($p=0.055$, by students ttest) and a trend to reduced overall weight at day 4 ($p=0.1$, by students ttest, Figure 5.3A). At day 1 there was a significant increase in wound size in LAR animals compared to FC ($p<0.001$,by students ttest, Figure 5.3B). Within the wound and spleen there was no significant difference in GAS CFU (colony forming units) in LAR mice (Figure 5.3C). However, there was a significant increase in CFU isolated from LAR blood compared to FC

animals by Wald-Wolfowitz test ($p<1x10^{-10}$, Figure 5.3E). This indicated that LAR mice had increased systemic infection and were unable to keep the infection localised.

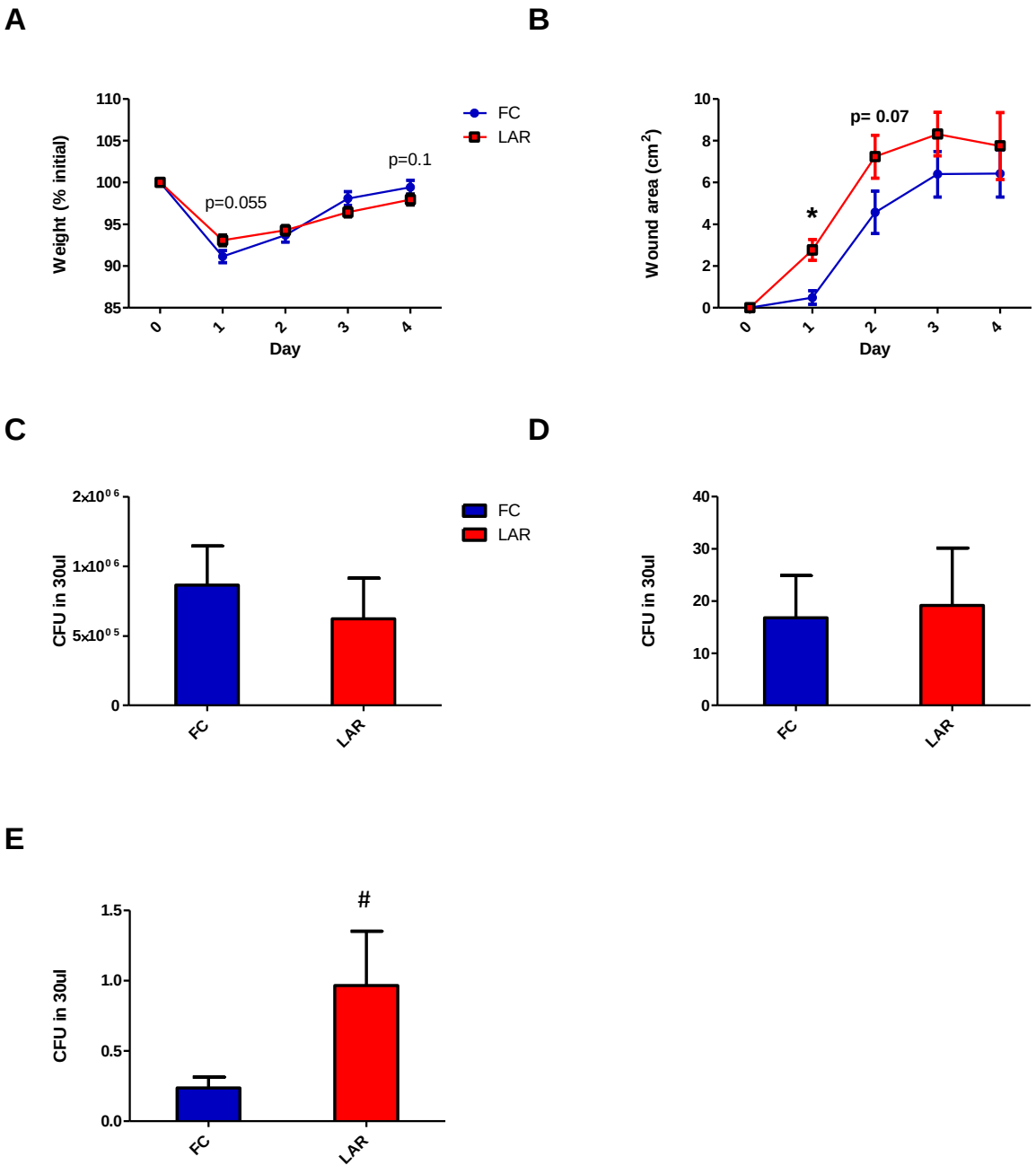

Figure 5.3 Response of LAR mice to GAS infection.
FC in blue (circles or bars) LAR mice in red (circles or bars). (A) Mouse weights after infection. (B) GAS wound size. (C) CFU isolated from skin. (D) CFU from spleen (E) CFU from blood. *p<0.05 by students ttest, #<0.05 by Wald-Wolfowitz test. SEM is shown (n=20-22/group).

The response of LAR mice to the skin transplant model was next assessed. There was a significant delay in Balb/c skin transplant rejection in LAR mice compared to FC by Log-rank (Mantel-Cox, p=0.0056, Figure 5.4A). There was no difference in rejection in the reciprocal transplant of LAR skin onto Balb/c mice, suggesting grossly normal presentation of antigens in LAR skin (Figure 5.4B). Interestingly, during these experiments it was noted that LAR mice appeared to have delayed healing after transplant rejection.

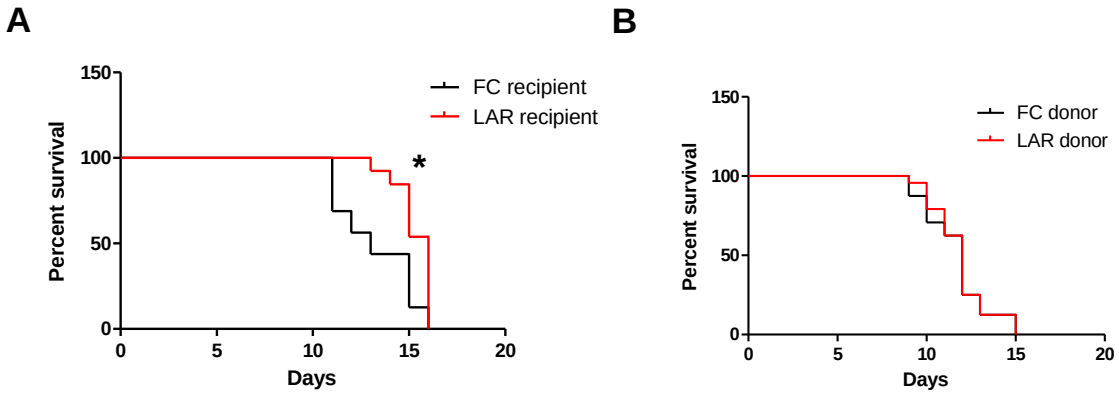

Figure 5.4 Survival curve of graft rejection.
Survival curve of Balbc graft onto FC recipient (black) and LAR recipient female mice (red) (A). Survival curve of reciprocal transplant from LAR donor (Red) or FC donor onto Balbc female mice. *p<0.05 by Mantel-Cox test (n=13-16/group).

5.4 LAR mice have delayed wound healing

Given the observed healing delay after transplant rejection in LAR animals we formally assessed wound healing in these mice (Figure 5.5A). LAR mice had significantly delayed wound healing at 2, 4 and 6 days by Students t-test ($p<0.001$, <0.001 and $=0.011$). Average tensile strength of LAR wounds, asessed with the assistance of Philip Boughton, was not significantly altered at day 18 by students ttest (Figure 5.5B). H&E and Trichrome Milligan's staining of wounds, Peformed by James Bonner, at day 4 is shown (Figure 5.6 A-F). The results show no major morphometric changes observed in LAR mice wound histology compared to FC animals.

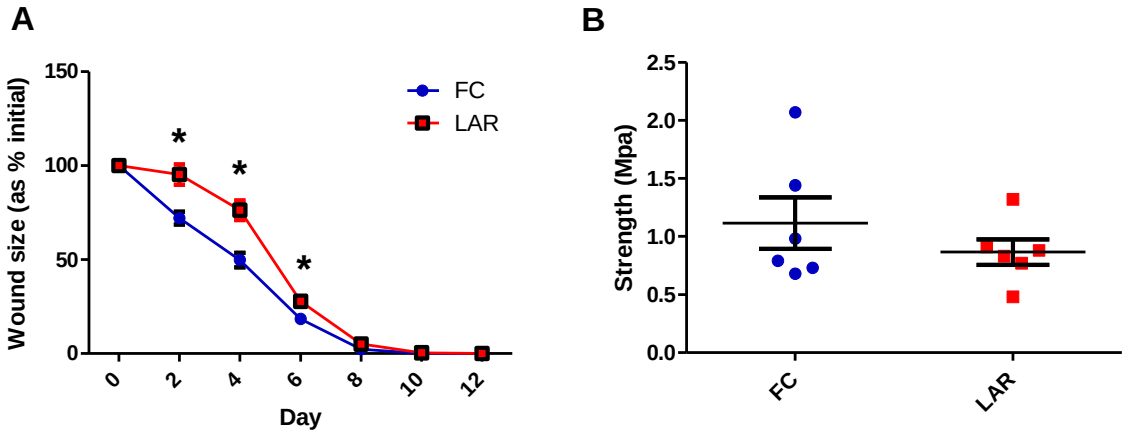

Figure 5.5 Wound healing in female LAR mice.
(A) Wound healing in FC (blue circles) and LAR (red squares), n=20/group. (B) Tensile strength of FC (blue circles) and LAR (red squares) of wounds at day 18 (n=6/group). Average +/- SEM is shown, * < 0.05 by students ttest.

Wounds were collected during the healing process (day 4) to examine gene expression. Cytokine expression in LAR animals was reduced with *Mcp-1* mRNA expression reduced to 32% ($p<0.0001$, students ttest) and *Il-6* mRNA to 14% ($p=0.02$, students ttest) of FC levels. *Tnf-α* was also reduced to 39% (not-normally distributed, Wald-Wolfowitz test $p=0.003$, Figure 5.7A). Messenger RNA expression of the key tissue remodelling gene, *Mmp9*, was reduced to 44% of FC level ($p=0.004$, students ttest) and there was a trend to reduced *Timp1* (47%, $p=0.058$, students ttest) and *Sma* (66%, $p=0.064$, students ttest). *Tgf-β1* was found to be reduced by Wald-Wolfowitz test as were *Col1a1*, *Sma*, *Timp1* and *Elastin* (Figure 5.7B). Interestingly although there was a reduction in cytokine and tissue remodelling gene expression, there was no significant change in macrophage marker *F4/80*

mRNA expression (Figure 5.7C). Together with unchanged numbers of thioglycollate-elicited macrophages, this indicated normal tissue migration in LAR macrophages.

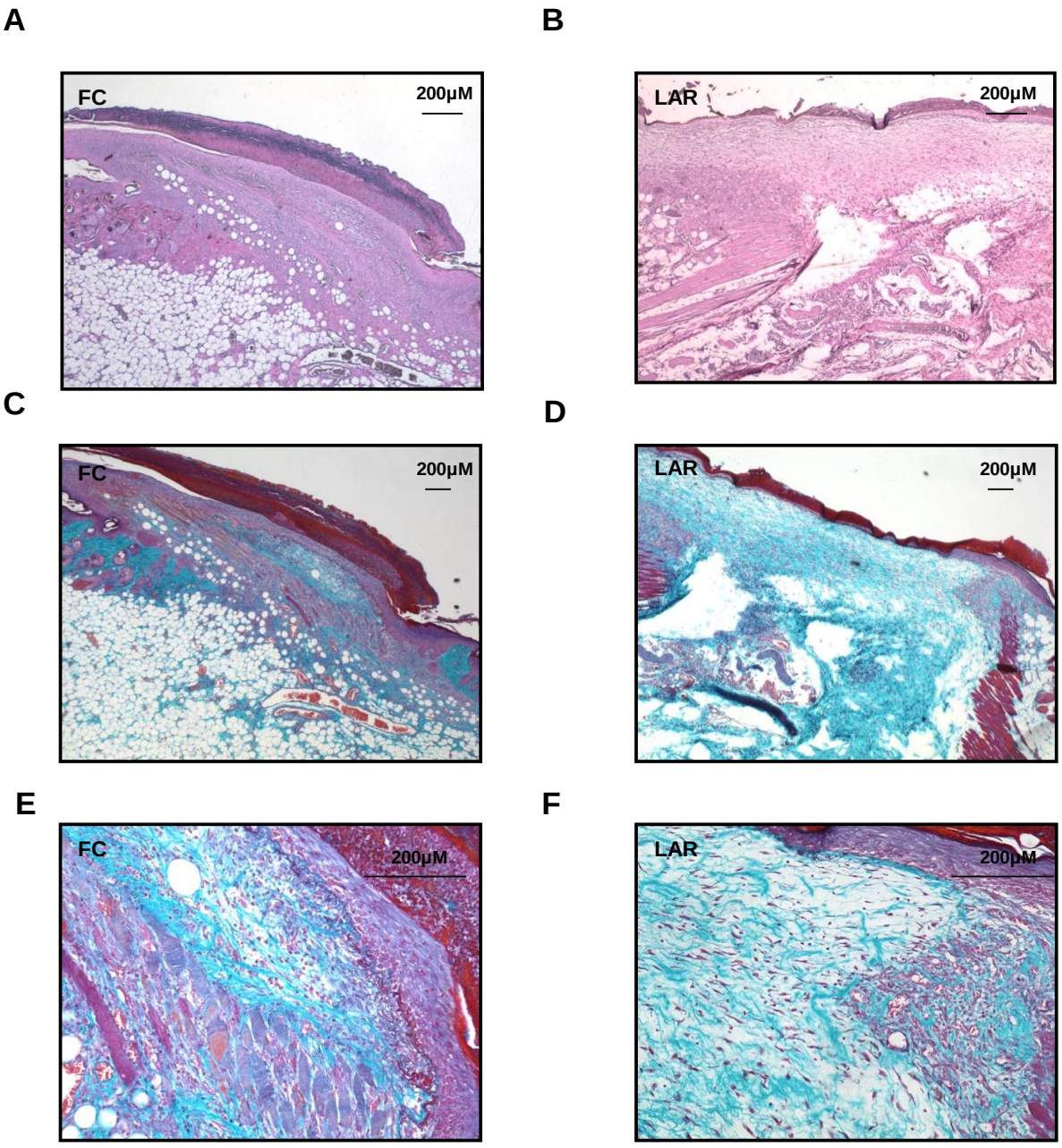

Figure 5.6 Wound histology. FC and LAR wounds at 4 days.
Representative H&E of (FC) (C) and LAR wound (D) at 40 X magnification. Trichrome milligan's stain of FC (E) and LAR wounds at 25 X magnification (F). Trichrome milligan's stain of FC (G) and LAR wounds (H) at 100 x Magnification at wound edge.

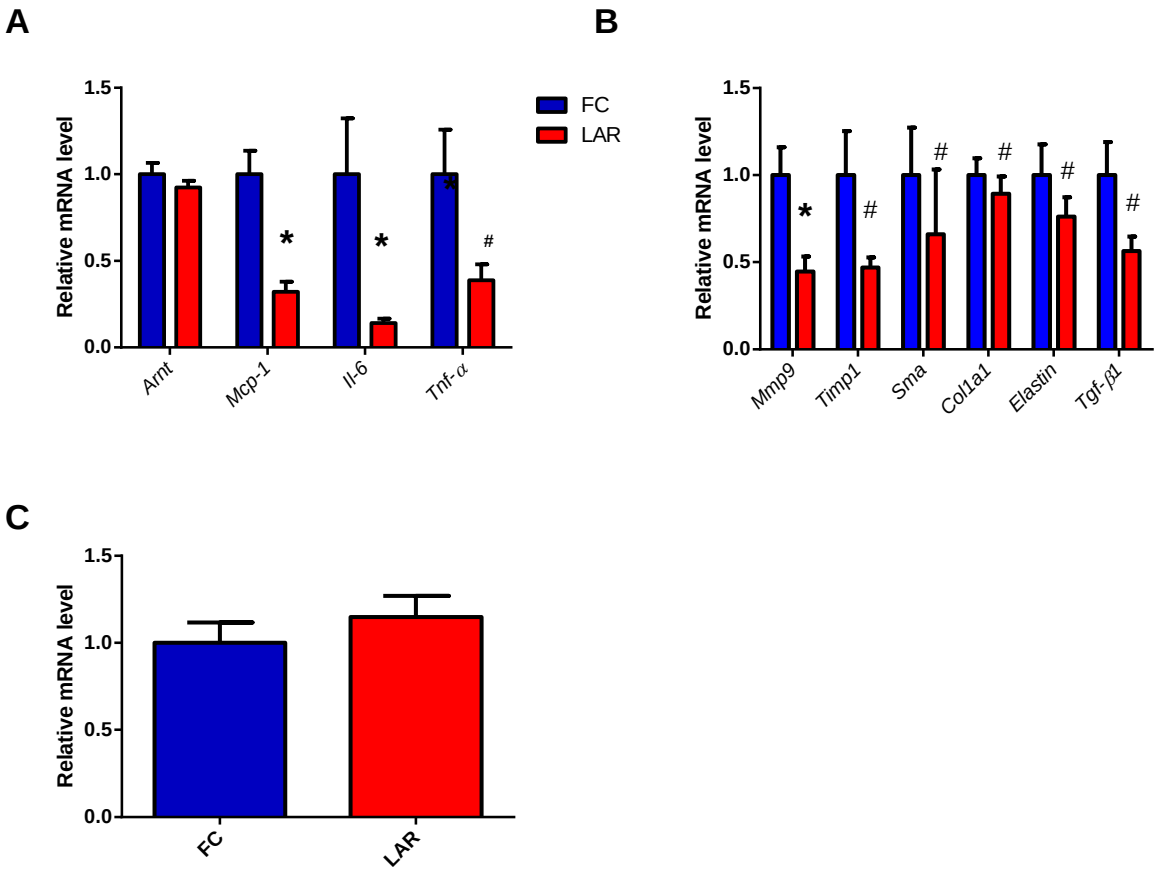

Figure 5.7 Day 4 wound mRNA expression.
(A) Cytokine expression in day 4 wounds. (B) Tissue remodelling expression in day four wounds. (C) F480 mRNA expression in day 4 wound. * = $p<0.05$ by students ttest. # = $p<0.05$ by Wald-Wolfowitz T test. SEM is shown, n=6/group.

Due to literature indicating that the ARNT partner HIF-1α is decreased in diabetic wounds and contributes to impaired wound healing, we investigated wound healing in LAR and control mice which were rendered diabetic as described in methods. Interestingly, the differences in wound healing in control and LAR animals were markedly reduced on a diabetic background (Figure 5.8A). This suggests that decreased ARNT-dimer activity in LysM expressing cells (including neutrophils, monocytes and macrophages) is a component of impaired wound healing in diabetes.

To delineate whether increasing transcriptional activity of the ARNT/HIF-1α complex in myeloid cells is part of the mechanism of DFO in improving healing in diabetic mice, we investigated the response

of diabetic FC and LAR mice to DFO treatment (Figure 5.8B and C). DFO treatment resulted in significant decreases in wound size of FC animals at 6 and 8 days (p=0.045 and p=0.03 by students ttest). In contrast, DFO treatment failed to significantly improve wound healing in LAR animals. This indicated that action of ARNT+HIF in myeloid cells in wounds is required for the full benefit of DFO

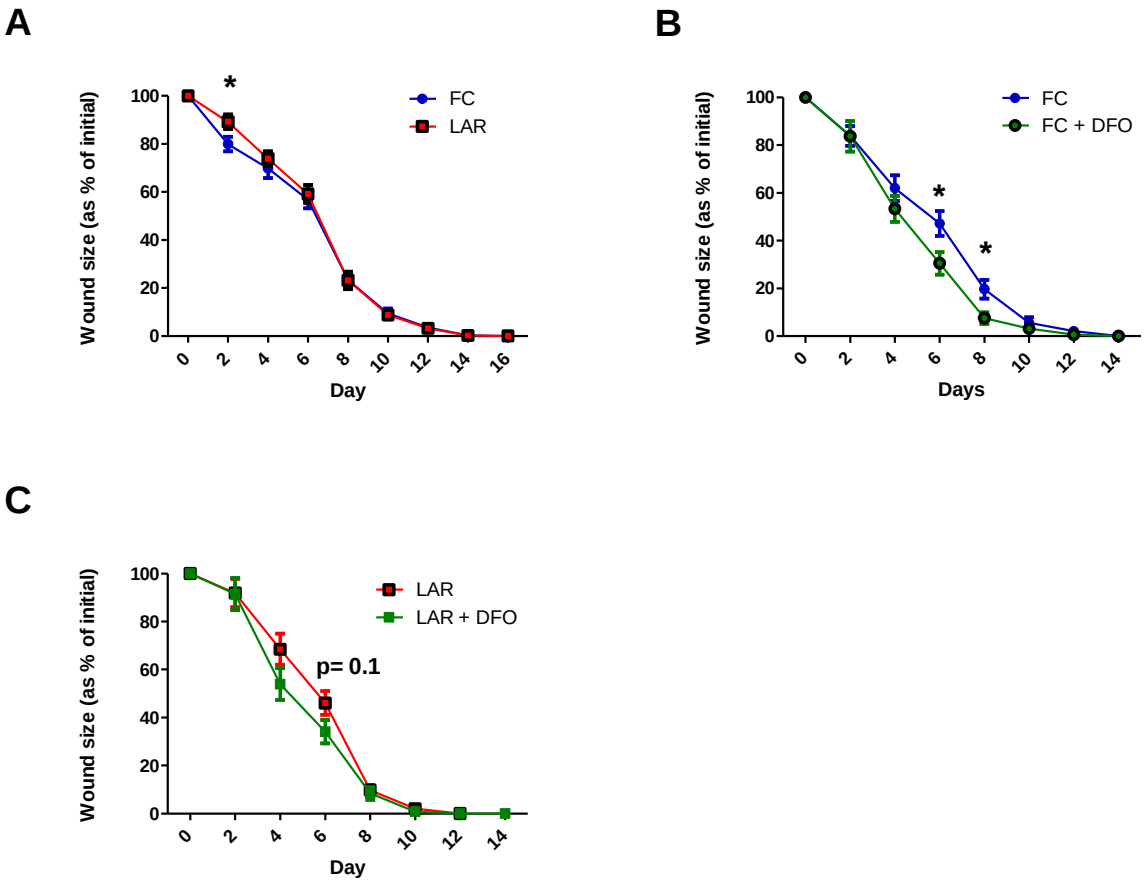

Figure 5.8 Wound healing in diabetic mice.
(A) FC (blue circles) and LAR (red squares) wound healing in diabetic mice (n=12-20/group). (B and C) FC and LAR wound healing with (green circles or squares) or without DFO (n=8-10/group). * = p<0.05 by students ttest. Average -/+ SEM is shown.

5.5 Human monocyte ARNT expression in diabetes

To test whether human myeloid cells from people with diabetes had lower ARNT, we measured ARNT mRNA in human blood monocytes. The monocyte cDNA and serum cytokine data were the kind gift of Sue Mclennon and Stephen Twigg (Department of Endocrinology, Royal Prince Alfred Hospital, Sydney, NSW, Australia). There was very wide inter-individual variability, and no significant differences in monocyte mRNA expression of ARNT observed between control and diabetic patients (p= 0.3 by students ttest, Figure 5.9A).

Interestingly, *ARNT* mRNA expression in human monocytes correlated negatively with serum levels of various cytokines. That is decreased *ARNT* expression in blood monocytes correlated with increased cytokine expression (Figure 5.9B - H) including IL-6 (p=0.01), IL-8 (p=0.02), MCP-1 (p=0.03) and TNF-α (p= 0.043, all by Pearson's correlations p-value from 2-tailed analysis is shown). There were no significant correlations between ARNT expression and IL-8, IFN-γ, IP-10 or MIP-1β.

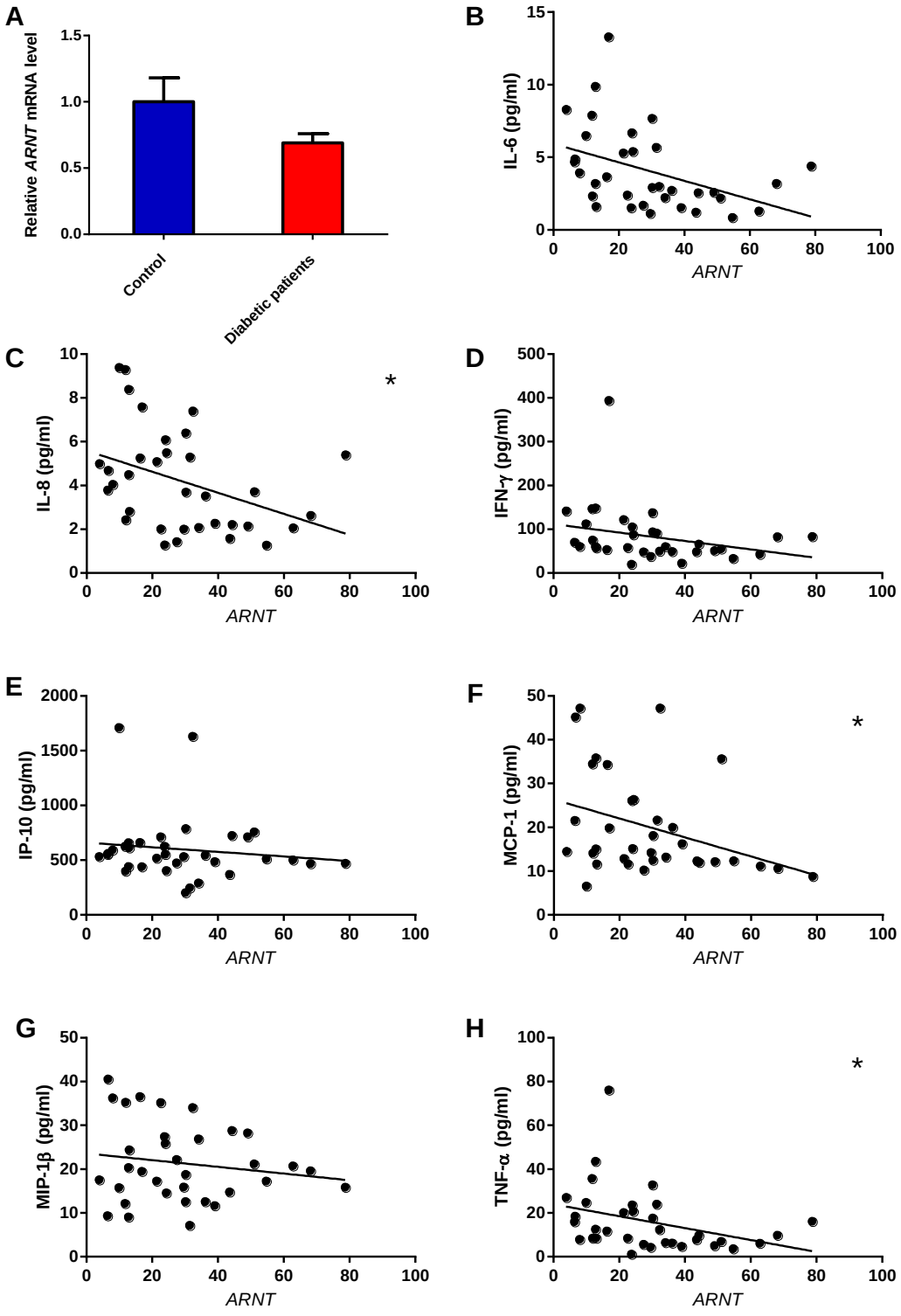

Figure 5.9 Human monocyte ARNT mRNA and expression.

ARNT level is expressed as the estimated relative fold change using the formula ARNT = 2*(40-CT). (A) *ARNT* mRNA expression in control (blue column, n=9) and diabetic (red column, n=25) patients. Average +/- SEM is shown. (B) IL- 6 pg/ml versus *ARNT* (C) IL- 8 pg/ml versus *ARNT*. (D) IFN-γ pg/ml versus *ARNT*. (E) IP-10 pg/ml versus *ARNT*. (F) MCP-1 pg/ml versus *ARNT*. (G) MIP-1β versus *ARNT* (H) TNF-α pg/ml versus *ARNT*. Pearson's correlations were calculated using PRISM 5 software, (n=34 patients). * = p <0.05.

5.6 Discussion

In this study, mice lacking ARNT in cells of the myeloid lineage displayed impairment of cytokine induction, phagocytosis, bacterial killing, skin inflammation, skin transplant rejection and wound healing. Interestingly impairment of LAR wound healing relative to FC mice was markedly reduced in diabetic mice. This suggested that reduced ARNT transcriptional activity in myeloid cells is a component of the diabetic wound phenotype. DFO administration failed to significantly increase wound healing in LAR mice, also suggesting that increasing ARNT/HIF1α in myeloid cells is integral to the mode of action of DFO in improving diabetic wound healing (380, 381). Interestingly *ARNT* mRNA in human blood monocytes correlated negatively with basal serum IL-6, IL-8, MCP-1 and TNF-α, which is consistent with increased cytokine mRNA observed basally in isolated macrophages. This also suggests that decreased ARNT in monocytes may paradoxically be linked to a chronic low-grade inflammation.

The impairment of phagocytosis and bacterial killing found in these animals is consistent with previous literature on myeloid cell HIF-1α knockout animals (238, 266, 267). In those experiments phagocytosis was increased in macrophages exposed to hypoxia in a HIF-1α dependant manner (268). Decreased bactericidal activity may also relate to decreased activity of proteases neutrophil elastase and cathepsin G, decreased cathelicidin-related antimicrobial peptide and decreased nitric oxide production (266). Interestingly impaired phagocytosis, bacterial killing and acute cytokine induction are all features of innate immune dysfunction in T2D (331).

Isolated macrophages also showed decreased mRNA expression of cytokines *Cxcl1*, *Mcp-1*, *Tgf-β1* and *Il-6*. Within wound biopsies, significantly reduced *Mcp-1*, *Il-6* and *Tnf-α* mRNA expression was found, suggesting an impaired acute inflammatory response in vivo. In addition IL-6 increases keratinocyte proliferation and migration, correspondingly mice lacking IL-6 have delayed wound healing (416). MCP-1 plays a role in wound healing with knockout animals displaying delayed wound re-epithelialisation, angiogenesis and collagen synthesis (417). Reduction of these cytokines coupled with impaired phagocytosis of bacteria and cellular debris may have contributed to the early delay in wound healing in this model. In support of the importance of monocytes, impaired monocyte phagocytosis and removal of inflammatory neutrophils has been shown to be a component of impaired wound healing in db/db diabetic mice (317). Reduction in the mRNAs for *Col1α1*, *Mmp9* and *Timp1* were found compared to FC animals and suggest impaired collagen deposition and altered wound remodelling. These results show that ARNT regulates myeloid cell function. Reduced ARNT

results in impairment of acute inflammatory response *in vitro* and *in vivo* models. It is now well accepted that HIF-1α expression is reduced in diabetic wounds and this reduction contributes to delayed wound healing (380-384). Importantly, delivery of agents and vectors to increase HIF-1α wounds are not cell specific. The results of this study suggest that increasing myeloid cell ARNT/HIF-1α in diabetic wounds may be a component to the improvements in would healing observed in the published literature. It is also important to note that LAR mice wound healing also deteriorated significantly on a diabetic background. A component of this deterioration could be decreased ARNT/HIF activity in myeloid cells with residual ARNT expression. However, it is likely that the observed impairment of wound healing is due to additional alterations in wound healing which occur in the diabetic mileu in addition to reduced ARNT/HIF function in other cell types including fibroblasts (324, 381).

Expression of *ARNT* in human monocytes was found to be highly variable, and larger studies may be required to determine if monocyte ARNT is in fact decreased in the setting of diabetes. In addition, measurement of monocyte ARNT with patients with sepsis and impaired wound healing would be interesting, as would assessment of ARNT levels in tissue macrophages exposed to the diabetic milieu.

The effect of DFO treatment on diabetic control mice wound healing in this study were not as marked as previous studies (381). Part of this may be the altered regime and decreased dosing of DFO compared to previous studies. Nonetheless DFO significantly decrease wound size in FC animals but not in mice lacking myeloid ARNT, suggesting a role for myeloid cell HIF-1α in mediating the effects of DFO.

The correlation of reduced monocyte ARNT with increased serum cytokines IL-6, IL-8, MCP-1 and TNF-α was a surprising finding. However results presented in section 4.4 show that mice lacking ARNT in myeloid cells have increased NASH and expression of *Mcp-1*, *Tgfβ1* and *Tnf-α* when placed on HFD. Also there have been recent reports which indicate myeloid cell ARNT/HIF-1α may be anti-inflammatory in certain situations. For example mice lacking HIF-1α in myeloid cells were reported to have had increased allergic response in both a house dust mite model and an OVA murine asthma model (418). This study went on to suggest that myeloid cell HIF-1α is also responsible for dampening down inflammation through the expression of cytokines like IL-10. It was also reported that HIF activation through myeloid cell Vhl deletion reduced inflammation in a model of chronic kidney

disease (419). Finally it was shown that macrophage HIF-1α deletion led to an increased immune response to cancer through de-repression of infiltrating cytotoxic T-cell activity (420). It may also be the case that the inflammatory environment produced by increased cytokine production results in decreased ARNT through ROS generation (421).

The results of these studies show that mice lacking ARNT in cells of the myeloid lineage had impaired cytokine induction, phagocytosis, bacterial killing, skin inflammation, skin transplant rejection and wound healing. The data presented here suggest that reduced ARNT activity in myeloid cells is a component of the diabetic phenotype and is consistent with the demonstrated impairment of immune function in these animals.

Chapter 6. Discussion and conclusions

6.1 Introduction

The results of the numerous studies reviewed in Section 1.7 support a role for ARNT and its partners in liver function. This work aimed to investigate the impact of long term ARNT deletion on whole body metabolism, non-alcoholic fatty liver disease (NAFLD), non-alcoholic steato-hepatitis (NASH) and liver fibrosis. Liver dysfunction is a key component of T2D and the metabolic syndrome and is both affected by and actively contributes to these phenotypes (147, 148). It is thought that it is primarily the elevated circulating lipids released from fat-laden adipocytes which leads to the increased prevalence of NAFLD and hence its sequelae NASH and cirrhosis (7). This liver lipid accumulation is further exacerbated by liver insulin resistance which leads to a paradoxical increase in de novo lipogenesis (7). The increased lipid content of the diabetic liver also spills over into the blood stream via increased export which contributes to the increased prevalence of cardiovascular disease in this population (48, 157, 158). In addition insulin resistance in the liver contributes to elevated fasting glucose by increased hepatic glucose production (HGP), another key feature of T2D (153, 154). A further feature of the diabetic liver is that hepatic glucose uptake is decreased and it is thought this may contribute to elevated blood glucose (152). Decreased uptake in the liver may account for 1/3 of the decrease in glucose disappearance in people with type 2 diabetes (155, 156). Perturbations of HIF-1α and other members of the bHLH/PAS protein family have been demonstrated to play a role in all of these processes in animal models.

The results of this work support a role for hepatic ARNT in HGP, glucose tolerance, post prandial lipid handling and ATP generation. Importantly, these changes became non-significant after HFD. Although there was no significant reduction in ARNT protein in animals after HFD, it is well known in other tissues that HIF-1α activity is reduced at high glucose concentrations (380-383). This coupled with the finding that ARNT mRNA is reduced in human livers (252) may suggest modulation of this pathway in the diabetic milieu.

The results of studies using HIF-1α knockout in myeloid cells suggested that perturbations in ARNT would affect immune function (238, 266, 267). This information combined with studies showing that ARNT mRNA was decreased in the liver and islets of patients with type two diabetes led us to hypothesise that myeloid cell ARNT may also be decreased and play a role in the diabetic phenotype (225, 252). We used myeloid cell specific deletion of ARNT to investigate the role of this transcription factor in normal immune function, metabolism during HFD and wound healing in a non-diabetic and diabetic milieu. The results of work with these animals showed that ARNT deletion, like that of HIF-1α, impaired myeloid cell function including decreased cytokine expression, decreased phagocytosis,

decreased bactericidal activity and impaired response to infection. These studies show for the first time that myeloid cell ARNT is important for normal wound healing. Further, the difference in wound healing between knockout and FC animals equilibrated in a diabetic milieu. DFO, which increases HIFs was more effective in improving wound healing in FC diabetic mice. All this information suggests that myeloid cell ARNT/ HIF-1α function is crucial for the full effects of DFO in improving wound healing. Interestingly, mice lacking ARNT in myeloid cells displayed impaired glucose tolerance on HFD and paradoxically increased liver inflammation. In human cells, ARNT mRNA correlated negatively with key serum cytokine levels including IL-6, IL-8, MCP-1 and TNF-α, although there was no significant reduction in monocyte ARNT in diabetic patients compared to controls.

6.2 ARNT and its partners in liver metabolism

Hepatocyte ARNT binds with its partners HIF-1α, HIF-2α or AhR. HIF-2α like HIF-1α is primarily regulated by cellular oxygen content (232). However as mentioned, it has been shown that HIF-1α can be stabilized by inflammation, TGF, IL-1β, PDGF and EGF (238, 239, 422). Maximal HIF-1α expression is dependent on functional NF-κB in fibroblasts and macrophages. Further, NF-κB signaling controls HIF-1α mRNA expression under both hypoxic and basal conditions (241). While the most relevant endogenous ligand for AhR is still contentious, there are many that have been found including bile acids, cAMP, curcumin, modified LDL and breakdown products from cruciferous vegetables (229-231, 423-425). The three ARNT-partners combined with ARNT regulate genes involved in hypoxic-responses, cell survival, proliferation, glycolysis, angiogenesis and response to xenobiotics (225-228). Importantly, alterations in the activation status of either partner could potentially decrease the availability of ARNT for another. A further complicating factor when considering the role of ARNT is the existence of the highly homologous ARNT-2. ARNT-2 can bind with AhR, HIF1-A or HIF2-A and is required for maximal expression of hypoxia inducible genes in neuronal cells (426-428). This suggests that ARNT-2 may be able to partially compensate the effects of ARNT deletion. However, after development ARNT-2 appears to be expressed at negiligable levels in the liver (429-432) . Although considered in the past as being constitutively expressed it is known that ARNT protein is decreased in livers of mice with streptozotocin induced diabetes and that mRNA is decreased in diabetic patients (252). Studies have shown that ARNT is increased by insulin and decreased by circumin (252, 421). Furthermore, it is reduced alongside AhR in co-cultures of Kupffer cells and hepatocytes after LPS treatment (433). We found that ARNT mRNA was reduced in mice on a HFD, but surprisingly there was no significant alteration in ARNT protein expression between fasted chow and HFD mice. The question of what actually occurs to ARNT's partners and functionality in

diabetic human liver remains unknown. It has however been reported that HIF-1α expression was transiently increased in the mouse livers after high fat/sucrose diet, and expression is also increased in the bile duct ligation model of liver fibrosis and in ethanol induced fatty liver (259, 400, 434). To add to the likelihood that HIF-1α activity is altered in the setting of diabetes evidence suggests that HIF-1α activity may be reduced at high glucose concentrations (380-383). Future studies assessing protein levels and function of liver AhR, HIF-2α and HIF-1α in models of diabetes would help to ascertain whether or not signalling through these transcription factors are in fact altered.

From the literature it could be predicted that ARNT deletion would result in a phenotypic copy of a combination of the effects of deletion of ARNT's partners. AhR deletion has been shown to increase liver fibrosis, increase insulin sensitivity and decrease gluconeogenic gene expression (244, 245, 250). While deletion or activation of AhR has been shown to increase hepatic lipid accumulation (244, 248, 249). It would appear that a lack of signalling through HIF-2α should lead to decreased fibrosis and triglyceride accumulation, which could negate some of the effects of loss of AhR function (257, 258). The results of studies using hepatocyte Vhl deletion suggest that excess HIF-1α inhibits gluconeogenesis (256). However, the interpretation of studies involving Vhl deletion is complicated by the finding that HIF proteins are also hydroxylated at asparagine residues by factor inhibiting HIF (FIH) to prevent interactions with co-activators (236). The effects of hepatocyte HIF-1α deletion have varied in different studies, with some producing contradicting results in similar models. In particular HIF-1α deletion has been shown to be protective in terms of fibrosis in a bile duct ligation model of fibrosis, while generating conflicting results in a model of ethanol-induced fatty liver (259, 400, 434). A further study showed impairment of glucose tolerance and hepatocyte glucose uptake after HIF-1α deletion on HFD (265). The results of the experiments of this thesis show findings most consistent with a phenotype of a combination of altered HIF-1α and HIF-2α function. Although there was no change in histological fibrosis scores between LARNT and FC mice after the TAA model of liver fibrosis, the quantity of collagen was decreased in LARNT mice. This is consistent with decreased signalling through HIFs. However, it also shows that HIF activity is not an absolute requirement for fibrosis initiation. Taken together, this work along with that of other groups suggest that physiological levels and function of liver ARNT and its partners are desirable in the diabetic environment. A reduction in signalling through ARNT would not contribute to the lipid accumulation observed in NAFLD or NASH but it may contribute to elevated fasting glucose and impaired glucose tolerance, through decreased liver glucose uptake and elevated HGP.

6.3 Myeloid cell ARNT and its partners in innate immune function, metabolism and wound healing.

Since the importance of HIF-1α in myeloid cells was discovered by Cramer et al 2003, increased HIF-1α has been demonstrated in a number of disorders characterised by a proinflammatory state including inflammatory bowel disease, asthma, psoriasis, atherosclerosis, and rheumatoid arthritis (435-438). It has become clear that myeloid cell HIF-1α both effects and is affected by inflammation, with molecules like TNF-α, IL-1β and LPS increasing HIF-1α mRNA and protein (439-441). An additional link between myeloid cell HIF and immunity is that NF-κB was been found to be crucial for maximal HIF-1α mRNA expression, while HIF-1α may also increase levels of NF-κB (241). It has also been shown that ARNT deletion in Kupffer cells prevented the upregulation of PDGF-β, VEGF, angiopoetin-1 and MCP-1 in hypoxia (269). The results of this research have indicated a decreased acute response of myeloid cells lacking ARNT in terms of phagocytosis, bacterial killing and cytokine expression. A complicating factor in this work is the low level of ARNT deletion found in macrophages and the non-myeloid-cell expression found in previous studies (411-413). Nonetheless we have found a phenotype both *in vitro* and *in vivo*. This data is consistent with the phenotype of myeloid cells lacking HIF-1α, suggesting that loss of HIF-1α signalling is a major cause of these effects (238, 266, 267). ARNT deletion led to defects in terms of increased infection, decreased inflammation and delayed wound healing. Paradoxically, this decreased immune response to infection was accompanied by increased liver inflammation and histological fibrosis score after HFD. The mechanisms of this finding were not investigated during this study, however it has recently been reported that in mice lacking ARNT/ HIF-1α signalling in myeloid cells have increased allergic response in both a house dust mite model and an OVA murine asthma model (418). This study goes on to suggest that myeloid cell HIF-1α is also responsible for dampening down inflammation through the expression of cytokines like IL-10. It was also reported that HIF activation through myeloid cell Vhl deletion reduced inflammation in a model of chronic kidney disease, and that macrophage HIF-1α deletion increased the immune response to cancer through de-repression of infiltrating cytotoxic T-cell activity (419, 420). Thus depending on the tissue and the nature of the stimulus HIF signalling through ARNT can be pro or anti-inflammatory. The importance of ARNT/HIF-1α signalling for macrophage phagocytosis has now been shown in a number of studies, and this suggests that it may

also be important for resolution of inflammation through phagocytosis of apoptotic neutrophils (238, 268, 442).

It is noteworthy that AhR has also been shown to be important for proper immune response to listeria infections (443). In addition it has been shown that LPS treatment of co-cultures of Kupffer cells and hepatocytes lead to a decrease in ARNT and AhR protein. This did not occur with monocultures of either cell type or when a membrane stopped direct cell to cell interaction. The effect was blocked by addition of anti-TNF-α and anti-IL-1β antibodies (433). Furthermore, the aryl hydrocarbon receptor has been shown to play a role in immune function, both in T cell and macrophage function (424, 444). In the second case it was shown that AhR knockout animals are sensitive to LPS induced septic shock and that this may be caused by elevated IL-1β production by macrophages. Intriguingly it appears that this effect was independent of ARNT indicating that AhR can also induce changes in gene expression independent of ARNT through an as yet undetermined mechanism (444). This model was not investigated in this research but further complicates the picture of signalling by ARNT and its partners. A further potentially complicating factor is again compensation by ARNT2, although expression in myeloid cells has not previously been reported (429, 431).

During the investigation of monocyte ARNT mRNA expression in diabetes we found a significant negative correlation ARNT and cytokine expression of IL-6, IL-8, MCP-1 and TNF-α. Cytokine expression is known to effect HIF-1α expression, and at this point a cause and effect relationship is speculative. However, in the context of our finding of increased inflammation and cytokine mRNA expression in LAR livers after HFD it is possible that the increase in inflammatory cytokines in these patients may be a result of chronically decreased ARNT expression in myeloid cells.

Another important finding of our research is that myeloid cell ARNT deletion generally impaired glucose tolerance on HFD. This is consistent with an important role for myeloid cells in metabolism metabolism (182-186). Surprisingly, although we found increased weight gain in female mice initially we did not find increased insulin resistance to explain the altered glucose tolerance in either sex. One possibility that was not investigated is that the tissue inflammation evidenced in these animals on HFD led to inflammation of pancreatic tissue and a decrease in insulin secretion by islets. This hypothesis requires further examination.

It is widely accepted that rapidly expanding adipose tissue in obesity becomes hypoxic as tissue growth occurs faster than the vasculature can keep pace with (270-273). In addition oxygen tension correlates negatively with macrophage infiltration suggesting hypoxia may be responsible for the inflammation observed (270). Correspondingly levels of HIF-1α are also known to increase (274, 445) and the effects of HIF-1α on adipose function have been explored in a number of studies. One study used the AP2 promoter to overexpress a constitutively active HIF-1α, and showed that these animals had increased adipose tissue inflammation and fibrosis alongside decreased glucose tolerance and increased weight gain on HFD (274). Complementary to this work it was shown that AP2-mediated HIF-1α or ARNT deletion resulted in reduced adipose tissue and improved glucose tolerance (275, 276). However Lee et al 2011 did not find reduced fat inflammation and fibrosis with adipocyte ARNT deletion suggesting it is not a requirement for these features (276). Again using the AP2 promoter Zhang et al (2010) showed that overexpression of a dominant negative form of HIF-1α led to increased obesity and impaired glucose tolerance on HFD (446). Work with a tamoxifen inducible AP2 HIF-1α knockout recapitulated findings of decreased adipose tissue, with improved glucose tolerance and insulin sensitivity. In addition these animals had increased beta oxidation in visceral adipose tissue (277). This work suggests that either too much or too little signalling through HIF-1α in adipose tissue is detrimental. Importantly the commonly used AP2 promoter, which was utilised to drive specific adipocyte expression, has also been found to be expressed in macrophages and other cells (278, 279). This suggests that some effects of these studies may be mediated through alteration of macrophage function. Repeating the aforementioned studies using the adipocyte specific promoter developed by Wang et al 2010 would be helpful to clarify the specific role of adipocyte HIF-1α and ARNT (447).

One unique finding of this research is that loss of myeloid ARNT led to delayed wound healing, and that the delay was markedly reduced on a diabetic background. This is consistent with signalling through the ARNT/ HIF-1α dimer and the reported decrease in HIF-1α activity in diabetic wounds (381, 383). Thus the beneficial effects of iron chelation seem to require myeloid cell ARNT for the full effects. As discussed this is likely to be the result of decreased cytokine expression and altered innate immune cell function. These defects may also be the result of delayed resolution of inflammation and subsequent elongation of healing time. Assessment of cytokine expression and inflammatory cell infiltration and clearance at multiple time points would be useful to determine if in fact non-resolving inflammation is a component of this phenotype.

6.4 The potential of ARNT in therapy.

Although ARNT was previously considered to be constitutively expressed, it has now been shown to be regulated in specific circumstances. ARNT protein has been reported to be down-regulated by ROS, possibly through miR-24 (448). As mentioned in the above section LPS treatment of co cultures of KCs and hepatocytes can lead to a decrease in both ARNT and AhR mRNA and protein (433). It has also been found that curcumin leads to destabilisation and reduction in ARNT protein (421). Coupled with this is the finding that ARNT mRNA is lower in livers and islets of diabetic patients, and that protein is decreased in the livers of mice with streptozocin induced diabetes (225, 252). These findings suggest that ARNT mRNA and protein are in fact regulated and that in the future drugs could be designed to specifically target this transcription factor.

The HIFα's have been modulated by iron chelators such as DFO and DFS, and by heavy metals such as $CoCL_2$ in animal models to increase HIF-1α (251, 381, 449). Specific PHD inhibition has also been used in animal models, apparently without untoward effects (450, 451). The idea of increasing HIF-1α in therapy is controversial due to mixed results seen with HIF-1α perturbations in different models and different tissues. In particular upregulation of the HIFα's via deletion of Vhl has been shown to be lead to impaired pancreatic function, and liver steatosis with inflammation (256, 452). In the case of the liver, it led to death if left uncountered. So certainly the supra-physiological level of HIFα's delivered with complete loss of Vhl function have negative consequences. Nonetheless modulation of HIF-1α using DFO was shown to improve islet survival and glucose tolerance on a HFD (251, 449). In other systems results have also varied depending on the model and the nature of HIF-1α modulation. For example, there is evidence that HIF-1α plays a role in proximal tubular epithelial cells to increase renal fibrosis and renal dysfunction in the unilateral ureteral obstruction model of chronic kidney disease (453). In contrast, global induction of HIFα's using cobalt infusion or prolyl hydroxylase inhibition with L-mimosine was found to be protective in a model of gentamycin induced kidney injury and subtotal nephrectomy respectively (450, 454). Not surprisingly in the lung the upregulation of MCP-1 in response to a model of allergic airway disease was reported to be dependent on HIF-1α, and global disruption of ARNT or HIF-1α signalling reduced inflammation(455, 456). In contrast to this HIF-1α deletion specifically in myeloid cells enhanced sensitivity to inflammation (418). A recent a paper showed that HIF-1α deletion in T cells led to increased colonic inflammation with a failure of hypoxia to induce Treg activation and coincident increased in TH17 cells (457). Suggesting that in T cells HIF-1α may be anti-inflammatory. In addition increasing colonic HIFs through dimethyloxalylglycine, prolyl hydroxylase (PHD) inhibitor (FG-4497) was shown to reduce inflammation. Further work showed that epithelial deletion of HIF-1α led to increased

inflammation and colonic damage with TNBS or oxazolone induced colitis (451, 458, 459). Nonetheless increasing HIF's with Vhl deletion or an activating mutation also led to increased colitis using the DSS model (460), as did whole body deletion of PHD3 (461). Thus the potential use of the use of HIFα modulation in disease management could be complicated by differing effects in different tissues and in different disease processes.

One example of increased human HIF-1α function is Vhl syndrome, which is an autosomal dominant disease characterised by the inheritance of one dysfunctional copy of VhL and predisposition to the development of various tumours through somatic mutation of the second functional copy including: haemangioblastomas, renal cysts, phaeochromocytoma and renal cell carcinoma (462). Although only one copy is mutated in this instant I was unable to find any articles suggesting a tumour-independent increase in prevalence of metabolic derangements, fatty liver, inflammation or fibrosis. Another point to make is that iron chelation with DFO and DFS, which leads to an increase in HIFα expression, has long been used to treat the toxic accumulation of iron in patients that result from the need for frequent transfusions (thalassemia, sickle cell disease, and aplastic anaemia) and haemochromatosis. Available evidence suggests that long term use of desferasirox within the therapeutic range is safe, with the most common adverse effects being associated with gastrointestinal disturbances and a rash (463, 464). Two studies looked at the use of iron chelation to treat diabetes. The first study showed that in those patients with diabetes and hyperferritinaemia of no known cause metabolic control was improved with iron chelation, however no effect was seen in diabetic patients with normal serum ferritin levels (465). The second found a small improvement in glycated haemoglobin in patients with hyperferritinaemia (466). However, I was unable to locate a paper which specifically assessed serum cytokine expression after DFO treatment (as a marker of possible increased inflammation).

Importantly these studies did not exclude AhR as being responsible for some of the effects of ARNT deletion. And AhR modulation may also hold future promise, as mentioned potential ligands for development could include bile acids and breakdown products from cruciferous vegetables (229-231). AhR has multiple ligands some of which we are exposed to on a regular basis in the form of polycyclic aromatic hydrocarbons (424). It has in fact been postulated that the increasing prevalence of exogenous AhR ligands in the environment may be linked with increasing inflammatory and autoimmune disease (424).

6.5 Future studies

As discussed multiple questions about the role of ARNT in liver and immune dysfunction remain. The most pressing being what happens to ARNT function in diabetic patients? Currently it is known that ARNT mRNA is decreased in the liver and pancreas but protein levels have not been assessed (252). Future studies should address this. The Arg554Lys polymorphism in AhR is described in the literature and predisposes to decreased levels of ARNT and AhR (407). To date this polymorphism has been associated with risk of male infertility and DNA damage in lymphocytes (467, 468). There have been mixed results in terms of risk of lung cancer and no association with endometriosis or breast cancer (469-472). To date there have been no studies investigating an association with obesity, T2D or innate immune function, it would be interesting to screen these populations to determine if this polymorphism is over-reperesented. This could suggest that intrinsically low ARNT could actually predispose individuals to the development of diabetes. We found a reduction in ARNT mRNA after HFD in mice we did not find a corresponding reduction in total protein. An additional experiment to address this would be to assess nuclear versus cytoplasmic ARNT to see if levels of nuclear/active ARNT are in fact altered, this would suggest decreased transcriptional activity. Neverless if the findings of this work translate into humans then modulation of liver ARNT could be used therapeutically to reduce gluconeogenesis and post prandial liver lipids.

In terms of the LARNT phenotype one unanswered question is the cause for increased serum lipids after feeding. Donnelley et al (2005) described a technique using multiple labeled substrates which could be used to delineate the liver uptake and lipogenesis, which we could use to investigate the phenotype (7). This finding also raises the possibility that polymorphisms like the Arg554Lys, which lead to alterations in liver ARNT expression, could predispose to elevated serum TG and cardiovascular disease. It would be interesting to assay serum of LARNT mice to see the relative amounts of LDL and HDL, and see if the lipid profile is altered in an atherogenic direction.

Assessment of ARNT in monocytes was hampered by the apparent variability of ARNT expression in control human monocyte humans. Larger studies would clarify this issue as would measurement of ARNT protein levels. The finding of a negative correlation between monocyte ARNT mRNA expression and key cytokine expression also raised the possibility that decreased ARNT could contribute to a low grade inflammation. It would have been interesting to assess serum cytokine levels in HFD fed LAR mice to see if the increased liver inflammation observed correlated with a systemic inflammatory response. Perfoming the TAA model on LAR animals would be another useful experiment to determine whether myeloid cell ARNT is involved in liver fibrosis. The cause of the

impaired glucose tolerance in HFD LAR mice was also unclear. Although a level of insulin resistance was found in female animals we found no consistent increase in insulin resistance in males to explain the impaired glucose tolerance observed in these animals. As mentioned in the text one possibility is pancreatic dysfunction caused by inflammation which could have led to decreased insulin secretion (201, 404). An easy way to assess this hypothesis would be to place male LAR animals on a short term HFD and assess glucose stimulated insulin secretion and pancreatic histology and mRNA expression. Another potential explanation could be altered hepatic function leading to alterations in gluconeogenesis. At 20 weeks we actually found decreased gluconeogenesis in males. However, at this time point male LAR mice no longer had impaired glucose tolerance compared to FC, and fasting glucose levels were lower. Assessment of gluconeogenesis at earlier timepoints would be useful and also ideally a labelled euglycemic– hyperinsulinaemic clamp to determine hepatic insulin resistance. In terms of the role of ARNT in wound healing it would be useful to assess monocyte ARNT specifically in diabetic and control patients with sepsis and impaired would healing. Also as mentioned it would be interesting to assess wound histology and cytokine expression at multiple time points in LAR mice wounds to determine if non-resolving inflammation is a component of the wound healing phenotype of these animals.

6.6 Summary

This work investigated the role of ARNT in the function of the liver and of the immune system. We found that ARNT is crucial for normal functioning of both systems and that perturbation in these cell types lead to changes with much in common with those observed in T2D. Importantly, in both instances we found evidence for alteration of normal ARNT signalling in a diabetic milieu. It is also apparent that the effects of the ARNT deletion are likely the result of a combination of disruptions in signalling in its multiple partners. Previous studies have shown that ARNT levels are altered in the liver and islets of people with diabetes, reduced in mouse models of T1D, and that the transcriptional activity of HIF-1α is reduced in the diabetic mileu. This accumulating evidence points to a potentially global down-regulation of ARNT function in the setting of diabetes. The results of this work in combination with previous studies also suggest that this reduced function of ARNT could be involved in multiple aspects of the diabetic phenotype in different tissues. This data adds to the growing body of evidence that in the future modulation of ARNT and its partners could be used therapeutically for the management of diabetes and its complications, as well as potentially other causes of immune dysfunction.

REFERENCES

1. Sherwood L. Human Physiology: From cells to systems. 6 ed. Adams P, editor. Australia: Thompson Brooks/Cole; 2007.
2. James MC. Liver and Bilary Tract. In: Kumar VA, A.K. & Fausto, N., editor. Robbins and Cotran Pathological Basis of Disease. 7 ed: Elsevier Saunders; 2005.
3. Gao B, Jeong WI, Tian Z. Liver: An organ with predominant innate immunity. Hepatology. 2008 Feb;47(2):729-36.
4. Voet D, Voet, Judith.G. & Pratt, Charlotte, W. Fundamentals of Biochemistry. Russell S, editor. New York: John Wiley & Sons, Inc.; 1999.
5. Pilkis SJ, Granner DK. Molecular physiology of the regulation of hepatic gluconeogenesis and glycolysis. Annu Rev Physiol. 1992;54:885-909.
6. Cherrington AD, Edgerton D, Sindelar DK. The direct and indirect effects of insulin on hepatic glucose production in vivo. Diabetologia. 1998 Sep;41(9):987-96.
7. Donnelly KL, Smith CI, Schwarzenberg SJ, Jessurun J, Boldt MD, Parks EJ. Sources of fatty acids stored in liver and secreted via lipoproteins in patients with nonalcoholic fatty liver disease. J Clin Invest. 2005 May;115(5):1343-51.
8. Qureshi K, Abrams GA. Metabolic liver disease of obesity and role of adipose tissue in the pathogenesis of nonalcoholic fatty liver disease. World J Gastroenterol. 2007 Jul 14;13(26):3540-53.
9. Lavoie JM, Gauthier MS. Regulation of fat metabolism in the liver: link to non-alcoholic hepatic steatosis and impact of physical exercise. Cell Mol Life Sci. 2006 Jun;63(12):1393-409.
10. Matsumoto M, Ogawa W, Akimoto K, Inoue H, Miyake K, Furukawa K, et al. PKClambda in liver mediates insulin-induced SREBP-1c expression and determines both hepatic lipid content and overall insulin sensitivity. J Clin Invest. 2003 Sep;112(6):935-44.
11. Horton JD, Goldstein JL, Brown MS. SREBPs: activators of the complete program of cholesterol and fatty acid synthesis in the liver. J Clin Invest. 2002 May;109(9):1125-31.
12. Zhang Y, Mangelsdorf DJ. LuXuRies of lipid homeostasis: the unity of nuclear hormone receptors, transcription regulation, and cholesterol sensing. Mol Interv. 2002 Apr;2(2):78-87.
13. Yamashita H, Takenoshita M, Sakurai M, Bruick RK, Henzel WJ, Shillinglaw W, et al. A glucose-responsive transcription factor that regulates carbohydrate metabolism in the liver. Proc Natl Acad Sci U S A. 2001 Jul 31;98(16):9116-21.
14. Iizuka K, Bruick RK, Liang G, Horton JD, Uyeda K. Deficiency of carbohydrate response element-binding protein (ChREBP) reduces lipogenesis as well as glycolysis. Proc Natl Acad Sci U S A. 2004 May 11;101(19):7281-6.
15. Iizuka K, Horikawa Y. ChREBP: a glucose-activated transcription factor involved in the development of metabolic syndrome. Endocr J. 2008 Aug;55(4):617-24.
16. Macdonald GA, Prins JB. Peroxisomal fatty acid metabolism, peroxisomal proliferator-activated receptors and non-alcoholic fatty liver disease. J Gastroenterol Hepatol. 2004 Dec;19(12):1335-7.
17. Schoen F, J. Blood Vessels. In: Kumar VA, A.K. & Fausto, N., editor. Robbins and Cotran: Pathological Basis of Disease. 7 ed: Elsevier Saunders; 2005.
18. Browning JD, Horton JD. Molecular mediators of hepatic steatosis and liver injury. J Clin Invest. 2004 Jul;114(2):147-52.
19. McCullough AJ, O'Connor JF. Alcoholic liver disease: proposed recommendations for the American College of Gastroenterology. Am J Gastroenterol. 1998 Nov;93(11):2022-36.
20. Wieckowska A, McCullough AJ, Feldstein AE. Noninvasive diagnosis and monitoring of nonalcoholic steatohepatitis: present and future. Hepatology. 2007 Aug;46(2):582-9.
21. Matteoni CA, Younossi ZM, Gramlich T, Boparai N, Liu YC, McCullough AJ. Nonalcoholic fatty liver disease: a spectrum of clinical and pathological severity. Gastroenterology. 1999 Jun;116(6):1413-9.

22. Kleiner DE, Brunt EM, Van Natta M, Behling C, Contos MJ, Cummings OW, et al. Design and validation of a histological scoring system for nonalcoholic fatty liver disease. Hepatology. 2005 Jun;41(6):1313-21.
23. Brunt EM, Janney CG, Di Bisceglie AM, Neuschwander-Tetri BA, Bacon BR. Nonalcoholic steatohepatitis: a proposal for grading and staging the histological lesions. Am J Gastroenterol. 1999 Sep;94(9):2467-74.
24. Skelly MM, James PD, Ryder SD. Findings on liver biopsy to investigate abnormal liver function tests in the absence of diagnostic serology. J Hepatol. 2001 Aug;35(2):195-9.
25. Browning JD, Szczepaniak LS, Dobbins R, Nuremberg P, Horton JD, Cohen JC, et al. Prevalence of hepatic steatosis in an urban population in the United States: impact of ethnicity. Hepatology. 2004 Dec;40(6):1387-95.
26. Farrell GC, Larter CZ. Nonalcoholic fatty liver disease: from steatosis to cirrhosis. Hepatology. 2006 Feb;43(2 Suppl 1):S99-S112.
27. Marchesini G, Bugianesi E, Forlani G, Cerrelli F, Lenzi M, Manini R, et al. Nonalcoholic fatty liver, steatohepatitis, and the metabolic syndrome. Hepatology. 2003 Apr;37(4):917-23.
28. Poonawala A, Nair SP, Thuluvath PJ. Prevalence of obesity and diabetes in patients with cryptogenic cirrhosis: a case-control study. Hepatology. 2000 Oct;32(4 Pt 1):689-92.
29. Bugianesi E, Leone N, Vanni E, Marchesini G, Brunello F, Carucci P, et al. Expanding the natural history of nonalcoholic steatohepatitis: from cryptogenic cirrhosis to hepatocellular carcinoma. Gastroenterology. 2002 Jul;123(1):134-40.
30. Adams LA, Lymp JF, St Sauver J, Sanderson SO, Lindor KD, Feldstein A, et al. The natural history of nonalcoholic fatty liver disease: a population-based cohort study. Gastroenterology. 2005 Jul;129(1):113-21.
31. Sozio MS, Chalasani N, Liangpunsakul S. What advice should be given to patients with NAFLD about the consumption of alcohol? Nat Clin Pract Gastroenterol Hepatol. 2009 Jan;6(1):18-9.
32. Kane ABK, V. Environmental and Nutritional Pathology. In: Kumar VA, A.K. & Fausto, N., editor. Robbins and Cotran: Pathological Basis of Disease. 7 ed: Elsevier Saunders; 2005. p. 415-68.
33. Linacre S. Australian Social Trends: Overweight and Obesity. Australian Bureau of Statistics; 2007 [updated 2007 7/08/2007; cited 2012]; Available from: http://www.abs.gov.au/ausstats/abs@.nsf/0/4DE3C28315518DCECA25732C002074E4?opendocument.
34. Stefan N, Kantartzis K, Machann J, Schick F, Thamer C, Rittig K, et al. Identification and characterization of metabolically benign obesity in humans. Arch Intern Med. 2008 Aug 11;168(15):1609-16.
35. Cornier MA, Dabelea D, Hernandez TL, Lindstrom RC, Steig AJ, Stob NR, et al. The metabolic syndrome. Endocr Rev. 2008 Dec;29(7):777-822.
36. Angulo P. Treatment of nonalcoholic fatty liver disease. Ann Hepatol. 2002 Jan-Mar;1(1):12-9.
37. Abrams GA, Kunde SS, Lazenby AJ, Clements RH. Portal fibrosis and hepatic steatosis in morbidly obese subjects: A spectrum of nonalcoholic fatty liver disease. Hepatology. 2004 Aug;40(2):475-83.
38. van der Poorten D, Milner KL, Hui J, Hodge A, Trenell MI, Kench JG, et al. Visceral fat: a key mediator of steatohepatitis in metabolic liver disease. Hepatology. 2008 Aug;48(2):449-57.
39. Adams LA, Angulo P. Recent concepts in non-alcoholic fatty liver disease. Diabet Med. 2005 Sep;22(9):1129-33.
40. Clark JM. The epidemiology of nonalcoholic fatty liver disease in adults. J Clin Gastroenterol. 2006 Mar;40 Suppl 1:S5-10.
41. Wanless IR, Lentz JS. Fatty liver hepatitis (steatohepatitis) and obesity: an autopsy study with analysis of risk factors. Hepatology. 1990 Nov;12(5):1106-10.
42. Maitra AA, A.K. The Endocrine System. In: Kumar VA, A.K. & Fausto, N., editor. Robbins and Cotran: Pathological Basis of Disease. 7 ed: Elsevier Saunders; 2005.

43. Diabetes in Australia: A Snapshot, 2007-08 Australian Bureau of Statistics; 2007-8 [updated 2007-8 16 September 2011; cited 2012 27th of September 2012]; Available from: http://www.abs.gov.au/ausstats/abs@.nsf/mf/4820.0.55.001.
44. Mendez-Sanchez N, Arrese M, Zamora-Valdes D, Uribe M. Current concepts in the pathogenesis of nonalcoholic fatty liver disease. Liver Int. 2007 May;27(4):423-33.
45. Cotrim HP, Andrade ZA, Parana R, Portugal M, Lyra LG, Freitas LA. Nonalcoholic steatohepatitis: a toxic liver disease in industrial workers. Liver. 1999 Aug;19(4):299-304.
46. Ouyang X, Cirillo P, Sautin Y, McCall S, Bruchette JL, Diehl AM, et al. Fructose consumption as a risk factor for non-alcoholic fatty liver disease. J Hepatol. 2008 Jun;48(6):993-9.
47. Postic C, Girard J. Contribution of de novo fatty acid synthesis to hepatic steatosis and insulin resistance: lessons from genetically engineered mice. J Clin Invest. 2008 Mar;118(3):829-38.
48. Biddinger SB, Hernandez-Ono A, Rask-Madsen C, Haas JT, Aleman JO, Suzuki R, et al. Hepatic insulin resistance is sufficient to produce dyslipidemia and susceptibility to atherosclerosis. Cell Metab. 2008 Feb;7(2):125-34.
49. Brown MS, Goldstein JL. Selective versus total insulin resistance: a pathogenic paradox. Cell Metab. 2008 Feb;7(2):95-6.
50. Semple RK, Sleigh A, Murgatroyd PR, Adams CA, Bluck L, Jackson S, et al. Postreceptor insulin resistance contributes to human dyslipidemia and hepatic steatosis. J Clin Invest. 2009 Feb;119(2):315-22.
51. Taniguchi CM, Ueki K, Kahn R. Complementary roles of IRS-1 and IRS-2 in the hepatic regulation of metabolism. J Clin Invest. 2005 Mar;115(3):718-27.
52. Shimomura I, Matsuda M, Hammer RE, Bashmakov Y, Brown MS, Goldstein JL. Decreased IRS-2 and increased SREBP-1c lead to mixed insulin resistance and sensitivity in livers of lipodystrophic and ob/ob mice. Mol Cell. 2000 Jul;6(1):77-86.
53. Tamura S, Shimomura I. Contribution of adipose tissue and de novo lipogenesis to nonalcoholic fatty liver disease. J Clin Invest. 2005 May;115(5):1139-42.
54. Charlton M, Sreekumar R, Rasmussen D, Lindor K, Nair KS. Apolipoprotein synthesis in nonalcoholic steatohepatitis. Hepatology. 2002 Apr;35(4):898-904.
55. Brady LJ, Brady PS, Romsos DR, Hoppel CL. Elevated hepatic mitochondrial and peroxisomal oxidative capacities in fed and starved adult obese (ob/ob) mice. Biochem J. 1985 Oct 15;231(2):439-44.
56. Li Z, Yang S, Lin H, Huang J, Watkins PA, Moser AB, et al. Probiotics and antibodies to TNF inhibit inflammatory activity and improve nonalcoholic fatty liver disease. Hepatology. 2003 Feb;37(2):343-50.
57. Sanyal AJ, Campbell-Sargent C, Mirshahi F, Rizzo WB, Contos MJ, Sterling RK, et al. Nonalcoholic steatohepatitis: association of insulin resistance and mitochondrial abnormalities. Gastroenterology. 2001 Apr;120(5):1183-92.
58. Chalasani N, Gorski JC, Asghar MS, Asghar A, Foresman B, Hall SD, et al. Hepatic cytochrome P450 2E1 activity in nondiabetic patients with nonalcoholic steatohepatitis. Hepatology. 2003 Mar;37(3):544-50.
59. Miele L, Grieco A, Armuzzi A, Candelli M, Forgione A, Gasbarrini A, et al. Hepatic mitochondrial beta-oxidation in patients with nonalcoholic steatohepatitis assessed by 13C-octanoate breath test. Am J Gastroenterol. 2003 Oct;98(10):2335-6.
60. Pessayre D, Fromenty B, Mansouri A. Mitochondrial injury in steatohepatitis. Eur J Gastroenterol Hepatol. 2004 Nov;16(11):1095-105.
61. Korenblat KM, Fabbrini E, Mohammed BS, Klein S. Liver, muscle, and adipose tissue insulin action is directly related to intrahepatic triglyceride content in obese subjects. Gastroenterology. 2008 May;134(5):1369-75.
62. Solga S, Alkhuraishe AR, Clark JM, Torbenson M, Greenwald A, Diehl AM, et al. Dietary composition and nonalcoholic fatty liver disease. Dig Dis Sci. 2004 Oct;49(10):1578-83.

63. Surwit RS, Feinglos MN, Rodin J, Sutherland A, Petro AE, Opara EC, et al. Differential effects of fat and sucrose on the development of obesity and diabetes in C57BL/6J and A/J mice. Metabolism. 1995 May;44(5):645-51.
64. Musso G, Gambino R, De Michieli F, Cassader M, Rizzetto M, Durazzo M, et al. Dietary habits and their relations to insulin resistance and postprandial lipemia in nonalcoholic steatohepatitis. Hepatology. 2003 Apr;37(4):909-16.
65. Soza A, Riquelme A, Gonzalez R, Alvarez M, Perez-Ayuso RM, Glasinovic JC, et al. Increased orocecal transit time in patients with nonalcoholic fatty liver disease. Dig Dis Sci. 2005 Jun;50(6):1136-40.
66. Yoshimatsu M, Terasaki Y, Sakashita N, Kiyota E, Sato H, van der Laan LJ, et al. Induction of macrophage scavenger receptor MARCO in nonalcoholic steatohepatitis indicates possible involvement of endotoxin in its pathogenic process. Int J Exp Pathol. 2004 Dec;85(6):335-43.
67. Wigg AJ, Roberts-Thomson IC, Dymock RB, McCarthy PJ, Grose RH, Cummins AG. The role of small intestinal bacterial overgrowth, intestinal permeability, endotoxaemia, and tumour necrosis factor alpha in the pathogenesis of non-alcoholic steatohepatitis. Gut. 2001 Feb;48(2):206-11.
68. Koteish A, Mae Diehl A. Animal models of steatohepatitis. Best Pract Res Clin Gastroenterol. 2002 Oct;16(5):679-90.
69. Yahagi N, Shimano H, Hasty AH, Matsuzaka T, Ide T, Yoshikawa T, et al. Absence of sterol regulatory element-binding protein-1 (SREBP-1) ameliorates fatty livers but not obesity or insulin resistance in Lep(ob)/Lep(ob) mice. J Biol Chem. 2002 May 31;277(22):19353-7.
70. Ingalls AM, Dickie MM, Snell GD. Obese, a new mutation in the house mouse. J Hered. 1950 Dec;41(12):317-8.
71. Mayer J, Bates MW, Dickie MM. Hereditary diabetes in genetically obese mice. Science. 1951 Jun 29;113(2948):746-7.
72. Anstee QM, Goldin RD. Mouse models in non-alcoholic fatty liver disease and steatohepatitis research. Int J Exp Pathol. 2006 Feb;87(1):1-16.
73. Biddinger SB, Almind K, Miyazaki M, Kokkotou E, Ntambi JM, Kahn CR. Effects of diet and genetic background on sterol regulatory element-binding protein-1c, stearoyl-CoA desaturase 1, and the development of the metabolic syndrome. Diabetes. 2005 May;54(5):1314-23.
74. Castrillo A, Tontonoz P. Nuclear receptors in macrophage biology: at the crossroads of lipid metabolism and inflammation. Annu Rev Cell Dev Biol. 2004;20:455-80.
75. Berger J, Moller DE. The mechanisms of action of PPARs. Annu Rev Med. 2002;53:409-35.
76. Bensinger SJ, Tontonoz P. Integration of metabolism and inflammation by lipid-activated nuclear receptors. Nature. 2008 Jul 24;454(7203):470-7.
77. Dreyer C, Keller H, Mahfoudi A, Laudet V, Krey G, Wahli W. Positive regulation of the peroxisomal beta-oxidation pathway by fatty acids through activation of peroxisome proliferator-activated receptors (PPAR). Biol Cell. 1993;77(1):67-76.
78. Kersten S, Seydoux J, Peters JM, Gonzalez FJ, Desvergne B, Wahli W. Peroxisome proliferator-activated receptor alpha mediates the adaptive response to fasting. J Clin Invest. 1999 Jun;103(11):1489-98.
79. Leone TC, Weinheimer CJ, Kelly DP. A critical role for the peroxisome proliferator-activated receptor alpha (PPARalpha) in the cellular fasting response: the PPARalpha-null mouse as a model of fatty acid oxidation disorders. Proc Natl Acad Sci U S A. 1999 Jun 22;96(13):7473-8.
80. Ibdah JA, Paul H, Zhao Y, Binford S, Salleng K, Cline M, et al. Lack of mitochondrial trifunctional protein in mice causes neonatal hypoglycemia and sudden death. J Clin Invest. 2001 Jun;107(11):1403-9.
81. Day CP, James OF. Steatohepatitis: a tale of two "hits"? Gastroenterology. 1998 Apr;114(4):842-5.
82. Day CP. Pathogenesis of steatohepatitis. Best Pract Res Clin Gastroenterol. 2002 Oct;16(5):663-78.

83. Yang SQ, Lin HZ, Lane MD, Clemens M, Diehl AM. Obesity increases sensitivity to endotoxin liver injury: implications for the pathogenesis of steatohepatitis. Proc Natl Acad Sci U S A. 1997 Mar 18;94(6):2557-62.
84. Chavin KD, Yang S, Lin HZ, Chatham J, Chacko VP, Hoek JB, et al. Obesity induces expression of uncoupling protein-2 in hepatocytes and promotes liver ATP depletion. J Biol Chem. 1999 Feb 26;274(9):5692-700.
85. Yu XX, Murray SF, Pandey SK, Booten SL, Bao D, Song XZ, et al. Antisense oligonucleotide reduction of DGAT2 expression improves hepatic steatosis and hyperlipidemia in obese mice. Hepatology. 2005 Aug;42(2):362-71.
86. Yamaguchi K, Yang L, McCall S, Huang J, Yu XX, Pandey SK, et al. Inhibiting triglyceride synthesis improves hepatic steatosis but exacerbates liver damage and fibrosis in obese mice with nonalcoholic steatohepatitis. Hepatology. 2007 Jun;45(6):1366-74.
87. Miele L, Grieco A, Armuzzi A, Candelli M, Zocco MA, Forgione A, et al. Nonalcoholic-steatohepatitis (NASH) and hepatic mitochondrial beta-oxidation. Journal of hepatology. 2003;38:197.
88. Cook GA, Gamble MS. Regulation of carnitine palmitoyltransferase by insulin results in decreased activity and decreased apparent Ki values for malonyl-CoA. J Biol Chem. 1987 Feb 15;262(5):2050-5.
89. Memon RA, Tecott LH, Nonogaki K, Beigneux A, Moser AH, Grunfeld C, et al. Up-regulation of peroxisome proliferator-activated receptors (PPAR-alpha) and PPAR-gamma messenger ribonucleic acid expression in the liver in murine obesity: troglitazone induces expression of PPAR-gamma-responsive adipose tissue-specific genes in the liver of obese diabetic mice. Endocrinology. 2000 Nov;141(11):4021-31.
90. De Craemer D, Pauwels M, Van den Branden C. Alterations of peroxisomes in steatosis of the human liver: a quantitative study. Hepatology. 1995 Sep;22(3):744-52.
91. Kelly LJ, Vicario PP, Thompson GM, Candelore MR, Doebber TW, Ventre J, et al. Peroxisome proliferator-activated receptors gamma and alpha mediate in vivo regulation of uncoupling protein (UCP-1, UCP-2, UCP-3) gene expression. Endocrinology. 1998 Dec;139(12):4920-7.
92. Nakatani T, Tsuboyama-Kasaoka N, Takahashi M, Miura S, Ezaki O. Mechanism for peroxisome proliferator-activated receptor-alpha activator-induced up-regulation of UCP2 mRNA in rodent hepatocytes. J Biol Chem. 2002 Mar 15;277(11):9562-9.
93. Enomoto N, Takei Y, Hirose M, Ikejima K, Miwa H, Kitamura T, et al. Thalidomide prevents alcoholic liver injury in rats through suppression of Kupffer cell sensitization and TNF-alpha production. Gastroenterology. 2002 Jul;123(1):291-300.
94. McClain CJ, Mokshagundam SP, Barve SS, Song Z, Hill DB, Chen T, et al. Mechanisms of non-alcoholic steatohepatitis. Alcohol. 2004 Aug;34(1):67-79.
95. Ghoshal AK, Ahluwalia M, Farber E. The rapid induction of liver cell death in rats fed a choline-deficient methionine-low diet. Am J Pathol. 1983 Dec;113(3):309-14.
96. George J, Pera N, Phung N, Leclercq I, Yun Hou J, Farrell G. Lipid peroxidation, stellate cell activation and hepatic fibrogenesis in a rat model of chronic steatohepatitis. J Hepatol. 2003 Nov;39(5):756-64.
97. Reddy JK. Nonalcoholic steatosis and steatohepatitis. III. Peroxisomal beta-oxidation, PPAR alpha, and steatohepatitis. Am J Physiol Gastrointest Liver Physiol. 2001 Dec;281(6):G1333-9.
98. Gao D, Wei C, Chen L, Huang J, Yang S, Diehl AM. Oxidative DNA damage and DNA repair enzyme expression are inversely related in murine models of fatty liver disease. Am J Physiol Gastrointest Liver Physiol. 2004 Nov;287(5):G1070-7.
99. Weltman MD, Farrell GC, Liddle C. Increased hepatocyte CYP2E1 expression in a rat nutritional model of hepatic steatosis with inflammation. Gastroenterology. 1996 Dec;111(6):1645-53.
100. Weltman MD, Farrell GC, Hall P, Ingelman-Sundberg M, Liddle C. Hepatic cytochrome P450 2E1 is increased in patients with nonalcoholic steatohepatitis. Hepatology. 1998 Jan;27(1):128-33.

101. Leung TM, Nieto N. CYP2E1 and oxidant stress in alcoholic and non-alcoholic fatty liver disease. J Hepatol. 2013 Feb;58(2):395-8.
102. Lieber CS. Cytochrome P-4502E1: its physiological and pathological role. Physiol Rev. 1997 Apr;77(2):517-44.
103. Aubert J, Begriche K, Knockaert L, Robin MA, Fromenty B. Increased expression of cytochrome P450 2E1 in nonalcoholic fatty liver disease: mechanisms and pathophysiological role. Clin Res Hepatol Gastroenterol. 2011 Oct;35(10):630-7.
104. Cai D, Yuan M, Frantz DF, Melendez PA, Hansen L, Lee J, et al. Local and systemic insulin resistance resulting from hepatic activation of IKK-beta and NF-kappaB. Nat Med. 2005 Feb;11(2):183-90.
105. Arkan MC, Hevener AL, Greten FR, Maeda S, Li ZW, Long JM, et al. IKK-beta links inflammation to obesity-induced insulin resistance. Nat Med. 2005 Feb;11(2):191-8.
106. Napetschnig J, Wu H. Molecular basis of NF-kappaB signaling. Annu Rev Biophys. 2013;42:443-68.
107. Hayden MS, West AP, Ghosh S. NF-kappaB and the immune response. Oncogene. 2006 Oct 30;25(51):6758-80.
108. Hotamisligil GS, Erbay E. Nutrient sensing and inflammation in metabolic diseases. Nat Rev Immunol. 2008 Dec;8(12):923-34.
109. Dela Pena A, Leclercq I, Field J, George J, Jones B, Farrell G. NF-kappaB activation, rather than TNF, mediates hepatic inflammation in a murine dietary model of steatohepatitis. Gastroenterology. 2005 Nov;129(5):1663-74.
110. Zordoky BN, El-Kadi AO. Role of NF-kappaB in the regulation of cytochrome P450 enzymes. Curr Drug Metab. 2009 Feb;10(2):164-78.
111. Videla LA, Tapia G, Rodrigo R, Pettinelli P, Haim D, Santibanez C, et al. Liver NF-kappaB and AP-1 DNA binding in obese patients. Obesity (Silver Spring). 2009 May;17(5):973-9.
112. Pessayre D, Berson A, Fromenty B, Mansouri A. Mitochondria in steatohepatitis. Semin Liver Dis. 2001;21(1):57-69.
113. Tokushige K, Takakura M, Tsuchiya-Matsushita N, Taniai M, Hashimoto E, Shiratori K. Influence of TNF gene polymorphisms in Japanese patients with NASH and simple steatosis. J Hepatol. 2007 Jun;46(6):1104-10.
114. Crespo J, Cayon A, Fernandez-Gil P, Hernandez-Guerra M, Mayorga M, Dominguez-Diez A, et al. Gene expression of tumor necrosis factor alpha and TNF-receptors, p55 and p75, in nonalcoholic steatohepatitis patients. Hepatology. 2001 Dec;34(6):1158-63.
115. Abiru S, Migita K, Maeda Y, Daikoku M, Ito M, Ohata K, et al. Serum cytokine and soluble cytokine receptor levels in patients with non-alcoholic steatohepatitis. Liver Int. 2006 Feb;26(1):39-45.
116. Kern PA, Saghizadeh M, Ong JM, Bosch RJ, Deem R, Simsolo RB. The expression of tumor necrosis factor in human adipose tissue. Regulation by obesity, weight loss, and relationship to lipoprotein lipase. J Clin Invest. 1995 May;95(5):2111-9.
117. Bataller R, Brenner DA. Liver fibrosis. J Clin Invest. 2005 Feb;115(2):209-18.
118. Kisseleva T, Brenner DA. Role of hepatic stellate cells in fibrogenesis and the reversal of fibrosis. J Gastroenterol Hepatol. 2007 Jun;22 Suppl 1:S73-8.
119. Marra F. Hepatic stellate cells and the regulation of liver inflammation. J Hepatol. 1999 Dec;31(6):1120-30.
120. Bouwens L, Baekeland M, De Zanger R, Wisse E. Quantitation, tissue distribution and proliferation kinetics of Kupffer cells in normal rat liver. Hepatology. 1986 Jul-Aug;6(4):718-22.
121. Smedsrod B, De Bleser PJ, Braet F, Lovisetti P, Vanderkerken K, Wisse E, et al. Cell biology of liver endothelial and Kupffer cells. Gut. 1994 Nov;35(11):1509-16.
122. Baffy G. Kupffer cells in non-alcoholic fatty liver disease: the emerging view. J Hepatol. 2009 Jul;51(1):212-23.

123. Park JW, Jeong G, Kim SJ, Kim MK, Park SM. Predictors reflecting the pathological severity of non-alcoholic fatty liver disease: comprehensive study of clinical and immunohistochemical findings in younger Asian patients. J Gastroenterol Hepatol. 2007 Apr;22(4):491-7.
124. Lefkowitch JH, Haythe JH, Regent N. Kupffer cell aggregation and perivenular distribution in steatohepatitis. Mod Pathol. 2002 Jul;15(7):699-704.
125. Rai RM, Loffreda S, Karp CL, Yang SQ, Lin HZ, Diehl AM. Kupffer cell depletion abolishes induction of interleukin-10 and permits sustained overexpression of tumor necrosis factor alpha messenger RNA in the regenerating rat liver. Hepatology. 1997 Apr;25(4):889-95.
126. Rai RM, Zhang JX, Clemens MG, Diehl AM. Gadolinium chloride alters the acinar distribution of phagocytosis and balance between pro- and anti-inflammatory cytokines. Shock. 1996 Oct;6(4):243-7.
127. Duffield JS, Forbes SJ, Constandinou CM, Clay S, Partolina M, Vuthoori S, et al. Selective depletion of macrophages reveals distinct, opposing roles during liver injury and repair. J Clin Invest. 2005 Jan;115(1):56-65.
128. Kolios G, Valatas V, Kouroumalis E. Role of Kupffer cells in the pathogenesis of liver disease. World J Gastroenterol. 2006 Dec 14;12(46):7413-20.
129. Shek FW, Benyon RC. How can transforming growth factor beta be targeted usefully to combat liver fibrosis? Eur J Gastroenterol Hepatol. 2004 Feb;16(2):123-6.
130. Boivin GP, O'Toole BA, Orsmby IE, Diebold RJ, Eis MJ, Doetschman T, et al. Onset and progression of pathological lesions in transforming growth factor-beta 1-deficient mice. Am J Pathol. 1995 Jan;146(1):276-88.
131. Schnur J, Olah J, Szepesi A, Nagy P, Thorgeirsson SS. Thioacetamide-induced hepatic fibrosis in transforming growth factor beta-1 transgenic mice. Eur J Gastroenterol Hepatol. 2004 Feb;16(2):127-33.
132. Qi Z, Atsuchi N, Ooshima A, Takeshita A, Ueno H. Blockade of type beta transforming growth factor signaling prevents liver fibrosis and dysfunction in the rat. Proc Natl Acad Sci U S A. 1999 Mar 2;96(5):2345-9.
133. Crean JK, Lappin D, Godson C, Brady HR. Connective tissue growth factor: an attractive therapeutic target in fibrotic renal disease. Expert Opin Ther Targets. 2001 Aug;5(4):519-30.
134. Knittel T, Mehde M, Kobold D, Saile B, Dinter C, Ramadori G. Expression patterns of matrix metalloproteinases and their inhibitors in parenchymal and non-parenchymal cells of rat liver: regulation by TNF-alpha and TGF-beta1. J Hepatol. 1999 Jan;30(1):48-60.
135. Shek FW, Benyon RC, Walker FM, McCrudden PR, Pender SL, Williams EJ, et al. Expression of transforming growth factor-beta 1 by pancreatic stellate cells and its implications for matrix secretion and turnover in chronic pancreatitis. Am J Pathol. 2002 May;160(5):1787-98.
136. Li G, Xie Q, Shi Y, Li D, Zhang M, Jiang S, et al. Inhibition of connective tissue growth factor by siRNA prevents liver fibrosis in rats. J Gene Med. 2006 Jul;8(7):889-900.
137. Tilg H, Moschen AR. Insulin resistance, inflammation, and non-alcoholic fatty liver disease. Trends Endocrinol Metab. 2008 Dec;19(10):371-9.
138. Utzschneider KM, Kahn SE. Review: The role of insulin resistance in nonalcoholic fatty liver disease. J Clin Endocrinol Metab. 2006 Dec;91(12):4753-61.
139. Czech MP. The nature and regulation of the insulin receptor: structure and function. Annu Rev Physiol. 1985;47:357-81.
140. Abdul-Ghani MA, Williams K, DeFronzo RA, Stern M. What is the best predictor of future type 2 diabetes? Diabetes Care. 2007 Jun;30(6):1544-8.
141. Maitra A, Abbas, A.K. The Endocrine System. Kumar V, Abbas, A.K. and Fausto, N., editor. Seattle: Elsevier Saunders; 2005.
142. Samuel VT, Liu ZX, Qu X, Elder BD, Bilz S, Befroy D, et al. Mechanism of hepatic insulin resistance in non-alcoholic fatty liver disease. J Biol Chem. 2004 Jul 30;279(31):32345-53.
143. Samuel VT, Shulman GI. Mechanisms for insulin resistance: common threads and missing links. Cell. 2012 Mar 2;148(5):852-71.

144. Weir GC, Bonner-Weir S. A dominant role for glucose in beta cell compensation of insulin resistance. J Clin Invest. 2007 Jan;117(1):81-3.
145. Masiello P. Animal models of type 2 diabetes with reduced pancreatic beta-cell mass. Int J Biochem Cell Biol. 2006;38(5-6):873-93.
146. Donath MY, Halban PA. Decreased beta-cell mass in diabetes: significance, mechanisms and therapeutic implications. Diabetologia. 2004 Mar;47(3):581-9.
147. Musso G, Gambino R, Cassader M. Non-alcoholic fatty liver disease from pathogenesis to management: an update. Obes Rev. 2010 Jun;11(6):430-45.
148. Rivera CA. Risk factors and mechanisms of non-alcoholic steatohepatitis. Pathophysiology. 2008 Aug;15(2):109-14.
149. Lo L, McLennan SV, Williams PF, Bonner J, Chowdhury S, McCaughan GW, et al. Diabetes is a progression factor for hepatic fibrosis in a high fat fed mouse obesity model of non-alcoholic steatohepatitis. J Hepatol. 2011 Aug;55(2):435-44.
150. Visinoni S, Fam BC, Blair A, Rantzau C, Lamont BJ, Bouwman R, et al. Increased glucose production in mice overexpressing human fructose-1,6-bisphosphatase in the liver. Am J Physiol Endocrinol Metab. 2008 November 1, 2008;295(5):E1132-41.
151. Basu R, Chandramouli V, Dicke B, Landau B, Rizza R. Obesity and type 2 diabetes impair insulin-induced suppression of glycogenolysis as well as gluconeogenesis. Diabetes. 2005 Jul;54(7):1942-8.
152. Basu R, Basu A, Johnson CM, Schwenk WF, Rizza RA. Insulin dose-response curves for stimulation of splanchnic glucose uptake and suppression of endogenous glucose production differ in nondiabetic humans and are abnormal in people with type 2 diabetes. Diabetes. 2004 Aug;53(8):2042-50.
153. Rizza RA. Pathogenesis of fasting and postprandial hyperglycemia in type 2 diabetes: implications for therapy. Diabetes 2010 Nov;59(11):2697-707.
154. Basu R, Schwenk WF, Rizza RA. Both fasting glucose production and disappearance are abnormal in people with "mild" and "severe" type 2 diabetes. Am J Physiol Endocrinol Metab. 2004 Jul;287(1):E55-62.
155. Basu A, Basu R, Shah P, Vella A, Johnson CM, Nair KS, et al. Effects of type 2 diabetes on the ability of insulin and glucose to regulate splanchnic and muscle glucose metabolism: evidence for a defect in hepatic glucokinase activity. Diabetes. 2000 Feb;49(2):272-83.
156. Caro JF, Triester S, Patel VK, Tapscott EB, Frazier NL, Dohm GL. Liver glucokinase: decreased activity in patients with type II diabetes. Horm Metab Res. 1995 Jan;27(1):19-22.
157. Ginsberg HN, Zhang YL, Hernandez-Ono A. Regulation of plasma triglycerides in insulin resistance and diabetes. Arch Med Res. 2005 May-Jun;36(3):232-40.
158. Ginsberg HN. Lipoprotein physiology in nondiabetic and diabetic states. Relationship to atherogenesis. Diabetes Care. 1991 Sep;14(9):839-55.
159. Ginsberg HN. Insulin resistance and cardiovascular disease. J Clin Invest. 2000 Aug;106(4):453-8.
160. Lewis GF. Fatty acid regulation of very low density lipoprotein production. Curr Opin Lipidol. 1997 Jun;8(3):146-53.
161. Sparks JD, Sparks CE. Insulin regulation of triacylglycerol-rich lipoprotein synthesis and secretion. Biochim Biophys Acta. 1994 Nov 17;1215(1-2):9-32.
162. Taghibiglou C, Rashid-Kolvear F, Van Iderstine SC, Le-Tien H, Fantus IG, Lewis GF, et al. Hepatic very low density lipoprotein-ApoB overproduction is associated with attenuated hepatic insulin signaling and overexpression of protein-tyrosine phosphatase 1B in a fructose-fed hamster model of insulin resistance. J Biol Chem. 2002 Jan 4;277(1):793-803.
163. Lewis GF, Uffelman KD, Szeto LW, Steiner G. Effects of acute hyperinsulinemia on VLDL triglyceride and VLDL apoB production in normal weight and obese individuals. Diabetes. 1993 Jun;42(6):833-42.

164. Malmstrom R, Packard CJ, Caslake M, Bedford D, Stewart P, Yki-Jarvinen H, et al. Defective regulation of triglyceride metabolism by insulin in the liver in NIDDM. Diabetologia. 1997 Apr;40(4):454-62.
165. Bourgeois CS, Wiggins D, Hems R, Gibbons GF. VLDL output by hepatocytes from obese Zucker rats is resistant to the inhibitory effect of insulin. Am J Physiol. 1995 Aug;269(2 Pt 1):E208-15.
166. Griffin ME, Marcucci MJ, Cline GW, Bell K, Barucci N, Lee D, et al. Free fatty acid-induced insulin resistance is associated with activation of protein kinase C theta and alterations in the insulin signaling cascade. Diabetes. 1999 Jun;48(6):1270-4.
167. Wellen KE, Hotamisligil GS. Inflammation, stress, and diabetes. J Clin Invest. 2005 May;115(5):1111-9.
168. Wellen KE, Hotamisligil GS. Obesity-induced inflammatory changes in adipose tissue. J Clin Invest. 2003 Dec;112(12):1785-8.
169. Hotamisligil GS, Shargill NS, Spiegelman BM. Adipose expression of tumor necrosis factor-alpha: direct role in obesity-linked insulin resistance. Science. 1993 Jan 1;259(5091):87-91.
170. Hotamisligil GS, Spiegelman BM. Tumor necrosis factor alpha: a key component of the obesity-diabetes link. Diabetes. 1994 Nov;43(11):1271-8.
171. Garg R, Tripathy D, Dandona P. Insulin resistance as a proinflammatory state: mechanisms, mediators, and therapeutic interventions. Curr Drug Targets. 2003 Aug;4(6):487-92.
172. Shirai K. Obesity as the core of the metabolic syndrome and the management of coronary heart disease. Curr Med Res Opin. 2004 Mar;20(3):295-304.
173. Berg AH, Combs TP, Scherer PE. ACRP30/adiponectin: an adipokine regulating glucose and lipid metabolism. Trends Endocrinol Metab. 2002 Mar;13(2):84-9.
174. Kershaw EE, Flier JS. Adipose tissue as an endocrine organ. J Clin Endocrinol Metab. 2004 Jun;89(6):2548-56.
175. Weisberg SP, McCann D, Desai M, Rosenbaum M, Leibel RL, Ferrante AW, Jr. Obesity is associated with macrophage accumulation in adipose tissue. J Clin Invest. 2003 Dec;112(12):1796-808.
176. Xu H, Barnes GT, Yang Q, Tan G, Yang D, Chou CJ, et al. Chronic inflammation in fat plays a crucial role in the development of obesity-related insulin resistance. J Clin Invest. 2003 Dec;112(12):1821-30.
177. Khazen W, M'Bika J P, Tomkiewicz C, Benelli C, Chany C, Achour A, et al. Expression of macrophage-selective markers in human and rodent adipocytes. FEBS Lett. 2005 Oct 24;579(25):5631-4.
178. Charriere G, Cousin B, Arnaud E, Andre M, Bacou F, Penicaud L, et al. Preadipocyte conversion to macrophage. Evidence of plasticity. J Biol Chem. 2003 Mar 14;278(11):9850-5.
179. Odegaard JI, Chawla A. Mechanisms of macrophage activation in obesity-induced insulin resistance. Nat Clin Pract Endocrinol Metab. 2008 Nov;4(11):619-26.
180. Donath MY, Shoelson SE. Type 2 diabetes as an inflammatory disease. Nat Rev Immunol. Feb;11(2):98-107.
181. Gordon S, Taylor PR. Monocyte and macrophage heterogeneity. Nat Rev Immunol. 2005 Dec;5(12):953-64.
182. Koliwad SK, Streeper RS, Monetti M, Cornelissen I, Chan L, Terayama K, et al. DGAT1-dependent triacylglycerol storage by macrophages protects mice from diet-induced insulin resistance and inflammation. J Clin Invest. 2010 Mar 1;120(3):756-67.
183. Sachithanandan N, Graham KL, Galic S, Honeyman JE, Fynch SL, Hewitt KA, et al. Macrophage deletion of SOCS1 increases sensitivity to LPS and palmitic acid and results in systemic inflammation and hepatic insulin resistance. Diabetes. 2011 Aug;60(8):2023-31.
184. Moran-Salvador E, Lopez-Parra M, Garcia-Alonso V, Titos E, Martinez-Clemente M, Gonzalez-Periz A, et al. Role for PPARgamma in obesity-induced hepatic steatosis as determined by hepatocyte- and macrophage-specific conditional knockouts. FASEB J. 2011 Aug;25(8):2538-50.

185. Serre-Beinier V, Toso C, Morel P, Gonelle-Gispert C, Veyrat-Durebex C, Rohner-Jeanrenaud F, et al. Macrophage migration inhibitory factor deficiency leads to age-dependent impairment of glucose homeostasis in mice. J Endocrinol. 2010 Sep;206(3):297-306.
186. Odegaard JI, Ricardo-Gonzalez RR, Goforth MH, Morel CR, Subramanian V, Mukundan L, et al. Macrophage-specific PPARgamma controls alternative activation and improves insulin resistance. Nature. 2007 Jun 28;447(7148):1116-20.
187. Goerdt S, Politz O, Schledzewski K, Birk R, Gratchev A, Guillot P, et al. Alternative versus classical activation of macrophages. Pathobiology. 1999;67(5-6):222-6.
188. Gordon S. Alternative activation of macrophages. Nat Rev Immunol. 2003 Jan;3(1):23-35.
189. Lumeng CN, Bodzin JL, Saltiel AR. Obesity induces a phenotypic switch in adipose tissue macrophage polarization. J Clin Invest. 2007 Jan;117(1):175-84.
190. Lumeng CN, Deyoung SM, Bodzin JL, Saltiel AR. Increased inflammatory properties of adipose tissue macrophages recruited during diet-induced obesity. Diabetes. 2007 Jan;56(1):16-23.
191. Ferrante AW, Jr. Obesity-induced inflammation: a metabolic dialogue in the language of inflammation. J Intern Med. 2007 Oct;262(4):408-14.
192. Bouloumie A, Curat CA, Sengenes C, Lolmede K, Miranville A, Busse R. Role of macrophage tissue infiltration in metabolic diseases. Curr Opin Clin Nutr Metab Care. 2005 Jul;8(4):347-54.
193. Uysal KT, Wiesbrock SM, Marino MW, Hotamisligil GS. Protection from obesity-induced insulin resistance in mice lacking TNF-alpha function. Nature. 1997 Oct 9;389(6651):610-4.
194. Perreault M, Marette A. Targeted disruption of inducible nitric oxide synthase protects against obesity-linked insulin resistance in muscle. Nat Med. 2001 Oct;7(10):1138-43.
195. Kanda H, Tateya S, Tamori Y, Kotani K, Hiasa K, Kitazawa R, et al. MCP-1 contributes to macrophage infiltration into adipose tissue, insulin resistance, and hepatic steatosis in obesity. J Clin Invest. 2006 Jun;116(6):1494-505.
196. Kamei N, Tobe K, Suzuki R, Ohsugi M, Watanabe T, Kubota N, et al. Overexpression of monocyte chemoattractant protein-1 in adipose tissues causes macrophage recruitment and insulin resistance. J Biol Chem. 2006 Sep 8;281(36):26602-14.
197. Inouye KE, Shi H, Howard JK, Daly CH, Lord GM, Rollins BJ, et al. Absence of CC chemokine ligand 2 does not limit obesity-associated infiltration of macrophages into adipose tissue. Diabetes. 2007 Sep;56(9):2242-50.
198. Nomiyama T, Perez-Tilve D, Ogawa D, Gizard F, Zhao Y, Heywood EB, et al. Osteopontin mediates obesity-induced adipose tissue macrophage infiltration and insulin resistance in mice. J Clin Invest. 2007 Oct;117(10):2877-88.
199. Maedler K, Sergeev P, Ris F, Oberholzer J, Joller-Jemelka HI, Spinas GA, et al. Glucose-induced beta cell production of IL-1beta contributes to glucotoxicity in human pancreatic islets. J Clin Invest. 2002 Sep;110(6):851-60.
200. Maedler K, Sergeev P, Ehses JA, Mathe Z, Bosco D, Berney T, et al. Leptin modulates beta cell expression of IL-1 receptor antagonist and release of IL-1beta in human islets. Proc Natl Acad Sci U S A. 2004 May 25;101(21):8138-43.
201. Ehses JA, Perren A, Eppler E, Ribaux P, Pospisilik JA, Maor-Cahn R, et al. Increased number of islet-associated macrophages in type 2 diabetes. Diabetes. 2007 Sep;56(9):2356-70.
202. Boni-Schnetzler M, Boller S, Debray S, Bouzakri K, Meier DT, Prazak R, et al. Free fatty acids induce a proinflammatory response in islets via the abundantly expressed interleukin-1 receptor I. Endocrinology. 2009 Dec;150(12):5218-29.
203. Schumann DM, Maedler K, Franklin I, Konrad D, Storling J, Boni-Schnetzler M, et al. The Fas pathway is involved in pancreatic beta cell secretory function. Proc Natl Acad Sci U S A. 2007 Feb 20;104(8):2861-6.
204. Carstensen M, Herder C, Kivimaki M, Jokela M, Roden M, Shipley MJ, et al. Accelerated increase in serum interleukin-1 receptor antagonist starts 6 years before diagnosis of type 2 diabetes: Whitehall II prospective cohort study. Diabetes. 2010 May;59(5):1222-7.

205. Abul KA, Lichtman, A.H. & Pillai, S. . Innate Immunity. In: Schmidt B, editor. Cellular and Molecular Immunology. Philadelphia: Saunders Elsevier; 2007. p. 19-47.
206. Takeda K, Kaisho T, Akira S. Toll-like receptors. Annu Rev Immunol. 2003;21:335-76.
207. Shi H, Kokoeva MV, Inouye K, Tzameli I, Yin H, Flier JS. TLR4 links innate immunity and fatty acid-induced insulin resistance. J Clin Invest. 2006 Nov;116(11):3015-25.
208. Kim F, Pham M, Luttrell I, Bannerman DD, Tupper J, Thaler J, et al. Toll-like receptor-4 mediates vascular inflammation and insulin resistance in diet-induced obesity. Circ Res. 2007 Jun 8;100(11):1589-96.
209. Nguyen MT, Favelyukis S, Nguyen AK, Reichart D, Scott PA, Jenn A, et al. A subpopulation of macrophages infiltrates hypertrophic adipose tissue and is activated by free fatty acids via Toll-like receptors 2 and 4 and JNK-dependent pathways. J Biol Chem. 2007 Nov 30;282(48):35279-92.
210. Odegaard JI, Ricardo-Gonzalez RR, Red Eagle A, Vats D, Morel CR, Goforth MH, et al. Alternative M2 activation of Kupffer cells by PPARdelta ameliorates obesity-induced insulin resistance. Cell Metab. 2008 Jun;7(6):496-507.
211. Kang K, Reilly SM, Karabacak V, Gangl MR, Fitzgerald K, Hatano B, et al. Adipocyte-derived Th2 cytokines and myeloid PPARdelta regulate macrophage polarization and insulin sensitivity. Cell Metab. 2008 Jun;7(6):485-95.
212. Kosteli A, Sugaru E, Haemmerle G, Martin JF, Lei J, Zechner R, et al. Weight loss and lipolysis promote a dynamic immune response in murine adipose tissue. J Clin Invest. 2010 Oct 1;120(10):3466-79.
213. Gregor MG, Hotamisligil GS. Adipocyte stress: The endoplasmic reticulum and metabolic disease. J Lipid Res. 2007 May 9.
214. Urano F, Wang X, Bertolotti A, Zhang Y, Chung P, Harding HP, et al. Coupling of stress in the ER to activation of JNK protein kinases by transmembrane protein kinase IRE1. Science. 2000 Jan 28;287(5453):664-6.
215. Deng J, Lu PD, Zhang Y, Scheuner D, Kaufman RJ, Sonenberg N, et al. Translational repression mediates activation of nuclear factor kappa B by phosphorylated translation initiation factor 2. Mol Cell Biol. 2004 Dec;24(23):10161-8.
216. Hu P, Han Z, Couvillon AD, Kaufman RJ, Exton JH. Autocrine tumor necrosis factor alpha links endoplasmic reticulum stress to the membrane death receptor pathway through IRE1alpha-mediated NF-kappaB activation and down-regulation of TRAF2 expression. Mol Cell Biol. 2006 Apr;26(8):3071-84.
217. Hirosumi J, Tuncman G, Chang L, Gorgun CZ, Uysal KT, Maeda K, et al. A central role for JNK in obesity and insulin resistance. Nature. 2002 Nov 21;420(6913):333-6.
218. Xue X, Piao JH, Nakajima A, Sakon-Komazawa S, Kojima Y, Mori K, et al. Tumor necrosis factor alpha (TNFalpha) induces the unfolded protein response (UPR) in a reactive oxygen species (ROS)-dependent fashion, and the UPR counteracts ROS accumulation by TNFalpha. J Biol Chem. 2005 Oct 7;280(40):33917-25.
219. Ron D, Walter P. Signal integration in the endoplasmic reticulum unfolded protein response. Nat Rev Mol Cell Biol. 2007 Jul;8(7):519-29.
220. Solinas G, Vilcu C, Neels JG, Bandyopadhyay GK, Luo JL, Naugler W, et al. JNK1 in hematopoietically derived cells contributes to diet-induced inflammation and insulin resistance without affecting obesity. Cell Metab. 2007 Nov;6(5):386-97.
221. Kewley RJ, Whitelaw ML, Chapman-Smith A. The mammalian basic helix-loop-helix/PAS family of transcriptional regulators. Int J Biochem Cell Biol. 2004 Feb;36(2):189-204.
222. McIntosh BE, Hogenesch JB, Bradfield CA. Mammalian Per-Arnt-Sim proteins in environmental adaptation. Annu Rev Physiol. 2010 Mar 17;72:625-45.
223. Massari ME, Murre C. Helix-loop-helix proteins: regulators of transcription in eucaryotic organisms. Mol Cell Biol. 2000 Jan;20(2):429-40.
224. Pongratz I, Antonsson C, Whitelaw ML, Poellinger L. Role of the PAS domain in regulation of dimerization and DNA binding specificity of the dioxin receptor. Mol Cell Biol. 1998 Jul;18(7):4079-88.

225. Gunton JE, Kulkarni RN, Yim S, Okada T, Hawthorne WJ, Tseng YH, et al. Loss of ARNT/HIF1beta Mediates Altered Gene Expression and Pancreatic-Islet Dysfunction in Human Type 2 Diabetes. Cell. 2005 Aug 12;122(3):337-49.
226. Kozak KR, Abbott BD, Hankinson O. ARNT-deficient mice and placental differentiation. Dev Biol. 1997;191(2):297-305.
227. Salceda S, Beck I, Caro JF. Absolute requirement of aryl hydrocarbon receptor nuclear translocator protein for gene activation by hypoxia. Arch Biochem Biophys. 1996;334(2):389-94.
228. Wang GL, Jiang BH, Rue EA, Semenza GL. Hypoxia-inducible factor 1 is a basic-helix-loop-helix-PAS heterodimer regulated by cellular O2 tension. PNAS. 1995 Jun 6;92(12):5510-4.
229. Oesch-Bartlomowicz B, Oesch F. Role of cAMP in mediating AHR signaling. Biochem Pharmacol. 2009 Feb 15;77(4):627-41.
230. Zollner G, Wagner M, Trauner M. Nuclear receptors as drug targets in cholestasis and drug-induced hepatotoxicity. Pharmacol Ther. 2010 Jun;126(3):228-43.
231. Li Y, Innocentin S, Withers DR, Roberts NA, Gallagher AR, Grigorieva EF, et al. Exogenous Stimuli Maintain Intraepithelial Lymphocytes via Aryl Hydrocarbon Receptor Activation. Cell. 2011 Oct 28;147(3):629-40.
232. Huang LE, Gu J, Schau M, Bunn HF. Regulation of hypoxia-inducible factor 1alpha is mediated by an O2-dependent degradation domain via the ubiquitin-proteasome pathway. Proc Natl Acad Sci U S A. 1998 Jul 7;95(14):7987-92.
233. Ivan M, Kondo K, Yang H, Kim W, Valiando J, Ohh M, et al. HIFalpha targeted for VHL-mediated destruction by proline hydroxylation: implications for O2 sensing. Science. 2001 Apr 20;292(5516):464-8.
234. Jaakkola P, Mole DR, Tian YM, Wilson MI, Gielbert J, Gaskell SJ, et al. Targeting of HIF-alpha to the von Hippel-Lindau ubiquitylation complex by O2-regulated prolyl hydroxylation. Science. 2001 Apr 20;292(5516):468-72.
235. Iwai K, Yamanaka K, Kamura T, Minato N, Conaway RC, Conaway JW, et al. Identification of the von Hippel-lindau tumor-suppressor protein as part of an active E3 ubiquitin ligase complex. Proc Natl Acad Sci U S A. 1999 Oct 26;96(22):12436-41.
236. Mahon PC, Hirota K, Semenza GL. FIH-1: a novel protein that interacts with HIF-1alpha and VHL to mediate repression of HIF-1 transcriptional activity. Genes Dev. 2001 Oct 15;15(20):2675-86.
237. Stroka DM, Burkhardt T, Desbaillets I, Wenger RH, Neil DA, Bauer C, et al. HIF-1 is expressed in normoxic tissue and displays an organ-specific regulation under systemic hypoxia. FASEB J. 2001 Nov;15(13):2445-53.
238. Cramer T, Yamanishi Y, Clausen BE, Forster I, Pawlinski R, Mackman N, et al. HIF-1alpha is essential for myeloid cell-mediated inflammation. Cell. 2003 Mar 7;112(5):645-57.
239. Pugh CW, Ratcliffe PJ. Regulation of angiogenesis by hypoxia: role of the HIF system. Nat Med. 2003 Jun;9(6):677-84.
240. Yu DH, Mace KA, Hansen SL, Boudreau N, Young DM. Effects of decreased insulin-like growth factor-1 stimulation on hypoxia inducible factor 1-alpha protein synthesis and function during cutaneous repair in diabetic mice. Wound Repair Regen. 2007 Sep-Oct;15(5):628-35.
241. Rius J, Guma M, Schachtrup C, Akassoglou K, Zinkernagel AS, Nizet V, et al. NF-kappaB links innate immunity to the hypoxic response through transcriptional regulation of HIF-1alpha. Nature. 2008 Jun 5;453(7196):807-11.
242. Jungermann K, Kietzmann T. Oxygen: modulator of metabolic zonation and disease of the liver. Hepatology. 2000 Feb;31(2):255-60.
243. Schmidt JV, Su GH, Reddy JK, Simon MC, Bradfield CA. Characterization of a murine Ahr null allele: involvement of the Ah receptor in hepatic growth and development. Proc Natl Acad Sci U S A. 1996 Jun 25;93(13):6731-6.
244. Fernandez-Salguero PM, Ward JM, Sundberg JP, Gonzalez FJ. Lesions of aryl-hydrocarbon receptor-deficient mice. Vet Pathol. 1997 Nov;34(6):605-14.

245. Zaher H, Fernandez-Salguero PM, Letterio J, Sheikh MS, Fornace AJ, Jr., Roberts AB, et al. The involvement of aryl hydrocarbon receptor in the activation of transforming growth factor-beta and apoptosis. Mol Pharmacol. 1998 Aug;54(2):313-21.
246. Park KT, Mitchell KA, Huang G, Elferink CJ. The aryl hydrocarbon receptor predisposes hepatocytes to Fas-mediated apoptosis. Mol Pharmacol. 2005 Mar;67(3):612-22.
247. Andreola F, Calvisi DF, Elizondo G, Jakowlew SB, Mariano J, Gonzalez FJ, et al. Reversal of liver fibrosis in aryl hydrocarbon receptor null mice by dietary vitamin A depletion. Hepatology. 2004 Jan;39(1):157-66.
248. Lee JH, Wada T, Febbraio M, He J, Matsubara T, Lee MJ, et al. A novel role for the dioxin receptor in fatty acid metabolism and hepatic steatosis. Gastroenterology. 2010 Aug;139(2):653-63.
249. Kawano Y, Nishiumi S, Tanaka S, Nobutani K, Miki A, Yano Y, et al. Activation of the aryl hydrocarbon receptor induces hepatic steatosis via the upregulation of fatty acid transport. Arch Biochem Biophys. 2010 Dec 15;504(2):221-7.
250. Wang C, Xu CX, Krager SL, Bottum KM, Liao DF, Tischkau SA. Aryl hydrocarbon receptor deficiency enhances insulin sensitivity and reduces PPAR-alpha pathway activity in mice. Environ Health Perspect. 2011 Dec;119(12):1739-44.
251. Cheng K, Ho K, Stokes R, Scott C, Lau SM, Hawthorne WJ, et al. Hypoxia-inducible factor-1alpha regulates beta cell function in mouse and human islets. J Clin Invest 2010 Jun 1;120(6):2171-83.
252. Wang XL, Suzuki R, Lee K, Tran T, Gunton JE, Saha AK, et al. Ablation of ARNT/HIF1beta in liver alters gluconeogenesis, lipogenic gene expression, and serum ketones. Cell Metab. 2009 May;9(5):428-39.
253. Mishra P, Nugent C, Afendy A, Bai C, Bhatia P, Afendy M, et al. Apnoeic-hypopnoeic episodes during obstructive sleep apnoea are associated with histological nonalcoholic steatohepatitis. Liver Int. 2008 Sep;28(8):1080-6.
254. Jouet P, Sabate JM, Maillard D, Msika S, Mechler C, Ledoux S, et al. Relationship between obstructive sleep apnea and liver abnormalities in morbidly obese patients: a prospective study. Obes Surg. 2007 Apr;17(4):478-85.
255. Haase VH, Glickman JN, Socolovsky M, Jaenisch R. Vascular tumors in livers with targeted inactivation of the von Hippel-Lindau tumor suppressor. Proc Natl Acad Sci U S A. 2001 Feb 13;98(4):1583-8.
256. Kucejova B, Sunny NE, Nguyen AD, Hallac R, Fu X, Pena-Llopis S, et al. Uncoupling hypoxia signaling from oxygen sensing in the liver results in hypoketotic hypoglycemic death. Oncogene. 2011 Jan 10;30(18):2147-60.
257. Rankin EB, Rha J, Selak MA, Unger TL, Keith B, Liu Q, et al. Hypoxia-inducible factor 2 regulates hepatic lipid metabolism. Mol Cell Biol. 2009 Aug;29(16):4527-38.
258. Qu A, Taylor M, Xue X, Matsubara T, Metzger D, Chambon P, et al. Hypoxia-inducible transcription factor 2alpha promotes steatohepatitis through augmenting lipid accumulation, inflammation, and fibrosis. Hepatology. 2011 Aug;54(2):472-83.
259. Nath B, Levin I, Csak T, Petrasek J, Mueller C, Kodys K, et al. Hepatocyte-specific hypoxia-inducible factor-1alpha is a determinant of lipid accumulation and liver injury in alcohol-induced steatosis in mice. Hepatology. 2011 May;53(5):1526-37.
260. McMahon S, Charbonneau M, Grandmont S, Richard DE, Dubois CM. Transforming growth factor beta1 induces hypoxia-inducible factor-1 stabilization through selective inhibition of PHD2 expression. J Biol Chem. 2006 Aug 25;281(34):24171-81.
261. Shi YF, Fong CC, Zhang Q, Cheung PY, Tzang CH, Wu RS, et al. Hypoxia induces the activation of human hepatic stellate cells LX-2 through TGF-beta signaling pathway. FEBS Lett. 2007 Jan 23;581(2):203-10.
262. Hong KH, Yoo SA, Kang SS, Choi JJ, Kim WU, Cho CS. Hypoxia induces expression of connective tissue growth factor in scleroderma skin fibroblasts. Clin Exp Immunol. 2006 Nov;146(2):362-70.

263. Zaouali MA, Ben Mosbah I, Boncompagni E, Ben Abdennebi H, Mitjavila MT, Bartrons R, et al. Hypoxia inducible factor-1alpha accumulation in steatotic liver preservation: role of nitric oxide. World J Gastroenterol. 2010 Jul 28;16(28):3499-509.
264. Tajima T, Goda N, Fujiki N, Hishiki T, Nishiyama Y, Senoo-Matsuda N, et al. HIF-1alpha is necessary to support gluconeogenesis during liver regeneration. Biochem Biophys Res Commun. 2009 Oct 2;387(4):789-94.
265. Ochiai D, Goda N, Hishiki T, Kanai M, Senoo-Matsuda N, Soga T, et al. Disruption of HIF-1alpha in hepatocytes impairs glucose metabolism in diet-induced obesity mice. Biochem Biophys Res Commun. 2011 Oct 22;415(3):445-9.
266. Peyssonnaux C, Datta V, Cramer T, Doedens A, Theodorakis EA, Gallo RL, et al. HIF-1alpha expression regulates the bactericidal capacity of phagocytes. J Clin Invest. 2005 Jul;115(7):1806-15.
267. Walmsley SR, Print C, Farahi N, Peyssonnaux C, Johnson RS, Cramer T, et al. Hypoxia-induced neutrophil survival is mediated by HIF-1alpha-dependent NF-kappaB activity. J Exp Med. 2005 Jan 3;201(1):105-15.
268. Anand RJ, Gribar SC, Li J, Kohler JW, Branca MF, Dubowski T, et al. Hypoxia causes an increase in phagocytosis by macrophages in a HIF-1alpha-dependent manner. J Leukoc Biol. 2007 Nov;82(5):1257-65.
269. Copple BL, Bai S, Moon JO. Hypoxia-inducible factor-dependent production of profibrotic mediators by hypoxic Kupffer cells. Hepatol Res. 2010 May;40(5):530-9.
270. Pasarica M, Sereda OR, Redman LM, Albarado DC, Hymel DT, Roan LE, et al. Reduced adipose tissue oxygenation in human obesity: evidence for rarefaction, macrophage chemotaxis, and inflammation without an angiogenic response. Diabetes. 2009 Mar;58(3):718-25.
271. Ye J, Gao Z, Yin J, He Q. Hypoxia is a potential risk factor for chronic inflammation and adiponectin reduction in adipose tissue of ob/ob and dietary obese mice. Am J Physiol Endocrinol Metab. 2007 Oct;293(4):E1118-28.
272. Hosogai N, Fukuhara A, Oshima K, Miyata Y, Tanaka S, Segawa K, et al. Adipose tissue hypoxia in obesity and its impact on adipocytokine dysregulation. Diabetes. 2007 Apr;56(4):901-11.
273. Kabon B, Nagele A, Reddy D, Eagon C, Fleshman JW, Sessler DI, et al. Obesity decreases perioperative tissue oxygenation. Anesthesiology. 2004 Feb;100(2):274-80.
274. Halberg N, Khan T, Trujillo ME, Wernstedt-Asterholm I, Attie AD, Sherwani S, et al. Hypoxia-inducible factor 1alpha induces fibrosis and insulin resistance in white adipose tissue. Mol Cell Biol. 2009 Aug;29(16):4467-83.
275. Jiang C, Qu A, Matsubara T, Chanturiya T, Jou W, Gavrilova O, et al. Disruption of hypoxia-inducible factor 1 in adipocytes improves insulin sensitivity and decreases adiposity in high-fat diet-fed mice. Diabetes. 2011 Oct;60(10):2484-95.
276. Lee KY, Gesta S, Boucher J, Wang XL, Kahn CR. The differential role of Hif1beta/Arnt and the hypoxic response in adipose function, fibrosis, and inflammation. Cell Metab. 2011 Oct 5;14(4):491-503.
277. Krishnan J, Danzer C, Simka T, Ukropec J, Walter KM, Kumpf S, et al. Dietary obesity-associated Hif1alpha activation in adipocytes restricts fatty acid oxidation and energy expenditure via suppression of the Sirt2-NAD+ system. Genes Dev. 2012 Feb 1;26(3):259-70.
278. Rolph MS, Young TR, Shum BO, Gorgun CZ, Schmitz-Peiffer C, Ramshaw IA, et al. Regulation of dendritic cell function and T cell priming by the fatty acid-binding protein AP2. J Immunol. 2006 Dec 1;177(11):7794-801.
279. Chakrabarti P. Promoting adipose specificity: the adiponectin promoter. Endocrinology. 2010 Jun;151(6):2408-10.
280. Gurtner GC, Werner S, Barrandon Y, Longaker MT. Wound repair and regeneration. Nature. 2008 May 15;453(7193):314-21.
281. Singer AJ, Clark RA. Cutaneous wound healing. N Engl J Med. 1999 Sep 2;341(10):738-46.
282. Falanga V. Wound healing and its impairment in the diabetic foot. Lancet. 2005 Nov 12;366(9498):1736-43.

283. Dijke PaI, K. Growth Factors for Wound Healing. Nature Biotechnology. 1989 1989;7(8):793-98.
284. Heldin CH, Westermark B. Mechanism of action and in vivo role of platelet-derived growth factor. Physiol Rev. 1999 Oct;79(4):1283-316.
285. Roberts AB. Transforming growth factor-beta: activity and efficacy in animal models of wound healing. Wound Repair Regen. 1995 Oct-Dec;3(4):408-18.
286. Bennett NT, Schultz GS. Growth factors and wound healing: biochemical properties of growth factors and their receptors. Am J Surg. 1993 Jun;165(6):728-37.
287. Cheng CF, Sahu D, Tsen F, Zhao Z, Fan J, Kim R, et al. A fragment of secreted Hsp90alpha carries properties that enable it to accelerate effectively both acute and diabetic wound healing in mice. J Clin Invest. 2011 Nov 1;121(11):4348-61.
288. Semenza GL. Life with oxygen. Science. 2007 Oct 5;318(5847):62-4.
289. Rezvani HR, Ali N, Nissen LJ, Harfouche G, de Verneuil H, Taieb A, et al. HIF-1alpha in epidermis: oxygen sensing, cutaneous angiogenesis, cancer, and non-cancer disorders. J Invest Dermatol. 2011 Sep;131(9):1793-805.
290. Grose R, Werner S. Wound-healing studies in transgenic and knockout mice. Mol Biotechnol. 2004 Oct;28(2):147-66.
291. Martin P, Leibovich SJ. Inflammatory cells during wound repair: the good, the bad and the ugly. Trends Cell Biol. 2005 Nov;15(11):599-607.
292. Tissue Renewal and Repair: Regeneration, Healing, and Fibrosis. In: Kumar V, Abbas, A.K. and Fausto, N., editor. Robbins and Cotran Pathological Basis of Disease. 7th ed. Seattle: Elsevier Saunders; 2005. p. 87-118.
293. Werner S, Grose R. Regulation of wound healing by growth factors and cytokines. Physiol Rev. 2003 Jul;83(3):835-70.
294. Raja, Sivamani K, Garcia MS, Isseroff RR. Wound re-epithelialization: modulating keratinocyte migration in wound healing. Front Biosci. 2007;12:2849-68.
295. Werner S, Krieg T, Smola H. Keratinocyte-fibroblast interactions in wound healing. J Invest Dermatol. 2007 May;127(5):998-1008.
296. Chmielowiec J, Borowiak M, Morkel M, Stradal T, Munz B, Werner S, et al. c-Met is essential for wound healing in the skin. J Cell Biol. 2007 Apr 9;177(1):151-62.
297. Howdieshell TR, Callaway D, Webb WL, Gaines MD, Procter CD, Jr., Sathyanarayana, et al. Antibody neutralization of vascular endothelial growth factor inhibits wound granulation tissue formation. J Surg Res. 2001 Apr;96(2):173-82.
298. Desmouliere A, Geinoz A, Gabbiani F, Gabbiani G. Transforming growth factor-beta 1 induces alpha-smooth muscle actin expression in granulation tissue myofibroblasts and in quiescent and growing cultured fibroblasts. J Cell Biol. 1993 Jul;122(1):103-11.
299. Schiro JA, Chan BM, Roswit WT, Kassner PD, Pentland AP, Hemler ME, et al. Integrin alpha 2 beta 1 (VLA-2) mediates reorganization and contraction of collagen matrices by human cells. Cell. 1991 Oct 18;67(2):403-10.
300. Woodley DT, Yamauchi M, Wynn KC, Mechanic G, Briggaman RA. Collagen telopeptides (cross-linking sites) play a role in collagen gel lattice contraction. J Invest Dermatol. 1991 Sep;97(3):580-5.
301. Xue M, Le NT, Jackson CJ. Targeting matrix metalloproteases to improve cutaneous wound healing. Expert Opin Ther Targets. 2006 Feb;10(1):143-55.
302. Trengove NJ, Stacey MC, MacAuley S, Bennett N, Gibson J, Burslem F, et al. Analysis of the acute and chronic wound environments: the role of proteases and their inhibitors. Wound Repair Regen. 1999 Nov-Dec;7(6):442-52.
303. Ladwig GP, Robson MC, Liu R, Kuhn MA, Muir DF, Schultz GS. Ratios of activated matrix metalloproteinase-9 to tissue inhibitor of matrix metalloproteinase-1 in wound fluids are inversely correlated with healing of pressure ulcers. Wound Repair Regen. 2002 Jan-Feb;10(1):26-37.

304. Chen P, Parks WC. Role of matrix metalloproteinases in epithelial migration. J Cell Biochem. 2009 Dec 15;108(6):1233-43.
305. Nwomeh BC, Liang HX, Diegelmann RF, Cohen IK, Yager DR. Dynamics of the matrix metalloproteinases MMP-1 and MMP-8 in acute open human dermal wounds. Wound Repair Regen. 1998 Mar-Apr;6(2):127-34.
306. Fisher C, Gilbertson-Beadling S, Powers EA, Petzold G, Poorman R, Mitchell MA. Interstitial collagenase is required for angiogenesis in vitro. Dev Biol. 1994 Apr;162(2):499-510.
307. Scott KA, Wood EJ, Karran EH. A matrix metalloproteinase inhibitor which prevents fibroblast-mediated collagen lattice contraction. FEBS Lett. 1998 Dec 11;441(1):137-40.
308. Mirastschijski U, Impola U, Karsdal MA, Saarialho-Kere U, Agren MS. Matrix metalloproteinase inhibitor BB-3103 unlike the serine proteinase inhibitor aprotinin abrogates epidermal healing of human skin wounds ex vivo. J Invest Dermatol. 2002 Jan;118(1):55-64.
309. Mirastschijski U, Haaksma CJ, Tomasek JJ, Agren MS. Matrix metalloproteinase inhibitor GM 6001 attenuates keratinocyte migration, contraction and myofibroblast formation in skin wounds. Exp Cell Res. 2004 Oct 1;299(2):465-75.
310. Jackson CJ, Xue M, Thompson P, Davey RA, Whitmont K, Smith S, et al. Activated protein C prevents inflammation yet stimulates angiogenesis to promote cutaneous wound healing. Wound Repair Regen. 2005 May-Jun;13(3):284-94.
311. Ramasastry SS. Acute wounds. Clin Plast Surg. 2005 Apr;32(2):195-208.
312. Bailey AJ, Bazin S, Sims TJ, Le Lous M, Nicoletis C, Delaunay A. Characterization of the collagen of human hypertrophic and normal scars. Biochim Biophys Acta. 1975 Oct 20;405(2):412-21.
313. Lovvorn HN, 3rd, Cheung DT, Nimni ME, Perelman N, Estes JM, Adzick NS. Relative distribution and crosslinking of collagen distinguish fetal from adult sheep wound repair. J Pediatr Surg. 1999 Jan;34(1):218-23.
314. Simpson DM, Ross R. The neutrophilic leukocyte in wound repair a study with antineutrophil serum. J Clin Invest. 1972 Aug;51(8):2009-23.
315. Dovi JV, He LK, DiPietro LA. Accelerated wound closure in neutrophil-depleted mice. J Leukoc Biol. 2003 Apr;73(4):448-55.
316. Leibovich SJ, Ross R. The role of the macrophage in wound repair. A study with hydrocortisone and antimacrophage serum. Am J Pathol. 1975 Jan;78(1):71-100.
317. Khanna S, Biswas S, Shang Y, Collard E, Azad A, Kauh C, et al. Macrophage dysfunction impairs resolution of inflammation in the wounds of diabetic mice. PLoS One. 2010;5(3):e9539.
318. Thepen T, van Vuuren AJ, Kiekens RC, Damen CA, Vooijs WC, van De Winkel JG. Resolution of cutaneous inflammation after local elimination of macrophages. Nat Biotechnol. 2000 Jan;18(1):48-51.
319. Martin P, D'Souza D, Martin J, Grose R, Cooper L, Maki R, et al. Wound healing in the PU.1 null mouse--tissue repair is not dependent on inflammatory cells. Curr Biol. 2003 Jul 1;13(13):1122-8.
320. Hopkinson-Woolley J, Hughes D, Gordon S, Martin P. Macrophage recruitment during limb development and wound healing in the embryonic and foetal mouse. J Cell Sci. 1994 May;107 (Pt 5):1159-67.
321. Goren I, Allmann N, Yogev N, Schurmann C, Linke A, Holdener M, et al. A transgenic mouse model of inducible macrophage depletion: effects of diphtheria toxin-driven lysozyme M-specific cell lineage ablation on wound inflammatory, angiogenic, and contractive processes. Am J Pathol. 2009 Jul;175(1):132-47.
322. Mirza R, DiPietro LA, Koh TJ. Selective and specific macrophage ablation is detrimental to wound healing in mice. Am J Pathol. 2009 Dec;175(6):2454-62.
323. Lucas T, Waisman A, Ranjan R, Roes J, Krieg T, Muller W, et al. Differential roles of macrophages in diverse phases of skin repair. J Immunol. 2010 Apr 1;184(7):3964-77.
324. Blakytny R, Jude E. The molecular biology of chronic wounds and delayed healing in diabetes. Diabet Med. 2006 Jun;23(6):594-608.

325. Christman AL, Selvin E, Margolis DJ, Lazarus GS, Garza LA. Hemoglobin A1c predicts healing rate in diabetic wounds. J Invest Dermatol. 2011 Oct;131(10):2121-7.
326. Margolis DJ, Allen-Taylor L, Hoffstad O, Berlin JA. Diabetic neuropathic foot ulcers: predicting which ones will not heal. Am J Med. 2003 Dec 1;115(8):627-31.
327. Brem H, Tomic-Canic M. Cellular and molecular basis of wound healing in diabetes. J Clin Invest. 2007 May;117(5):1219-22.
328. Lerman OZ, Galiano RD, Armour M, Levine JP, Gurtner GC. Cellular dysfunction in the diabetic fibroblast: impairment in migration, vascular endothelial growth factor production, and response to hypoxia. Am J Pathol. 2003 Jan;162(1):303-12.
329. Galkowska H, Wojewodzka U, Olszewski WL. Chemokines, cytokines, and growth factors in keratinocytes and dermal endothelial cells in the margin of chronic diabetic foot ulcers. Wound Repair Regen. 2006 Sep-Oct;14(5):558-65.
330. Waltenberger J, Lange J, Kranz A. Vascular endothelial growth factor-A-induced chemotaxis of monocytes is attenuated in patients with diabetes mellitus: A potential predictor for the individual capacity to develop collaterals. Circulation. 2000 Jul 11;102(2):185-90.
331. Geerlings SE, Hoepelman AI. Immune dysfunction in patients with diabetes mellitus (DM). FEMS Immunol Med Microbiol. 1999 Dec;26(3-4):259-65.
332. Wierusz-Wysocka B, Wysocki H, Wykretowicz A, Szczepanik A, Siekierka H. Phagocytosis, bactericidal capacity, and superoxide anion (O2-) production by polymorphonuclear neutrophils from patients with diabetes mellitus. Folia Haematol Int Mag Klin Morphol Blutforsch. 1985;112(5):658-68.
333. Rosner K, Ross C, Karlsmark T, Petersen AA, Gottrup F, Vejlsgaard GL. Immunohistochemical characterization of the cutaneous cellular infiltrate in different areas of chronic leg ulcers. APMIS. 1995 Apr;103(4):293-9.
334. Loots MA, Lamme EN, Zeegelaar J, Mekkes JR, Bos JD, Middelkoop E. Differences in cellular infiltrate and extracellular matrix of chronic diabetic and venous ulcers versus acute wounds. J Invest Dermatol. 1998 Nov;111(5):850-7.
335. Wetzler C, Kampfer H, Stallmeyer B, Pfeilschifter J, Frank S. Large and sustained induction of chemokines during impaired wound healing in the genetically diabetic mouse: prolonged persistence of neutrophils and macrophages during the late phase of repair. J Invest Dermatol. 2000 Aug;115(2):245-53.
336. Thomson SE, McLennan SV, Hennessy A, Boughton P, Bonner J, Zoellner H, et al. A novel primate model of delayed wound healing in diabetes: dysregulation of connective tissue growth factor. Diabetologia. 2010 Mar;53(3):572-83.
337. Ferguson MW, Herrick SE, Spencer MJ, Shaw JE, Boulton AJ, Sloan P. The histology of diabetic foot ulcers. Diabet Med. 1996;13 Suppl 1:S30-3.
338. Peleg AY, Weerarathna T, McCarthy JS, Davis TM. Common infections in diabetes: pathogenesis, management and relationship to glycaemic control. Diabetes Metab Res Rev. 2007 Jan;23(1):3-13.
339. Xu L, McLennan SV, Lo L, Natfaji A, Bolton T, Liu Y, et al. Bacterial load predicts healing rate in neuropathic diabetic foot ulcers. Diabetes Care. 2007 Feb;30(2):378-80.
340. Loots MA, Lamme EN, Mekkes JR, Bos JD, Middelkoop E. Cultured fibroblasts from chronic diabetic wounds on the lower extremity (non-insulin-dependent diabetes mellitus) show disturbed proliferation. Arch Dermatol Res. 1999 Feb-Mar;291(2-3):93-9.
341. Hehenberger K, Kratz G, Hansson A, Brismar K. Fibroblasts derived from human chronic diabetic wounds have a decreased proliferation rate, which is recovered by the addition of heparin. J Dermatol Sci. 1998 Jan;16(2):144-51.
342. Rafehi H, El-Osta A, Karagiannis TC. Genetic and epigenetic events in diabetic wound healing. Int Wound J. 2010 Feb;8(1):12-21.
343. Stojadinovic O, Brem H, Vouthounis C, Lee B, Fallon J, Stallcup M, et al. Molecular pathogenesis of chronic wounds: the role of beta-catenin and c-myc in the inhibition of epithelialization and wound healing. Am J Pathol. 2005 Jul;167(1):59-69.

344. Brem H, Stojadinovic O, Diegelmann RF, Entero H, Lee B, Pastar I, et al. Molecular markers in patients with chronic wounds to guide surgical debridement. Mol Med. 2007 Jan-Feb;13(1-2):30-9.
345. Tepper OM, Galiano RD, Capla JM, Kalka C, Gagne PJ, Jacobowitz GR, et al. Human endothelial progenitor cells from type II diabetics exhibit impaired proliferation, adhesion, and incorporation into vascular structures. Circulation. 2002 Nov 26;106(22):2781-6.
346. Fadini GP, Miorin M, Facco M, Bonamico S, Baesso I, Grego F, et al. Circulating endothelial progenitor cells are reduced in peripheral vascular complications of type 2 diabetes mellitus. J Am Coll Cardiol. 2005 May 3;45(9):1449-57.
347. Gallagher KA, Liu ZJ, Xiao M, Chen H, Goldstein LJ, Buerk DG, et al. Diabetic impairments in NO-mediated endothelial progenitor cell mobilization and homing are reversed by hyperoxia and SDF-1 alpha. J Clin Invest. 2007 May;117(5):1249-59.
348. Ferrara N. Molecular and biological properties of vascular endothelial growth factor. J Mol Med (Berl). 1999 Jul;77(7):527-43.
349. Altavilla D, Saitta A, Cucinotta D, Galeano M, Deodato B, Colonna M, et al. Inhibition of lipid peroxidation restores impaired vascular endothelial growth factor expression and stimulates wound healing and angiogenesis in the genetically diabetic mouse. Diabetes. 2001 Mar;50(3):667-74.
350. Ferrara N, Davis-Smyth T. The biology of vascular endothelial growth factor. Endocr Rev. 1997 Feb;18(1):4-25.
351. Bitar MS, Labbad ZN. Transforming growth factor-beta and insulin-like growth factor-I in relation to diabetes-induced impairment of wound healing. J Surg Res. 1996 Feb 15;61(1):113-9.
352. Jude EB, Blakytny R, Bulmer J, Boulton AJ, Ferguson MW. Transforming growth factor-beta 1, 2, 3 and receptor type I and II in diabetic foot ulcers. Diabet Med. 2002 Jun;19(6):440-7.
353. Castronuovo JJ, Jr., Ghobrial I, Giusti AM, Rudolph S, Smiell JM. Effects of chronic wound fluid on the structure and biological activity of becaplermin (rhPDGF-BB) and becaplermin gel. Am J Surg. 1998 Aug;176(2A Suppl):61S-7S.
354. Doxey DL, Ng MC, Dill RE, Iacopino AM. Platelet-derived growth factor levels in wounds of diabetic rats. Life Sci. 1995;57(11):1111-23.
355. Wieman TJ, Smiell JM, Su Y. Efficacy and safety of a topical gel formulation of recombinant human platelet-derived growth factor-BB (becaplermin) in patients with chronic neuropathic diabetic ulcers. A phase III randomized placebo-controlled double-blind study. Diabetes Care. 1998 May;21(5):822-7.
356. Wang XJ, Han G, Owens P, Siddiqui Y, Li AG. Role of TGF beta-mediated inflammation in cutaneous wound healing. J Investig Dermatol Symp Proc. 2006 Sep;11(1):112-7.
357. Anand P, Terenghi G, Warner G, Kopelman P, Williams-Chestnut RE, Sinicropi DV. The role of endogenous nerve growth factor in human diabetic neuropathy. Nat Med. 1996 Jun;2(6):703-7.
358. Graiani G, Emanueli C, Desortes E, Van Linthout S, Pinna A, Figueroa CD, et al. Nerve growth factor promotes reparative angiogenesis and inhibits endothelial apoptosis in cutaneous wounds of Type 1 diabetic mice. Diabetologia. 2004 Jun;47(6):1047-54.
359. Yiangou Y, Facer P, Sinicropi DV, Boucher TJ, Bennett DL, McMahon SB, et al. Molecular forms of NGF in human and rat neuropathic tissues: decreased NGF precursor-like immunoreactivity in human diabetic skin. J Peripher Nerv Syst. 2002 Sep;7(3):190-7.
360. Werner S, Breeden M, Hubner G, Greenhalgh DG, Longaker MT. Induction of keratinocyte growth factor expression is reduced and delayed during wound healing in the genetically diabetic mouse. J Invest Dermatol. 1994 Oct;103(4):469-73.
361. Conde J, Scotece M, Gomez R, Gomez-Reino JJ, Lago F, Gualillo O. At the crossroad between immunity and metabolism: focus on leptin. Expert Rev Clin Immunol. 2010 Sep;6(5):801-8.
362. Fahey TJ, 3rd, Sadaty A, Jones WG, 2nd, Barber A, Smoller B, Shires GT. Diabetes impairs the late inflammatory response to wound healing. J Surg Res. 1991 Apr;50(4):308-13.
363. Pradhan L, Cai X, Wu S, Andersen ND, Martin M, Malek J, et al. Gene expression of pro-inflammatory cytokines and neuropeptides in diabetic wound healing. J Surg Res. 2011 May 15;167(2):336-42.

364. Galiano RD, Tepper OM, Pelo CR, Bhatt KA, Callaghan M, Bastidas N, et al. Topical vascular endothelial growth factor accelerates diabetic wound healing through increased angiogenesis and by mobilizing and recruiting bone marrow-derived cells. Am J Pathol. 2004 Jun;164(6):1935-47.
365. Greenhalgh DG, Sprugel KH, Murray MJ, Ross R. PDGF and FGF stimulate wound healing in the genetically diabetic mouse. Am J Pathol. 1990 Jun;136(6):1235-46.
366. Schafer M, Werner S. Oxidative stress in normal and impaired wound repair. Pharmacol Res. 2008 Aug;58(2):165-71.
367. Roy S, Khanna S, Nallu K, Hunt TK, Sen CK. Dermal wound healing is subject to redox control. Mol Ther. 2006 Jan;13(1):211-20.
368. Ojha N, Roy S, He G, Biswas S, Velayutham M, Khanna S, et al. Assessment of wound-site redox environment and the significance of Rac2 in cutaneous healing. Free Radic Biol Med. 2008 Feb 15;44(4):682-91.
369. Mudge BP, Harris C, Gilmont RR, Adamson BS, Rees RS. Role of glutathione redox dysfunction in diabetic wounds. Wound Repair Regen. 2002 Jan-Feb;10(1):52-8.
370. Palka J, Bankowski E, Wolanska M. Changes in IGF-binding proteins in rats with experimental diabetes. Ann Biol Clin (Paris). 1993;51(7-8):701-6.
371. Cechowska-Pasko M, Palka J, Bankowski E. Decrease in the glycosaminoglycan content in the skin of diabetic rats. The role of IGF-I, IGF-binding proteins and proteolytic activity. Mol Cell Biochem. 1996 Jan 12;154(1):1-8.
372. Craig RG, Yu Z, Xu L, Barr R, Ramamurthy N, Boland J, et al. A chemically modified tetracycline inhibits streptozotocin-induced diabetic depression of skin collagen synthesis and steady-state type I procollagen mRNA. Biochim Biophys Acta. 1998 Apr 24;1402(3):250-60.
373. Cechowska-Pasko M, Palka J, Bankowski E. Decreased biosynthesis of glycosaminoglycans in the skin of rats with chronic diabetes mellitus. Exp Toxicol Pathol. 1999 May;51(3):239-43.
374. Goodson WH, 3rd, Hunt TK. Wound collagen accumulation in obese hyperglycemic mice. Diabetes. 1986 Apr;35(4):491-5.
375. Tsilibary EC, Charonis AS, Reger LA, Wohlhueter RM, Furcht LT. The effect of nonenzymatic glucosylation on the binding of the main noncollagenous NC1 domain to type IV collagen. J Biol Chem. 1988 Mar 25;263(9):4302-8.
376. Hasegawa G, Hunter AJ, Charonis AS. Matrix nonenzymatic glycosylation leads to altered cellular phenotype and intracellular tyrosine phosphorylation. J Biol Chem. 1995 Feb 17;270(7):3278-83.
377. Ito A, Sato T, Iga T, Mori Y. Tumor necrosis factor bifunctionally regulates matrix metalloproteinases and tissue inhibitor of metalloproteinases (TIMP) production by human fibroblasts. FEBS Lett. 1990 Aug 20;269(1):93-5.
378. Chen C, Schultz GS, Bloch M, Edwards PD, Tebes S, Mast BA. Molecular and mechanistic validation of delayed healing rat wounds as a model for human chronic wounds. Wound Repair Regen. 1999 Nov-Dec;7(6):486-94.
379. Trengove NJ, Bielefeldt-Ohmann H, Stacey MC. Mitogenic activity and cytokine levels in non-healing and healing chronic leg ulcers. Wound Repair Regen. 2000 Jan-Feb;8(1):13-25.
380. Thangarajah H, Yao D, Chang EI, Shi Y, Jazayeri L, Vial IN, et al. The molecular basis for impaired hypoxia-induced VEGF expression in diabetic tissues. Proc Natl Acad Sci U S A. 2009 Aug 11;106(32):13505-10.
381. Botusan IR, Sunkari VG, Savu O, Catrina AI, Grunler J, Lindberg S, et al. Stabilization of HIF-1alpha is critical to improve wound healing in diabetic mice. Proc Natl Acad Sci U S A. 2008 Dec 9;105(49):19426-31.
382. Mace KA, Yu DH, Paydar KZ, Boudreau N, Young DM. Sustained expression of Hif-1alpha in the diabetic environment promotes angiogenesis and cutaneous wound repair. Wound Repair Regen. 2007 Sep-Oct;15(5):636-45.
383. Catrina SB, Okamoto K, Pereira T, Brismar K, Poellinger L. Hyperglycemia regulates hypoxia-inducible factor-1alpha protein stability and function. Diabetes. 2004 Dec;53(12):3226-32.

384. Liu L, Marti GP, Wei X, Zhang X, Zhang H, Liu YV, et al. Age-dependent impairment of HIF-1alpha expression in diabetic mice: Correction with electroporation-facilitated gene therapy increases wound healing, angiogenesis, and circulating angiogenic cells. J Cell Physiol. 2008 Nov;217(2):319-27.
385. Sarkar K, Rey S, Zhang X, Sebastian R, Marti GP, Fox-Talbot K, et al. Tie2-dependent knockout of HIF-1 impairs burn wound vascularization and homing of bone marrow-derived angiogenic cells. Cardiovasc Res. 2011 Jan 1;93(1):162-9.
386. Li W, Li Y, Guan S, Fan J, Cheng CF, Bright AM, et al. Extracellular heat shock protein-90alpha: linking hypoxia to skin cell motility and wound healing. EMBO J. 2007 Mar 7;26(5):1221-33.
387. Tomita S, Sinal CJ, Yim SH, Gonzalez FJ. Conditional disruption of the aryl hydrocarbon receptor nuclear translocator (Arnt) gene leads to loss of target gene induction by the aryl hydrocarbon receptor and hypoxia-inducible factor 1alpha. Mol Endocrinol. 2000 Oct;14(10):1674-81.
388. Clausen BE, Burkhardt C, Reith W, Renkawitz R, Forster I. Conditional gene targeting in macrophages and granulocytes using LysMcre mice. Transgenic Res. 1999 Aug;8(4):265-77.
389. Michael MD, Kulkarni RN, Postic C, Previs SF, Shulman GI, Magnuson MA, et al. Loss of insulin signaling in hepatocytes leads to severe insulin resistance and progressive hepatic dysfunction. Molecular Cell. 2000;6(1):87-97.
390. Valera A, Pujol A, Pelegrin M, Bosch F. Transgenic mice overexpressing phosphoenolpyruvate carboxykinase develop non-insulin-dependent diabetes mellitus. Proceedings of the National Academy of Sciences of the United States of America. 1994 September 13, 1994;91(19):9151-4.
391. Gunton JE, Kulkarni RN, Yim S, Okada T, Hawthorne WJ, Tseng YH, et al. Loss of ARNT/HIF1beta mediates altered gene expression and pancreatic-islet dysfunction in human type 2 diabetes. Cell. 2005 Aug 12;122(3):337-49.
392. Postic C, Shiota M, Niswender KD, Jetton TL, Chen Y, Moates JM, et al. Dual roles for glucokinase in glucose homeostasis as determined by liver and pancreatic beta cell-specific gene knock-outs using Cre recombinase. J Biol Chem. 1999 Jan 1;274(1):305-15.
393. Gomez-Valades AG, Mendez-Lucas A, Vidal-Alabro A, Blasco FX, Chillon M, Bartrons R, et al. Pck1 gene silencing in the liver improves glycemia control, insulin sensitivity, and dyslipidemia in db/db mice.(ORIGINAL ARTICLE). Diabetes. 2008;57(8):2199(12).
394. Burchell A, Cain DI. Rat hepatic microsomal glucose-6-phosphatase protein levels are increased in streptozotocin-induced diabetes. Diabetologia. 1985;28(11):852-6.
395. Hanson RW, Reshef L. REGULATION OF PHOSPHOENOLPYRUVATE CARBOXYKINASE (GTP) GENE EXPRESSION. Annual Review of Biochemistry. 1997;66(1):581-611.
396. Postic C, Dentin R, Girard J. Role of the liver in the control of carbohydrate and lipid homeostasis. Diabetes & Metabolism. 2004;30(5):398-408.
397. Szendroedi J, Chmelik M, Schmid AI, Nowotny P, Brehm A, Krssak M, et al. Abnormal hepatic energy homeostasis in type 2 diabetes. Hepatology. 2009 Oct;50(4):1079-86.
398. Schmid AI, Szendroedi J, Chmelik M, Krssak M, Moser E, Roden M. Liver ATP synthesis is lower and relates to insulin sensitivity in patients with type 2 diabetes. Diabetes Care. 2011 Feb;34(2):448-53.
399. Noordeen NA, Khera TK, Sun G, Longbottom ER, Pullen TJ, da Silva Xavier G, et al. Carbohydrate-responsive element-binding protein (ChREBP) is a negative regulator of ARNT/HIF-1beta gene expression in pancreatic islet beta-cells. Diabetes. 2010 Jan;59(1):153-60.
400. Nishiyama Y, Goda N, Kanai M, Niwa D, Osanai K, Yamamoto Y, et al. HIF-1alpha induction suppresses excessive lipid accumulation in alcoholic fatty liver in mice. J Hepatol. 2012 Feb;56(2):441-7.
401. Donath MY, Shoelson SE. Type 2 diabetes as an inflammatory disease. Nat Rev Immunol. 2011 Feb;11(2):98-107.

402. Hellmann J, Tang Y, Kosuri M, Bhatnagar A, Spite M. Resolvin D1 decreases adipose tissue macrophage accumulation and improves insulin sensitivity in obese-diabetic mice. FASEB J. 2011 Jul;25(7):2399-407.
403. Cusi K. Nonalcoholic fatty liver disease in type 2 diabetes mellitus. Curr Opin Endocrinol Diabetes Obes. 2009 Apr;16(2):141-9.
404. Wang C, Guan Y, Yang J. Cytokines in the Progression of Pancreatic beta-Cell Dysfunction. Int J Endocrinol. 2010;2010:515136.
405. Larsen CM, Faulenbach M, Vaag A, Volund A, Ehses JA, Seifert B, et al. Interleukin-1-receptor antagonist in type 2 diabetes mellitus. N Engl J Med. 2007 Apr 12;356(15):1517-26.
406. Ehses JA, Boni-Schnetzler M, Faulenbach M, Donath MY. Macrophages, cytokines and beta-cell death in Type 2 diabetes. Biochem Soc Trans. 2008 Jun;36(Pt 3):340-2.
407. Helmig S, Seelinger JU, Dohrel J, Schneider J. RNA expressions of AHR, ARNT and CYP1B1 are influenced by AHR Arg554Lys polymorphism. Mol Genet Metab. 2011 Sep-Oct;104(1-2):180-4.
408. Silhi N. Diabetes and wound healing. J Wound Care. 1998 Jan;7(1):47-51.
409. Koh TJ, DiPietro LA. Inflammation and wound healing: the role of the macrophage. Expert Rev Mol Med. 2011;13:e23.
410. Sindrilaru A, Peters T, Wieschalka S, Baican C, Baican A, Peter H, et al. An unrestrained proinflammatory M1 macrophage population induced by iron impairs wound healing in humans and mice. J Clin Invest. 2011 Mar 1;121(3):985-97.
411. Hume DA. Applications of myeloid-specific promoters in transgenic mice support in vivo imaging and functional genomics but do not support the concept of distinct macrophage and dendritic cell lineages or roles in immunity. J Leukoc Biol. 2010 Apr;89(4):525-38.
412. Miyake Y, Kaise H, Isono K, Koseki H, Kohno K, Tanaka M. Protective role of macrophages in noninflammatory lung injury caused by selective ablation of alveolar epithelial type II Cells. J Immunol. 2007 Apr 15;178(8):5001-9.
413. Stadtfeld M, Ye M, Graf T. Identification of interventricular septum precursor cells in the mouse embryo. Dev Biol. 2007 Feb 1;302(1):195-207.
414. Faust N, Varas F, Kelly LM, Heck S, Graf T. Insertion of enhanced green fluorescent protein into the lysozyme gene creates mice with green fluorescent granulocytes and macrophages. Blood. 2000 Jul 15;96(2):719-26.
415. Jakubzick C, Bogunovic M, Bonito AJ, Kuan EL, Merad M, Randolph GJ. Lymph-migrating, tissue-derived dendritic cells are minor constituents within steady-state lymph nodes. J Exp Med. 2008 Nov 24;205(12):2839-50.
416. Gallucci RM, Simeonova PP, Matheson JM, Kommineni C, Guriel JL, Sugawara T, et al. Impaired cutaneous wound healing in interleukin-6-deficient and immunosuppressed mice. FASEB J. 2000 Dec;14(15):2525-31.
417. Low QE, Drugea IA, Duffner LA, Quinn DG, Cook DN, Rollins BJ, et al. Wound healing in MIP-1alpha(-/-) and MCP-1(-/-) mice. Am J Pathol. 2001 Aug;159(2):457-63.
418. Toussaint M, Fievez L, Drion PV, Cataldo D, Bureau F, Lekeux P, et al. Myeloid hypoxia-inducible factor 1alpha prevents airway allergy in mice through macrophage-mediated immunoregulation. Mucosal Immunol. 2012 Sep 12.
419. Kobayashi H, Gilbert V, Liu Q, Kapitsinou PP, Unger TL, Rha J, et al. Myeloid cell-derived hypoxia-inducible factor attenuates inflammation in unilateral ureteral obstruction-induced kidney injury. J Immunol. 2012 May 15;188(10):5106-15.
420. Doedens AL, Stockmann C, Rubinstein MP, Liao D, Zhang N, DeNardo DG, et al. Macrophage expression of hypoxia-inducible factor-1 alpha suppresses T-cell function and promotes tumor progression. Cancer Res. 2010 Oct 1;70(19):7465-75.
421. Choi H, Chun YS, Kim SW, Kim MS, Park JW. Curcumin inhibits hypoxia-inducible factor-1 by degrading aryl hydrocarbon receptor nuclear translocator: a mechanism of tumor growth inhibition. Mol Pharmacol. 2006 Nov;70(5):1664-71.

422. Lee JW, Bae SH, Jeong JW, Kim SH, Kim KW. Hypoxia-inducible factor (HIF-1)alpha: its protein stability and biological functions. Exp Mol Med. 2004 Feb 29;36(1):1-12.
423. McMillan BJ, Bradfield CA. The aryl hydrocarbon receptor is activated by modified low-density lipoprotein. Proc Natl Acad Sci U S A. 2007 Jan 23;104(4):1412-7.
424. Esser C, Rannug A, Stockinger B. The aryl hydrocarbon receptor in immunity. Trends Immunol. 2009 Sep;30(9):447-54.
425. Hu W, Sorrentino C, Denison MS, Kolaja K, Fielden MR. Induction of cyp1a1 is a nonspecific biomarker of aryl hydrocarbon receptor activation: results of large scale screening of pharmaceuticals and toxicants in vivo and in vitro. Mol Pharmacol. 2007 Jun;71(6):1475-86.
426. Hirose K, Morita M, Ema M, Mimura J, Hamada H, Fujii H, et al. cDNA cloning and tissue-specific expression of a novel basic helix-loop-helix/PAS factor (Arnt2) with close sequence similarity to the aryl hydrocarbon receptor nuclear translocator (Arnt). Mol Cell Biol. 1996 Apr;16(4):1706-13.
427. Sekine H, Mimura J, Yamamoto M, Fujii-Kuriyama Y. Unique and overlapping transcriptional roles of arylhydrocarbon receptor nuclear translocator (Arnt) and Arnt2 in xenobiotic and hypoxic responses. J Biol Chem. 2006 Dec 8;281(49):37507-16.
428. Keith B, Adelman DM, Simon MC. Targeted mutation of the murine arylhydrocarbon receptor nuclear translocator 2 (Arnt2) gene reveals partial redundancy with Arnt. Proc Natl Acad Sci U S A. 2001 Jun 5;98(12):6692-7.
429. Jain S, Maltepe E, Lu MM, Simon C, Bradfield CA. Expression of ARNT, ARNT2, HIF1 alpha, HIF2 alpha and Ah receptor mRNAs in the developing mouse. Mech Dev. 1998 Apr;73(1):117-23.
430. Freeburg PB, Abrahamson DR. Divergent expression patterns for hypoxia-inducible factor-1beta and aryl hydrocarbon receptor nuclear transporter-2 in developing kidney. J Am Soc Nephrol. 2004 Oct;15(10):2569-78.
431. Aitola MH, Pelto-Huikko MT. Expression of Arnt and Arnt2 mRNA in developing murine tissues. J Histochem Cytochem. 2003 Jan;51(1):41-54.
432. Drutel G, Kathmann M, Heron A, Schwartz JC, Arrang JM. Cloning and selective expression in brain and kidney of ARNT2 homologous to the Ah receptor nuclear translocator (ARNT). Biochem Biophys Res Commun. 1996 Aug 14;225(2):333-9.
433. Wu R, Cui X, Dong W, Zhou M, Simms HH, Wang P. Suppression of hepatocyte CYP1A2 expression by Kupffer cells via AhR pathway: the central role of proinflammatory cytokines. Int J Mol Med. 2006 Aug;18(2):339-46.
434. Moon JO, Welch TP, Gonzalez FJ, Copple BL. Reduced liver fibrosis in hypoxia-inducible factor-1alpha-deficient mice. Am J Physiol Gastrointest Liver Physiol. 2009 Mar;296(3):G582-92.
435. Giatromanolaki A, Sivridis E, Maltezos E, Papazoglou D, Simopoulos C, Gatter KC, et al. Hypoxia inducible factor 1alpha and 2alpha overexpression in inflammatory bowel disease. J Clin Pathol. 2003 Mar;56(3):209-13.
436. Lee SY, Kwon S, Kim KH, Moon HS, Song JS, Park SH, et al. Expression of vascular endothelial growth factor and hypoxia-inducible factor in the airway of asthmatic patients. Ann Allergy Asthma Immunol. 2006 Dec;97(6):794-9.
437. Tovar-Castillo LE, Cancino-Diaz JC, Garcia-Vazquez F, Cancino-Gomez FG, Leon-Dorantes G, Blancas-Gonzalez F, et al. Under-expression of VHL and over-expression of HDAC-1, HIF-1alpha, LL-37, and IAP-2 in affected skin biopsies of patients with psoriasis. Int J Dermatol. 2007 Mar;46(3):239-46.
438. Giatromanolaki A, Sivridis E, Maltezos E, Athanassou N, Papazoglou D, Gatter KC, et al. Upregulated hypoxia inducible factor-1alpha and -2alpha pathway in rheumatoid arthritis and osteoarthritis. Arthritis Res Ther. 2003;5(4):R193-201.
439. Thornton RD, Lane P, Borghaei RC, Pease EA, Caro J, Mochan E. Interleukin 1 induces hypoxia-inducible factor 1 in human gingival and synovial fibroblasts. Biochem J. 2000 Aug 15;350 Pt 1:307-12.

440. Westra J, Brouwer E, Bos R, Posthumus MD, Doornbos-van der Meer B, Kallenberg CG, et al. Regulation of cytokine-induced HIF-1alpha expression in rheumatoid synovial fibroblasts. Ann N Y Acad Sci. 2007 Jun;1108:340-8.
441. Frede S, Stockmann C, Freitag P, Fandrey J. Bacterial lipopolysaccharide induces HIF-1 activation in human monocytes via p44/42 MAPK and NF-kappaB. Biochem J. 2006 Jun 15;396(3):517-27.
442. Ortiz-Masia D, Diez I, Calatayud S, Hernandez C, Cosin-Roger J, Hinojosa J, et al. Induction of CD36 and thrombospondin-1 in macrophages by hypoxia-inducible factor 1 and its relevance in the inflammatory process. PLoS One. 2012;7(10):e48535.
443. Shi LZ, Faith NG, Nakayama Y, Suresh M, Steinberg H, Czuprynski CJ. The aryl hydrocarbon receptor is required for optimal resistance to Listeria monocytogenes infection in mice. J Immunol. 2007 Nov 15;179(10):6952-62.
444. Sekine H, Mimura J, Oshima M, Okawa H, Kanno J, Igarashi K, et al. Hypersensitivity of aryl hydrocarbon receptor-deficient mice to lipopolysaccharide-induced septic shock. Mol Cell Biol. 2009 Dec;29(24):6391-400.
445. Rausch ME, Weisberg S, Vardhana P, Tortoriello DV. Obesity in C57BL/6J mice is characterized by adipose tissue hypoxia and cytotoxic T-cell infiltration. Int J Obes (Lond). 2008 Mar;32(3):451-63.
446. Zhang X, Lam KS, Ye H, Chung SK, Zhou M, Wang Y, et al. Adipose tissue-specific inhibition of hypoxia-inducible factor 1{alpha} induces obesity and glucose intolerance by impeding energy expenditure in mice. J Biol Chem. 2010 Oct 22;285(43):32869-77.
447. Wang ZV, Deng Y, Wang QA, Sun K, Scherer PE. Identification and characterization of a promoter cassette conferring adipocyte-specific gene expression. Endocrinology. 2010 Jun;151(6):2933-9.
448. Oda Y, Nakajima M, Mohri T, Takamiya M, Aoki Y, Fukami T, et al. Aryl hydrocarbon receptor nuclear translocator in human liver is regulated by miR-24. Toxicol Appl Pharmacol. 2012 May 1;260(3):222-31.
449. Stokes RA, Cheng K, Deters N, Lau SM, Hawthorne WJ, O'Connell PJ, et al. Hypoxia-inducible factor 1alpha (HIF-1alpha) potentiates beta-cell survival after islet transplantation of human and mouse islets. Cell Transplant. 2012 Jun 15.
450. Yu X, Fang Y, Ding X, Liu H, Zhu J, Zou J, et al. Transient hypoxia-inducible factor activation in rat renal ablation and reduced fibrosis with L-mimosine. Nephrology (Carlton). 2012 Jan;17(1):58-67.
451. Robinson A, Keely S, Karhausen J, Gerich ME, Furuta GT, Colgan SP. Mucosal protection by hypoxia-inducible factor prolyl hydroxylase inhibition. Gastroenterology. 2008 Jan;134(1):145-55.
452. Cantley J, Selman C, Shukla D, Abramov AY, Forstreuter F, Esteban MA, et al. Deletion of the von Hippel-Lindau gene in pancreatic beta cells impairs glucose homeostasis in mice. J Clin Invest. 2009 Jan;119(1):125-35.
453. Higgins DF, Kimura K, Bernhardt WM, Shrimanker N, Akai Y, Hohenstein B, et al. Hypoxia promotes fibrogenesis in vivo via HIF-1 stimulation of epithelial-to-mesenchymal transition. J Clin Invest. 2007 Dec;117(12):3810-20.
454. Ahn JM, You SJ, Lee YM, Oh SW, Ahn SY, Kim S, et al. Hypoxia-inducible factor activation protects the kidney from gentamicin-induced acute injury. PLoS One. 2012;7(11):e48952.
455. Baay-Guzman GJ, Bebenek IG, Zeidler M, Hernandez-Pando R, Vega MI, Garcia-Zepeda EA, et al. HIF-1 expression is associated with CCL2 chemokine expression in airway inflammatory cells: implications in allergic airway inflammation. Respir Res. 2012;13:60.
456. Zhou H, Chen X, Zhang WM, Zhu LP, Cheng L. HIF-1alpha inhibition reduces nasal inflammation in a murine allergic rhinitis model. PLoS One. 2012;7(11):e48618.
457. Clambey ET, McNamee EN, Westrich JA, Glover LE, Campbell EL, Jedlicka P, et al. Hypoxia-inducible factor-1 alpha-dependent induction of FoxP3 drives regulatory T-cell abundance and function during inflammatory hypoxia of the mucosa. Proc Natl Acad Sci U S A. 2012 Oct 9;109(41):E2784-93.

458. Cummins EP, Seeballuck F, Keely SJ, Mangan NE, Callanan JJ, Fallon PG, et al. The hydroxylase inhibitor dimethyloxalylglycine is protective in a murine model of colitis. Gastroenterology. 2008 Jan;134(1):156-65.
459. Karhausen J, Furuta GT, Tomaszewski JE, Johnson RS, Colgan SP, Haase VH. Epithelial hypoxia-inducible factor-1 is protective in murine experimental colitis. J Clin Invest. 2004 Oct;114(8):1098-106.
460. Shah YM, Ito S, Morimura K, Chen C, Yim SH, Haase VH, et al. Hypoxia-inducible factor augments experimental colitis through an MIF-dependent inflammatory signaling cascade. Gastroenterology. 2008 Jun;134(7):2036-48, 48 e1-3.
461. Walmsley SR, Chilvers ER, Thompson AA, Vaughan K, Marriott HM, Parker LC, et al. Prolyl hydroxylase 3 (PHD3) is essential for hypoxic regulation of neutrophilic inflammation in humans and mice. J Clin Invest. 2011 Mar;121(3):1053-63.
462. Barontini M, Dahia PL. VHL disease. Best Pract Res Clin Endocrinol Metab. 2010 Jun;24(3):401-13.
463. Cappellini MD. Long-term efficacy and safety of deferasirox. Blood Rev. 2008 Dec;22 Suppl 2:S35-41.
464. Roberts DJ, Rees D, Howard J, Hyde C, Alderson P, Brunskill S. Desferrioxamine mesylate for managing transfusional iron overload in people with transfusion-dependent thalassaemia. Cochrane Database Syst Rev. 2005(4):CD004450.
465. Cutler P. Deferoxamine therapy in high-ferritin diabetes. Diabetes. 1989 Oct;38(10):1207-10.
466. Redmon JB, Pyzdrowski KL, Robertson RP. No effect of deferoxamine therapy on glucose homeostasis and insulin secretion in individuals with NIDDM and elevated serum ferritin. Diabetes. 1993 Apr;42(4):544-9.
467. Safarinejad MR, Shafiei N, Safarinejad S. Polymorphisms in Aryl Hydrocarbon Receptor Gene Are Associated With Idiopathic Male Factor Infertility. Reprod Sci. 2013 May 23.
468. Chen Y, Bai Y, Yuan J, Chen W, Sun J, Wang H, et al. Association of polymorphisms in AhR, CYP1A1, GSTM1, and GSTT1 genes with levels of DNA damage in peripheral blood lymphocytes among coke-oven workers. Cancer Epidemiol Biomarkers Prev. 2006 Sep;15(9):1703-7.
469. Chen D, Tian T, Wang H, Liu H, Hu Z, Wang Y, et al. Association of human aryl hydrocarbon receptor gene polymorphisms with risk of lung cancer among cigarette smokers in a Chinese population. Pharmacogenet Genomics. 2009 Jan;19(1):25-34.
470. Kawajiri K, Watanabe J, Eguchi H, Nakachi K, Kiyohara C, Hayashi S. Polymorphisms of human Ah receptor gene are not involved in lung cancer. Pharmacogenetics. 1995 Jun;5(3):151-8.
471. Tsuchiya M, Katoh T, Motoyama H, Sasaki H, Tsugane S, Ikenoue T. Analysis of the AhR, ARNT, and AhRR gene polymorphisms: genetic contribution to endometriosis susceptibility and severity. Fertil Steril. 2005 Aug;84(2):454-8.
472. Le Marchand L, Donlon T, Kolonel LN, Henderson BE, Wilkens LR. Estrogen metabolism-related genes and breast cancer risk: the multiethnic cohort study. Cancer Epidemiol Biomarkers Prev. 2005 Aug;14(8):1998-2003.